

Photovoltaics

International

THE TECHNOLOGY RESOURCE FOR PV PROFESSIONALS

Solar Intelligence Competing PV cell technologies set to co-exist out to 2020

ISFH The PERC+ cell: More output power for less aluminium paste

ISC Konstanz Cost/kWh thinking and bifaciality: Two allies for low-cost PV of the future

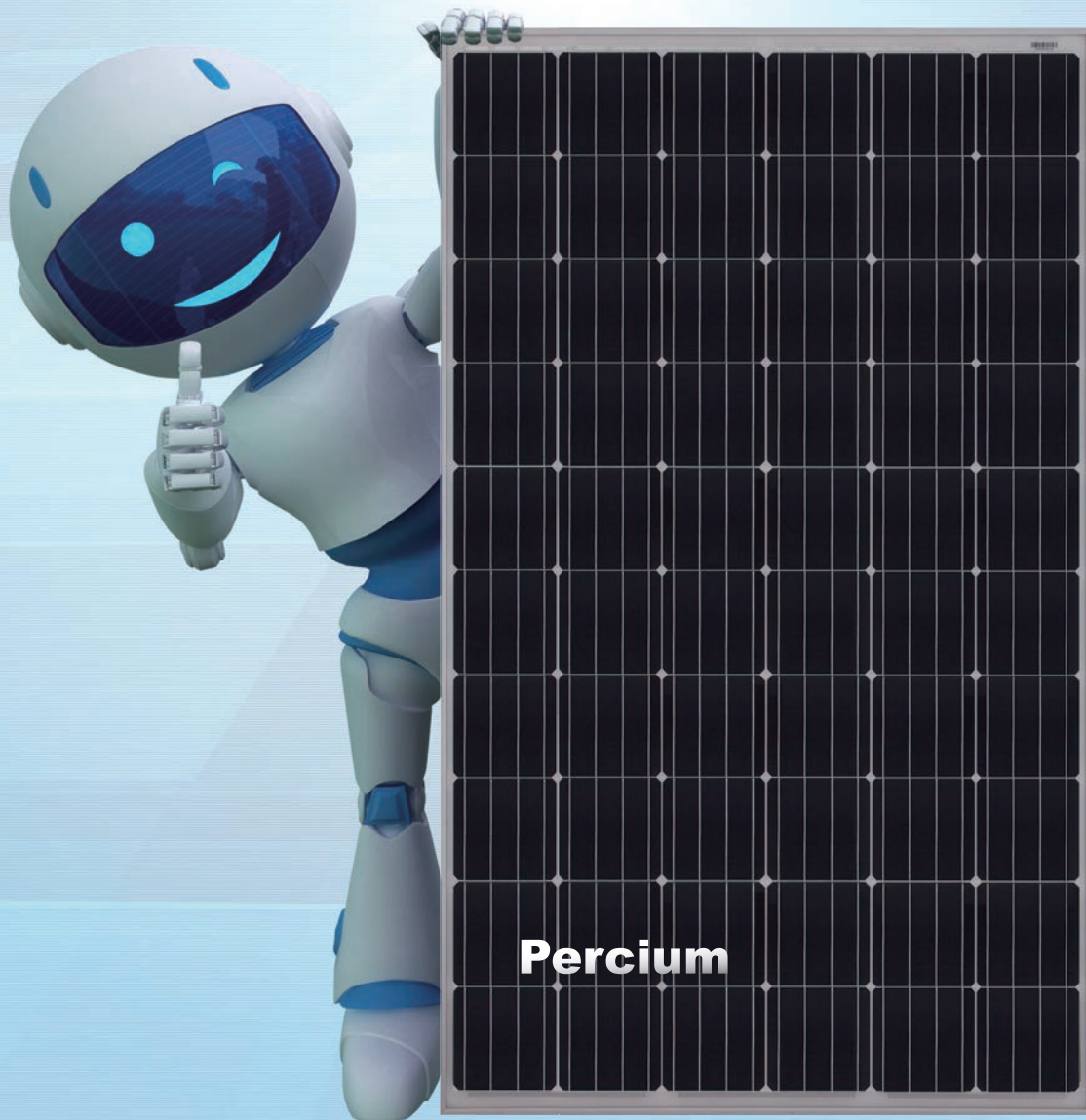
MiaSolé Predicting moisture-induced degradation of flexible PV modules in the field

CSEM Metallization and interconnection for silicon heterojunction solar cells and modules

Suntech Reliability and durability comparison of PV module backsheets

JA SOLAR

www.jasolar.com



Harvest the Sunshine

Premium Cells, Premium Modules

JA Solar Holdings Co., Ltd.

Building No.8, Nuode Center, Automobile Museum East Road, Fengtai District, Beijing

Tel: +86 (10) 63611888 Fax: +86 (10) 63611999 Email: sales@jasolar.com; market@jasolar.com

Published by:
Solar Media Ltd.,
3rd Floor, America House, 2 America Square
London EC3N 2LU, UK
Tel: +44 (0) 207 871 0122
Fax: +44 (0) 207 871 0101
E-mail: info@pv-tech.org
Web: www.pv-tech.org

Publisher: Chris Riley

Head of Content: Ben Willis
Deputy Head of Content: John Parnell
Commissioning Editor: Adam Morrison
Sub-Editor: Steve D. Brierley
Senior News Editor: Mark Osborne
Reporters: Andy Colthorpe, Tom Kenning,
David Pratt
Design: Tina Davidian
Production: Daniel H Brown, Sarah-Jane Lee

Sales Director: David Evans
Account Managers: Adam Morrison,
Graham Davie, Lili Zhu, Colin Michael, Matthew
Bosnjak

While every effort has been made to ensure
the accuracy of the contents of this journal, the
publisher will accept no responsibility for any
errors, or opinion expressed, or omissions, or for
any loss or damage, consequential or otherwise,
suffered as a result of any material here published.

Cover image: Flipper turning wafers mid-
processing.

Image courtesy of Hanwha Q CELLS.

Printed by Buxton Press
Photovoltaics International
Thirtieth Edition
Fourth Quarter 2015
Photovoltaics International is a quarterly
journal published in February, May, August and
December.

Distributed in the USA by Mail Right
International, 1637 Stelton Road B4, Piscataway,
NJ 08854.

ISSN: 1757-1197

The entire contents of this publication are
protected by copyright, full details of which are
available from the publisher. All rights reserved.
No part of this publication may be reproduced,
stored in a retrieval system or transmitted in any
form or by any means – electronic, mechanical,
photocopying, recording or otherwise – without
the prior permission of the copyright owner.

USPS Information
USPS Periodical Code: 025 313

Periodicals Postage Paid at
New Brunswick, NJ
Postmaster: Send changes to:
Photovoltaics International,
Solar Media Ltd., C/o 1637 Stelton
Road, B-4, Piscataway, NJ 08854, USA

Foreword

With PV supply and demand finding equilibrium once again, manufacturers are turning their attention to the next big question they must face: what their technology of choice will be for the next round of production expansions they are planning, announcements of which are now coming thick and fast. As such, this is arguably the key strategic decision manufacturers now have to make as the industry enters a new phase of growth.

If anything, 2015 has demonstrated that there seems to be no single answer emerging to that question. Manufacturers are embracing a broad range of technologies depending on what downstream strategies they are pursuing, as most now are. This raises the prospect of a number of competing PV cell technologies co-existing for the next few years, rather than one prevailing approach to new technology development.

That is the key conclusion of some exclusive preview findings we present in this issue of *Photovoltaics International* (p.111) from research undertaken by Finlay Colville, head of our new Solar Intelligence activities. Colville will be publishing a full report on next-generation cell technologies in the new year, ahead of the PVCellTech event we will be hosting in Kuala Lumpur, Malaysia in March 2016. Together the report and event promise to bring some much-needed focus to the debate around cell technology evolution, which is happening against the backdrop of break-neck growth in the solar industry worldwide.

Just how fast the industry is growing is explored in our latest capacity expansion analysis on p.13. For over the past year, we have been tracking the production capacity announcements of the leading manufacturers. The volume of those announcements has now reached an all-time high, and 2016 and beyond looks set to be a busy and hopefully profitable period for manufacturers.

Other highlights of this issue include an account of the potential benefits of bifacial module design (p.88). Scientists from ISC Konstanz, who have written for us before on the kWh cost-reduction benefits of bifaciality, take up the theme once again, this time focusing on the performance gains offered by the technology at a system level.

As the year draws to a close, the team at *Photovoltaics International* would like to thank you for your ongoing support for our work. Next year looks set to be an exciting one for the global PV industry as plans instigated this year come to fruition. We look forward to bringing you the latest from the cutting edge of PV technology again in 2016.

Ben Willis

Head of Content
Solar Media Ltd

Photovoltaics International's primary focus is on assessing existing and new technologies for "real-world" supply chain solutions. The aim is to help engineers, managers and investors to understand the potential of equipment, materials, processes and services that can help the PV industry achieve grid parity. The Photovoltaics International advisory board has been selected to help guide the editorial direction of the technical journal so that it remains relevant to manufacturers and utility-grade installers of photovoltaic technology. The advisory board is made up of leading personnel currently working first-hand in the PV industry.



Editorial Advisory Board

Our editorial advisory board is made up of senior engineers from PV manufacturers worldwide. Meet some of our board members below:



Prof Armin Aberle, CEO, Solar Energy Research Institute of Singapore (SERIS), National University of Singapore (NUS)

Prof Aberle's research focus is on photovoltaic materials, devices and modules. In the 1990s he established the Silicon Photovoltaics Department at the Institute for Solar Energy Research (ISFH) in Hamelin, Germany. He then worked for 10 years in Sydney, Australia as a professor of photovoltaics at the University of New South Wales (UNSW). In 2008 he joined NUS to establish SERIS (as Deputy CEO), with particular responsibility for the creation of a Silicon PV Department.



Dr. Markus Fischer, Director R&D Processes, Hanwha Q Cells

Dr. Fischer has more than 15 years' experience in the semiconductor and crystalline silicon photovoltaic industry. He joined Q Cells in 2007 after working in different engineering and management positions with Siemens, Infineon, Philips, and NXP. As Director R&D Processes he is responsible for the process and production equipment development of current and future c-Si solar cell concepts. Dr. Fischer received his Ph.D. in Electrical Engineering in 1997 from the University of Stuttgart. Since 2010 he has been a co-chairman of the SEMI International Technology Roadmap for Photovoltaic.



Dr. Thorsten Dullweber, R&D Group Leader at the Institute for Solar Energy Research Hamelin (ISFH)

Dr. Dullweber's research focuses on high efficiency industrial-type PERC silicon solar cells and ultra-fine-line screen-printed Ag front contacts. His group has contributed many journal and conference publications as well as industry-wide recognized research results. Before joining ISFH in 2009, Dr. Dullweber worked for nine years in the microelectronics industry at Siemens AG and later Infineon Technologies AG. He received his Ph. D. in 2002 for research on Cu(In,Ga)Se₂ thin-film solar cells.



Dr. Wei Shan, Chief Scientist, JA Solar

Dr. Wei Shan has been with JA Solar since 2008 and is currently the Chief Scientist and head of R&D. With more than 30 years' experience in R&D in a wider variety of semiconductor material systems and devices, he has published over 150 peer-reviewed journal articles and prestigious conference papers, as well as six book chapters.



Jim Zhu, Chief Scientist, Wuxi Suntech

Jim Zhu has bachelor and master's degrees from Fundan University and a Ph.D. from the Shanghai Institute of Technical Physics of the Chinese Academy of Sciences. In 2007 he joined Suntech as group VP with responsibility for customer service, quality management and R&D. He has been the company's Chief Scientist since 2013.



Florian Clement, Head of Group, MWT solar cells/printing technology, Fraunhofer ISE

Dr. Clement received his Ph.D in 2009 from the University of Freiburg. He studied physics at the Ludwigs-Maximilian-University of Munich and the University of Freiburg and obtained his diploma degree in 2005. His research is focused on the development, analysis and characterization of highly efficient, industrially feasible MWT solar cells with rear side passivation, so called HIP-MWT devices, and on new printing technologies for silicon solar cell processing.



Sam Hong, Chief Executive, Neo Solar Power

Dr. Hong has more than 30 years' experience in solar photovoltaic energy. He has served as the Research Division Director of Photovoltaic Solar Energy Division at the Industry Technology Research Institute (ITRI), and Vice President and Plant Director of Sinonar Amorphous Silicon Solar Cell Co., the first amorphous silicon manufacturer in Taiwan. Dr. Hong has published three books and 38 journal and international conference papers, and is a holder of seven patents. In 2011 he took office as Chairman of Taiwan Photovoltaic Industry Association.



Matt Campbell, Senior Director, Power Plant Products, SunPower

Matt Campbell has held a variety of business development and product management roles since joining the SunPower, including the development of the 1.5MW AC Oasis power plant platform, organized SunPower's power plant LCOE reduction programmes, and the acquisition of three power plant technology companies. Campbell helped form a joint venture in Inner Mongolia, China for power plant project development and manufacturing. He holds an MBA from the University of California at Berkeley and a BBA in Marketing, Finance, and Real Estate from the University of Wisconsin at Madison.



Ru Zhong Hou, Director of Product Center, ReneSola

Ru Zhong Hou joined ReneSola as R&D Senior Manager in 2010 before being appointed Director of R&D in 2012. Before joining ReneSola he was a researcher for Microvast Power Systems, a battery manufacturer. His work has been published in numerous scientific journals. He has a Ph.D. from the Institute of Materials Physics & Microstructures, Zhejiang University, China.



No matter where you are
together we *GREEN* the future.

**WORLD FUTURE
ENERGY SUMMIT**

PART OF ABU DHABI SUSTAINABILITY WEEK 2016

18-21 JANUARY 2016
ABU DHABI NATIONAL EXHIBITION CENTRE

*We sincerely invite you
to visit our booth at Hall 8*

#8110

 **SUNTECH**
BE UNLIMITED

Contents

07 Product Reviews

10 Section 1 Fab & Facilities

+ NEWS

Page 13

Quarterly analysis of PV manufacturing capacity expansion plans

Mark Osborne, Senior News Editor, *Photovoltaics International*

Page 23

From service provider to partner: optimal logistics opportunities in PV manufacturing

Holger Meyer, Solar United & Hellmann Renewable Logistics



26 Section 2 Materials

+ NEWS

Page 28

Inline quality rating of multicrystalline wafers – Relevance, approach and performance of Al-BSF and PERC processes

Matthias Demant¹, Theresa Strauch¹, Kirsten Sunder², Oliver Anspach², Jonas Haunschild¹ & Stefan Rein¹

¹Fraunhofer Institute for Solar Energy Systems ISE, Freiburg;

²PV Crystallox Solar Silicon GmbH, Erfurt, Germany



38 Section 3 Cell Processing

+ NEWS

Page 41

The PERC+ cell: More output power for less aluminium paste

Thorsten Dullweber, Christopher Kranz, Robby Peibst, Ulrike Baumann & Helge Hannebauer, Institute for Solar Energy Research Hamelin (ISFH), Emmerthal, & Alexander Fülle, Stefan Steckemetz, Torsten Weber, Martin Kutzer, Matthias Müller, Gerd Fischer, Phedon Palinginis & Holger Neuhaus, SolarWorld Innovations GmbH, Freiberg, Germany

Page 52

Metallization: The technology with highest efficiency gain potential for c-Si cells

Radovan Kopecek, Lejo J. Koduvelikulathu, Enrique Cabrera, Dominik Rudolph & Thomas Buck, International Solar Energy Research Center (ISC) Konstanz, Germany

Page 61

Metallization and interconnection for silicon heterojunction solar cells and modules

Matthieu Despeisse, Christophe Ballif, Antonin Faes & Agata Lachowicz, CSEM, Neuchâtel, Switzerland



RENOLIT REFLEXOLAR

The One-Step Multilayer Backsheet

DEVELOPING
PRODUCTS FOR
TOMORROW

Reaching new heights in reflection & endurance.

RENOLIT REFLEXOLAR is a totally new class of backsheets in the Solar PV industry. RENOLIT REFLEXOLAR is an engineered, highly white reflective, flexible Polyolefin-Polyamide multilayer construction. It has a synergetic dynamic barrier system, managing low moisture and oxygen concentrations inside the module but allowing the acetic acid to escape, hence offering extended durability to the module. Rely on it.



Rely on it.

For further information, visit: renolit.reflexolar.com

Contents

69 Section 4 Thin Film

+ NEWS

Page 72

Predicting moisture-induced degradation of flexible PV modules in the field

Kedar Hardikar, Todd Krajewski & Kris Toivola, MiaSolé, Santa Clara, California, USA



69

85 Section 5 PV Modules

+ NEWS

Page 88

Cost/kWh thinking and bifaciality: Two allies for low-cost PV of the future

Radovan Kopecek, Ismail Shoukry & Joris Libal, ISC Konstanz, Germany

Page 98

Reliability and durability comparison of PV module backsheets

Haidan Gong & Guofeng Wang, Wuxi Suntech Power Co., Ltd., Wuxi, China



85

107 Section 6 Market Watch

+ NEWS

Page 111

Competing PV cell technologies set to co-exist out to 2020

Finlay Colville, Head of Market Intelligence, Solar Media Ltd.



107

116 Subscription / Advertisers Index

Product Reviews

Despatch Industries



Despatch Industries provides retrofit inline LID prevention technology

Product Outline: Despatch Industries has introduced its patent-pending in-line 'PowerLock' light-induced degradation (LID) prevention technology that eliminates the need for material handling that can be retrofitted into existing Despatch tools and will be offered on all 'Safire' firing furnaces.

Problem: LID, which reduces the efficiency of passivated emitter rear cell (PERC) cells by up to 6% after they are installed, has been a persistent problem for PV manufacturers. Several furnace manufacturers have introduced solutions to the problem but they are all claimed to require the purchase of stand-alone equipment that takes up valuable floor space and requires additional material handling steps.

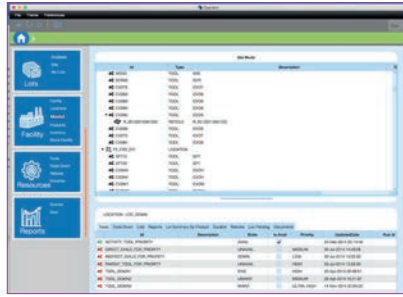
Solution: Despatch has developed an in-line solution that integrates into its metallization firing furnace line and reduces LID to around 1%. The patent-pending in-line PowerLock LID prevention technology eliminates the need for material handling and saves floor space. PowerLock uses LED lamps which have a 20SUN maximum intensity that achieves the desired result in just 3.6 meters. These lamps allow the dwell time to be reduced significantly, enabling an in-line process that maintains furnace throughput speeds, according to the company.

Applications: PERC-based cell processing using Despatch furnaces.

Platform: PowerLock can be retrofitted into existing Despatch tools and will be offered on all new Safire Firing Furnaces. Despatch CF-Series Firing Furnaces can also be ordered with PowerLock. The Safire tool features PowerLock technology which suppresses LID on PERC cells from 3-6% down to ~1%, according to the company.

Availability: Already available.

Eyelit



Eyelit's version 5.2 MES software lowers the cost of factory automation and improves productivity

Product Outline: Manufacturing software provider Eyelit has announced the general availability of version 5.2 of its 'Eyelit Manufacturing' and 'Eyelit Semiconductor Edition' suites of software.

Problem: Many of the new Manufacturing Execution System (MES) features were driven by customers that migrated to Eyelit from Camstar, Applied Materials (FactoryWorks, PROMIS and WorkStream) and IBM (SiView) legacy systems. They recognized that Eyelit's software enables them to dramatically reduce their overall costs and the number of systems required.

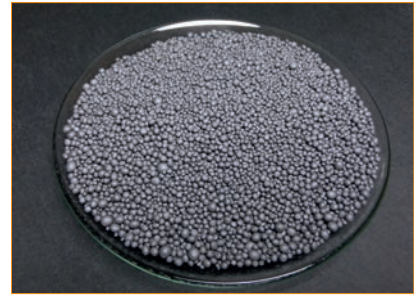
Solution: Eyelit Manufacturing version 5.2 and Semiconductor Edition version 5.2 feature many product enhancements developed in collaboration with customers that are implementing large-scale factory automation projects. Automation requirements drove major enhancements to equipment reservation and data collection. A Run-to-Run (R2R) integration template is introduced and utilizes the 'Eyelit Recipe Management System' and the 'Eyelit FactoryConnect' module for integration with external Advanced Process Control controllers and equipment. This enables dynamic adjustment of equipment processing through feed-forward controls to help extend the time between preventive maintenance tasks to increase throughput.

Applications: PV manufacturing execution systems.

Platform: The Eyelit platform has a graphical 'scenario builder' for end-users to configure flexible conditional manufacturing, as well as business-process and quality-management workflows..

Availability: Already available.

SiTec



SiTec's 'Genesis' FBR technology designed to drastically lower production costs

Product Outline: SiTec, a subsidiary of centrotherm photovoltaics, is developing 'Genesis', a new technology aimed at reducing monosilane fluid-bed reactor (FBR) polysilicon production capital and operating costs by approximately 45% each, compared to legacy FBR decomposition processes.

Problem: Legacy FBR processes typically fluidize reaction beds by blowing a mixture of monosilane gas up through a bed of small silicon particles. Decomposition and particle growth occur when monosilane gas contacts hot granules in the bed. Resultant epitaxial growth increases particle size until sufficiently large to be harvested. Previous attempts to increase hydraulic fluid bed reactor productivity by operating at high pressure and high monosilane feed concentration have resulted in excessively high rates of dust formation and unacceptably low yield.

Solution: SiTec's Genesis technology fluidizes the granular reaction bed by mechanically induced vibration as opposed to hydraulic fluidization used by legacy processes. Coupled with SiTec's proprietary monosilane process technology, known as 'STAR', SiTec forecasts polysilicon plant investment and energy consumption will be reduced by approximately 35% each compared to legacy FBR processes.

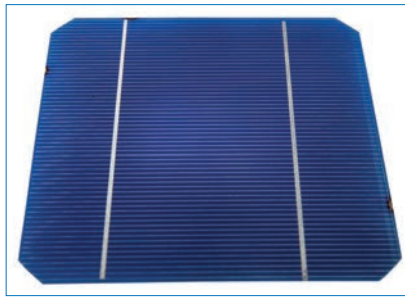
Applications: High-volume, low-cost FBR polysilicon production.

Platform: Genesis reaction rates are expected to be fast due to the reactor's ability to run at high temperature and pressure. These high temperatures, pressures and feed composition make for fast reaction rate and economical, highly efficient, small-sized reactors.

Availability: September 2016 onwards.

Product Reviews

PV Nano Cell



PV Nano Cell's 'Sicrys' silver and copper nano-metric digital inks boost cell efficiencies

Product Outline: PV Nano Cell is to enter the US solar market with its 'Sicrys' silver and copper inks. The inks are expected to accelerate the adoption of PV by reducing the cost of silicon solar cell production, using an efficient process that produces sustainable inks without the use of hazardous wastes and by increasing solar cell efficiencies at a mass production scale.

Problem: With the solar industry under enormous pressure to accelerate cost reductions while continuing an environmentally responsible production process, the search is underway for new printing technologies that reduce the costs of producing solar cells and increase solar cell efficiency, thus allowing more energy to be harvested from each cell.

Solution: PV Nano Cell's Sicrys silver and copper inks are said to reduce costs because they can be used with innovative non-contact digital inkjet printing, instead of traditional screen printing. Because it does not involve contact with the cell, inkjet printing reduces the amount of cell breakage, reducing the wastage of silicon; in addition, it also enables the use of thinner wafers, also saving on silicon costs. Implementing Sicrys silver nano-metric inkjet inks allows manufacturers to reduce the amount of silver needed in the cell. The level of silver consumption reduction can reach up to 70%, saving on the cost of silver, which is the most expensive material used in the production of solar cells.

Applications: Solar cell metallization of silver and copper.

Platform: PV Nano Cell's inks increase solar cell efficiency by more than 0.2% absolute, according to the company.

Availability: Currently available.

M10 Industries



M10 Industries 'Kubus' multi-tray stringer offers up to 5,000 cells per hour throughput

Product Outline: M10 Industries has launched 'Kubus', a new multi-tray stringer. The device deploys decoupled processes that are claimed to guarantee uninterrupted production and an output of up to 5,000 cells per hour.

Problem: A key problem for PV module manufacturers is a lack of space and manpower to operate assembly tools with high throughput in existing facilities. This limits the potential for debottlenecking and expanding existing nameplate capacity at low capital expenditure levels.

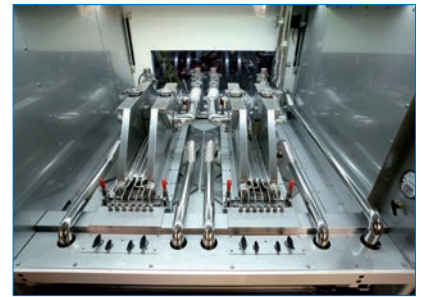
Solution: The Kubus multi-tray stringer enables PV modules to be produced at 45 second intervals, or up to 80 modules per hour, at least three times as many as with previous stringers, according to the company. The stringer solders up to six solar cells side by side to form a complete cell matrix for modules. For this purpose the cells are transported on tooling plates – or "trays". Up to now only single 'strings' have been generated which have to be placed by side by side in a module. This step of the process can be entirely omitted with and therefore also the risk of cell breakage. Kubus can be operated by a single staff member and by taking up 90 square metres does not require more space than previous stringers, despite its higher throughput.

Applications: High-volume flexible stringing of two- to five-busbar cells and 6" half-cells.

Platform: The Kubus can handle soldering cells with up to five busbars and 6" half-cells. The modular approach enables the system to be maintained at all times, thereby enabling greater efficiency such as ribbon coils that can be exchanged at any time without interrupting the production process.

Availability: Already available.

Schmid



Schmid's APCVD tool provides versatile deposition of multiple films

Product Outline: Schmid's Atmospheric Pressure Chemical Vapor Deposition (APCVD) technology allows for a variety of doped and un-doped films to be deposited in-line, boosting solar cell conversion efficiencies for a wide range of solar cell architectures for high-volume production such as PERC and PERT.

Problem: One of the main drivers to adopt n-type solar cells regards LID, which occurs in p-type silicon after being exposed to light. Doping n-type silicon with boron can be done using either ion implantation or thermal diffusion using boron precursors. However, when introduced inside the tube, the boron depletes resulting in poor uniformity across the wafers. Moreover, precursor byproducts leave a residue which can cause both the wafer carrier and wafers themselves to stick. In addition, thermal diffusion leads to doping of both surfaces of the wafer unless additional masking steps are applied. Lastly, the process leaves a boron oxygen-rich layer on the cell surface which must be removed requiring further steps.

Solution: SCHMID's APCVD technology allows for a variety of doped and un-doped films to be deposited in-line. The APCVD can deposit un-doped silicon glass, phosphorus silicate glass, boron silicate glass and titanium oxide, to fit a variety of cell designs.

Applications: APCVD has been used for creating high-efficiency boron-doped n-type cells, IBC cells, back junction and bifacial cell architectures.

Platform: SCHMID's APCVD systems are offered in belt or roller variants. They can be configured for multiple films and film stacks in a single pass. Film thickness can reach up to 200nm with finely controlled dopant concentration and uniformity.

Availability: Currently available.

Fab & Facilities



Page 10
News

Page 13
Quarterly analysis of PV
manufacturing capacity
expansion plans

Mark Osborne, Senior News Editor,
Photovoltaics International

Page 23
From service provider to
partner: Optimal logistics
opportunities in PV
manufacturing

Holger Meyer, Solar United &
Hellmann Renewable Logistics



JA Solar launches new 400MW cell plant in Malaysia

JA Solar has ramped its 400MW cell plant in Malaysia as part of its wider capacity expansion plans. JA Solar said it also planned to increase ingot/wafer production for the first time in many years to 1.5GW, up 500MW from 1GW.

Both solar cell and module nameplate capacity will be increased to 5GW by mid-2016, equating to both being increased by 1.4GW from planned 2015 nameplate capacity levels of 3.6GW.

The company recently starting ramping its new 400MW solar cell manufacturing facility in Penang, Malaysia. JA Solar said in May 2015 that it was planning a solar cell plant in Malaysia to avoid the US anti-dumping duties and said that expected the plant to be completed and start ramping in the fourth quarter of 2015. The plant is JA Solar's first outside China and is located at the Bayan Lepas Industrial Park, Pulau, Pinang in Malaysia and will produce p-type multicrystalline solar cells.

Management said that the Malaysian plant had a nameplate capacity of 800MW to 1,000MW.



Credit: JA Solar

The Malaysia cell plant is JA Solar's first outside China.

India

Trina inks MOU for new module plant in India's Andhra Pradesh

Trina Solar has signed a provisional agreement to build a new PV manufacturing plant in the Indian state of Andhra Pradesh.

The government of Andhra Pradesh confirmed the memorandum of understanding with Trina in November, revealing that the deal would be worth INR2,800 crore (US\$422 million) and employ some 3,500 workers.

Few further details have been disclosed on the deal, other than that the plant will be built in the state's Atchutapuram Visakhapatnam district.

Reports earlier this year suggested Trina was looking at India as a new manufacturing location for exports to Europe and the USA, where Chinese modules and cells are subject to punitive import duties. In May the company agreed a deal with local firm Welspun for 500MW each of cell and module manufacturing capacity in India.

Swelect ramps up Bangalore module manufacturing to 100MW, aims for 1GW by 2020

India-based module manufacturer HHV Solar Technologies, a wholly-owned subsidiary of renewable energy firm Swelect Energy, has ramped up its crystalline and thin film PV module manufacturing line in Dabaspur, Bangalore, from 40MW to 100MW.

The firm also aims to reach 1GW

capacity in a phased programme over the next five years.

The new manufacturing line has advanced process automation and uses German machinery, according to R. Chellappan, managing director of HHV. The facility is spread across 40,000 sq. ft. using Electro Luminescence testing in compliance with IEC and UL standards among others.

Furthermore HHV has won an order to supply modules for a 10MW PV project in the US to be shipped by April next year.

Chellappan also named some of the firm's leading customers including BHEL, SunEdison, Swelect, Bosch, Godrej & Boyce, Mahindra Reva, Larson & Toubro, Huawei, Rich Phytocare, Indian Institutes of Technology and Indian Parliament House



Credit: Trina Solar

Trina is looking for a new manufacturing base where trade duties will apply less pressure.

Global expansions

Zhongli Talesun starts production at 500MW PERC production plant in Thailand

PV manufacturer Zhongli Talesun has become the first of a wave of Chinese firms planning to establish manufacturing operations in Thailand to begin production in the Southeast Asian country.

The company said this week that it had begun the first phase of production at its new 500MW integrated solar cell and module assembly plant in the Thai-China Industrial Park in Rayong, Thailand, announced in February. Zhongli Talesun had also previously said that the plant would produce PERC (passivated

Credit: CSUN



China Sunergy is to expand its manufacturing footprint overseas.

emitter and rear cell) technology for its new 'Hipro' 285W+ modules that were launched at SNEC in May. Talesun had said that the new PV modules would deploy solar cells with 20.3% conversion efficiencies, providing module conversion efficiencies of 17.55%.

The company noted in a financial filing in China that the start of production in Thailand would help the company further develop its PV business in Southeast Asia as well as across the world due to

"effectively avoiding the impact of anti-dumping and anti-subsidies", which included the US and EU.

China Sunergy to restructure manufacturing footprint

Struggling PV manufacturer China Sunergy (CSUN) is planning to relocate its manufacturing operations in China and expand its manufacturing footprint overseas in a major new move.

CSUN said that the actions were intended to improve its cost competitiveness and counter anti-dumping actions in the US, EU and potentially in other regions in the future.

Tingxiu Lu, chairman and CEO of China Sunergy said: "Since the inception of our first oversea[s] plant, in Turkey, our efforts to diversify CSUN's manufacturing base [has] never stop [sic]. The move helps to enhance our global supply chain, gain access to local customers and minimise potential negative impacts from anti-dumping cases in the US, EU, or elsewhere. Looking ahead, we will continue to improve our cost competitiveness and strengthen our global footprint by the combination of moving our existing facilities in mainland China and building new facilities in the countries which have cost and geographic advantages."

The company announced the plans in a press release celebrating the formal volume production ramp at its new 200MW solar cell plant in Incheon, South Korea. CSUN noted that trial production had successfully started in May 2015 and said the company would consider expanding production to 500MW with additional production lines once the facility has reached around 50% utilisation rates. CSUN-branded solar modules would be produced by local Korean module assembly firms, according to the company.

VON ARDENNE

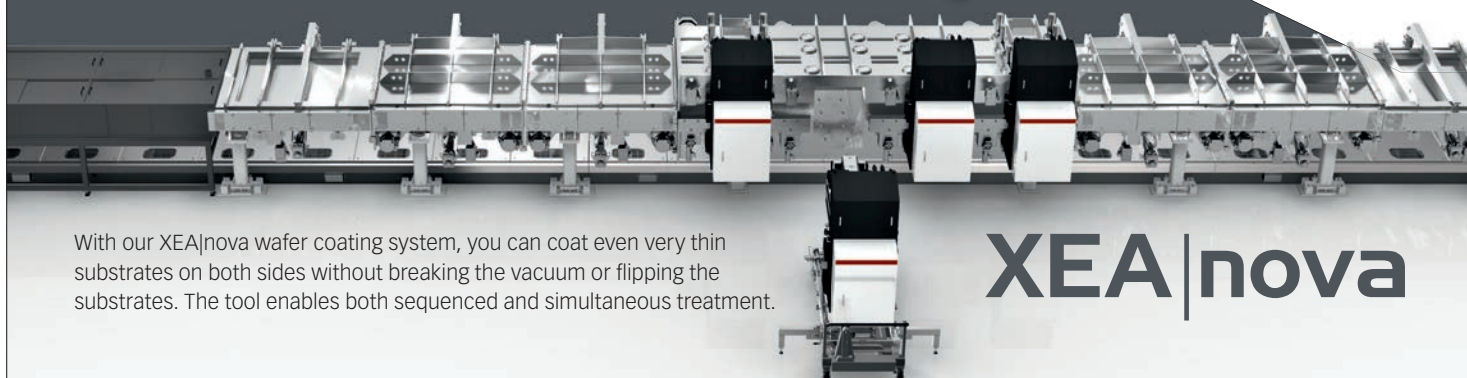


www.vonardenne.biz

EASY AND PRECISE

SIMULTANEOUS DOUBLE-SIDED

VACUUM COATING



With our XEA|nova wafer coating system, you can coat even very thin substrates on both sides without breaking the vacuum or flipping the substrates. The tool enables both sequenced and simultaneous treatment.

XEA|nova

Solargiga and Motech JV adding 600MW of module capacity in China

Major Taiwanese PV manufacturer Motech Industries is making an investment in a PV module manufacturing subsidiary of monocrystalline solar cell producer Solargiga Energy that will drive an additional 600MW of new capacity at the plant in China through 2016.

The PV module subsidiary of Solargiga is expected to expand PV module capacity by 400MW and enter volume production in February 2016. A second phase of expansion totalling 200MW is follow and start ramping in the third quarter of 2016.

According to Solargiga, annual production would total 1.2GW once the second phase of expansion was completed. The company noted that the capacity expansion was needed to support customer demand and its PV project business. Motech's China-based operations, Motech (Suzhou) Renewable Energy Co is making the investment of RMB11.4 million (US\$1.78 million) and will have a 19% stake in the module manufacturing subsidiary. A further RMB8.6 million (US\$1.34 million) is to be contributed by Solargiga subsidiary, Jinzhou Jinmao which owns the PV module company.

Closures

GD Solar shutting down 640MW of production line capacity

China-based PV manufacturer and project developer GD Solar, a subsidiary of Guodian Technology & Environment Group Corporation, is discontinuing certain solar cell, module and thin-film production lines due to financial weakness on the back of weak demand.

The parent company said in a financial statement that GD Solar would shutter 180MW of c-Si solar cell production line capacity, 400MW of PV module production capacity and 60MW of a-Si thin-film capacity. GD Solar was said to have "faced operating and financial challenges, for example, low utilisation rates of its production lines, high production costs, and difficulties in market expansion".

The parent company noted that it did not rule out further actions to reduce the financial impact of its subsidiary on its operations, noting that the production line closures would impact its profitability for the full year, due to impairment charges.

Sonali Solar doubles India module production to 100MW, plans for 300MW

India-based module manufacturer Sonali Solar completed the ramp up of its



Credit: SolarWorld

SolarWorld CEO Frank Asbeck said planned capacity expansions were "a few months" behind schedule

polycrystalline module manufacturing facility in Gujarat, India, from 50MW to 100MW.

Sonali Solar president and chief executive Pankaj Desai said that the company also plans to ramp up to 300MW by the end of 2015 or in Q1 2016.

The company has already purchased the new assembly line to produce its polycrystalline PV modules with a range between 3W to 320W. The Gujarat plant, which has been running for seven years, supplies modules to PV developers across India. Sonali Solar also owns a 25MW module manufacturing facility in Michigan, which has been running for more than three years. The firm plans to expand the plant to 100MW once the Gujarat facility has reached 200-300MW.

Desai said: "The India market is getting more dynamic and we see a lot of demand coming up for Indian-made modules, as well as in US [where] we are getting much better market share through our distributor network."

Factory upgrade delays hit SolarWorld earnings

German manufacturer SolarWorld has said delays implementing planned production capacity expansions and new production technologies will impact on its 2015 earnings.

In its Q3 report, SolarWorld said the delays would mean its earnings before interest and tax (EBIT) would remain negative in 2015, though the company is expecting an improvement on 2014's EBIT figure of €-43.8 million.

PV Tech understands that the delays have set the company back by around three to six months, and relate to a combination of the shifts to PERC technology at its US and Freiburg plants, capacity expansions and other measures such as changes to its administrative systems. "In light of the wealth of ambitious measures we implemented this year, a few delays could not be completely avoided," said CEO

Frank Asbeck in his foreword to the Q3 report.

"All in all, we are running a few months behind our original plans. As a result and contrary to our expectations, we will not be able to return to positive territory with the operating result for the full fiscal year 2015."

Tool makers

Amtech's solar sales slide in fiscal fourth quarter

PV manufacturing equipment specialist Amtech Systems has reported a significant slump in solar related sales, order backlog and new orders in its fiscal fourth quarter.

Amtech reported group revenue in the fiscal fourth quarter of US\$28.2 million, while solar segment revenue totalled US\$12.8 million, down from US\$37.5 million in the previous quarter.

Total backlog for solar segment orders stood at US\$19.6 million at the end of September 2015, compared to US\$32.4 million in the previous quarter. Backlog includes deferred revenue and customer orders that are expected to ship within the next 12 months.

Solar segment new orders were US\$2.8 million, compared to US\$13 million in the previous quarter.

The company had US\$52.7 million in new orders booked in fiscal 2015, compared to around US\$33 million in fiscal 2014, mirroring a recovery in solar capital spending seen building since last year.

Solar revenue for the fiscal full year was US\$50.2 million, up from US\$37.6 million in fiscal 2014.

Fokko Pentinga, chief executive officer of Amtech Systems said: "Although we experienced an anticipated lull in fourth quarter equipment orders, we are pleased to report a 79% increase in bookings from one year ago and robust quoting activity with both current and prospective customers."

Quarterly analysis of PV manufacturing capacity expansion plans

Mark Osborne, Senior News Editor, *Photovoltaics International*

ABSTRACT

This quarterly report will focus on the third quarter of 2015, which was expected to be the low point in new capacity expansion announcements during the year. Momentum seen during the first half of the year, however, carried through, and so a full nine-month analysis is also provided, to further characterize developments in 2015. Finally, developments in October and the record-setting month of November will also be covered, ahead of a full-year analysis of all expansion announcements over the last 24 months that were converted into 'effective' capacity in the next quarterly report.

July the joker

Global PV manufacturing expansion plans for the month of July 2015 could have provided a longer-term picture of future expansions, rather than more-immediate decisions that might have resulted in newly added capacity within the next 12 months. In July global PV manufacturing expansion plan announcements totalled 3.68GW, up by over 30% from June, which amounted to 2.75GW.

In the first half of the year, May was

the high point of announcements, which totalled 6.7GW, as well as the most active month in terms of the number of companies announcing new plans for capacity expansions. Despite the 3.68GW of announcements for the month of July, that figure proved to be the second largest to May's record.

The challenge with the majority of planned expansions announced in July was that most lacked either a definitive timeline or a definitive location, while some lacked both.

In one particular case, an initial plan was for 160MW of integrated PERC cell/module production in India as part of a more ambitious target of 1GW of production that was also announced for future years without any specific timelines being given for execution. Adding to the challenge of qualifying the majority of the announcements in July is the lack of details regarding financing. Consequently, announcements in July fell significantly below the meaningful



Credit: JA Solar

Figure 1. November this year saw a record surge in cell and module production capacity expansion announcements.

Fab & Facilities

Materials

Cell Processing

Thin Film

PV Modules

Market Watch

capacity qualification criteria, compared with the many that met the mark in February, March and May.

Even in May's record level of announcements, however, close to 1GW of announced expansions can already be eliminated from the total. This is because a 900MW a-Si thin-film plant by Hanergy Thin Film was cancelled after the Hong Kong stock market commission began investigating the company. Its shares remain frozen through the end of November 2015. Several other small module assembly expansions from start-ups bring the total close to the 1GW level, as obtaining financing for such projects can often take more than a year to arrange, if this done at all.

“July stands out because of the 1GW of planned monocrystalline solar cell capacity in China, from a single company.”

The month of July also stands out because of the 1GW of planned monocrystalline solar cell capacity in China, from a single company. The expansion schedule is understandably phased over an unspecified number of years, but does have substance for several reasons. First, there is a renaissance under way in high-efficiency monocrystalline wafer/cell production. Second, the announcement was made by a leading Chinese monocrystalline wafer producer as part of its strategy to support growth of monocrystalline production overall to enable low-cost competitive modules. Third, overall solar cell capacity expansions have trailed module assembly expansion plans in 2014, yet the first half of 2015 has been notable for the resurgence in cell expansion plans as companies start to rebalance production.

Another project that materialized in July comes from a Tier-1 integrated PV manufacturer in Asia, with an expected 400MW expansion of multicrystalline PERC production. The company has been capacity constrained and running at 100% utilization rates.

Dedicated solar cell capacity expansions announced in July topped 2.1GW, while integrated cell/module expansions totalled 1.4GW. Dedicated module assembly expansions were only 180MW.

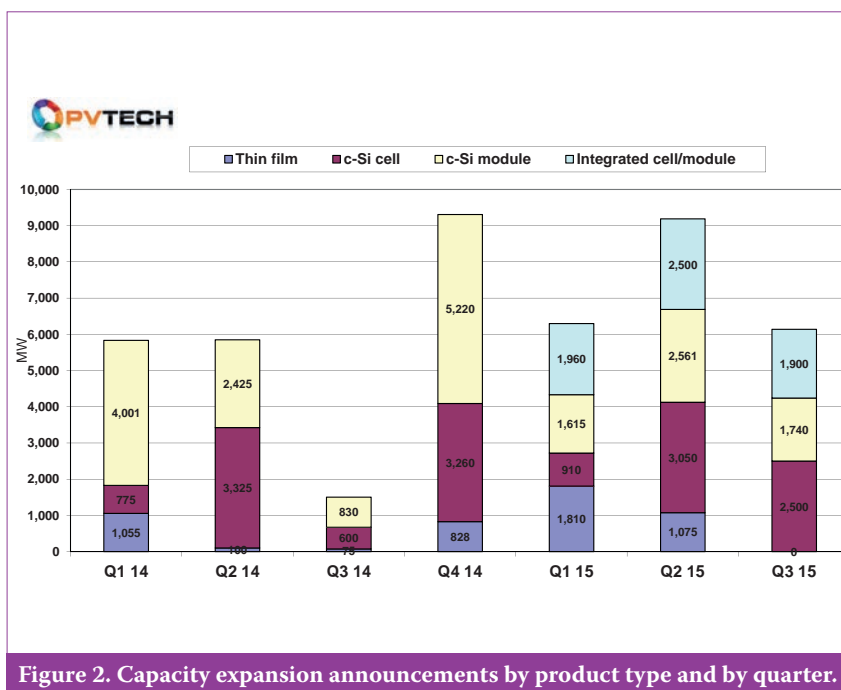


Figure 2. Capacity expansion announcements by product type and by quarter.

USA dominates August

Global PV manufacturing expansion plans announced for the month of August 2015 neatly totalled 1GW, down by over 72% from 3.68GW in the previous month, but significantly higher than announcements made in August a year ago, which only totalled 50MW. The majority (800MW) of capacity expansions were for PV module facilities, which included 320MW of capacity additions at existing facilities and 480MW for new module assembly plants.

Only four companies announced plans in August; these included Suniva on its acquisition by Shunfeng/Suntech, Silfab Solar, Amerisolar and Globo Brazil, which was a new facility that officially opened in the month. Significantly for the month of August, virtually all the announcements (820MW) related to North America, with 700MW concerning the USA.

Despite the booming US market and stiffened anti-dumping duties against China and Taiwan, only 1GW of new capacity plans had been announced for the USA by the end of August.

September slumber

The expectation for September was that after the record capacity expansion level set in May (6.7GW), new announcements would decline through to the fourth quarter, when major new announcements from some of the major PV manufacturers could be expected during third-quarter financial conference calls. Though the trend has been downward as expected,

a total of almost 1.5GW of new capacity plans were announced from five companies – a much higher figure than the 1GW announced from five companies in August.

Similarly to August, the announced September capacity plans were dominated by dedicated solar cell (200MW) and integrated cell and module (500MW) expansions, while dedicated module assembly plans totalled 760MW. There were zero capacity expansions announced for thin-film production, and zero for the third quarter of 2015.

The main expansion announced (700MW) was that of China-based Seraphim Solar System; this was an expansion of previously revealed plans in May (300MW) of module assembly in Jackson, Mississippi. The company has since said that it would be using solar cells procured from merchant cell producers in South Korea, which would include multi and mono products.

The surprise news of the month was the planned introduction of 200MW of solar cell capacity at aleo solar's module assembly plant in Germany. Despite the European end-market being in decline, European producers are mostly running at full capacity.

Once again, a level of caution should be applied to more than 500MW of plans for India announced by LONGi Silicon Materials (for a 500MW integrated facility) and by GCL Integrated Technology Co/Adani Group joint venture (unspecified). The recent GCL/Adani announcement simply lacks any details at all, especially with regard to financing,

DISCOVER THE WORLD OF INTERSOLAR



Intersolar India | Mumbai | November 18–20, 2015

Intersolar Europe | Munich | June 22–24, 2016

Intersolar North America | San Francisco | July 12–14, 2016

Intersolar South America | São Paulo | August 23–25, 2016

Intersolar Summits | Worldwide



Discover the World's Leading
Exhibition Series for the Solar Industry
www.intersolarglobal.com

suggesting that both companies have issues with raising new capital.

Impressively, around 2GW of planned expansions by cell/module subsidiary Lerri Photovoltaic have recently received financing through a private placement of shares in the parent company, while the remaining capacity plans have yet to be finalized.

Third-quarter analysis

As expected, total capacity announcements declined from the highs of 9.2GW in the second quarter of 2015 to just over 6GW in the third quarter (Fig. 2). The drop-off was not as significant as expected, however, especially when only 1.4GW was announced in the same period in 2014. The strength of announcements for Q3 mirrors that for Q1, and is similar in size to that for the first two quarters of 2014.

“Total capacity announcements declined from the highs of 9.8GW in the second quarter of 2015 to just over 6GW in the third quarter.”

The third quarter also confirmed that emphasis at a MW level has most definitely switched to capacity plans for both dedicated solar cell expansions and integrated cell/module expansions. A total of 2.5GW of dedicated solar cell expansion announcements were made in the third quarter, while at least 1.9GW of integrated production plans were announced. Dedicated module assembly plans totalled around 1.7GW, slightly ahead of first quarter plans, but down significantly from the second quarter's 2.5GW.

Nine-month analysis

The most important trend in the first half of 2015 was arguably the geographical shift in planned expansions. With the wise precaution of excluding announcements made by Hanergy Thin Film, no new capacity announcements were made in China in the first six months of the year. That dry spell ended abruptly in July, however, when LONGi began announcing 5.5GW of expansions in China. Nevertheless, LONGi was the only Chinese producer to announce major plans in China in the third quarter of the year, clearly indicating

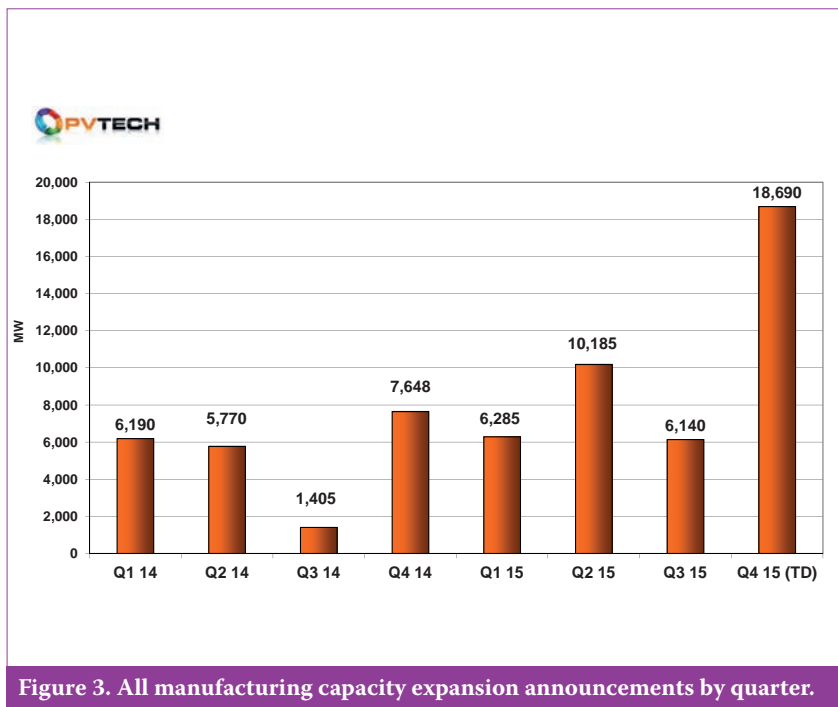


Figure 3. All manufacturing capacity expansion announcements by quarter.

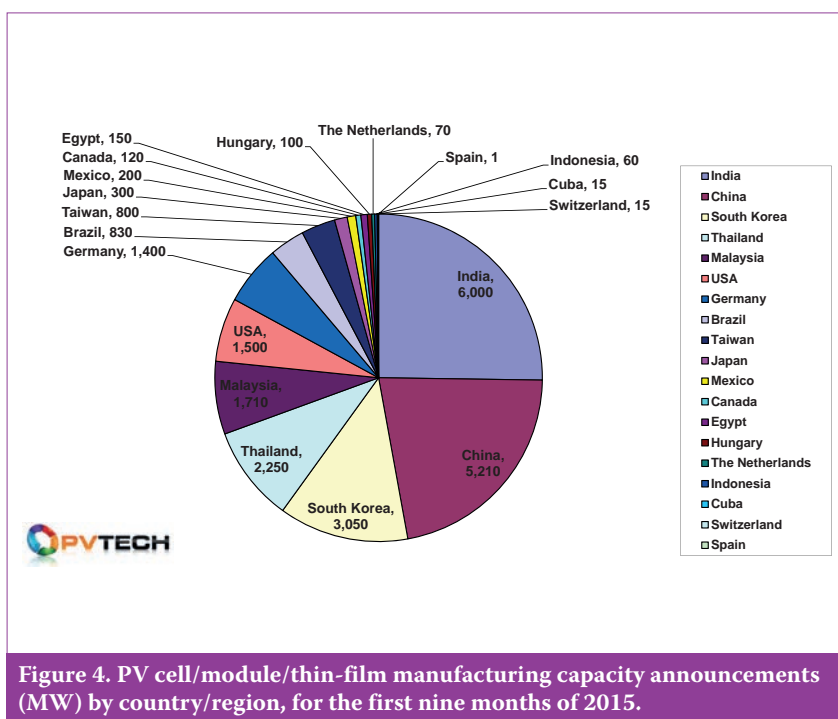


Figure 4. PV cell/module/thin-film manufacturing capacity announcements (MW) by country/region, for the first nine months of 2015.

that a significant hold on capacity expansions remains in place.

In the first nine months of 2015, a total of over 22GW of new capacity expansions were announced, compared with over 13GW during the same period in 2014 (Fig. 3). Clearly, strong momentum has been building.

Geographical trends

A total of 1,843MW of capacity expansion announcements were made for the USA in 2014, with 1,000MW being attributed to SolarCity. Interestingly, around 530MW of the

2014 announcements for the USA have become operational, and are classified as effective capacity increases to date. Around 8.5GW of capacity expansion announcements in Asia since the start of 2014 have primarily been made to circumvent or capitalize on the anti-dumping duties in the USA.

PV Tech recently highlighted the seismic shift that occurred in the first half of 2015, which saw few, if any, new capacity plans by Chinese producers for manufacturing in China. Instead, Chinese silicon-based PV manufacturers announced more than 6.7GW of planned capacity expansions

in a number of overseas countries that included India, Malaysia, Thailand, South Korea, Brazil and the USA.

The announcements in 2015 for capacity expansions in the USA have included three Chinese firms, Seraphim, Shunfeng and Amerisolar, totalling 800MW so far this year.

The promise of India

The Indian government's plans to install 100GW of PV by 2022 has sparked a significant wave of pledges and MOUs to build PV manufacturing facilities in the country, covering polysilicon, ingot/wafers, solar cells and PV modules. Much of this promise has yet to convert from hype and hope to any actual meaningful new effective capacity.

The assessment of significant double-digit gigawatts of pledges boils down to around 6GW (at the end of September 2015) of potential expansions of cell and module production at some point in the future. Though much remains speculation, the 6GW figure is based on such projects having a much higher probability of happening, which catapults India to the top of the list of locations for planned capacity expansion announcements in the first nine months of 2015 (Fig. 4).

Changing China

Another major change, as already reported in the previous quarterly report, was the seismic shift away from new capacity announcements in China. Discounting (because of Hanergy's financial and stock market issues) a-Si and CIGS thin-film announcements by Hanergy of over 2.1GW, there were no expansions announced in China in the first half of 2015. That trend was broken in July, however, with LONGi announcing ingot/wafer and module production expansions in China. Several months then went by before further announcements were made. Chinese PV manufacturers instead announced many plans to start production outside China, a trend that continued through the end of November.

If Hanergy's plans with others for expansions in China in the first nine months of the year are included, a total of around 5.2GW of announcements were made, still making China the second largest to India with regard to capacity expansion plans.

Perhaps the most significant trend of where meaningful capacity expansions were occurring was the rise of South

East Asia, notably Malaysia (1.7GW) and Thailand (2.2GW), with South Korea (3GW) being the surprise draw in Asia, after Hanwha and several other companies selected that country in 2015 (Fig. 4).

Less dependence on expansions in China in 2015 led to an overall broader potential global manufacturing footprint, a trend further supported by announcements made in October and November, covered next.

October calm

New capacity expansion announcements reached 1.1GW in October, covering a sprinkling of thin film, c-Si solar cell and module assembly. Overall expansion plans were in line with expected rates, as the lull seen during August to October 2014 was repeated in the same months in 2015, but the 2015 figures were slightly higher, despite October 2014 and October 2015 producing identical announcements (1.1GW).

Although the announcements in October of both years were the same, the product mix was very different. In October 2014, c-Si module assembly expansions dominated (950MW), while 150MW was provided by dedicated solar cell expansions. By contrast, in October 2015, thin film contributed 300MW, dedicated solar cell expansions totalled 500MW, and 310MW was attributed to c-Si module assembly. No integrated solar cell/module assembly expansions were announced in October 2015.

The relatively few capacity expansion announcements reflected once again the small number of companies (six) that declared plans. Nevertheless, some of the plans demonstrated bigger ambitions over the next few years, as seen in July 2015.

The CIGS thin-film plans of ADVANCIS are worth noting because, although the initial first-phase capacity expansion is 300MW at a new facility in China, ambitious plans were announced for subsequent build-out totalling 1.5GW of capacity at a single facility. The other big ambition relates to 1366 Technologies' initial 250MW 'Direct Wafer' production plant in the USA, with future plans to expand capacity to 3GW in coming years.

Staying with upstream manufacturing, Elkem Solar announced plans to restart multicrystalline ingot production at the former REC plant in Herøya, Norway. Although planned production levels were not disclosed, the plant had a capacity of 650MW and several hundred employees. Elkem Solar is

expecting to initially create around 70 to 80 jobs, indicating that initial production would be low.

There have been few new multicrystalline wafer capacity expansions announced in more than two years, apart from an additional meaningful 1GW of capacity at GCL-Poly, taking nameplate capacity to 14GW. Overcapacity and weak ASPs have limited expansions in this upstream sector.

In mid-October China Sunergy (CSUN) announced that it had officially started the volume production ramp-up at a new 200MW solar cell plant in Incheon, South Korea, after having had trial production successfully undertaken in May. The NASDAQ-listed PV manufacturer had not previously disclosed any specific plans for production in South Korea. The cash-strapped company is believed to have transferred tools from its facilities in China, and said it was considering expanding production to 500MW with additional production lines, once the facility has reached around 50% utilization rates; this is against the backdrop of a restructuring of its manufacturing footprint to circumvent US and EU anti-dumping duties.

Technically, CSUN's announcement would not be classified as a capacity expansion announcement, but as simply a relocation of nameplate capacity. In recent years, however, the company has experienced low utilization rates, and the shift of tools to South Korea would bring idled capacity back into being 'effective' capacity.

November storm

Global PV capacity expansion announcements in November 2015 set several new major benchmarks: of the big six Silicon Module Super League (SMSL) members, five (Trina Solar, Canadian Solar, JinkoSolar, JA Solar and Hanwha Q CELLS), as expected, announced further expansions to meet growing demand in 2016.

A total of 17.5GW of new capacity expansions were announced in November, across dedicated solar cell and dedicated module assembly. Notably, no integrated cell/module capacity expansions were announced that month, primarily because of the dominance of announcements by SMSL members. This is by far the highest figure set during the two years 2014–15, and is almost triple the benchmark capacity announcements of 6.7GW set earlier in the year in May.

The number of companies announcing expansions totalled 14 in November 2015, beating the previous benchmark of 11, set in May. Interestingly, three SMSL members – Trina Solar, JinkoSolar and Hanwha Q CELLS – participated in setting the May and the November benchmark figures.

“The number of companies announcing expansions totalled 14 in November 2015, beating the previous benchmark of 11, set in May.”

SMSL dominance

Overall, five of the six SMSL members dominated capacity expansion announcements in November. Canadian Solar announced a total of over 4GW of expansions across ingot/wafer, dedicated solar cell and dedicated PV module assembly. Expansions or new plants in various regions were announced, including Canada, China, Brazil, Indonesia and Vietnam, as well as plans for a 400MW solar cell plant somewhere in South East Asia.

JA Solar kept things simpler on the geographical front, announcing that a total of 1.4GW of new solar cell capacity would be added in China and Malaysia, while a similar figure of dedicated module assembly would be added in China. Including 500MW of new ingot/wafer capacity in China, a total of 3.3GW of new expansions was announced by the company in November.

JinkoSolar also announced in this month a total of 1.8GW of expansions, across ingot/wafer, dedicated solar cell and module assembly. The company has not yet decided the split of manufacturing between China and Malaysia. The situation was also similar with Hanwha Q CELLS, who announced module assembly expansions of 1GW, while not disclosing the location and capacity levels between China, South Korea and Malaysia. Leading global PV manufacturer Trina Solar announced a total of 2.8GW of new capacity. Once again, geographical locations were not forthcoming.

The SMSL members' capacity expansion announcements totalled around 13GW in November 2015 alone.

Dedicated solar cell capacity announcements in November reached 6.2GW, significantly higher than the previous benchmark of 2.7GW set in May 2015. Including SunPower's re-announced IBC cell plant and further planned phases of solar cell capacity expansions over the next five years that were announced in November, the total for the month reaches an astonishing 13.1GW.

Similar significant figures were announced for dedicated PV module assembly expansions, which totalled 11.38GW in November 2015. The previous monthly benchmark for dedicated module assembly expansions was set at 3.11GW in November 2014, while the integrated cell/module benchmark of 2.96GW was set in February 2015.

Another interesting development was further announcements surrounding expansions of multi c-Si ingot and wafer production by several integrated PV manufacturers, such as JA Solar, JinkoSolar, Canadian Solar and Trina Solar, from the big six SMSL. In total, 1.6GW of multi c-Si ingot/wafer expansions and upgrades were announced in November. Although a sign that outsourced wafer capacity may be finally tightening, it does not yet indicate that wafer supply is heading for major constraints.

Leading multi c-Si ingot/wafer producer GCL-Poly, however, has yet to announce capacity expansion plans in 2015, after increasing capacity in 2014 by 1GW, to 14GW. The company is currently attempting to close on a major deal to sell its coal-fired power station and steam-generation businesses in order to raise major new funding for expansions in solar cell (joint venture with Canadian Solar) and ingot/wafer production.

Seismic shift rebalance

As a result of the unspecified locations for much of the planned expansions in November, excluding Canadian Solar, it is difficult at this time to put an accurate figure on the latest expansions planned in China. Nevertheless, the announcements made in November indicate that at least 6.1GW is clearly earmarked in China, which brings the total for the first 11 months of 2015 (including Hanergy) to 11.31GW.

Malaysia is also expected to be a key location for further expansions, but once again the lack of details at this time precludes specifying an accurate

figure past the figures that have been provided for the first nine months of 2015.

Meaningful capacity additions

In tracking capacity expansion announcements, one of the perennial topics for discussion is the conversion rate to actual production; to address this point, several levels of assessment are made.

First, the term 'meaningful capacity additions' is used when assessing announcements from the likes of Tier-1 manufacturers, for whom the likelihood of conversion is typically greater. This is no guarantee of this happening, however, and several major announcements made by such manufacturers in 2014 have been cancelled or are currently still pending.

Second, assessments are made on key metrics surrounding the details provided in initial announcements. The lack of information about expansion schedules and locations, as well as about the ability to finance such expansions, are all taken into account.

An assessment of 2014 capacity expansion announcements categorized as 'meaningful' indicates that around 85% of the plans have progressed to the under-construction, tool-installation or ramping-up phase. The high rate of conversion of meaningful capacity additions from announcements in 2014 was simply due to a key number of larger or long-standing manufacturers executing plans; those executed capacity expansions then pass from being 'meaningful' additions to 'effective' additions. Effective capacity relates to not only capacity that exists, but also in the real world to the manufactured products that will be sold on the market.

At the beginning of 2014, effective global PV module capacity stood at around 45GW, compared with a nameplate capacity of more than 60GW. A disconnect also exists between capacity announcements, meaningful additions and effective capacities from the massive expansions made through 2011. With the new wave of expansions that started again in 2014, the same disconnects are occurring.

Tracking manufacturing-equipment orders, backlogs and delivery schedules from leading suppliers is also used to assess meaningful capacity additions. Again, it is clear that order intake at equipment suppliers tracks meaningful capacity additions. In 2014,

however, it was not as straightforward as one might have expected, looking at the period through 2011.

A sizeable disconnect existed between meaningful capacity additions and order intake in 2014. One of the key reasons for this was the emphasis on PV module assembly expansions and the regional dominance of China in those announcements. Lower capital expenditure requirements for back-end assembly equipment, coupled with a shift to using domestic equipment suppliers for expansions compared with the last expansion phase when western suppliers were dominant, were behind the disconnect.

Lead times for solar cell equipment, from ordering to tool installation to qualification, for example, have been taking between six and nine months since 2014, and have remained relatively unchanged since the prior expansion phase. This has again led to a typical lapse in revenue generated by suppliers before customers announce meaningful capacity additions, as the next phase of capacity expansions gets under way.

A detailed appraisal of meaningful capacity additions announced over the first seven months of 2015 indicates that a total of 9.3GW could come on

stream in the next four to eighteen months, on the basis of a grand total of capacity announcements in this period of around 19GW. Although around 10GW fail the meaningful capacity test, this does not mean that many of the plans would not meet the test in the future.

Eliminating the possibility of Hanergy's plans ever happening, however, is treated as being prudent in the current circumstances the company finds itself in; this elimination accounts for 3.6GW since 2014. Yet it should be noted that Hanergy's plans to build 600MW of CIGS capacity, using technology from its acquisitions of Solibro and MiaSolé, recently met our meaningful capacity addition test, as some equipment suppliers, one in particular, publicly confirmed advanced payment.

Several potential gigawatts of capacity expansions announced in the first half of 2015 include joint ventures with major PV manufacturers, notably in the form of plans to establish production in India. Many of these could indeed progress to meet meaningful capacity criteria metrics in the next 12 to 18 months, with the potential for some to happen sooner than that. July, however, still

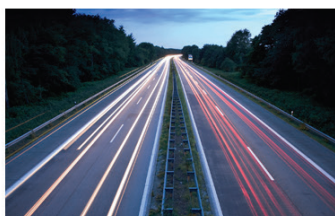
stands out as the weakest month in 2015 for meeting meaningful capacity criteria metrics, despite its top-line 3.68GW figure. When that aspect is taken into account, the month of July in 2014 had less than 800MW of announcements (with around 200MW since then) converted to actual production.

“A new meaningful capacity expansion phase is clearly under way and gaining momentum.”

Conclusion

Despite the highlighted disconnects, a new meaningful capacity expansion phase is clearly under way and gaining momentum. Capacity announcements have increased in 'intensity', as seen by the announcements made in November, representing larger nameplate figures than those announced in 2014.

In the first 11 months of 2015, a total of over 41GW of capacity expansions was announced (Table1, on next page), compared with a total of just over 21GW for the full-year 2014.



SECURE SUPPLY CHAIN COST CUTTING BY GLOBAL 24/7 PRODUCT VISIBILITY

Do you know what happens with your modules when they leave the factory? Where and when do micro cracks occur while your cargo is in transit? Who is accountable? Are you affected by irregular decrease of module efficiency over 25 years due to careless handling? If these questions crossed your mind before, we have a solution that can save you money. Get in touch with us and find out more.

www.hellmann.net/secureSupplyChain



hellmann
Worldwide Logistics

Company	Announcement date	Manufacturing location	New nameplate capacity	Production product type
Jetion Solar	Jan-15	Thailand	200MW	Integrated c-Si cell/module
Renovasol	Jan-15	Brazil	70MW	Multi c-Si module assembly
Hanwha Q CELLS	Jan-15	Cyberjaya, Malaysia	230MW	(Relocated) PERC multi c-Si solar cell
Hanwha Q CELLS	Jan-15	Cyberjaya, Malaysia	130MW	(Relocated) multi c-Si module assembly
PT Len	Jan-15	Indonesia	60MW	Integrated c-Si cell/module
E-Ton Solar Tech	Jan-15	Tainan, Taiwan	60MW	PERC cell upgrade
Surana Solar	Jan-15	Fab City, Hyderabad, India	110MW	Multi c-Si solar cell
SolarPark Korea	Feb-15	South Korea	600MW	Integrated c-Si cell/module
LG Electronics	Feb-15	South Korea	200MW	n-type bi-facial mono c-Si cells and modules
Zhongli Talesun	Feb-15	Rayong, Thailand	500MW	Integrated PERC c-Si cell/module
Silevo/SolarCity	Feb-15	California, USA	32MW	(Relocated) Pilot and R&D line
Waaree Energies	Feb-15	Surat, Gujarat, India	750MW	Multi c-Si module assembly
Empresa de Componentes Electrónicos	Feb-15	Cuba	15MW	Multi c-Si module assembly
Tainergy Tech	Feb-15	Taiwan	300MW	Multi c-Si solar cell
Hanergy Thin Film/ Shangdong Macrolink New Resources Technology	Feb-15	China	600MW	a-Si thin-film BIPV plant
SolarWorld	Mar-15	Arnstadt, Germany	500MW	Mono c-Si ingot production
SolarWorld	Mar-15	Arnstadt, Germany	700MW	Upgrade PERC cell production
Vietnam Government	Mar-15	Hanoi, Vietnam	20MW	Multi/mono c-Si module assembly
Ener Brazil	Mar-15	Brazil	50MW	Semi-automated c-Si PV module assembly plant
Woongjin Energy Co	Mar-15	South Korea	1GW	n-type and p-type ingot/wafer plant
SAS/ Sunrise Global	Mar-15	Taiwan	350MW	PERC, p-type mono cell expansion
JA Solar	Mar-15	Penang, Malaysia	400MW–1GW	Integrated c-Si cell/module
JinkoSolar	Mar-15	Malaysia	500MW	Multi c-Si PERC solar cell
JinkoSolar	Mar-15	Malaysia	450MW	Multi c-Si module assembly
Hanergy Thin Film/ Inner Mongolia Manshi Investment Group	Mar-15	China	600MW	a-Si thin-film BIPV plant
Hanergy Thin Film/ Baota Petrochemical Group	Mar-15	China	600MW	a-Si thin-film BIPV plant
Flextronics	Apr-15	Ciudad Juarez, Mexico	200MW	Multi/mono c-Si module assembly
Eclipse Brasil	Apr-15	Limoeiro do Norte, Ceará, Brazil	100MW	Multi c-Si module assembly
Orange Solar Power	Apr-15	The Netherlands	70MW	15MW 'monoflex' and 55MW multi c-Si module assembly
Hanergy Thin Film	Apr-15	Wuhan, China	10MW	Thin-film GaAs R&D/pilot line
Onyx Solar	Apr-15	Spain	1MW	c-Si BIPV
Sunrise Global Solar	Apr-15	Taiwan	350MW	Multi c-Si PERC solar cell
Hanergy Thin Film/ Hanergy Group	May-15	China	900MW	a-Si thin-film BIPV plant
Trina Solar	May-15	Rayong, Thailand	700MW	Multi c-Si solar cell (PERC)
Trina Solar	May-15	Rayong, Thailand	500MW	Multi c-Si module assembly
Gintech Energy	May-15	Thailand	350MW	Multi c-Si solar cell (incl. PERC)
Seraphim Solar System	May-15	Jackson, Mississippi, USA	300MW	Multi c-Si module assembly
Intéling soluções inteligentes	May-15	Bento Gonçalves, Brazil	Unknown	Multi c-Si module assembly

Panasonic Corp	May-15	Shimane, Japan	150MW	HJ mono c-Si cell
Panasonic Corp	May-15	Shiga, Japan	150MW	HJ mono c-Si module assembly
JA Solar/Essel Group JV	May-15	India	500MW	c-Si cell plant
JA Solar/Essel Group JV	May-15	India	500MW	c-Si module assembly
Trina Solar/Welspun JV	May-15	India	500MW	Integrated c-Si cell/module
Vikram Solar	May-15	India	250MW	c-Si mono/multi assembly
Vikram Solar	May-15	India	250MW	c-Si mono/multi assembly
BYD Company	May-15	São Paulo, Brazil	400MW	Multi c-Si module assembly
Hanwha Q CELLS	May-15	South Korea	250MW	Multi c-Si module assembly
Hanwha Q CELLS	May-15	Jincheon, South Korea	1.5GW	Multi c-Si PERC solar cell
Flisom	Jun-15	Niederhasli-Zurich, Switzerland	15MW	Flex-CIGS thin film
Central Electronics Limited	Jun-15	Sahibabad, Ghaziabad, India	40MW	Multi c-Si automated module assembly line
Sunprism Energy	Jun-15	Cairo, Egypt	50MW	Multi c-Si module assembly
CNPV Power	Jun-15	Saemangeum, South Korea	500MW(E)	Integrated c-Si cell/module
Trina Solar	Jun-15	India	2GW	Integrated PERC c-Si cell/module
Hulk Energy Technology	Jun-15	Taiwan	150MW	CIGS thin film
Central Electronics Limited	Jun-15	India	40MW	Multi c-Si module assembly
ARECO/Z-One	Jul-15	Alexandria, Egypt	52–100MW	Multi c-Si module assembly
Lerri Photovoltaic Science & Technology Co/Xi'an LONGi Silicon Materials	Jul-15	Taizhou City, Jiangsu, China	2GW	Mono-c-Si PERC PV cell plant
Xi'an LONGi Silicon Materials	Jul-15	Yinchuan City, China	3GW	Mono c-Si ingot/wafer production
Xi'an LONGi Silicon Materials	Jul-15	Yinchuan City, China	500MW	Mono c-Si module assembly plant
REC Solar	Jul-15	South East Asia (TBC)	400MW	Integrated PERC cell/multi c-Si module assembly
EcoSolifer AG	Jul-15	Brazil (TBC)	80MW	Mono-Si (HJ) module assembly
EcoSolifer AG	Jul-15	Csorna, Hungary	90–100MW	Mono-Si (HJ) cell plant
Hareon SolarTechnology/ Dalmia Group JV	Jul-15	India (TBC)	160MW–1GW	Integrated PERC cell/multi c-Si module assembly
Shunfeng/Suniva Inc.	Aug-15	Michigan, USA	200MW	n-type mono-c-Si Cell
Shunfeng/Suniva Inc.	Aug-15	Michigan, USA	200MW	n-type mono module assembly
Silfab Solar	Aug-15	Ontario, Canada	120MW	n-type BiSoN module assembly
Amerisolar	Aug-15	USA/ TBC	300MW	c-Si PV module plant
Globo Brasil	Aug-15	São Paulo, Brazil	180MW	c-Si PV module plant
Seraphim Solar System	Sep-15	Jackson, Mississippi, USA	700MW	Multi c-Si module assembly expansion
aleo solar/SAS/aleo Sunrise GmbH	Sep-15	Prenzlau, Germany	200MW	Multi/mono c-Si solar cell production
Xi'an LONGi Silicon Materials	Sep-15	Sri City, Chittoor region, Andhra Pradesh, India	500MW	Integrated mono cell/module plant
GCL Integrated Technology Co/Adani Group	Sep-15	Mundra, India	TBC	c-Si integrated ingot/wafer/cell/module
HHV Solar Technologies	Sep-15	Bengaluru, India	60MW	c-Si/mono module expansion
1366 Technologies	Oct-15	Genesee County, New York, USA	250MW–3GW	Multi c-Si 'direct wafer' production
Elkem Solar	Oct-15	Herøya, Norway	650MW	Multi c-Si ingot production restart
Heckert Solar	Oct-15	Chemnitz, Germany	60MW	Multi c-Si module assembly expansion
AVANCIS/CNBM	Oct-15	Bengbu, Anhui Province, China	300MW–1.5GW	CIGS thin film

Sonali Solar	Oct-15	Gujarat, India	250MW	Multi c-Si module assembly expansion
China Sunergy (CSUN)	Oct-15	Incheon, South Korea	200–500MW	Multi c-Si solar cell production
Hyundai Heavy Industries (HHI)	Oct-15	Eumseong, South Korea	200MW	Mono c-Si PERL solar cell upgrade
Kaneka Corporation	Oct-15	Japan	Pilot line	n-type mono HJ solar cell line
Canadian Solar	Nov-15	Luoyang plant, Henan Province, China	600MW	Ingot/wafer expansion
Canadian Solar	Nov-15	Suzhou plant, Jiangsu Province, China	500MW	Multi-c-Si solar cell expansion
Canadian Solar	Nov-15	Funning plant, Jiangsu Province, China	600MW	Multi-c-Si solar cell expansion
Canadian Solar	Nov-15	South East Asia (TBC)	400MW	Multi-c-Si solar cell plant
Canadian Solar	Nov-15	Changshu, Jiangsu Province, China	200MW	c-Si module assembly
Canadian Solar	Nov-15	Luoyang, Henan Province, China	600MW	c-Si module assembly
Canadian Solar	Nov-15	Canada	500MW	c-Si module assembly
Canadian Solar	Nov-15	Brazil (TBC)	300MW	c-Si module assembly
Canadian Solar	Nov-15	Vietnam (TBC)	300MW	c-Si module assembly
Canadian Solar	Nov-15	Indonesia	30MW	c-Si module assembly
SunPower	Nov-15	South East Asia (TBC)	800MW	n-type mono IBC Cell production plant
SunPower	Nov-15	Multiple locations (TBC)	2GW	Multi/mono c-Si module assembly (P Series)
Motech/ Solargiga JV Jiansu Aide Solar Energy Technology	Nov-15	China	400–600MW	c-Si module assembly expansion
Sunew/CSEM Brasil	Nov-15	Belo Horizonte, Brazil	TBC	OPV thin-film module plant
JA Solar	Nov-15	China	500MW	Multi c-Si ingot/wafer expansion
JA Solar	Nov-15	China, Malaysia TBC	1.4GW	Multi c-Si cell expansion
JA Solar	Nov-15	China	1.4GW	Multi c-Si module assembly
Tongwei Group	Nov-15	Hefei, China	1–5GW	Multi c-Si cell plant (3–5 year plan)
JinkoSolar	Nov-15	China	300MW	Multi c-Si ingot/wafer upgraded
JinkoSolar	Nov-15	China/Malaysia TBC	500MW	Multi c-Si solar cell expansion
JinkoSolar	Nov-15	China/Malaysia TBC	1GW	Multi c-Si module assembly expansion
Hanwha Q CELLS	Nov-15	China/Malaysia/Korea TBC	1GW	Multi c-Si module assembly expansion
Trina Solar	Nov-15	China	100MW	Multi c-Si ingot production upgrade
Trina Solar	Nov-15	China	100MW	Multi c-Si wafer production upgrade
Trina Solar	Nov-15	TBC	1.3GW	Multi c-Si solar cell expansion
Trina Solar	Nov-15	TBC	1.3GW	Multi c-Si module assembly expansion
Lanco Infratech	Nov-15	Rajnandgaon, Chhattisgarh, India	100MW–2.2GW	Multi c-Si solar cell plant
Lanco Infratech	Nov-15	Rajnandgaon, Chhattisgarh, India	250MW	Multi c-Si module assembly plant
Jiangsu Aide Solar Energy Technology	Nov-15	China	500MW	Multi c-Si module assembly expansion
HHV Solar Technologies	Nov-15	India	900MW	c-Si/mono module expansion over 5 years
ZNshine Solar/Chongqing Silian Optoelectronic Technology JV	Nov-15	China	500MW	Mono/multi c-Si module assembly plant
Neo Solar Power (NSP)	Nov-15	South East Asia TBC	TBC	Relocating c-Si solar cell production
Inventec Solar Energy	Nov-15	Taiwan	400MW	Multi c-Si solar cell expansion

Table 1. PV manufacturing capacity expansion announcements in 2015.

From service provider to partner: Optimal logistics opportunities in PV manufacturing

Holger Meyer, Solar United & Hellmann Renewable Logistics

ABSTRACT

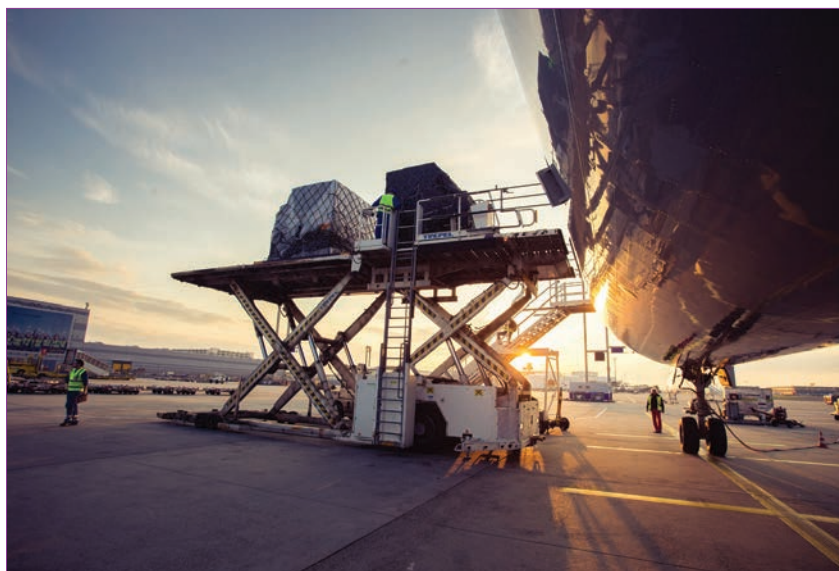
With global business an increasing reality for PV, the role of logistics is transforming from service provider to true partner. This article makes the case for integrated partnerships to move plant, products and business in the right direction, at the right time.

The availing of logistics opportunities means appreciating service providers as more than a replaceable link in the value-added chain, and recognizing them as partners in implementing company objectives. But how can advantages for the PV industry be generated via a logistics service provider, above and beyond pure transportation lines? In order to answer this question, it is helpful to look at the classic perception of the logistician and how this has developed in recent years.

For a long time, logisticians were seen purely as transporters. However the increasing globalization among client companies has spurred logistics firms to internationalize operations. At the same time, the hunger for transparency and information on the market and among market participants requires systems that greatly exceed classic transport services. Only those who recognized this trend early, considered their client requirements accordingly and created a global presence, mastered the transformation from traditional transporter to provider of intelligent logistics systems.

Logistics and the PV value chain

To illustrate this, let's take a look at the PV value-added chain. The first stage is choosing a location for suitable production plants, where cost is most often the decisive factor. However, purchasing parts from Asia or opening production plants beyond domestic borders necessitates increased coordination and steering. Here is where the support of a logistics company as a partner is an advantage. Network-planning tools for optimum planning in the logistics network with respect to the transition points, warehouse locations and transport routes can be made available to the client early on as



Logistics is an increasingly integral part of the PV value chain.

valuable decision-making supports. The customer's procurement and revenue information are processed within such planning tools. The resulting simulation of various goods-flow scenarios enables the creation of efficient solutions with respect to minimizing transport costs and lead-times, thus reducing cash flow within the entire delivery chain.

Should the customer decide to implement one of these scenarios, it is recommended to entrust the implementation to a dedicated logistics service provider as the 'architect of the value-added chain'. In so doing, many interfaces are reduced and unnecessary internal and external coordination and communication are minimized. To achieve this, it is imperative to choose a logistics partner with an international presence and its own branch network. Coupled with excellent information technology, the synergies within the value added chain might be exploited effectively.

Furthermore, comparatively large logistics service providers offer many

additional consulting services for customers' international development. Close cooperation with prestigious partners in the areas of tax and product testing is only one example of a most useful service, as new logistics scenarios usually directly affect these areas. One such example is the construction of production plants overseas. Close cooperation between logisticians and tax consultants can provide you with a solid evaluation from one source as to whether the tax relief in situ is of value when considering country-specific restrictions such as export regulations or logistics wage costs. Furthermore, logistics partners, with many years of local experience and contacts, often offer support in setting up companies abroad, whether in finding offices or first contacts to gather market data or making initial contact with the local industry.

Parallel to the increase in consulting requirements, the area of product testing at the supplier's production location has also shifted into greater

Credit: Hellmann

Fab &
Facilities

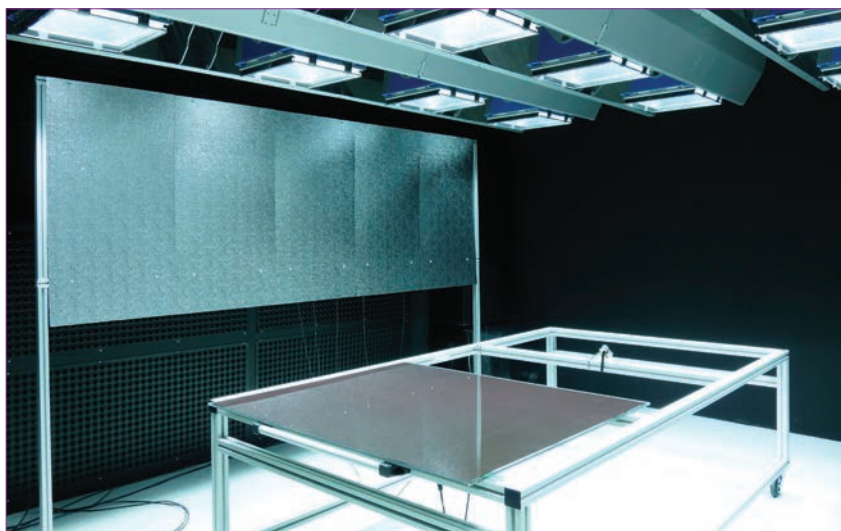
Materials

Cell
Processing

Thin
Film

PV
Modules

Market
Watch



Module testing is just one additional service a logistics provider can offer.

focus with the growth of globalization. Unnecessary transport costs can largely be avoided, if tests have already been carried out in the country of origin. Whole deliveries may be stopped prior to transportation, where discrepancies occur. The logistics service provider at the procurement location can offer so-called HUB inspections as a value-added service. Thus, modules may be flashed in the dispatch warehouse and wafers and ingots may be tested prior to transportation. Depending on the scope of the required tests, visual checks and simple functionality tests may be carried out by the service provider. Independent international test agencies, partners of the logistics provider, are available to carry out special technical tests. A medium-term homogenization of standards, according to the automobile industry's VDA regulations, in the photovoltaic sector, along the value-added chain, would accommodate the manufacturers and service providers.

The automobile industry and logistics sector have been cooperating successfully for a number of years in product testing by means of specifically defined process standards. The logistic partner's taking over production logistics directly "at the conveyor belt" has also been proven to make perfect sense and be very profitable for both sides. Transferring this success to the PV sector is surely a promising opportunity, which should be seriously considered.

Packaging and storage

Considering the importance of packaging in the transport chain in regards of quality and cost efficiency, dedicated packaging solutions are more and more required by the module manufacturers. This requires the

logistics provider to find simple and smart ways to increase the number of modules stored in the containers, trucks or warehouses. In addition, transport damage has to be prevented and the packaging has to be reusable and environmentally friendly. For this purpose, some logistics providers have already started to develop high-quality solutions.

Looking closely at the physical flow of goods in the value-added chain, there is great potential for cost reduction in procurement logistics. The automobile and electronic industries offer models for success here. Cost-efficient bundling and steering of procurement flows from Asia are incumbent upon the logistics provider. The customer merely gives instructions as to when certain parts are to arrive at the production point. It is then the task of intelligent logistics planning to bundle the various parts or groups of parts in such a manner as to reduce transport costs and deliver to deadline. In this model, the logistician is a dedicated partner responsible for the customer's procurement transportation, who communicates with the suppliers in situ regarding all logistics and quality issues.

This solution is supported by respective IT systems. Thus, supply-chain tools, connected to the customer's inventory management system via respective interfaces, enable access to purchase order data. Furthermore, suppliers and other partners may access the logistics provider's supply chain tool in order to inform the customer's employees of the production status, deadline alterations or quality issues in a timely fashion.

The use of such supply chain tools has the additional advantage that batch numbers may be tracked seamlessly. Thus product recall campaigns in the after sales area can be traced back as

far as the supplier. It also enables the logistics partner to carry out product testing at the customer's behest, exchanging any damaged parts with a central warehouse according to processes previously agreed upon with the PV customer.

The high-tech industry recognized this as an interesting growth sector years ago and began developing intelligent exchange and maintenance systems with the support of logistics partners. Such processes save costs and time, in turn contributing to the continued success of the sector.

A further important factor in trusting cooperation with a logistics partners is cargo visibility. Some of them already provide a full real-time visibility along the transport chain. Accessible via a web-based portals, these systems continuously transmit data pertaining to the transport route or changes to the container, such as shocks or unauthorized opening. Thus, damage or transport delays may immediately be checked and the customer informed. Also insurance fees can be reduced by using this kind of service.

Logistics service providers offer a variety of cooperation possibilities above and beyond transport. Apart from the examples mentioned, common interests in e-commerce are also conceivable. The logistics service provider is also readily available with these types of solutions, as today, it is essentially also an IT specialist committed to creating global transparency.

Like any real partnership, this one is based on mutual trust. In order to prepare the groundwork for and guarantee sustainable, solid growth in the PV industry for the future, it is worth rethinking the existing value-added chain with a logistician. This is true for companies that act globally and for those just starting out on that path.

About the author



Holger Meyer has been a member of the advisory board of SOLARUNITED since 2013 (formerly known as International Photovoltaic Equipment Association, IPVEA). As chairman of the body's supply chain strategy committee since 2014, he launched a new campaign, the Solar Supply Chain Forum. The task of this forum is to increase the knowhow within the solar industry along the entire supply chain to create a more cost-efficient as well as process-oriented global set-up to deliver solar projects. He is also global director of Hellmann Renewable Logistics.

Materials



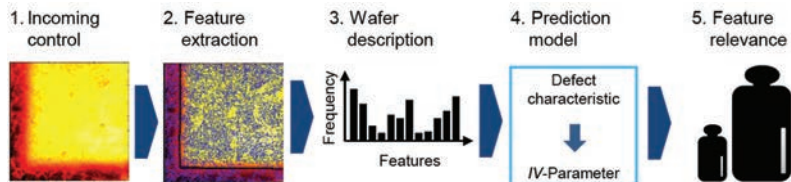
26

Page 26
News

Page 28
Inline quality rating of
multicrystalline wafers –
Relevance, approach and
performance of Al-BSF and
PERC processes

Matthias Demant¹, Theresa Strauch¹,
Kirsten Sunder², Oliver Anspach²,
Jonas Haunschild¹ & Stefan Rein¹

¹Fraunhofer Institute for Solar Energy
Systems ISE, Freiburg; ²PV Crystalox
Solar Silicon GmbH, Erfurt, Germany



28

Mono and multi c-Si wafer prices converging – EnergyTrend

Tight supply and strong demand for multicrystalline wafers, and overcapacity and weak demand for monocrystalline market, are leading to closer price convergence of the two wafer types, according to Taiwan-based market research firm, EnergyTrend.

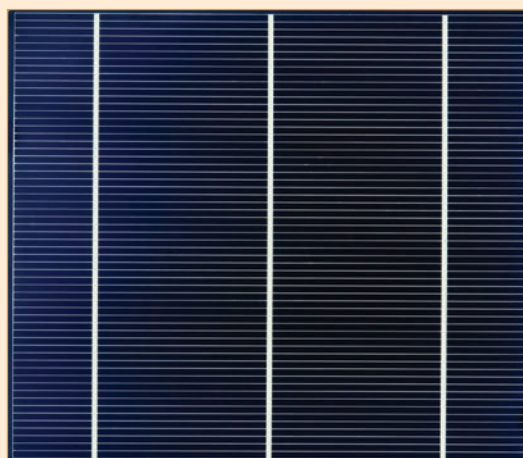
EnergyTrend estimated global mono wafer capacity stood at around 15GW but demand in 2015 would not reach 10GW, causing prices to fall from US\$1.04/pc at the start of this year to the current price of US\$0.92~0.93/pc.

In comparison, multi wafer prices had reached RMB 6.15/pc in China and are moving towards US\$0.84/pc in Taiwan. However, prices in China for some mainstream mono cell products are now at around RMB 2.35/W, matching the prices of multi-Si cells for the first time.

But the market research firm said it expected mono wafer capacity to increase by around 20% in 2016, due to increased demand.

Greater acceptance of mono-Si products in the PV power plant market would be a key driver of this.

Another driver is that PV cell manufacturers have found that passivated emitter rear cell (PERC) technology, a cell production process that is being increasingly widely used, produces better efficiency results on mono-Si cells than multi. PERC solutions from different companies are expected to drive the mono-Si market next year when they have become more mature.



Credit: GT Advanced Technologies

Pricing for mono and multi c-Si wafers are converging, EnergyTrend has said.

Wafers

Comtec's mono c-Si wafer sales and revenue up in Q3

Monocrystalline wafer producer Comtec Solar Systems Group reported third-quarter preliminary results showing higher wafer shipments and increased revenue, but gross margins continue to decline.

Comtec reported third-quarter 2015 revenue of RMB314,740,000 (US\$49.2 million), up slightly from US\$44.2 million in the previous quarter.

The unaudited consolidated gross profit was approximately RMB8,815,000 (US\$1.37 million), flat with results posted in the prior two quarters of 2015.

However, gross margin continued to decline over the last two years. Comtec reported a third quarter 2015 gross margin of 2.8%, compared to 7.4% in the prior year period. Gross margin in the first six months of 2015 had declined to 3.2%.

Comtec also sold excess inventory of raw materials (mainly polysilicon) during the quarter totalling RMB107.8 million (US\$16.8 million).

Sealants/adhesives

H.B. Fuller leveraging acquired TONSAN on new sealants and adhesives for PV manufacturers

US-listed Industrial adhesives supplier

H.B. Fuller is working to develop new technologies for PV manufacturers, after the acquisition of China-based adhesives specialist, TONSAN Adhesive earlier in the year.

H.B. Fuller was exploring a number of advanced technologies to address PV manufacturers' product issues that would employ its materials such as new liquid sealants, tapes and adhesives dispensing equipment.

TONSAN's popular silicone frame sealant, 1527, and junction box potting material, 1521, would still be available to customers.

"Through this acquisition, we're able to provide a powerful combination of global resources and advanced adhesive technologies that puts innovation on a fast track to give manufacturers the edge they need to maintain a competitive advantage," said Patrick Trippel, senior vice president of market development at H.B. Fuller.

STR Holdings secures module encapsulant deals with Trina Solar & Talesun

PV encapsulant producer STR Holdings reported another quarter of disappointing financial results, although the corner may have been turned after it secured major supply deals with Trina Solar and Talesun.

STR reported third quarter sales of US\$6.6 million, down 23% from the previous quarter and 31% down from the prior year period. Encapsulant volumes declined 20% quarter-on-quarter and ASPs fell 4%. The majority of revenue was

received from majority owner, China-based PV project developer Zhenfa via US\$3.2 million of cash from Zhenfa as an installment payment and the highly unusual solar modules-for-encapsulant swap deal with former customer ReneSola.

The company noted that after successful material qualification by Trina Solar and Talesun it had started shipments in China and was currently in the process of adding approximately 2GW of material capacity to meet demand.

Business

Dow and DuPont to merge

Industrial materials manufacturers Dow and DuPont are to merge creating a new company with a market capitalisation of US\$130 billion.

The new company DowDuPont will trade as three separate entities, one focused on agriculture, one on materials science and the third based around products for sectors including the Dow Electronic Materials business and DuPont's electronics business.

The combination of both firms' PV offerings could lead to redundancies. Savings of US\$3 billion are expected from the merger.

Andrew N. Liveris, president, CEO and chairman of Dow will become executive chairman of the new firm.

New DuPont CEO Edward D. Breen, will be CEO of the new venture.



Credit: Dow

Materials giants Dow and DuPont are to merge, to form DowDuPont.

Court ruling leaves hole in SolarWorld's defence in US\$700 million Hemlock lawsuit

The main line of defence in SolarWorld's US\$700 million lawsuit with Hemlock Semiconductor has crumbled after a court in the US ruled it invalid.

The company was quick to stress that the anti-trust defence was just one defence of several with "equal value" and downplayed the impact of latest development in the three-year old case.

SolarWorld was looking to claim that the polysilicon supply contracts at the heart of the dispute with Hemlock breached anti-trust rules and so were invalid. In its annual report the anti-trust defence was specifically cited by SolarWorld as the reason the case's risk was assigned low probability, despite the potentially huge damages it faces paying if it loses.

The anti-trust defence is now null and void but SolarWorld claims this does not impact the likelihood of it being forced to pay damages.

In February 2014, SolarWorld paid a "double digit" million euro charge related to a separate polysilicon contract.

SolarWorld's annual report states that if it were forced to pay damages it would have "considerable negative impact" on

the company's liquidity "possibly even threatening the company's continued existence".

The company's Q2 financial statement lists cash and cash equivalents of just over €141 million.

The case continues.

Polysilicon

REC Silicon continues job and production cuts

Polysilicon producer REC Silicon has been forced to make further cuts to production output and shed more jobs as it reacts to the current US/China trade tariff war and subsequent lower polysilicon sales to China.

A total of 45 jobs would be lost, bringing its head count down from 720 to 675.

REC Silicon would also defer maintenance outages and limit capital expenditures to critical maintenance of facilities only to reduce operating costs and further lower production to cut inventory and overall costs.

REC Silicon reported third quarter 2015 revenue of US\$87.5 million, down from US\$93 million in the previous quarter and a negative EBITDA of US\$14.1 million, compared to a EBITDA of US\$5.8 million in the previous quarter.

Wacker's polysilicon sales up 4% in Q3

Major polysilicon producer Wacker had a slight increase in polysilicon revenue for the third quarter of 2015 as production capacity remains fully utilised.

Wacker's Polysilicon segment reported third quarter sales of €271.4 million, a 4% increase from sales of €261.3 million in the prior quarter. Higher volume shipments from the prior year period

were said to have offset declining market prices of polysilicon.

ASP declines were not reported but Wacker noted overcapacity remained an issue.

Third-quarter EBITDA totalled €91.8 million, compared to €180.3 million in the prior year period, a 49% decline. EBITDA margin was 33.8%, compared to 71.4% in the prior year period, due to the reduction in lower special income from advance payments retained and damages received from PV customers.

GCL-Poly raises US\$110 million from new bond, struggles to keep up with polysilicon and wafer demand

The largest polysilicon producer GCL-Poly Energy Holdings has secured approximately US\$110 million from a new corporate bond from qualified investors in China.

GCL-Poly's polysilicon subsidiary Jiangsu Zhongneng issued the first tranche of the bond and will use the net proceeds for general working capital needs. The first tranche bond maturity is set for October 23, 2018.

GCL-Poly's polysilicon and wafer operations were also at full capacity in the Q3 2015. Polysilicon production in the third quarter reached 19,003MT, up 10.2% from the third quarter of 2014.

GCL-Poly said that wafer production was 10,928MW, 14.0% higher than the first nine months of 2014, while third quarter production topped 3,826MW, up only 3.9% on capacity constraints of adding 1GW of extra production in 2014 to bring total capacity to 14GW.

Paste

Heraeus Photovoltaics to start silver paste production in Taiwan

PV metallization paste producer Heraeus Photovoltaics has begun manufacturing front-side metallization paste in Taipei, Taiwan.

The company is adding front-side metallization paste production in Taiwan to support existing back-side paste production, which started in 2012.

Andreas Liebheit, president of Heraeus Photovoltaics said: "In order for us to offer customisation and shorten lead times for customers, it is vital to have a strong operational presence where our customers are, and Taiwan has grown to become an important market for us."

Taiwan is home to the largest merchant solar cell producers such as Motech, Gintech and NSP.



Credit: SolarWorld

A key element of SolarWorld's defence in a US\$700m lawsuit has been declared invalid by a judge.

Inline quality rating of multicrystalline wafers – Relevance, approach and performance of Al-BSF and PERC processes

Matthias Demant¹, Theresa Strauch¹, Kirsten Sunder², Oliver Anspach², Jonas Haunschild¹ & Stefan Rein¹

¹Fraunhofer Institute for Solar Energy Systems ISE, Freiburg; ²PV Crystalox Solar Silicon GmbH, Erfurt, Germany

ABSTRACT

With the transition of the cell structure from aluminium back-surface field (Al-BSF) to passivated emitter and rear cell (PERC), the efficiency of multicrystalline silicon (mc-Si) solar cells becomes more and more sensitive to variations in electrical material quality. Moreover, the variety of multicrystalline materials has increased with the introduction of high-performance multicrystalline (HPM) silicon. For these reasons, a reliable and verifiable assessment of the electrical material quality of multicrystalline wafers gains importance: to this end, a rating procedure based on photoluminescence (PL) imaging has been developed. The material quality is characterized by the distribution of crystallization-related defects, which are successfully correlated with the solar cell quality of PERC and Al-BSF solar cells. The applied image-processing and machine-learning techniques are outstandingly good because of their robustness, transparency and precision. This is demonstrated by an evaluation of the approach using a large database of wafers and cells from 72 bricks from nine different wafer manufacturers, which represent a broad spectrum of currently available materials. The quality prediction leads to mean absolute prediction errors of 2.2mV and 2.9mV for Al-BSF and PERC solar cells respectively, in a true blind test. The proposed wafer rating is of benefit to both wafer and cell manufacturers, and can be established during the pre-delivery inspection in wafer production, and the incoming inspection in solar cell production. While wafer manufacturers can improve material quality as a result of an immediate quality feedback after wafering, cell manufacturers can improve production yield because of an appropriate wafer selection.

Relevance and possibilities for a quality rating

The electrical quality of the wafer material has considerable impact on the achievable cell efficiency. Especially for passivated emitter and rear cells (PERC), solar cell efficiency is less limited by the surface recombination on the rear side, compared with solar cells with an aluminium back-surface field (Al-BSF); thus other factors gain importance. The quality of PERC solar cells is more sensitive to bulk recombination and hence to variations in the material quality. Since PERC cells are progressively replacing Al-BSF solar cells in mass production, an improved material quality and a reliable material selection are essential.

Recent developments of feedstock and the crystallization process have led to an improved class of material, the so-called 'high-performance' multicrystalline (HPM) Si [1]. Despite large differences in the price and quality of wafer materials, no specification in terms of the electrical material quality has yet been verified and established. The focus of this work is a reproducible quality description

of standard and HPM wafers based on photoluminescence (PL) imaging techniques [2].

“The establishment of a defect description requires a meaningful quantification of crystal defects and an evaluation of the rating capability for a broad set of materials.”

Feedstock and the crystallization process determine the types and distributions of defects. The quality of the feedstock can be quantified by the impurity grade of the granules. A more challenging task, however, is the characterization of material defects which form during the crystallization process and reduce charge-carrier lifetime. On the one hand, impurities from the coated crystallization crucible diffuse into the crystallized ingot; this leads to edge regions with increased metal contamination (e.g. Schubert et

al. [3] and Schindler et al. [4]). On the other hand, structural defects, such as grain boundaries and dislocations, form during the growth process. The novel concept of HPM reduces the generation and multiplication of dislocations. The different types of defect distribution have to be considered in a wafer rating.

PL imaging [2] already allows these structural defects and contaminated regions to be measured inline at the as-cut stage [5]. This technique's applicability is evaluated in the ISE approach for a wide range of wafer and solar cell data from different manufacturers and crystallization processes. Physically relevant defect features are quantified by means of image-processing techniques to form the basis of a wafer characterization. The presented detection and quantification of crystal defects allows a more detailed wafer description than currently available approaches in industry. The classification itself is based on machine-learning techniques. For this purpose, a regression model is trained in order to predict the expected solar cell quality.

The establishment of a defect

description requires a meaningful quantification of crystal defects and an evaluation of the rating capability for a broad set of materials, including material from unknown manufacturers, which was not part of the training data for the model. This level of distinction was first encountered by Demant et al. [6] and is presented in this paper.

Existing approaches for quality rating

Structural defects and impurities lead to an increased recombination of charge carriers at the defect location; these recombination-active defects become visible in PL images through a reduced luminescence signal. Alternative methods for lifetime measurement are, for example, the quasi-steady-state photoconductance (QSSPC) approach [7], which averages the carrier lifetime over larger areas, and the microwave-detected photoconductance approach (MDP) [8], which allows spatially resolved lifetime maps. The focus in this paper will be on PL imaging, since the method permits a quick investigation of defect structures, with the highest spatial resolution in the range of $160\mu\text{m}/\text{pixel}$. Commercial inline PL systems with megapixel resolution have been reported (e.g. Chunduri [9]).

On surface-passivated samples, the measured PL intensity directly reflects the electrical quality of the wafer bulk (e.g. Michl et al. [10]). Although the measured PL intensity of an as-cut wafer does not directly reflect the electrical quality of the wafer bulk, the geometrical structure of the structural defects present is already completely visible at the as-cut stage. PL measurements are therefore well suited to a 100% inline control at the as-cut stage. Four representative samples with different defect signatures, along with the corresponding solar cell efficiencies, are illustrated in Fig. 1.

The defect structures determined in PL images of as-cut wafers correlate with solar cell performance [5,11,12]. Features for assessing material quality have been included in multivariate rating models [13–15]. This paper describes a multivariate, feature-based prediction approach that was published in greater detail by Demant et al. [6]. The richness of the underlying data set surpasses all recent investigations in this field. The data set allows different levels of difficulty in classification to be distinguished; in particular, the prediction of unknown manufacturers is necessary for a sound rating model created on the basis of a

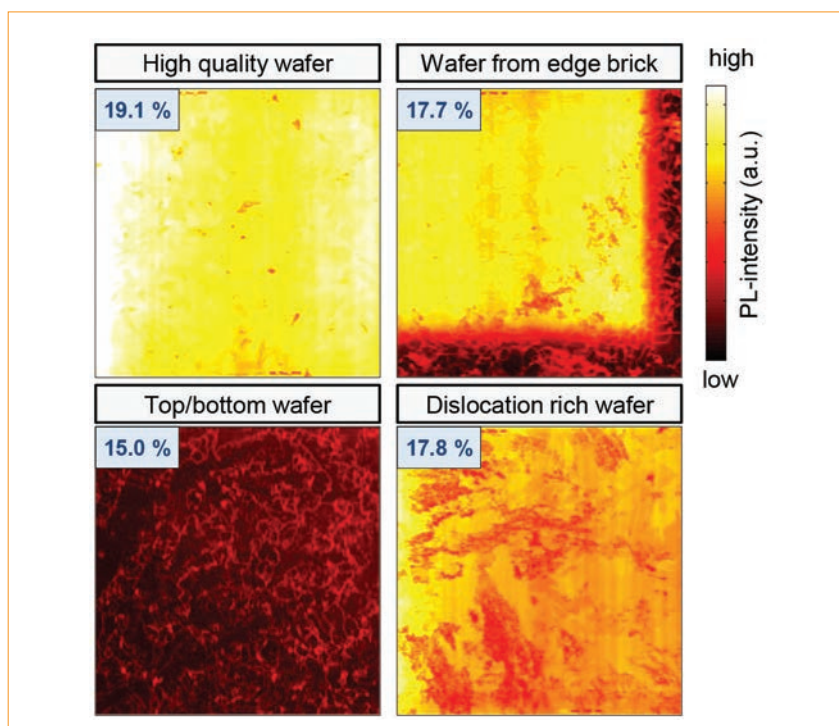


Figure 1. PL images of different bricks and brick positions, along with the conversion efficiencies of PERC cells manufactured from those wafers.

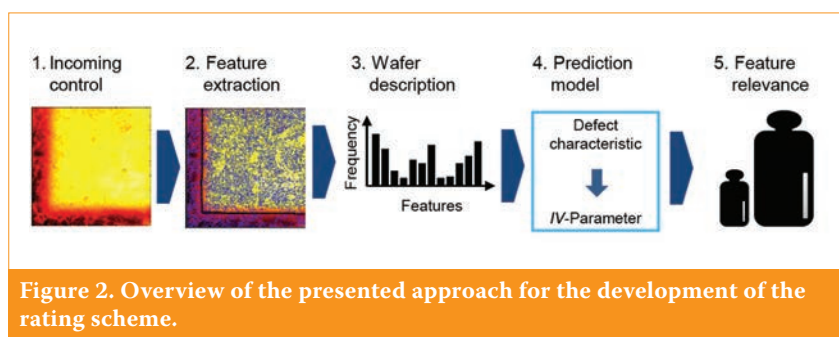


Figure 2. Overview of the presented approach for the development of the rating scheme.

powerful multivariate data analysis.

The impact of defect features on solar cell performance also shows a direct dependency on the solar cell process, for example via gettering during emitter diffusion [16]. Different types of structural defect have been distinguished in terms of their appearance and development during the cell process [17,18]. The local density of these structural defects may be connected to the development of different defect types [19]. In the approach presented in this paper, the issue is addressed by a quantification of the local defect density which is used to describe the wafer characteristics. Moreover, crystal defects inside and outside the contaminated regions are distinguished within the ISE approach, as a beneficial effect of crystal defects on the gettering behaviour in the contaminated regions has been shown by Bentzen & Holt [20]. The relevance of these features can be observed with the proposed classification model via a regularized form of multivariate regression.

Novel machine-learning-based approach for quality rating

Overview

The principal goal is to establish a prediction model to forecast the solar cell quality from PL images of as-cut wafers, and to identify the most relevant features for devising a rating of the material quality. The target parameter of the rating model is the open-circuit voltage V_{oc} , which strongly correlates with material quality and is quite robust with respect to process variations. The rating model is outlined in Fig. 2 and comprises the following steps:

- 1. Incoming control:** the wafer first passes an incoming control with inline PL imaging.
- 2. Feature extraction:** special image-processing techniques are applied in order to detect crystal defects, despite variations in contrast.

3. Wafer description: the defects are quantified within a defect characterization to describe the wafer.

4. Prediction model: the rating scheme is trained to predict the solar cell quality on the basis of the empirical data of the as-cut measurements and the corresponding cell performances. It is

essential to evaluate the quality of the model for unknown data.

5. Feature relevance: the prediction model enables the relevance of the features to be analysed; therefore, differences in the solar cell processes can be compared, and a deeper understanding can be gained by means of reference measurements.

Extraction of PL image features

Crystal defects and contaminated regions

The most important defect features are structural defects, such as dislocations and grain boundaries, which appear as dark, blurred line structures. Wafers with in-diffused impurities from the coated crystallization crucible exhibit large-area contaminated regions with reduced average PL intensities, which mostly appear on wafers from the top or bottom of the brick or on wafers taken from the edge or the corner bricks of an ingot.

As depicted in Fig. 3(a), the crystal defects appear as light structures within the contaminated regions; this reflects the gettering effect of the crystal defects in these regions. To allow a quantification of all structural defects, the structures of the PL images are extracted, as shown in Fig. 3(b). In a second step, all crystal defects are quantified according to the phase congruency model of edge detection [21], which leads to a contrast-invariant localization of crystal defects, shown in Fig. 3(c). The first defect feature, Feature 1, equals the area fraction of crystal defects (see Fig. 3(c)).

Since crystal defects are slightly blurred in the PL images, the defect structures are thinned. The second defect feature, Feature 2, quantifies the area fraction of

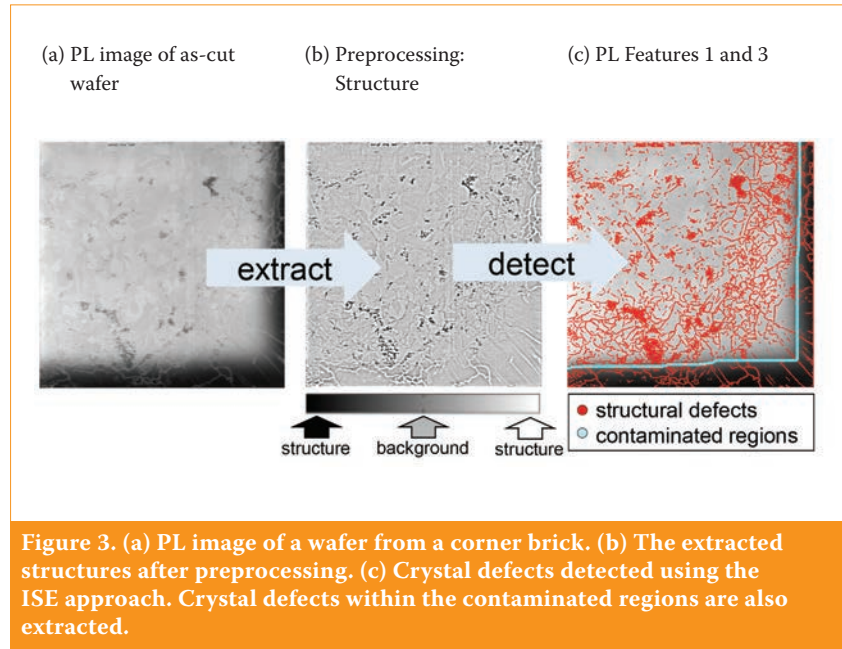


Figure 3. (a) PL image of a wafer from a corner brick. (b) The extracted structures after preprocessing. (c) Crystal defects detected using the ISE approach. Crystal defects within the contaminated regions are also extracted.

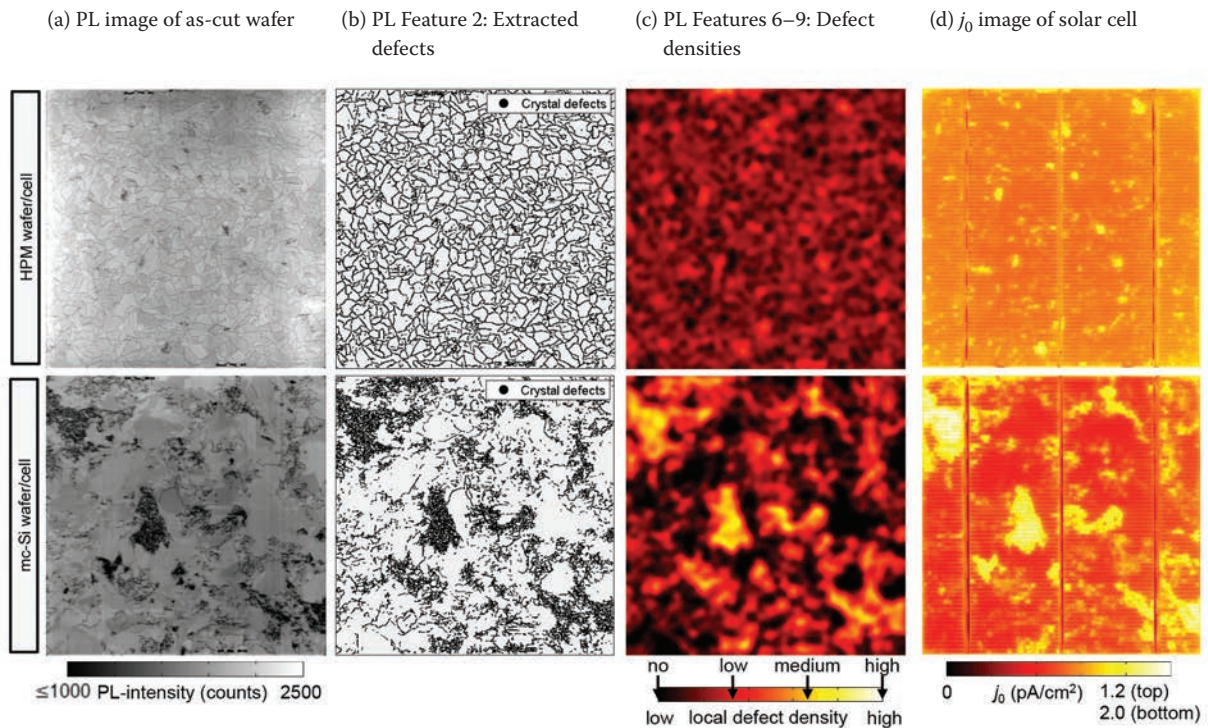


Figure 4. Appearance of crystal defects in a HPM Si wafer (top row) and a regular mc-Si wafer (bottom row). (a) PL images taken at the as-cut stage. (b) Extracted defects. (c) Corresponding local defect densities, revealing a difference between the materials – the HPM wafer (top) contains equally distributed defects, whereas the standard mc-Si wafer (bottom) contains dense dislocation clusters, as well as defect-free regions. These differences are quantified in the four parameters of the area fraction: no, low, medium and high local defect density. (d) The j_0 images of the solar cells are in good agreement with the features observed in the as-cut stage.

thinned crystal defects (see Fig. 4(b)). The area fraction of the contaminated region, Feature 3, is also added to the ISE wafer description (see Fig. 3(c)); this is computed using basic image-processing techniques. The information about the contaminated regions allows the quantification of crystal defects in regions with low lifetime due to the contaminant's in-diffusion from the crucible (Feature 4), and distinguishes them from crystal defects within non-contaminated wafer areas (Feature 5). The differentiation is beneficial because defect clusters may act as gettering sites within contaminated regions [20]. To the best of the authors' knowledge, these features are not detected in most industrial algorithms, which frequently consider only two or three features.

Distribution of crystal defects and intensities

The distribution of crystal defects throughout the wafer plane also influences the solar cell quality, as simulated by Isenberg et al. [22]. These material differences are quantified by computing local defect densities by a Gaussian averaging. Regions with no, low, medium and high (Features 6 to 9; see Fig. 4(c)) local defect densities are distinguished.

With HPM, crystallization dislocations are avoided because of a large quantity of small grains with random grain boundaries. Regions of low defect densities are therefore observed in HPM wafers, whereas a large number of dense crystal defects, mostly dislocations, can be observed in standard mc-Si wafers, as shown in Fig. 4. The correlation of defect regions of medium or high dislocation density with the corresponding image region of the dark-saturation current density (j_0 images) confirms the relevance of these features. In addition, structural defect densities in contaminated regions and non-contaminated regions are quantified separately and added to the set of features (Features 10 to 17).

Further features are the average PL intensity (Feature 18), the doping normalized PL intensity (Feature 19), and the area fractions of regions with increasing levels of average PL intensity (Features 20 to 24; see Fig. 5). Finally, whether the wafer originates from the top/bottom region of the brick and shows completely inverted PL contrasts (Feature 25) is analysed.

Regression models

A challenge in multivariate data analysis is avoiding models that over-fit the training data and lead to a poor prediction quality of unknown samples. On the other hand, models of very low complexity may

not be capable of describing complex relationships, which leads to a bias in the data. The optimum model can be identified within a model-selection step using a validation set of data. According to Occam's razor, a simple prediction model should be preferred to more complex models, provided it can explain the given relationship. Three models with different model complexities were therefore analysed.

“A challenge in multivariate data analysis is avoiding models that over-fit the training data and lead to a poor prediction quality of unknown samples.”

The first method is a support vector regression (SVR): this is a supervised machine-learning technique, which can predict non-linear relationships. A regression model is trained to rate an input feature vector $\vec{x} = (x_1, \dots, x_p)$

according to a quality parameter γ . The algorithm primarily learns the mapping from features to the output (open-circuit voltage) from training data. Vapnik's ε -SV regression model [23] is trained with a radial basis kernel. The meta-parameters ε and c are determined via a grid search on a validation subset of the data.

Second, a multilinear prediction model is used to predict the solar cell quality y_i on the basis of the set of features $x_{i,j}$ with $j \in \{0, \dots, p\}$ for sample $i \in \{0, \dots, n\}$. More precisely, the goal is to determine the coefficients β_k with $k \in \{0, \dots, p\}$ that minimize the prediction error for the training set with n elements according to

$$\hat{\beta} = \operatorname{argmin}_{\beta} \left\{ \frac{1}{2n} \sum_{i=1}^n (y_i - \beta_0 - \sum_{j=1}^p x_{i,j} \beta_j)^2 + \lambda P(\hat{\beta}) \right\} \quad (1)$$

At this stage, Occam's razor is followed by applying a regularized form of regression – the elastic-net algorithm [24]. The number of coefficients is penalized according to a penalty function $P(\hat{\beta})$ with a regularization term λ ; with a lower value of λ a more complex model is

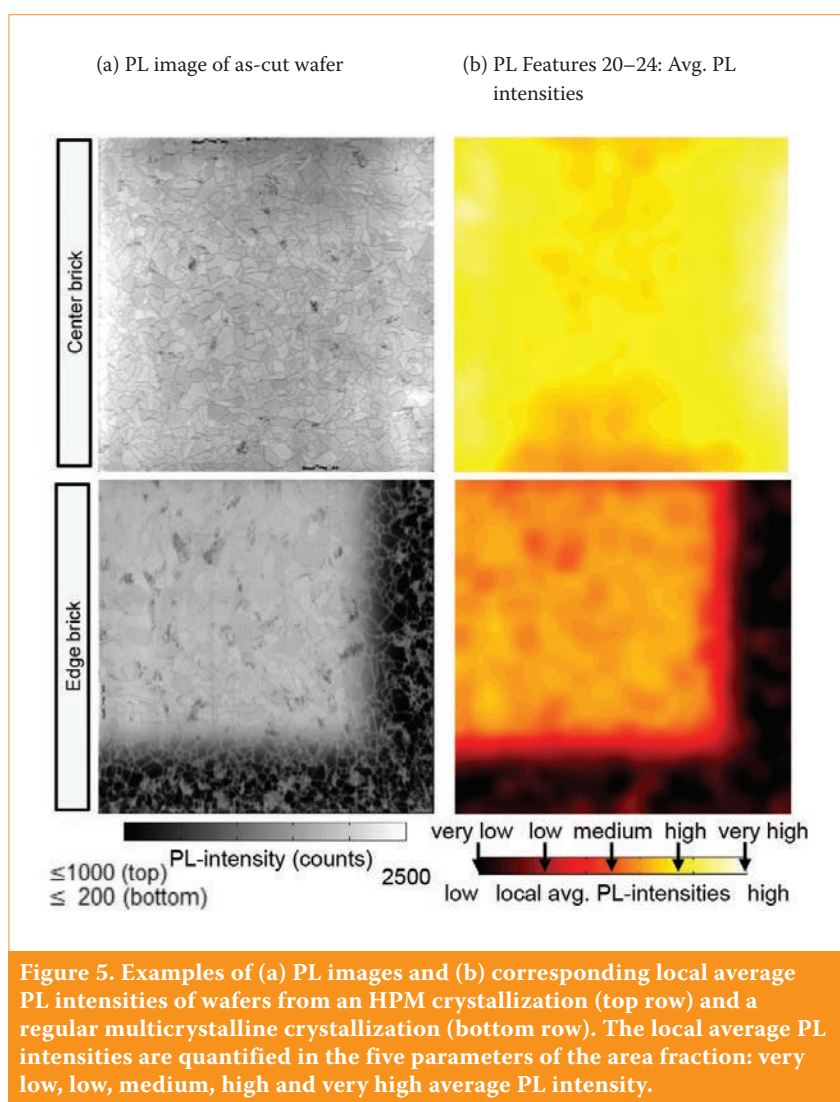


Figure 5. Examples of (a) PL images and (b) corresponding local average PL intensities of wafers from an HPM crystallization (top row) and a regular multicrystalline crystallization (bottom row). The local average PL intensities are quantified in the five parameters of the area fraction: very low, low, medium, high and very high average PL intensity.

Source: Demant et al. [6].

allowed. The penalty function can be the ℓ_2 norm ($P(\hat{\beta}) = \|\hat{\beta}\|_2$) or the ℓ_1 norm ($P(\hat{\beta}) = \|\hat{\beta}\|_1$) or a value in between, as proposed in the elastic-net approach. In the last two cases, fewer active features are preferred to solutions with many active features. The most robust model is identified within the model selection step. Finally, the predicted solar cell quality \hat{y} is given by $\hat{y} = \hat{\beta}(\vec{x}^T, 1)^T$.

The third method is a simple two-feature approach. The two features quantify dislocation clusters x_{clust} and the area of contaminated regions x_{cont} ; these are extracted on the basis of morphological operations. The calculation of the expected quality \hat{y} is based on the maximum expected solar cell quality q_{max} , where $q_{\text{max}} = V_{\text{oc,max}}$, according to

$$\hat{y} = q_{\text{max}} - \beta_{\text{clust}} x_{\text{clust}} - \beta_{\text{cont}} (x_{\text{cont}} - \beta_{\text{fix}}) \quad (2)$$

with coefficients β_{clust} , β_{cont} and β_{fix} . The parameter β_{fix} describes an expected positive gettering effect on contaminated edge regions, similar to the approach of Birkmann et al. [12].

Experimental approach for the qualification of a wafer rating

Materials and experimental approach

A large set of about 7,500 wafers from nine manufacturers was investigated using two different production processes, as shown in Fig. 6. Most

of the material (7,000 wafers) was selected from wafer sets with known ingot and brick positions provided by nine different manufacturers. To create a wafer set which represents the full spectrum of possible defect constellations, the wafers were systematically sampled from different brick positions of 72 bricks, the bricks being selected from 16 ingots from different ingot positions within the crystallization crucible. Additional material was sampled from 27 boxes from two manufacturers.

In the as-cut state, all wafers were subjected to an initial incoming control using commercially available inline measurement equipment (including conductivity and thickness measurements and micro-crack detection) and an inline PL system. The rating model is developed using this comprehensive data set, collected in the incoming control operation.

The wafer material was split into two sets for use in two different solar cell processes, one with 6,450 wafers and one with 1,050 wafers. The batch with 6,450 wafers was used to fabricate PERC solar cells in an industrial cell production line; the other batch, with 1,050 wafers, was used to create Al-BSF solar cells with screen-printed and fired, Ag and Al front- and rear-side metal contacts in the PV-TEC research line [25]. In both cases, neighbouring wafers were processed to ensure comparability of the rating. Furthermore, a representative subset of 47 bricks was

selected for the smaller batch (the Al-BSF process) from all 72 bricks considered within the PERC process.

The two material classes HPM and mc-Si were distinguished qualitatively according to their grain structure. In the outgoing quality control operation, the current–voltage (I – V) characteristics were measured under standard test conditions. To allow a spatially resolved analysis of the defect structure in the final cells, the images of the dark-saturation current density j_0 were generated for selected samples by C-DCR imaging accordant with Glatthaar et al. [26].

Evaluation set-up

A set of characteristic PL features is extracted using the data of the incoming control. The doping concentration (Feature 26), which was determined from inductive conductivity measurements [27], and the total thickness variation (Feature 27), are also added to the set of features. The proposed machine-learning techniques are applied and compared with respect to the prediction accuracy of the V_{oc} . The mean absolute error (MAE) between predicted and measured V_{oc} is selected as the quality metric. Furthermore, the root mean square error (RMS) and Pearson correlation coefficient (Corr) are determined.

In general, the application of powerful machine-learning techniques requires the evaluation of ‘unknown’ data; therefore, the data sets are split into disjoint training and testing sets for a valid evaluation of the prediction model. Frequently, a random selection of data is utilized. An advanced randomization can be used with the k -fold cross validation (e.g. Bishop [28]); by randomly splitting the data into k folds, all the data can be analysed. One of the k folds is iteratively predicted with a model trained by the remaining $(k-1)$ folds.

The challenge of a prediction model to make an accurate prediction increases with a decreasing degree of similarity between training and test sets. The analysis of data from unknown manufacturers, which represents the most challenging case, is considered in the second evaluation in this work. Iteratively, the data set of each manufacturer is selected as a test set and evaluated with a rating model trained on the data set containing all remaining manufacturers; each classification model is evaluated for these training/testing configurations. The elastic-net regression returns the most relevant features for both solar cell processes, which are then compared with respect to the most-influencing material

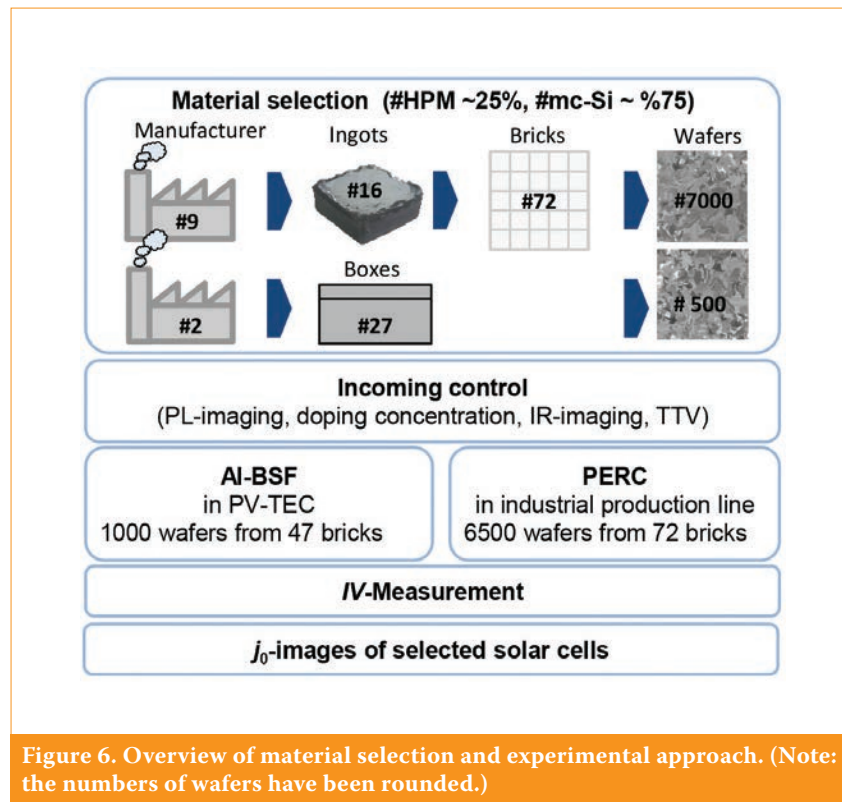


Figure 6. Overview of material selection and experimental approach. (Note: the numbers of wafers have been rounded.)

features. Finally, the appearance of these relevant features in both processes and material classes (HPM and mc-Si) are considered within a more detailed comparison based on the j_0 images of the final cells.

Quality of the different rating approaches

The PL images were analysed on the basis of the algorithm described in detail by Demant et al. [6]. The wafers were processed into solar cells, with V_{oc} values in the range 600–630 mV for the Al-BSF process and 610–650 mV for the PERC process (neglecting outliers). The broad V_{oc} range directly reflects the broad material spectrum. As expected, the PERC process reacts more sensitively than the Al-BSF process to the variations in material quality. The

main evaluation results are listed in Table 1 and discussed next.

The prediction of V_{oc} using a random selection of data ('Evaluation 1') yields very good results for the Al-BSF process, with MAE values of 1.3 mV, 2.0 mV and 2.1 mV for the SVR, elastic-net and two-feature approaches respectively. The evaluation of the prediction quality of the set of PERC data, however, shows larger differences between the models. The qualities of the rating models are nevertheless ordered the same, with SVR achieving the smallest error (MAE=1.4 mV). The elastic-net approach yields a slight increase in prediction error (MAE=2.5 mV), whereas the simple two-feature model completely fails to predict the solar cell quality within an industrial PERC process (MAE=6.9 mV). The complex SVR therefore performs best for

randomly selected data, regardless of the solar cell process. The high prediction quality reflects the quality of the approach but is also due to the remaining similarity between the training and test sets. Even for a random selection, however, the training and test sets do not include neighbouring wafers within the data set used.

In the case of forecasting material from an unknown manufacturer, this similarity is completely eliminated. The results in Fig. 7 show an example for the prediction of wafers from two unknown manufacturers ('Evaluation 2a') with HPM and standard mc-Si material for the Al-BSF and PERC processes. For the Al-BSF process, the elastic-net algorithm yields the best performance (MAE=1.8 mV), followed by the SVR method (MAE=2.0 mV) and the two-feature approach (MAE=2.1 mV), with

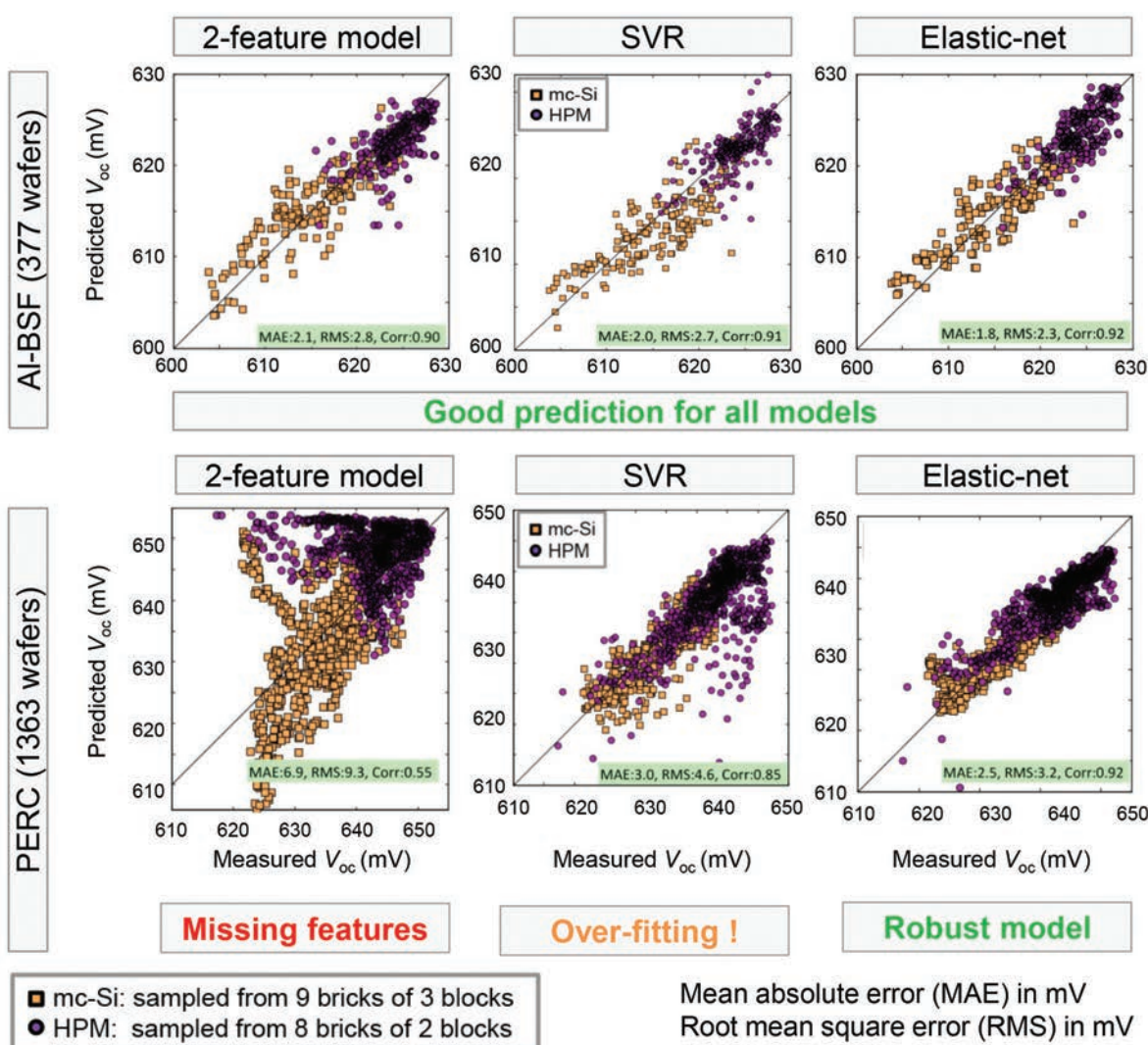


Figure 7. Prediction results for wafers from two unknown manufacturers (Evaluation 2a) for both solar cell processes, PERC and Al-BSF, obtained using the simple two-feature (left), complex SVR (middle) and elastic-net (right) approaches. The Al-BSF data prediction (top row) shows high correlations for all three prediction models. The PERC data prediction (bottom row) can be achieved with the SVR and elastic-net approaches, while the two-feature method fails completely.

Model	Solar cell process	Two-feature model [mV]	Support vector regression [mV]	Elastic-net algorithm [mV]
Complexity		Simple	Robust and non-linear	Linear, with optimized features
Evaluation 1: Random test set selection with fivefold cross-validation (MAE)	Al-BSF	2.1	1.3	2.0
	PERC	6.9	1.4	2.5
Evaluation 2a: Prediction of materials from two unknown manufacturers with HPM and standard wafers (MAE, cf. Fig. 7)	Al-BSF	2.1	2.0	1.8
	PERC	6.9	3.0	2.5
Evaluation 2b: Systematic prediction of wafers from each manufacturer, on the basis of training with wafers from the remaining manufacturers (overall MAE)	Al-BSF	2.1	2.2	2.2
	PERC	5.6	3.5	2.9

Table 1. Overview of the prediction quality of the investigated regression models for different training and test configurations and solar cell data. Prediction qualities are quantified by the mean absolute error (MAE) of the prediction. (The term ‘unknown manufacturer’ denotes that no material from this manufacturer was represented in the training data.)

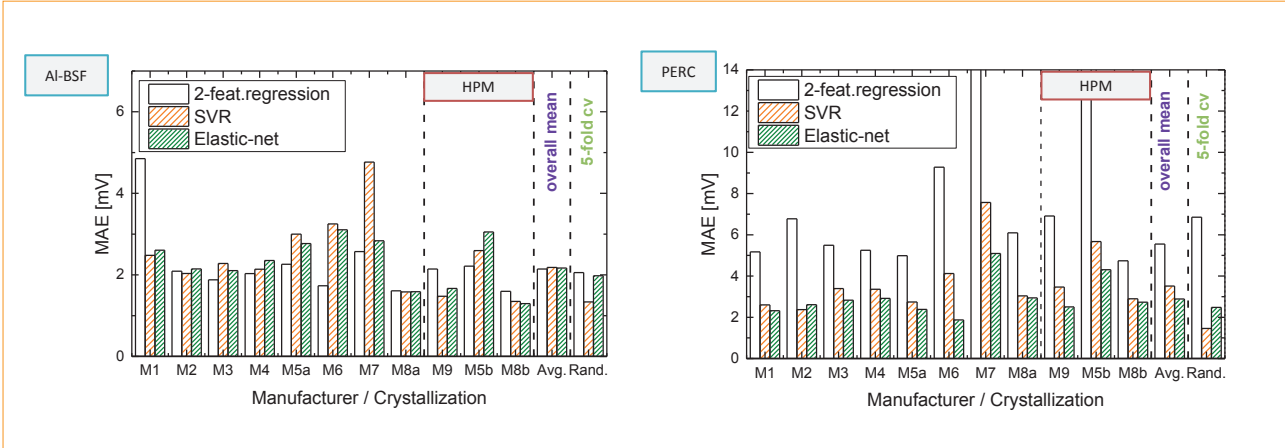


Figure 8. Prediction quality of material from an unknown manufacturer. The MAE is given for each manufacturer and is based on models trained using the remaining materials. The last two columns indicate the overall mean prediction result (‘Avg.’) and the prediction result on randomly selected test data (‘Rand.’). The elastic-net approach demonstrates the lowest overall MAE for the PERC prediction data.

slightly higher prediction errors. This ranking is even more distinct for the PERC prediction: while the elastic-net approach produces low prediction errors (MAE=2.5mV), the prediction errors are higher for the SVR model (MAE=3.0mV), and the simple two-feature-model fails completely (MAE=6.9mV).

In addition, for unknown material, the prediction quality of the three approaches was systematically evaluated (‘Evaluation 2b’): the material from each of the manufacturers was rated consecutively with the three models, each of the models being trained using the material from all the other manufacturers. The results are presented in Fig. 8, which shows the MAE values of the prediction for each manufacturer and all three prediction models; the overall MAE summarizes the result for all manufacturers. The classification accuracy for the Al-BSF process is high with all three approaches.

As regards the PERC process, it can be seen in Fig. 8 that the simple two-feature approach mostly fails for all the different

manufacturers (overall MAE=5.6mV). The prediction quality for SVR is also poor (overall MAE=3.5mV), which may be connected to an overfitting to the training data. In this most challenging task the robust elastic-net algorithm performs best (overall MAE=2.9mV); this can be interpreted as a very good result, considering the broad distribution of V_{oc} values ranging from 40mV and above, and the pure process- and measurement-related V_{oc} variations in the range of ~2mV.

Identification of relevant features

The applied elastic-net regression model allows the V_{oc} to be predicted and the relevance of the features to be simultaneously selected and rated. The model selection identifies a robust model with the most relevant features only. For normalized features, the coefficients of the linear regression model indicate the importance of the parameters.

The most important features for the

prediction of samples from both types of solar cell are the area fraction of thinned dislocations (Feature 2), and the area fraction of regions with low (Feature 7) and medium (Feature 8) local defect densities. Feature 2 represents dislocations or grain boundaries, which are thinned to their centres. As expected, the predicted solar cell quality decreases with the number of thinned structural defects and clusters of structural defects (Feature 8). On the other hand, it increases with the number of sparse structural defects (Feature 7), such as grain boundaries, which represent most structural defects identified in HPM wafers (see Fig. 4). These structures are less critical than dislocation clusters. For both types of solar cell, the distribution of PL structures and PL intensities plays an important role. The doping concentration was also considered to be a relevant feature in the rating model.

For PERC cells the second most important feature is different from that in the Al-BSF results: it quantifies instead the area fraction of regions

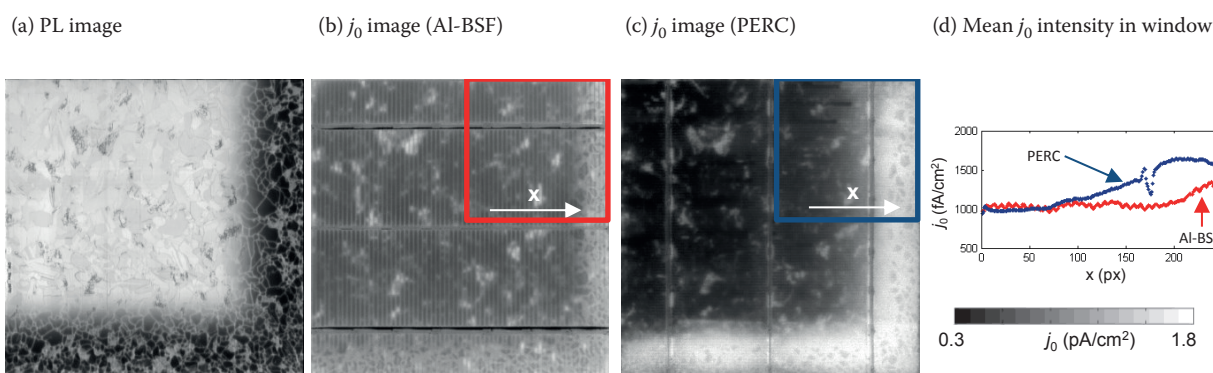


Figure 9. (a) PL image of a wafer from a corner brick. (b) The j_0 image obtained from the C-DCR method on an Al-BSF solar cell manufactured from the investigated wafer and a neighbouring wafer. (c) Corresponding j_0 image for a PERC cell. (d) Mean intensity profiles and j_0 values near the edges of the wafer, showing the effects of the diffusion processes.

with very low luminescence intensity (Feature 20) and has a strong negative impact on cell performance. According to the authors' empirical evaluation, the area fraction of very low luminescence intensity replaces the quantification of contaminated regions (Feature 3).

The differences between PERC and Al-BSF cells were investigated by comparing the images of dark-saturation current of two neighbouring wafers from a corner brick. The contaminated regions are visible in the PL image shown in Fig. 9(a). The contrast between the j_0 value in the contaminated regions and the non-contaminated regions is larger for PERC cells than for Al-BSF cells. This advantage of the Al-BSF process results from: 1) an enhanced phosphorus gettering during the two-sided emitter diffusion (which is reduced in the PERC process because of a one-sided emitter diffusion); and 2) the full-area aluminium gettering during rear-side contact formation (which no longer occurs in the PERC process because of the local contacting of the passivated rear side).

Conclusion and outlook

A classification scheme has been developed to simultaneously predict the solar cell quality of standard mc-Si and HPM wafers. The development was based on a representative set of 7,500 industrially available wafers from 72 bricks and nine manufacturers, which were intensively characterized in the as-cut state in an incoming inspection and then processed into solar cells using an Al-BSF and a PERC method.

“The results demonstrate the quality of the proposed elastic-net approach.”

The quantification of the defects that showed up in the PL images was improved by means of robust image-processing algorithms. Using regularized regression (elastic-net approach), the prediction of the open-circuit voltage for standard mc-Si and HPM material from ‘unknown’ manufacturers yielded average MAEs of 2.2mV for the Al-BSF solar cell process and 2.9mV for the PERC one. For an industrial PERC process, the prediction of the quality for unknown wafer manufacturers was slightly less accurate using the SVR approach (MAE=3.5mV), but completely failed using the simple two-feature approach (MAE=5.6mV). The results demonstrate the quality of the proposed elastic-net approach.

Most of the structural defects in HPM can be traced back to grain boundaries, which are quantified as regions with low local defect density and which marginally affect cell quality. Thus a rating scheme has to differentiate between different levels of defect density in order to rate both types of material under investigation. Different feature weights are also deemed necessary for Al-BSF and PERC solar cells.

In follow-up investigations, higher-order input parameters will be analysed. A modelling of relevant features as proposed by Demant et al. [29] by considering spatially resolved quality data (e.g. Glatthaar et al. [26]) can also be used to further refine the rating scheme. Moreover, advanced image-processing techniques have been developed at ISE to analyse the crystallization process in more detail using PL images of as-cut wafers; the extracted parameters allow the defect development to be rated during crystallization. The application of new computer-vision technologies, such as the so-called ‘deep learning’,

can further boost the material rating method. To implement such promising and data-intensive approaches, strong cooperation between industry and research will be necessary.

Acknowledgements

This work was supported by the German Ministry for Education and Research (BMBF) under the framework of the ‘Q-Wafer’ project (03SF0409).

References

- [1] Lan, C.W. et al. 2012, “Grain control in directional solidification of photovoltaic silicon”, *J. Cryst. Growth*, Vol. 360, pp. 68–75.
- [2] Trupke, T. et al. 2006, “Photoluminescence imaging of silicon wafers”, *Appl. Phys. Lett.*, Vol. 89, pp. 1–3.
- [3] Schubert, M.C. et al. 2013, “Impact of impurities from crucible and coating on mc-silicon quality – The example of iron and cobalt”, *IEEE J. Photovolt.*, Vol. 3, pp. 1250–1258.
- [4] Schindler, F. et al. 2014, “Solar cell efficiency losses due to impurities from the crucible in multicrystalline silicon”, *IEEE J. Photovolt.*, Vol. 4, pp. 122–129.
- [5] Haunschild, J. et al. 2010, “Quality control of as-cut multicrystalline silicon wafers using photoluminescence imaging for solar cell production”, *Sol. Energy Mater. Sol. Cells*, Vol. 94, pp. 2007–2012.
- [6] Demant, M. et al. 2015, “Inline quality rating of multi-crystalline wafers based on photoluminescence images”, *Prog. Photovoltaics Res. Appl.*, doi: 10.1002/ppa.2706.
- [7] Sinton, R.A., Cuevas, A. & Stuckings, M. 1996, “Quasi-steady-state photoconductance, a new method for solar cell material and device characterization”, *Proc. 25th IEEE*

- PVSC, Washington DC, USA, pp. 457–460.
- [8] Dornich, K. et al. 2013, “Fast, high resolution, inline contactless electrical semiconductor characterization for photovoltaic applications by microwave detected photoconductivity”, *Mater. Sci. Eng. B*, Vol. 178, pp. 676–681.
- [9] Chunduri, S.K. 2011, “Market survey on luminescence imaging systems and cameras”, *Photon International*, Vol. 1, pp. 158–193.
- [10] Michl, B. et al. 2012, “Efficiency limiting bulk recombination in multicrystalline silicon solar cells”, *Sol. Energy Mater. Sol. Cells*, Vol. 98, pp. 441–447.
- [11] Nagel, H. et al. 2010, “Luminescence imaging – a key metrology for crystalline silicon PV”, *Proc. 20th Worksh. Cryst. Si. Sol. Cells & Mod.*, Breckenridge, Colorado, USA.
- [12] Birkmann, B. et al. 2011, “Analysis of multicrystalline wafers originating from corner and edge bricks and forecast of cell properties”, *Proc. 26th EU PVSEC*, Hamburg, Germany, pp. 1–4.
- [13] Demant, M. et al. 2010, “Analysis of luminescence images applying pattern recognition techniques”, *Proc. 25th EU PVSEC*, Valencia, Spain, pp. 1078–1082.
- [14] McMillan, W. et al. 2010, “In-line monitoring of electrical wafer quality using photoluminescence imaging”, *Proc. 25th EU PVSEC*, Valencia, Spain, pp. 1346–1351.
- [15] Demant, M. et al. 2013, “Evaluation and improvement of a feature-based classification framework to rate the quality of multicrystalline silicon wafers”, *Proc. 28th EU PVSEC*, Paris, France, pp. 1650–1654.
- [16] Glatthaar, M. et al. 2010, “Luminescence imaging for quantitative solar cell material and process characterization”, *Proc. 25th EU PVSEC*, Valencia, Spain, pp. 1825–1827.
- [17] Bakowskie, R. et al. 2011, “Comparison of recombination active defects in multicrystalline silicon by means of photoluminescence imaging and reverse biased electroluminescence”, *Proc. 26th EU PVSEC*, Hamburg, Germany, pp. 1839–1842.
- [18] Lausch, D. & Hagendorf, C. 2015, “Influence of different types of recombination active defects on the integral electrical properties of multicrystalline silicon solar cells”, *J. Sol. Energy*, Vol. 2015, pp. 1–9.
- [19] Johnston, S. et al. 2012, “Comparison of photoluminescence imaging on starting multi-crystalline silicon wafers to finished cell performance”, *Proc. 38th IEEE PVSC*, Austin, Texas, USA, pp. 2161–2166.
- [20] Bentzen, A. & Holt, A. 2009, “Overview of phosphorus diffusion and gettering in multicrystalline silicon”, *Mater. Sci. Eng. B*, Vol. 159–160, pp. 228–234.
- [21] Kovesi, P. 2003, “Phase congruency detects corners and edges”, *Austral. Patt. Recog. Soc. Conf.: DICTA 2003*, Sydney, Australia, pp. 309–318.
- [22] Isenberg, J. et al. 2003, “Imaging method for laterally resolved measurement of minority carrier densities and lifetimes: Measurement principle and first applications”, *J. Appl. Phys.*, Vol. 93, pp. 4268–4275.
- [23] Vapnik, V. 1995, *The Nature of Statistical Learning Theory*. New York: Springer.
- [24] Hastie, T. et al. 2009, “Linear methods for regression”, in *The Elements of Statistical Learning*, 2nd edn. New York: Springer, pp. 43–100.
- [25] Biro, D. et al. 2009, “PV-TEC: Retrospection to the three years of operation of a production oriented research platform”, *Proc. 24th EU PVSEC*, Hamburg, Germany, pp. 1901–1905.
- [26] Glatthaar, M. et al. 2010, “Spatially resolved determination of dark saturation current and series resistance of silicon solar cells”, *physica status solidi (RRL)*, Vol. 4, pp. 13–15.
- [27] Spitz, M., Belledin, U. & Rein, S. 2007, “Fast inductive inline measurement of the emitter sheet resistance in industrial solar cell fabrication”, *Proc. 22nd EU PVSEC*, Milan, Italy, pp. 47–50.
- [28] Bishop, C.M. 2006, *Pattern Recognition and Machine Learning*. New York: Springer.
- [29] Demant, M. et al. 2012, “Modelling of physically relevant features in photoluminescence images”, *Energy Procedia*, Vol. 27, pp. 247–252.

About the Authors



Matthias Demant studied computer science at the University of Freiburg, Germany. Since 2009 he has been a researcher at Fraunhofer ISE. He is currently working on his Ph.D., which involves the inline characterization of wafers and solar cells by means of pattern-recognition techniques.



Theresa Strauch received her diploma degree in mathematics from the University of Freiburg in 2012. Since then she has been

working at Fraunhofer ISE on image processing with applications in wafer characterization. For her Ph.D. thesis, she is focusing on grain structure and dislocation development in silicon ingots.



Kirsten Sunder completed her physics diploma, with a focus on material physics, at the University of Münster, Germany. She continued working at the Institute of Materials Physics and received her Ph.D. for her work on network former diffusion in silicate glasses. Since 2011 she has been working as a scientist at PV Crystallox Solar Silicon GmbH in Erfurt, Germany.



Oliver Anspach studied geology at the Universities of Jena and Edinburgh, and received his Ph.D. from the Otto-Schott Institute for Glass Chemistry at the University of Jena. Since 2005 he has been working for PV Crystallox Solar PLC, and for the past eight years he has been responsible for R&D in the field of multiwire sawing.



Jonas Haunschild leads the inline wafer analysis team at Fraunhofer ISE. He studied physics at the Philipp University of Marburg and received a diploma degree in 2007, followed by his Ph.D. in 2012 for his work on luminescence-based methods for quality control in industrial solar cell production.



Stefan Rein is head of the inline measurement techniques and quality assurance group at Fraunhofer ISE, which focuses on metrology, production control, solar cell simulation and new silicon materials. He studied physics at the University of Freiburg and received his Ph.D. in 2004 for his work on lifetime spectroscopy for defect characterization in silicon.

Enquiries

Matthias Demant
PV Production Technology and Quality Assurance Dept.
Fraunhofer Institute for Solar Energy Systems ISE
Heidenhofstraße 2, 79110 Freiburg Germany

Tel: +49 (0) 761/4588-5651

Email:

matthias.demant@ise.fraunhofer.de

Cell Processing



38

Page 38
News

Page 41
The PERC+ cell: More output power for less aluminium paste

Thorsten Dullweber, Christopher Kranz, Robby Peibst, Ulrike Baumann & Helge Hannebauer, Institute for Solar Energy Research Hamelin (ISFH), Emmerthal, & Alexander Fülle, Stefan Steckemetz, Torsten Weber, Martin Kutzer, Matthias Müller, Gerd Fischer, Phedon Palinginis & Holger Neuhaus, SolarWorld Innovations GmbH, Freiberg, Germany

Page 52
Metallization: The technology with highest efficiency gain potential for c-Si cells

Radovan Kopecek, Lejo J. Koduvelikulathu, Enrique Cabrera, Dominik Rudolph & Thomas Buck, International Solar Energy Research Center (ISC) Konstanz, Germany

Page 61
Metallization and interconnection for silicon heterojunction solar cells and modules

Matthieu Despeisse, Christophe Ballif, Antonin Faes & Agata Lachowicz, CSEM, Neuchâtel, Switzerland



41



61

Trina Solar sets 21.25% multicrystalline cell efficiency record

PV manufacturer Trina Solar has set a new world record conversion efficiency for p-type multicrystalline silicon (mc-Si) solar cells.

Developed and produced at its State Key Laboratory of PV Science and Technology of China, Trina Solar's record total-area efficiency of 21.25% on standard 156×156mm substrates was achieved using advanced 'Honey Plus' processing technologies including back surface passivation and local back surface field on volume production equipment.

Pierre Verlinden, vice president and chief scientist of Trina Solar said: "To the best of our knowledge, this is the first time ever that a multicrystalline silicon solar cell has been able to achieve a conversion efficiency of over 21%. This exciting result shows that the development path toward higher efficiencies continues to be bright, even for silicon. Our aim is to continuously integrate innovative technological developments to improve the efficiency and lower the cost of our PV products. This technology advancement in efficiency will strengthen our leadership in the PV industry and allow us to continue providing affordable solar power to the world."

Trina Solar noted that the record cell efficiencies had been independently confirmed by the Fraunhofer ISE CalLab in Germany. The company had previously set the record at 20.76% in late 2014.



Credit: Trina Solar

Trina has reached an efficiency of 21.25% with p-type multi cell.

Global

'Silicon Module Super League' big-six to reach 50% global market share in 2016

The big-six c-Si module suppliers in the solar PV industry today – Canadian Solar, Hanwha Q CELLS, JA Solar, JinkoSolar, Trina Solar and Yingli Green – collectively known now as the 'Silicon Module Super League' (SMSL), are forecast to increase market share again in 2016, taking their collective market share of global module supply to almost 50%.

The figures come from an analysis by the Solar Intelligence research team, within Photovoltaics International's parent company Solar Media, which fully modelled out the expected capacity, production and shipment forecasts for each of the SMSL companies to the end of 2016.

The analysis noted that under this consolidation, the prospects of competing with companies shipping 5-6GW of modules annually, as part of diversified third-party/in-house supply channels via global sales outlets, are limited at best.

PV manufacturing capacity expansion announcements reach record 17.5GW in November

PV capacity expansion announcements in November 2015 set several new major benchmarks as some of the big-six SMSL

members announced further expansions to meet growing demand in 2016.

A total of 17.5GW of new capacity expansions were announced in November, across dedicated solar cell and dedicated module assembly. Notably, no integrated cell/module capacity expansions were announced in the month, primarily due to the dominance of announcements by SMSL members.

This is by far the highest figure set in the last two years, almost triple the benchmark capacity announcements set earlier this year in May of 6.78GW. The number of companies announcing expansions totalled 14 in November, beating the previous benchmark of 11, set in May 2015.

East Asia

Hanwha Q CELLS set to reach 5.2GW of cell and module capacity by mid-2016

SMSL member Hanwha Q CELLS expects to reach nameplate capacity of 5.2GW for both solar cells and modules by the middle of 2016 as the company continues major expansions in 2015.

In Q3 financial results, in-house production capacities for solar cells and modules had both reached 3.55GW and the company was on target to reach 4.3GW by the end of the year.

Further expansions underway would mean both cell and module production would reach 5.2GW by mid-2016.

Furthermore 600MW of new solar cell capacity expansions would come from Hanwha Q CELLS Korea in 2015, with a further 900MW in 2016.

The company also noted that in-house ingot production stood at 1.35GW and wafer production stood at 900MW at the end of the first nine months of 2015.

Latest heterojunction c-Si 'record breaker' among Japan's space and time-saving solar gadgets

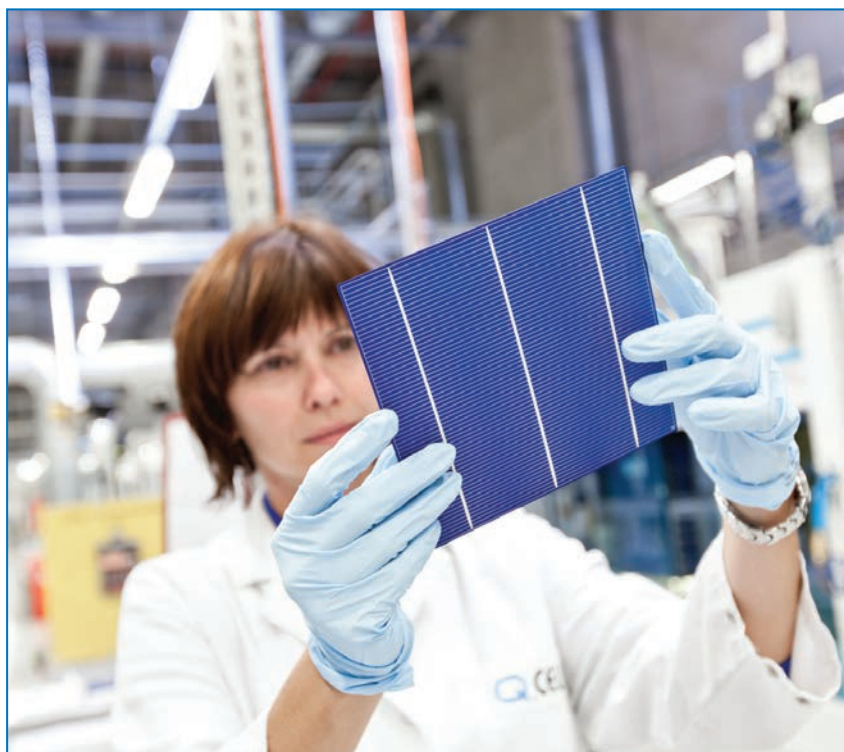
A heterojunction c-Si solar cell with a conversion efficiency of 25.1% has been showcased by its maker, a branch of Japanese chemicals manufacturer Kaneka Corporation in collaboration with NEDO, at an event hosted by the Japanese government to exhibit technological innovations in "new energy".

Kaneka's new device is a double-sided crystalline silicon cell, with the conversion efficiency verified by Germany's Fraunhofer ISE. The company is targeting pilot production for the cells. Kaneka and NEDO are targeting cost reductions that could take the cost of energy down to Y14/kWh by 2020 and then halve that to Y7/kWh by 2030.

Neo Solar Power hits record revenue for 2015 in October

Taiwan-based merchant solar cell producer Neo Solar Power (NSP) reported its highest monthly sales in October for the year to date.

NSP reported October 2015 revenue of NT\$2,410 million (US\$73.5 million), up



Hanwha Q CELLS is set to reach 5.2GW of cell and module capacity by mid-2016.

27.29% from the previous month and up 17.4% year-on-year.

The company attributed the growth in revenue to strong market demand, increased shipment volume, ASP increase and revenue contribution from selling solar farms owned by subsidiary, General Energy Solutions (GES).

NSP has also reached a new monocrystalline solar cell conversion efficiency milestone, with its 'Black 21' cell, certified by the Taiwan Industrial Technology Research Institute (ITRI) at 21.1% conversion efficiency.

JA Solar increasing cell and module capacity to 5GW by mid-2016

SMSL member JA Solar said it would make significant manufacturing capacity expansions by mid-2016 to meet demand.

It planned to increase ingot/wafer production for the first time in many years to 1.5GW, up 500MW from 1GW.

Both solar cell and module nameplate capacity would be increased to 5GW by mid-2016, equating to both being increased by 1.4GW from planned 2015 nameplate capacity levels of 3.6GW.

The company recently starting ramping its new 400MW solar cell manufacturing facility in Penang, Malaysia.

Motech sales at record high in October

Major Taiwan-based merchant solar cell producer Motech Industries has reported

record sales for October, 2015 of NT\$2,584 million (US\$79.5 million), an increase of 1.76% over the previous month and up 66.74% year-on-year.

The company had third quarter revenue of NT\$7.098 billion (US\$218.4 million).

Motech's sales have benefited from its merger with Topcell Solar in 2015.

A fire was said to have occurred at an idled processing tool at its FAB 5 production facility in Tainan Science Park on November 5, 2015 but was it was quickly extinguished and had little impact on production and did not cause any injuries.

The company is also expanding module production at a subsidiary in China by around 300MW.



JA Solar is increasing cell and module capacity to 5GW by mid 2016.

Europe

Teams combine perovskite and silicon cells to reach record 18% efficiency

Teams from solar cell research institute Helmholtz-Zentrum Berlin (HZB) and the university École Polytechnique Fédérale de Lausanne (EPFL) in Switzerland have combined a silicon heterojunction solar cell with a perovskite solar cell monolithically into a tandem device and reached a record efficiency of 18%.

Perovskite layers absorb light in the blue region of the spectrum, which means they are useful to combine with silicon layers that mostly convert long-wavelength red and near-infrared light.

However, constructing these two types of cell in tandem is difficult, but the teams managed to manufacture this kind of monolithic tandem cell and now claim there is even potential to reach efficiency levels as high as 30%.

North America

Canadian Solar making substantial manufacturing capacity expansion in 2016

Canadian Solar is to allocate around US\$401 million in capital expenditures through the end of 2016 to significantly increase in-house wafer, cell and module production capacity and locate new plants in multiple countries.

To meet "expected strong growth in global demand for solar modules in the quarters ahead," Canadian Solar will increase in-house wafer production from 400MW to 1GW by mid-2016, while solar cell capacity would be expanded from 2.5GW currently to 3.4GW

by the end of 2016, a 900MW increase.

However, the biggest capacity increase is PV module production which will be expanded from 4.33GW, which the company expects to be achieved by the end of 2015, to 5.63GW by the end of 2016, a 1GW increase.

Canadian Solar's wafer manufacturing capacity at its plant in Luoyang, Henan Province, is expected to reach 1GW by June of 2016, while its cell manufacturing capacity at its plant in Suzhou, Jiangsu Province, is expected to reach 2GW by the end of 2015. Cell manufacturing capacity at its Funning plant in Jiangsu Province is expected to reach 1.0GW by July of 2016.

1366 Technologies 'Direct Wafer' reaches verified 19.1% cell efficiency

US-Based 'Direct Wafer' producer, 1366 Technologies, has reported a champion cell that has achieved a cell efficiency of 19.1%, verified by Fraunhofer ISE. 1366 Technologies used its standard size kerfless multicrystalline wafer technology.

Frank van Mierlo, CEO of 1366 Technologies said: "The disruptive nature of the Direct Wafer process is not only evident in the cost and material savings it provides, but in its ability to break the technology limitations of conventional wafer manufacturing. The rapid and significant efficiency gains we've achieved will be further increased by new wafer features made possible only with our process."

The firm is targeting 20% plus cell efficiencies in the first half of 2016.

Recently, 1366 Technologies announced plans to build its first volume manufacturing hub in Genesee County, New York with an initial 250MW capacity.

India

Indian solar cell manufacturers request second anti-dumping investigation

Solar cell manufacturers in India put in a request to the government to investigate anti-dumping duties on the import of solar cells.

Domestic manufacturers claim that cheap imported solar cells now account for 90% of the market and have therefore called for duties on the US, EU, China, Malaysia and Taiwan for dumping.

The anti-dumping issue was first raised back in 2012 when Indian manufacturers filed an application with the Directorate General of Anti-dumping and Allied duties (DGAD) at the Ministry of Commerce and Industry. At that point, they claimed that foreign imports had a 60% market share.



Credit: Canadian Solar

Canadian Solar is expanding cell production capacity to 3.4GW in 2016.

A new letter from Indian Solar Manufacturer's Association to the DGS cited the current "aggravated situation" of imports and "injury" to the domestic industry.

Lanco Infratech signs 100MW solar cell plant MoU with Chhattisgarh government

India-based conglomerate Lanco Infratech is planning to build a 100MW solar cell production facility at new dedicated Solar SEZ in Rajnandgaon district of Chhattisgarh, India.

Lanco Infratech signed an MoU with the Chhattisgarh government to build the solar cell plant that would occupy around 150 acres within the SEZ, which would become a 'plug and play' zone with approvals for land, water and power sources intended to attract domestic as well as overseas PV manufacturers.

The initiative by the Chhattisgarh government supports the national solar mission and is in-line with the 'Make-in-India' initiative of the current Indian government. The bigger plan is to occupy a

250 acre site within the SEZ to achieve cell production of 2,200MW per annum.

Longi Silicon planning 500MW mono-cell and module plant in India

Monocrystalline wafer producer Longi Silicon Materials has signed an MoU with the provincial government of Andhra Pradesh to build and operate a 500MW solar cell and module production plant.

The plant is expected to need an investment of around CNY1.5 billion (US\$234.8 million) and to be located in Sri City, Chittoor region.

Longi has made several major announcements in 2015, totalling 6GW.

The firm is planning a 3GW capacity expansion of monocrystalline ingot/wafer production, a 2GW monocrystalline solar cell plant in Jiangsu, China via its subsidiary, Leye Photovoltaic Science & Technology, and a 500MW monocrystalline module plant in Yinchuan City, China ahead of the latest 500MW of integrated cell and module capacity in India.

The PERC+ cell: More output power for less aluminium paste

Thorsten Dullweber, Christopher Kranz, Robby Peibst, Ulrike Baumann & Helge Hannebauer, Institute for Solar Energy Research Hamelin (ISFH), Emmerthal, & **Alexander Fülle, Stefan Steckemetz, Torsten Weber, Martin Kutzer, Matthias Müller, Gerd Fischer, Phedon Palinginis & Holger Neuhaus**, SolarWorld Innovations GmbH, Freiberg, Germany

ABSTRACT

Passivated emitter and rear cell (PERC) technology has been forecast to become mainstream in the next few years, gaining around a 30% market share. This paper presents a novel PERC solar cell design in which a screen-printed rear aluminium (Al) finger grid is used instead of the conventional full-area Al rear layer, while implementing the same PERC manufacturing sequence. This novel cell concept, called 'PERC+', offers several advantages over PERC. In particular, the Al paste consumption for PERC+ cells is drastically reduced to 0.15g per wafer, as opposed to 1.6g per wafer for conventional PERC cells. The aluminium back-surface fields (Al-BSFs) created by the Al fingers are 2µm deeper, which increases the open-circuit voltage by 3mV. Moreover, the five-busbar Al finger grid enables the use of PERC+ cells in bifacial applications, offering front-side efficiencies of up to 21.2% and rear-side efficiencies of up to 16.6%, measured with a black chuck, and a corresponding bifaciality of up to 78%. When a reflective brass chuck is used for measurement, PERC+ cells demonstrate efficiencies of up to 21.5%, compared with 21.1% for conventional PERC cells. The PERC+ efficiency is higher, since the deeper aluminium back-surface field (Al-BSF) increases the open-circuit voltage and also because the reflective brass chuck increases the internal rear reflectance, leading to higher short-circuit currents. PERC+ cells are therefore expected to be an attractive candidate for both bifacial glass–glass modules and monofacial modules with a white backsheets. While ISFH developed the aforementioned PERC+, SolarWorld independently pioneered a very similar bifacial PERC+ cell process that has been successfully transferred to mass production. Novel glass–glass bifacial PERC+ modules based on a very simple, lean and cost-effective bifacial cell process were launched at Intersolar 2015. These new bifacial PERC+ modules have demonstrated an increase in annual energy yield between 5 and 25% in simulations, which has also been confirmed by the first outdoor measurements.

Introduction

Passivated emitter and rear cells (PERCs) are currently being introduced into mass production by several leading solar cell manufacturers, such as SolarWorld, Hanwha Q-Cells, Trina Solar and others [1–5]. In May 2015 SolarWorld demonstrated a record efficiency of 21.67% with an industrial p-type Cz-Si five-busbar PERC solar cell, an achievement that was externally certified by Fraunhofer-ISE CalLab in Germany. The latest photovoltaic technology roadmap ITRPV forecasts a market share for PERC solar cells of 35% by 2019 [6]. These industrial PERC cells use p-type wafers and a full-area screen-printed aluminium (Al) rear layer, which only locally contacts the silicon wafer in areas where the rear passivation has been removed by laser contact opening (LCO). Furthermore, the lab-type PERC cell of Blakers et al. in 1989 [7] employed a full-area evaporated Al rear contact. Full-area aluminium layers, however, consume a large amount of Al paste of around 1.0 to 1.5g per wafer; they also prevent any transmission of sunlight from the rear side into the silicon wafer, and hence any bifacial applications of these industrial PERC cells are ruled out.

“ITRPV predicts a market share for bifacial solar cell technologies of 15% by 2019.”

Bifacial solar cell concepts, on the other hand, are increasingly drawing a lot of interest for use in various applications, particularly in PV power plants, where the electricity produced can be increased by up to 20% using bifacial instead of monofacial solar cells [8,9]. Accordingly, the photovoltaic technology roadmap ITRPV predicts a market share for bifacial solar cell technologies of 15% by 2019 [6].

At the moment, industrial bifacial solar cell concepts mainly use n-type wafers, such as passivated emitter and rear totally diffused (PERT) solar cells [10–13] or heterojunction solar cells [14,15]. One of the challenges of these two cell concepts is that they typically involve screen-printed silver (Ag) finger grids on both sides of the wafer, and hence the consumption of a large amount of expensive Ag paste. Moreover, n-PERT cells entail single-sided boron and phosphorus doping, which requires additional or alternative process steps compared with p-type

PERC cell processing.

Bifacial silicon solar cell concepts using p-type wafers and a screen-printed Al rear finger grid have also been under investigation. In 2001 ISFH introduced a bifacial p-type solar cell in which the rear Al grid fires through the SiN_x rear passivation layer without using any LCO or rear-side boron doping [16]; ECN further developed this approach, offering the so-called 'p-PASHA' cell concept [17,18]. The published efficiencies, however, are very similar to those obtained with full-area Al-BSF cells, but are significantly lower than those of typical industrial PERC cells.

Recently, the company RCT Solutions reported a bifacial PERCT cell concept using p-type multicrystalline wafers, LCO and a screen-printed Al finger grid, resulting in front-side efficiencies of up to 18.6% [19,20]. However, this entailed an additional BBr₃ diffusion for the PERCT rear-side doping [19,20], which may increase the number of process steps compared with conventional monofacial PERC cell processing.

This paper presents high-efficiency bifacial PERC solar cells fabricated at ISFH SolarTeC using a typical

Fab & Facilities

Materials

Cell Processing

Thin Film

PV Modules

Market Watch

industrial PERC process flow (e.g. with $\text{AlO}_x/\text{SiN}_y$ rear passivation and LCO, but without rear boron doping), involving the application of a screen-printed Al finger grid on the rear side instead of a full-area Al layer. In the past, the low conductivity of screen-printed Al has been a concern for Al finger grid designs. However, with modern Al pastes, and in particular the use of a greater number of busbars (such as five-busbar H-pattern designs [21,22]), the Al conductivity is no longer a major limitation, as will be explored in this paper.

In the work reported here, the impact of the Al finger grid on the Al paste consumption and on the Al–Si contact formation was investigated. The front- and rear-side efficiencies of the resulting bifacial PERC solar cells were measured, and the implications of a white backsheet for its use in conventional monofacial modules were studied. This novel PERC cell design with screen-printed rear Al grid has been named ‘PERC+’, where the ‘+’ indicates the inherent advantages reported in this paper of the Al finger grid compared with a full-area Al rear metallization. In parallel to the aforementioned R&D activities at ISFH, SolarWorld independently pioneered the bifacial PERC+ cell process, with feasibility studies starting in 2014. This paper reports on the successful transfer to mass production of PERC+ cells at SolarWorld as well as on the novel glass–glass bifacial modules incorporating these cells. The added value to the PV industry of bifacial modules based on a very simple, lean and cost-effective bifacial cell process is discussed.

PERC+ solar cell process at ISFH

Boron-doped, $2\Omega\text{cm}$, $156\text{mm} \times 156\text{mm}$, Czochralski-grown silicon wafers are used in the work reported in this paper. After cleaning, the rear side is coated with a protection layer, which acts as a barrier in the subsequent alkaline texturing and phosphorus diffusion, resulting in an emitter sheet resistance of

$100\Omega/\text{sq}$. The rear protection layer and the phosphorus glass are removed by wet chemistry. An $\text{AlO}_x/\text{SiN}_y$ stack is deposited as the rear surface passivation. The thickness of the SiN_y capping layer is set to 80nm to obtain low reflection of the rear side of the bifacial PERC+ cells; the monofacial reference PERC cells with full-area Al layer receive a 200nm-thick SiN_y capping layer. The front side is passivated with plasma-enhanced chemical vapour deposition (PECVD) SiN_x . Line-shaped LCOs are formed on the PERC+ rear side, with a pitch p exceeding that of the monofacial PERC cells by a factor of 1.5; the larger LCO pitch of PERC+ cells is intended to reduce the rear metal coverage, thereby reducing the shadowing loss when the rear side receives illumination.

The Ag front grid is printed using a dual-print process similar to that described in Hannebauer et al. [21]: first the five busbars are screen-printed using a non-firing-through Ag paste, and then the Ag fingers are printed with a stencil using a firing-through Ag paste. For the Al screen print, a commercially available Al paste is used. The monofacial reference PERC cells are full-area screen printed, whereas the bifacial PERC+ cells use an Al finger grid screen design with a five-busbar H pattern. The aluminium screen has a finger opening width of $100\mu\text{m}$ and a pitch identical to the LCO pitch. The Al finger opening width is significantly wider than the LCO widths; hence, the Al–Si rear contact width and the Al grid line width can be optimized individually by the LCO and Al screen parameters. In the case of PERC+ cells, the Al fingers are printed in alignment with the LCOs.

As shown in Table 1, the monofacial PERC cells (group 1) consume 1.6g of Al paste per wafer, measured directly after printing, while the Al paste consumption of the bifacial PERC+ cells (group 2) is dramatically reduced to 0.15g per wafer, because of the finger grid design. The front and rear contacts are fired in a conventional belt furnace, during which the Al paste locally alloys with the silicon wafer in areas where the rear passivation has been removed by laser ablation.

“Al paste consumption of the bifacial PERC+ cells is dramatically reduced to 0.15g per wafer, because of the finger grid design.”

Schematic drawings of the resulting bifacial PERC+ and monofacial PERC solar cells are presented in Fig. 1; photographs of the front and rear surface of the PERC and PERC+ solar cells are shown in Fig. 2. Table 1 summarizes the various PERC and PERC+ process parameters.

Aluminium finger grid properties

The Al finger geometries of the PERC+ solar cells are analysed using a light microscope and an optical profilometer after firing. The Al finger height is similar to that of the full-area Al layer. The final Al finger widths are much wider than the $100\mu\text{m}$ screen-opening width, since the Al paste is not optimized for high aspect ratio prints. The Al finger width corresponds to an area fraction of 12.6% of the Al fingers on the PERC+ cell. If the area fraction of the five aluminium busbars of 1.6% is taken into account, the total metallization area fraction of the Al finger grid works out at 14.2%.

The wafer bow of four PERC and five PERC+ solar cells is measured as the maximum value of the distance of the solar cell to a flat surface. The bifacial PERC+ cells are almost perfectly flat, with a wafer bow of only $0.2 \pm 0.1\text{mm}$, whereas the monofacial PERC cells exhibit a wafer bow of $2.5 \pm 0.5\text{mm}$. This is to be expected, since the bifacial PERC+ cells are fairly symmetric, with both wafer surfaces being coated with dielectric layers and metal grid lines, thus reducing the mechanical stress within the wafers compared with PERC cells with a full-area Al layer.

In order to assess the impact of the Al grid design on the series resistance of the PERC solar cells, the grid line resistance of the Al fingers

Group	Solar cell type	Rear SiN thickness [nm]	LCO pitch [a.u.]	Al finger width [μm]	Al area fraction [%]	Al paste consumption [g]
1	PERC	200	p	N/A	100	1.6
2	PERC+	80	$1.5 p$	100	14.2	0.15

Table 1. PERC and PERC+ process parameters. Although the principal process flows for the two types of cell are identical, several process parameters were adjusted for the PERC+ cell in order to optimize the bifaciality. (The Al finger width refers to the Al screen-opening width, and the Al area fraction includes the fingers and busbars.)

is determined by four-point probe measurements on final PERC+ solar cells and on test wafers with and without LCOs below the Al fingers. When the finger length and the average cross-sectional area of the Al fingers as measured with an optical profilometer are taken into account, the calculation of the specific resistivity of the Al fingers works out to be $20 \pm 5 \mu\Omega\text{cm}$. Interestingly, very similar values are obtained with and without LCOs beneath the Al fingers, indicating that the Al-Si eutectic layer below the Al fingers provides only a minor contribution to the lateral conductivity. The series resistance contribution of the Al finger grid, calculated on the basis of the layout and the specific resistivity, is $0.1 \Omega\text{cm}^2$; this represents a relative increase of 20% compared with the total series resistance of $0.55 \Omega\text{cm}^2$ of the monofacial reference PERC cells. The relatively small resistance contribution of the Al finger grid, despite the rather high specific resistivity, is a consequence of the five-busbar grid design, which reduces the grid line resistance because of the reduced finger length compared with conventional three-busbar designs [22].

Another interesting aspect is the impact of the Al finger grid on the Al-Si contact formation and, in particular, on the depth of the Al-BSF. Fig. 3 shows two typical scanning electron microscope (SEM) images of the resulting local aluminium contacts for the monofacial reference PERC cell as well as for the bifacial PERC+ cell: the depth of the Al-BSF of the monofacial reference PERC cell (Fig. 3(a)) is $3.5 \pm 1.5 \mu\text{m}$ (taken as the average value of eight measured local Al contacts), whereas the bifacial PERC+ cell (Fig. 3(b)) exhibits Al-BSF depths of $5.5 \pm 1.5 \mu\text{m}$ [23]. The increased Al-BSF depth in the case of the bifacial PERC+ cell is due to the Al finger layout. During furnace firing, silicon from the wafer diffuses through the laser contact opening into the Al paste layer [24]. During the cool-down phase, the liquid silicon in the aluminium layer epitaxially regrows at the silicon wafer surface, incorporating Al up to the solid-solubility limit, thereby forming the Al-BSF.

In the full-area Al layer, the area of high silicon content is $520 \mu\text{m}$ wide, as can be observed in the darker busbar area on the light microscope image in Fig. 4. The wide Si out-diffusion leads to low silicon concentrations in the aluminium layer, and hence to shallow Al-BSF depths. This effect has been quantitatively described in Müller et al. [25] and Lauermann et al. [26]. In contrast, in the case of the PERC+ cells, the Al finger confines the silicon diffusion to the Al finger width, as illustrated in Fig. 4, leading to higher silicon concentrations in the Al finger, and hence deeper Al-BSFs. Additionally, for the PERC+ cells the depth of the Al-Si eutectic layer is found to be shallower than for the PERC cells, as seen in Fig. 3; moreover, the number of voids in the local Al contacts is significantly reduced for the PERC+ cells compared with the PERC cells. It is very likely that both effects are a consequence of the confinement of the silicon diffusion of the Al grid, since the higher Si content in the Al grid reduces the chemical potential gradient that drives the Si diffusion from the silicon wafer to the Al finger. The reduced number of voids contributes to the deeper Al-BSF of the PERC+ cells, since quite often voids cause locally shallower Al-BSFs. The deeper Al-BSF lowers the contact recombination [27] and hence potentially enables higher open-circuit voltages to be obtained with PERC+ solar cells.

“The deeper Al-BSF lowers the contact recombination and hence potentially enables higher open-circuit voltages to be obtained with PERC+ solar cells.”

THE FASTEST WAY TO

GET INTO

PERC!



G.PLASMA

The most versatile PECVD system for anti-reflective coatings, passivation and masking layers

- Dielectric AlO_x / SiN_x stack with best passivation properties
- More than 5% abs. higher uptime compared to inline systems
- Low cost of ownership due to optimized CAPEX, less maintenance, low TMA consumption and minimum footprint
- Fast and easy upgrade of all centrotherm PECVD systems with minimum space requirements

www.centrotherm-pv.com



UPGRADE SOLUTION OR
COMPLETE SYSTEM AVAILABLE
WITH SHORT DELIVERY TIME

I-*V* parameters of bifacial PERC+ solar cells processed at ISFH

The current–voltage (*I*–*V*) parameters of the PERC and PERC+ cells under study are measured in-house at ISFH directly after processing, since previous results [28] have shown that PERC cell efficiencies measured directly after processing are comparable to the efficiencies measured after boron-oxygen deactivation (e.g. by thermal

treatment). The monofacial PERC solar cells are measured using a reflective brass chuck, which electrically contacts the full rear surface of the solar cell. The *I*–*V* tester is calibrated using an ISE CalLab certified monofacial reference PERC solar cell.

The best monofacial PERC cell of group 1 in Table 1 achieves 21.1% efficiency η , as shown in Table 2; the average efficiency of all five corresponding PERC cells is 20.9%.

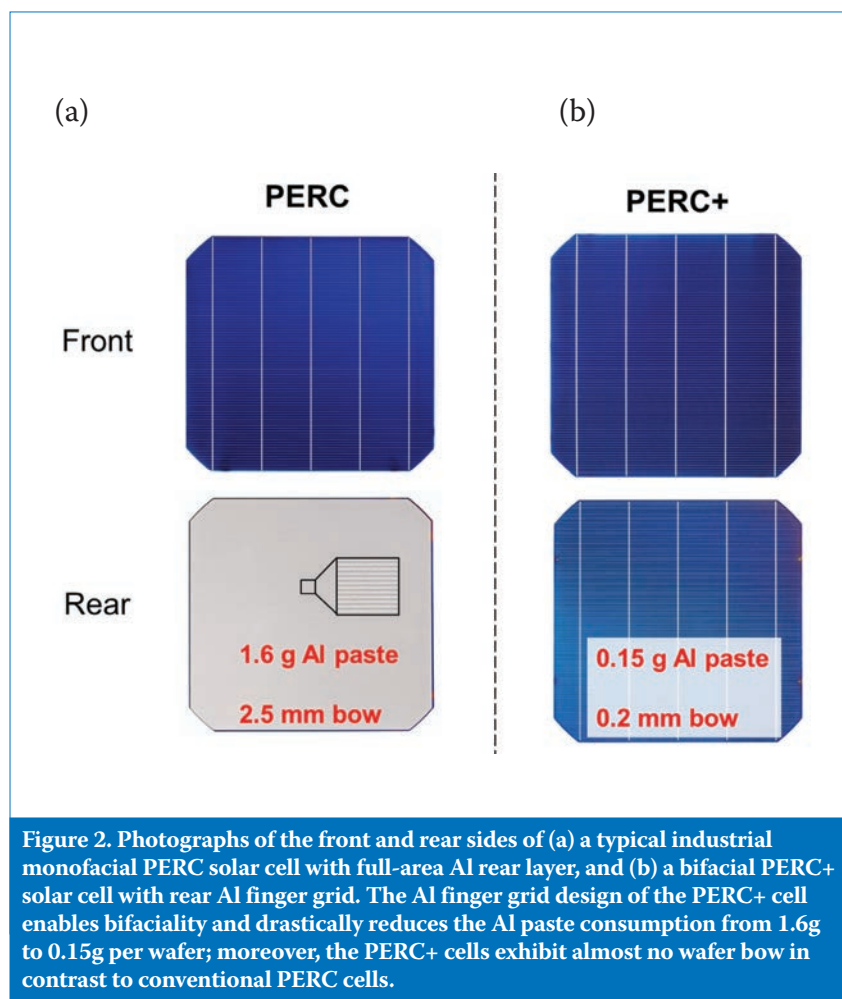
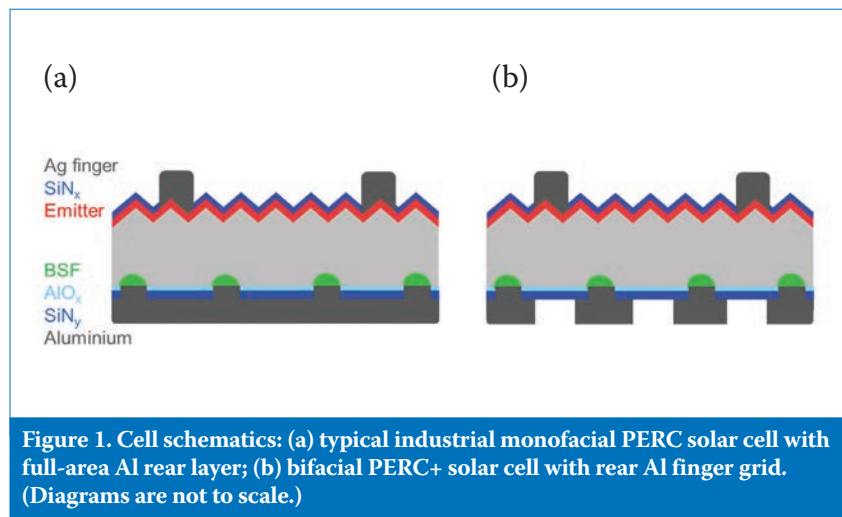
The bifacial PERC+ cells are measured in-house at ISFH using the same *I*–*V* tester and the same calibration method as for the monofacial PERC cells. When the reflective brass chuck, which contacts the full-rear Al grid, is used, the best PERC+ cell demonstrates 21.5% efficiency, as shown in Table 2 [29]. The average efficiency of all seven corresponding PERC+ cells is 21.0%.

The short-circuit current density J_{sc} for the PERC+ cell is 40.1 mA/cm², and hence slightly higher than the J_{sc} of 39.8 mA/cm² for the PERC cell. The open-circuit voltage V_{oc} for the PERC+ cell is 666 mV, and hence 6 mV higher than the V_{oc} of 660 mV for the monofacial PERC solar cell. The higher V_{oc} of the PERC+ cells is due partly to the deeper Al-BSF (as shown in Fig. 3) and partly to the larger LCO pitch of the PERC+ cells (see Table 1).

The PERC+ cells exhibit on average a 0.5% abs. lower *FF* and a 0.13 Ω cm² higher series resistance R_s compared with the average values for the monofacial PERC cells when both are measured with the full-area contacting brass chuck. This difference in series resistance is due to the larger LCO pitch (see Table 1) of the PERC+ cells, which (according to the model of Saint-Cast [30]) increases the spreading resistance of the wafer bulk from 0.2 Ω cm² for the PERC cells to 0.3 Ω cm² for the PERC+ cells.

To assess the bifacial performance of the PERC+ cells, for example when installed in bifacial glass–glass modules, the PERC+ cells are measured using a black chuck, where the front and rear metal grids are contacted at only the five busbars, and not at the fingers. With front-side illumination (Ag metal grid), the PERC+ cell in Table 2 achieves an efficiency of 21.2%, which is 0.3% abs. lower than the corresponding *I*–*V* measurement with the brass chuck. The reasons for this are twofold: 1) the J_{sc} is 0.2 mA/cm² lower when measured with a black chuck, since the reflected light of the brass chuck is absent; 2) the *FF* is on average 0.4% lower when measured with the black chuck, since now the resistance of the Al finger grid contributes to the total series resistance R_s . The average R_s value of all PERC+ cells when measured with the black chuck was found to be 0.77 Ω cm², and hence 0.12 Ω cm² higher than the measurement with the brass chuck. This measured value corresponds well to the calculated series resistance of the Al finger grid of 0.10 Ω cm², as explained in the previous section.

When illuminated from the rear side (Al metal grid), the PERC+ cells exhibit



efficiencies of up to 16.6%, as shown in Table 2. The short-circuit current J_{sc} is only $31.3\text{mA}/\text{cm}^2$, and hence $8.6\text{mA}/\text{cm}^2$ lower than the measurement with front-side illumination; this is the main reason for the considerably lower rear-side efficiency. The V_{oc} values of the PERC+ cells when illuminated from the rear are 6mV lower than with front-side illumination, which is a result of the lower J_{sc} . The root cause of the slightly higher FF values with rear illumination is not yet understood. The front- and rear-side efficiencies of respectively 21.2% and 16.6% correspond to a bifaciality $B = \eta_{\text{rear}}/\eta_{\text{front}} = 78\%$. Other PERC+ cells of this batch demonstrated slightly higher bifacialities, of up to 80%

Quantum efficiency and reflectance of bifacial PERC+ solar cells

The internal quantum efficiency (IQE) and the reflectance of the monofacial PERC solar cell in Table 2 are measured using a brass chuck, whereas for the PERC+ cell in Table 2 a black chuck illuminated from the front side is used. As shown in Fig. 5, both the IQE (top curves) and the reflectance (bottom curves) of the PERC and PERC+ cells are very similar. However, at a wavelength of around $1,100\text{nm}$, the PERC+ cell exhibits slightly higher IQE values than those for PERC cells, indicating reduced carrier recombination at the rear surface or rear Al contacts in the case of the PERC+ cells.

The reflectance of the PERC+ cell is then measured again by gluing a white backsheet foil onto the black measurement chuck. This measurement set-up is intended to assess the effective rear-side reflectance of the PERC+ cells when used in conventional modules with a white backsheet. As can be seen in Fig. 5, the reflectance increases from 0.44 to 0.51 at a wavelength of $1,200\text{nm}$ when measured with a white backsheet instead of the black chuck.

The values for the rear reflectance R_b , the Lambertian fraction Λ , and the effective rear-surface recombination velocity S_{rear} are extracted by means of analytical modelling [31]; these are summarized in Table 3.

The S_{rear} values for the PERC cells are around 100cm/s ; the PERC+ cells achieve S_{rear} values below 40cm/s , which is the resolution limit for this methodology, indicating that Al contact recombination is reduced because of the increased Al-BSF depth.

The R_b values of around 88% are

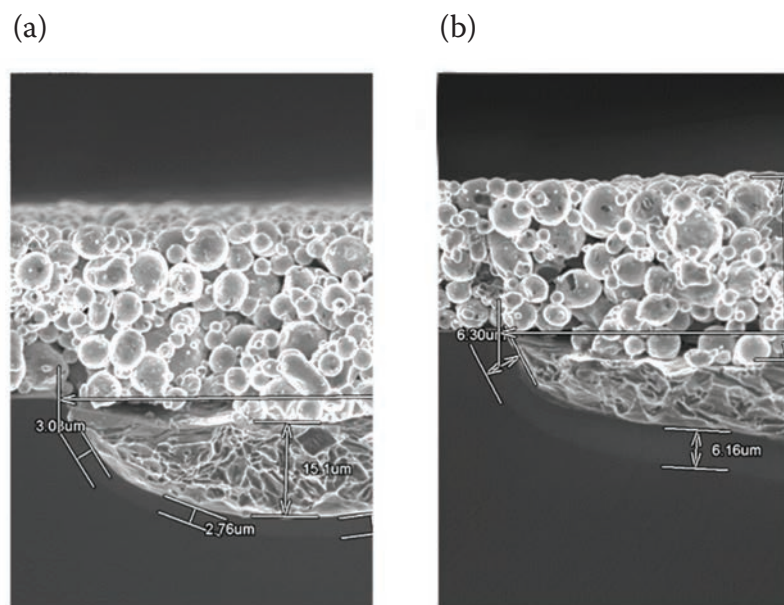


Figure 3. SEM images of the local aluminium contacts: (a) monofacial reference PERC cell; and (b) bifacial PERC+ cell. The deeper Al-BSF of the bifacial PERC+ cells is a result of confinement of the silicon diffusion to the Al finger width (as shown in Fig. 4).

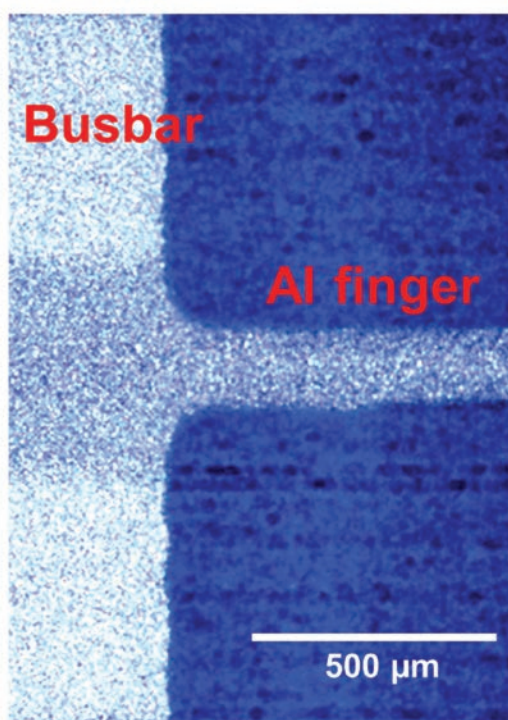


Figure 4. Light microscope image of the Al finger grid, displaying a part of the busbar on the left and one Al finger on the right. The darker area in the middle of the busbar shows the area of increased silicon content in the Al paste, caused by the Si diffusion from the wafer through the LCO into the Al paste during furnace firing. The width of the area with high Si content is in the range of $520\mu\text{m}$ and hence similar to that for PERC cells with full-area rear Al layer. In contrast, the Al finger confines the Si diffusion to the Al finger width, resulting in higher Si concentrations in the Al paste during furnace firing, and hence in deeper Al-BSFs (as seen in Fig. 3).

Group	Solar cell type	Al area fraction [%]	Side of illumination	Chuck type	η [%]	J_{sc} [mA/cm ²]	V_{oc} [mV]	FF [%]	R_s [Ω cm ²]
1	PERC	100	Front	Brass	21.1	39.8	660	80.5	0.53
2	PERC+	14.2	Front	Brass	21.5	40.1	666	79.7	0.55
2	PERC+	14.2	Front	Black	21.2	39.9	666	79.1	0.67
2	PERC+	14.2	Rear	Black	16.6	31.3	660	80.7	0.60

Table 2. Solar cell parameters measured at ISFH under AM1.5 standard test conditions of the best monofacial PERC cell of group 1 and of the best bifacial PERC+ cell of group 2 in Table 1. Both cells were measured using a brass chuck; additionally, the PERC+ cell was measured using a black chuck that was illuminated from either the front or the rear, in order to assess the bifaciality.

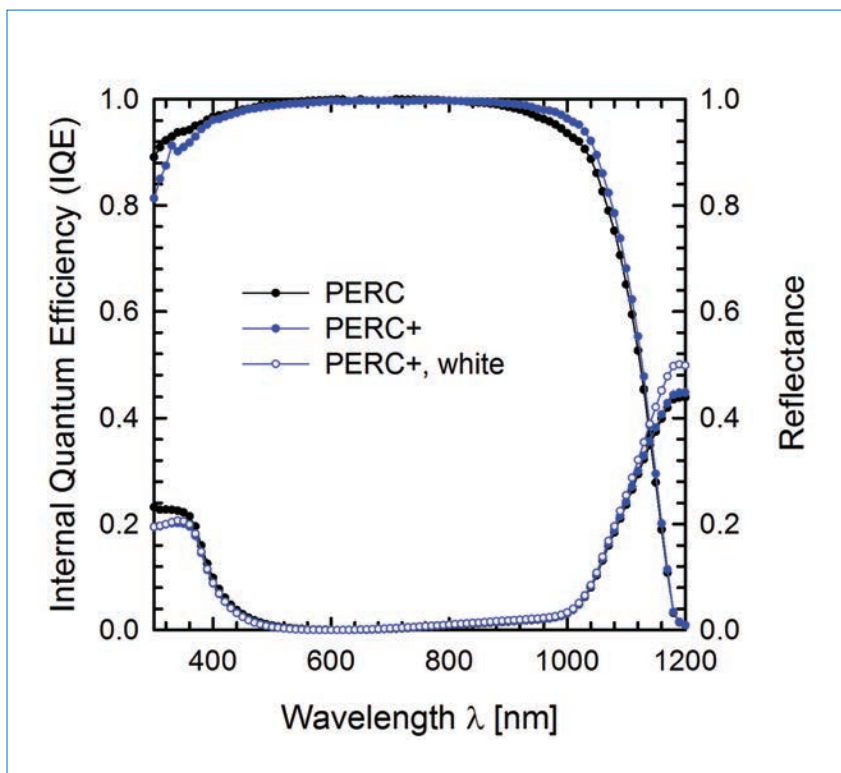


Figure 5. IQE (top curves) and reflectance (bottom curves) of the bifacial PERC+ cell and the monofacial PERC cell in Table 2, measured with front-side illumination (Ag grid). For both IQE and reflectance, the PERC cell was measured using a brass chuck, whereas the PERC+ cell was measured using a black chuck. Additionally, the reflectance of the PERC+ cell with a white backsheet glued on the chuck was measured, resulting in the highest reflectance in the long-wavelength regime.

very similar for both PERC+ cells (measured with a black chuck) and monofacial PERC cells. The R_b value increases to 90.4%, however, when the PERC+ cell is measured with the white chuck. The increase in R_b from 88.1% (black chuck) to 90.4% (white chuck) corresponds to an increase in J_{sc} of 0.17 mA/cm², as calculated with the solar cell analysis software SCAN, which was developed in-house and uses the analytical model for the QE introduced in Brendel et al. [31]. This value is in good agreement with the measured increase in J_{sc} of 0.2 mA/cm² when the $I-V$

measurements of the PERC+ cell in Table 2 with a brass chuck and a black chuck are compared.

Pilot production of bifacial PERC+ cells at SolarWorld

As mentioned earlier, in parallel to the bifacial PERC+ development at ISFH, SolarWorld has been independently pursuing the bifacial PERC+ cell process, described in this section, with feasibility studies on their Solar Cell Pilot Line at SolarWorld Innovations having begun in 2014. The monofacial production baseline PERC solar cell process was

modified to achieve suitable bifaciality of the resulting cells, without major modifications of the well-established production process. A transfer to mass production (announced at the end of 2014 [32]) has been successfully accomplished, and novel glass–glass bifacial modules based on this bifacial PERC+ cell variant were launched at Intersolar 2015 [33], introducing the added value to the PV industry of bifacial modules based on a very simple, lean and cost-effective bifacial cell process.

Starting with the monofacial production baseline PERC solar cell process, the following process steps have been modified: 1) the SiN capping layer of the rear passivation; 2) the ablation pattern of the contact openings; and 3) the Al grid. The bifacial PERC+ solar cell process was tested in a pilot production run, consisting of 100,000 bifacial cells with three busbars, on the PERC solar cell production line at SolarWorld. The average $I-V$ parameters of the bifacial PERC+ solar cells are very similar to those of the monofacial PERC production baseline. The efficiency of the PERC+ solar cells is marginally lower (1.5% rel.) than that of the monofacial PERC cells; the reasons for this are mainly the increased series resistance of the Al grid compared with a full-area Al contact and the inferior passivation quality of the rear stack with a reduced thickness of the SiN capping layer. The bifaciality $B = \eta_{rear}/\eta_{front}$ of the PERC+ cells is in the range 63–65%. Process development is ongoing in order to increase front-side efficiencies and bifaciality. Transparent glass–glass modules were built from these bifacial PERC+ cells: Fig. 6 gives a visual impression of a module from the rear and front sides. Note that the module bifaciality is higher than the cell bifaciality because of light-trapping effects.

In order to analyse the consumer benefits of the bifacial PERC+ modules, simulations of the annual energy yield

CONFERENCE **PVCELLTECH**

📍 Kuala Lumpur, Malaysia 📅 16 - 17 March 2016

The only event where senior decision makers of the top-20 c-Si cell manufacturers in the solar industry today showcase their technology roadmaps for 2016/17

Over 25 speakers confirmed including:



Holger Neuhaus,
Managing Director,
SolarWorld Innovations



Dr Hao Jin, Chief
Scientist, **JinkoSolar**



Paul Ni, CTO,
Zhongli Talesun



Hannes Rostan,
CTO, **REC Solar**



Pierre Verlinden,
Chief Scientist and Vice-
Chair of the State Key
Laboratory of PV Science and
Technology, **Trina Solar**



Peter Cousins,
VP Technology &
Development, **SunPower**



Markus Fischer,
Director R&D Processes,
Hanwha Q-Cells



Akira Terakawa,
Eco Solutions Company,
Panasonic Corporation

Confirmed Technical Advisory Board:

- Finlay Colville (PV-Tech, Conference Chair) • Pierre Verlinden (Trina Solar) • Markus Fischer (Hanwha Q-Cells)
- Peter Pauli (Meyer Burger) • Fokko Pentinga (Amtech) • Christian Buchner (Schmid) • Weiming Zhang (Heraeus)
- Don Cullen (MacDermid) • Homer Antoniadis (DuPont) • Armin Aberle (SERIS) • Mark Osborne (PV-Tech)
- David Owen (PV-Tech)



Why attend?

- Find out how PERC upgrades and expansions will evolve in the next two years and how you should prepare now
- Discover the key factors driving high-efficiency upgrades for both mono and multi cell lines
- Understand cell manufacturing capex plans from the leading producers in the industry

**To get involved either as a speaker,
partner or attendee please contact
Rosie: rriley@solarmedia.co.uk**

celltech.solarenergyevents.com



Group	PERC type	Chuck type	R_b [%]	Λ [%]	S_{rear} [cm/s]
1	PERC	Brass	87.8	69.2	128
2	PERC+	Black	88.1	67.4	< 40
2	PERC+	White	90.4	67.8	–

Table 3. Rear reflectance R_b , Lambertian fraction Λ , and effective rear-surface recombination velocity S_{rear} , as extracted from the IQE and reflectance measurements of the PERC and PERC+ cells in Fig. 5. The PERC+ cell measured with a white backsheets yields the highest R_b value of 90.2%, demonstrating the benefit of the external rear reflector, as sketched in Fig. 8(b)).



Figure 6. Rear and front sides of an industrial three-busbar bifacial PERC+ module, launched as the SolarWorld Sunmodule Protect 360° duo at Intersolar 2015 [33].

were carried out for various module-mounting surfaces having different albedo values. Fraunhofer ISE kindly provided these simulations, which used an in-house simulation package to calculate the annual energy yield of module installations, taking into account the local conditions of direct and diffuse light, ground reflection and shadowing effects.

Fig. 7 shows the simulated increase in annual energy yield for a PERC+ module with an STC front power of 270W and a bifaciality of 70%. In this simulation the modules were south oriented at a 30° tilt and landscape mounted, with several modules per row and a row pitch of 2.5m; a central location in Germany was also chosen. Depending on ground reflection, an increase of up to 25% in energy yield was predicted in the simulation. Note that normal grassland has an albedo of around 20%, whereas sand has an albedo of up to 40%. With optimized mounting systems, in combination with special reflective elements (e.g. white roof top foil), an albedo of up to 80% is possible.

Five bifacial PERC+ modules and one reference PERC module were installed in Freiberg, with a mounting configuration indicated by the yellow star in Fig. 7, and a predicted increase in energy yield of 5%. On the basis of the first measurements of these modules in June 2015, the PERC+ modules achieved a 5.5% higher energy yield than monofacial PERC reference modules. These outdoor measurements therefore provide an initial verification of the simulation, as well as reinforcing the increases in annual energy yield of bifacial PERC+ modules.

Conclusions and outlook

A novel industrial PERC solar cell design, given the name ‘PERC+’, which entails the screen printing of an Al rear metal grid instead of the conventional full-area aluminium rear metallization, has been introduced. The resulting Al finger grid, in combination with the five-busbar layout, corresponds to a metallization area fraction of 14.2%. Accordingly, the Al paste consumption of the PERC+ cells is considerably reduced to 0.15g per wafer, which compares with 1.6g per wafer for conventional PERC cells with a full-area Al layer. In contrast to conventional PERC cells, the PERC+ cells, because of the symmetric device structure, exhibit no wafer bow.

The specific Al grid line resistance has been determined to be $20 \pm 5 \mu\Omega/\text{cm}$, which corresponds to a series resistance contribution of $0.1 \Omega/\text{cm}^2$ from the five-busbar Al finger grid.

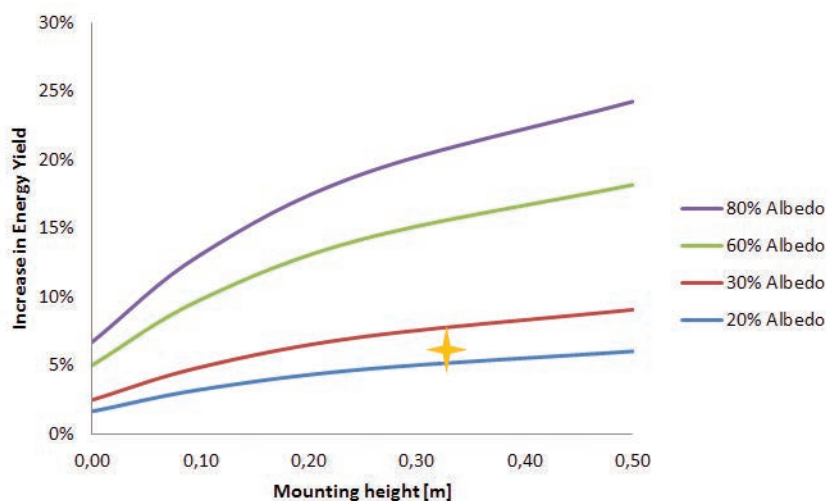


Figure 7. Simulated increase in annual energy yield for PERC+ modules compared with PERC modules, for various installation heights and albedo values of the ground at a central location in Germany. The yellow star indicates the installation conditions of the field test (grassland, 30cm above ground), with a predicted increase in energy yield of around 5%.

The slightly increased series resistance of the PERC+ cells decreases the efficiency by approximately 0.2% abs. Compared with full-area Al rear layers, the Al fingers confine the Si diffusion during furnace firing to the Al finger width; this leads to higher Si concentrations in the Al-Si melt, and hence to a deeper Al-BSF of 5.5 μm , as opposed to 3.5 μm for the full-area Al layer. The deeper Al-BSF reduces the rear contact recombination and hence increases the V_{oc} of PERC+ cells to 666mV, compared with 660mV for conventional PERC cells.

The PERC+ cells achieve front-side efficiencies, measured with a black chuck, of up to 21.2% and rear-side efficiencies of up to 16.6%, which equates to a bifaciality factor of 78%. PERC+ cells can therefore be used in bifacial module designs, such as the glass-glass module depicted in Fig. 8(a). The rear-side efficiency of 16.6% is limited mainly by the high Al metallization fraction of 14.2% and by the high reflection of the polished and passivated rear surface.

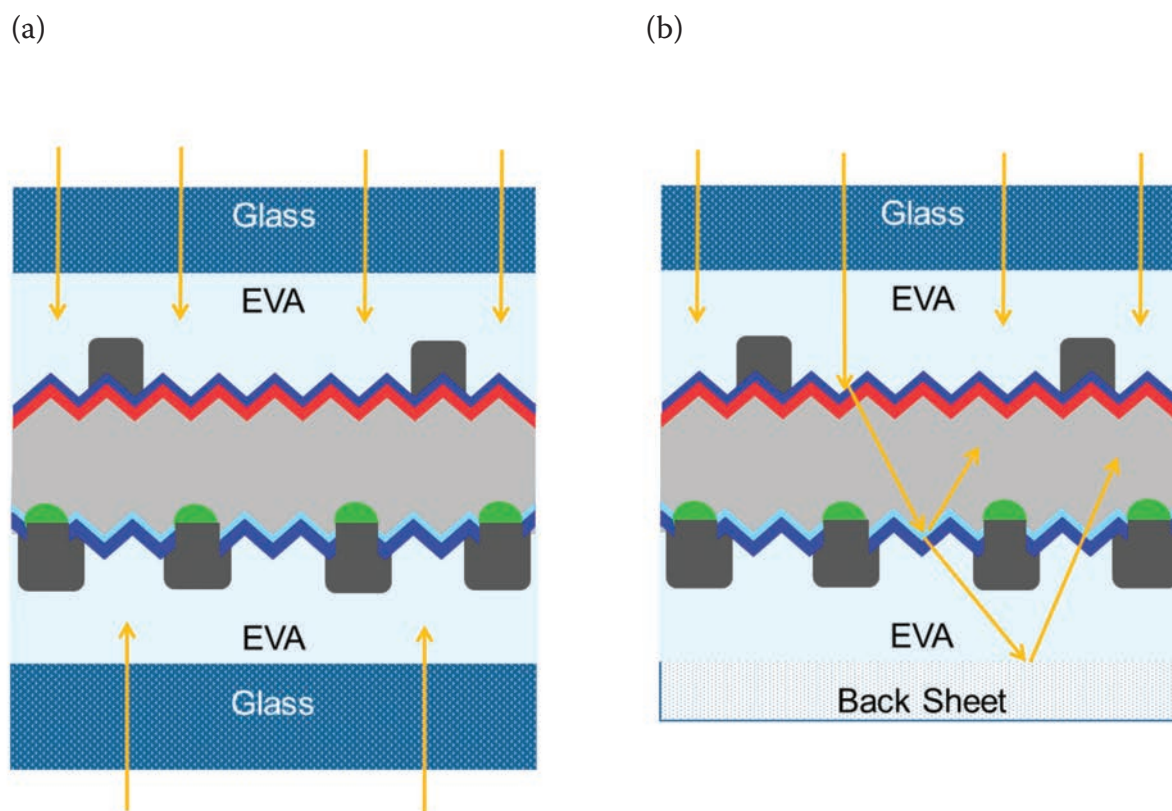


Figure 8. Schematic drawings of two potential applications of PERC+ solar cells: (a) bifacial glass-glass modules; (b) monofacial modules with a white backsheet, which serves as an external rear reflector for the PERC+ cells, leading to a higher effective rear reflectance compared with monofacial PERC cells (see Table 3).

“Bifacial modules incorporating PERC+ cells demonstrate an increase in annual energy yield between 5 and 25% in simulations.”

When a white backsheet is placed at the rear of the PERC+ cell, similarly to the set-up of a conventional monofacial module, the white backsheet acts as an external rear reflector, increasing the rear reflectance of the PERC+ cells by 2.3%, to a value of 90.4%. Accordingly, when PERC+ cells are incorporated in a monofacial module with a white backsheet, as shown in Fig. 8(b), the higher Al grid resistance is compensated by the deeper Al-BSF and higher rear reflectance, leading to PERC+ efficiencies that are at least comparable to those of monofacial PERC cells. The best PERC+ efficiency is 21.5%, measured with a reflective brass chuck contacting the full Al finger grid. In summary, the PERC+ concept reduces the Al paste consumption by a factor of 10, enables bifacial applications, and performs on a par with conventional monofacial PERC cells when incorporated in monofacial modules with a white backsheet.

In addition to the results obtained at ISFH, a very similar bifacial PERC+ solar cell process has been independently developed by SolarWorld. To the authors' knowledge, SolarWorld is the first industry player to pioneer this cell technology employing an industrially relevant cell process. Novel glass–glass bifacial modules based on this cell technology and with a three-busbar layout were launched successfully at Intersolar 2015. These new bifacial modules incorporating PERC+ cells demonstrate an increase in annual energy yield of between 5 and 25% in simulations. The first outdoor measurements have been performed and corroborate the simulation results. Further development of the process is under way, with the aim of increasing front-side efficiencies and bifaciality.

Acknowledgements

We thank our ISFH colleagues K. Bothe, T. Brendemühl and T. Gandy for their help in obtaining the *I*–*V* measurements, and R. Brendel for his continued support of the industrial cell research at ISFH. Furthermore, we would like to acknowledge the support of D. Schulze and K. Meyer of SolarWorld in transferring the process to a mass-production

environment and running the first pilot runs. Many thanks also to C. Reise from Fraunhofer-ISE for providing simulations of the annual energy yield of bifacial PERC+ modules under different installation conditions. Parts of this work were funded by the German Federal Ministry for Economic Affairs and Energy under Contract No. 0325716A.

References

- [1] Fischer, G. et al. 2015, “Model based continuous improvement of industrial p-type PERC technology beyond 21% efficiency”, *Proc. 5th SiliconPV*, Konstanz, Germany.
- [2] SolarWorld 2015, Press Release (Mar.) [<http://www.solarworld.de/en/group/investor-relations/news-announcements/corporate-news/single-ansicht/article/solarworld-expands-production-in-arnstadt/>].
- [3] Hanwha Q CELLS 2015, Press Release (Apr.) [<http://investors.hanwha-qcells.com/releasedetail.cfm?ReleaseID=907243>].
- [4] Verlinden, P.J. et al. 2014, “Strategy, development and mass production of high-efficiency crystalline silicon PV modules”, *Proc. 6th WCPEC*, Kyoto, Japan.
- [5] Trina Solar 2015, Press Release (Jan.) [http://www.pv-tech.org/news/trina_solar_starts_perc_technology_volume_production].
- [6] SEMI PV Group Europe 2015, “International technology roadmap for photovoltaic (ITRPV): 2014 results”, 6th edn (Apr.) [<http://www.itrpv.net/Reports/Downloads/>].
- [7] Blakers, A.W. et al. 1989, “22.8% efficient silicon solar cell”, *Appl. Phys. Lett.*, Vol. 55, pp. 1363–1365.
- [8] Guo, S. et al. 2013, “Vertically mounted bifacial photovoltaic modules: A global analysis”, *Energy*, Vol. 61, pp. 447–454.
- [9] Janssen, G.J.M. et al. 2015, “Outdoor performance of bifacial modules by measurements and modelling”, *Proc. 5th SiliconPV*, Konstanz, Germany.
- [10] Romijn, I.G. et al. 2013, “Industrial cost effective n-PASHA solar cells with >20% cell efficiency”, *Proc. 28th EU PVSEC*, Paris, France, pp. 736–740.
- [11] Song, D. et al. 2012, “Progress in n-type Si solar cell and module technology for high efficiency and low cost”, *Proc. 38th IEEE PVSC*, Austin, Texas, USA, pp. 3004–3008.
- [12] Mihailetchi, V.D. et al. 2010, “Screen printed n-type silicon solar cells for industrial application”, *Proc. 26th EU PVSEC*, Hamburg, Germany, pp. 1446–1448.
- [13] Larionova, Y. et al. 2015, “Industrial ion implanted co-annealed and fully screen-printed bifacial n-PERT solar cells with low-doped back-surface fields”, Presentation at 5th nPV Worksh., Konstanz, Germany.
- [14] Taguchi, M. et al. 2014, “24.7% record efficiency HIT solar cell on thin silicon wafer”, *IEEE J. Photovolt.*, Vol. 4, pp. 96–99.
- [15] Strahm, B. et al. 2014, “The Swiss Inno-HJT project: Fully integrated R&D to boost Si-HJT module performance”, *Proc. 29th EU PVSEC*, Amsterdam, The Netherlands, pp. 467–471.
- [16] Steckemetz, S. et al. 2001, “Thin Cz-silicon solar cells with rear silicon nitride passivation and screen printed contacts”, *Proc. 17th EU PVSEC*, Munich, Germany, pp. 1902–1905.
- [17] Cesar, I. et al. 2008, “Benchmark of open rear side solar cell with improved Al-BSF process at ECN”, *Proc. 23rd EU PVSEC*, Valencia, Spain, pp. 1770–1775.
- [18] Vermont, P. et al. 2012, “Spatial ALD Al₂O₃ film integrated in low-cost, high-performance bifacial solar cells”, *Proc. 27th EU PVSEC*, Frankfurt, Germany, pp. 1757–1760.
- [19] Teppe, A. et al. 2014, “Novel technology approach based on standard quality mc wafer achieving solar cell efficiencies significantly above 18% in an industrial production environment”, *Proc. 29th EU PVSEC*, Amsterdam, The Netherlands, pp. 1310–1313.
- [20] Teppe, A. et al. 2015, “Bifacial multicrystalline solar cells with efficiencies above 18% processed in an industrial production environment”, *Proc. 30th EU PVSEC*, Hamburg, Germany.
- [21] Hannebauer, H. et al. 2014, “21.2%-efficient fineline-printed PERC solar cell with 5 busbar front grid”, *physica status solidi (RRL)*, Vol. 8, pp. 675–679.
- [22] Dullweber, T. et al. 2014, “Fineline printed 5 busbar PERC solar cells with conversion efficiencies beyond 21%”, *Proc. 29th EU PVSEC*, Amsterdam, The Netherlands, pp. 621–626.
- [23] Dullweber, T. et al. 2015, “PERC+: Industrial PERC solar cells with rear Al grid enabling

bifaciality and reduced Al paste consumption", *Prog. Photovoltaics Res. Appl.* [forthcoming].

- [24] Urrejola, E. et al. 2011, "Silicon diffusion in aluminum for rear passivated solar cells", *Appl. Phys. Lett.*, Vol. 98, p. 153508.
- [25] Müller, J. et al. 2012, "Modeling the formation of local highly aluminum-doped silicon regions by rapid thermal annealing of screen-printed aluminum", *physica status solidi (RRL)*, Vol. 6, pp. 111–113.
- [26] Lauermann, T. et al. 2013, "Diffusion-based model of local Al back surface field formation for industrial passivated emitter and rear cell solar cells", *Prog. Photovoltaics Res. Appl.*, Vol. 23, pp. 10–18.
- [27] Gatz, S. et al. 2012, "Analysis and optimization of the bulk and rear recombination of screen-printed PERC solar cells", *Energy Procedia*, Vol. 27, pp. 95–102.
- [28] Dullweber, T. et al. 2013, "Silicon wafer material options for highly efficient p-type PERC solar cells", *Proc. 39th IEEE PVSC*, Tampa, Florida, USA, pp. 3074–3078.
- [29] Dullweber, T. et al. 2015, "The PERC+ cell: A 21%-efficient bifacial PERC solar cell", *Proc. 30th EU PVSEC*, Hamburg, Germany.
- [30] Saint-Cast, P. 2012, "Passivation of Si surfaces by PECVD aluminum oxide", Ph.D. dissertation, University of Konstanz, Germany.
- [31] Brendel, R. et al. 1996, "Quantum efficiency analysis of thin-layer silicon solar cells with back surface fields and optical confinement", *IEEE Trans. Electron Dev.*, Vol. 43, pp. 1104–1113.
- [32] *Handelsblatt* 2014, "Asbeck versucht Neustart", Newspaper Article (Dec. 15).
- [33] SolarWorld 2015, Press Release (May) [http://www.pv-tech.org/news/intersolar_europe_solarworld_to_launch_glass_glass_bifacial_modules].

About the Authors



Dr. Thorsten Dullweber leads the industrial solar cells R&D group at ISFH. His research focuses on high-efficiency industrial-type PERC silicon solar cells and ultra-fine-line screen-printed Ag front contacts. Before joining ISFH in 2009, Dr. Dullweber worked for nine years as a project leader in the microelectronics

industry at Siemens AG and later at Infineon Technologies AG.



Christopher Kranz received his diploma degree in physics from the University of Münster in 2011, after which he started a Ph.D. programme at ISFH in the industrial solar cells R&D group. He currently carries out research on screen-printed solar cells with passivated emitter and rear side.



Dr. Robby Peibst received his diploma degree in technical physics in 2005. In 2010 he received his Ph.D. from the Leibniz University of Hanover, with a thesis on germanium-nanocrystal-based memory devices. He joined ISFH in 2010 and has led the emerging solar technologies group since 2013. His research focuses on the development of techniques enabling the production of high-efficiency silicon solar cells.



Ulrike Baumann graduated in 2011 as a laboratory technical assistant in chemistry, after which she joined the industrial solar cells R&D group at ISFH, where she is in charge of processing industrial PERC solar cells. She is also responsible for the optimization and maintenance of a production-type wet-chemical batch processing tool.



Helge Hannebauer studied technical physics at the Leibniz University of Hanover from 2005 to 2009. The work for his diploma thesis, carried out at ISFH, involved the optimization of screen-printed solar cells. In 2010 he started his Ph.D. at ISFH, focusing on advanced screen printing and selective emitters.

Alexander Fülle received his diploma degree in technical physics from the University of Applied Sciences Zwickau (FH) in 2006, after which he spent two years in the microsystems department there. Since 2008 he has been working at SolarWorld, where he leads the process integration team.

Stefan Steckemetz received his diploma in technical physics from the University of Applied Sciences Aachen in 1993. He then worked on crystalline

Si solar cells at ISFH and Sunways AG, and joined SolarWorld in 2006, where he focuses on screen-printing metallization for high-efficiency solar cells.



Torsten Weber received his diploma degree in physics from the University of Hanover in 2006. He currently works as a senior R&D engineer at SolarWorld, where his research and expertise focus on the transfer and integration of high-efficiency solar cell and module concepts, from the laboratory scale to high-volume production.



Dr. Matthias Müller received his diploma degree in physics from Leipzig University in 2009, followed by his Ph.D. from Leibniz University Hanover in 2014. From 2007 he worked for Q-Cells SE, GP Inspect GmbH and Magdeburg-Stendal University of Applied Sciences, before joining SolarWorld in 2011, where he is responsible for numerical device simulation.

Dr. Phedon Palinginis leads the solar cell development group at SolarWorld. Before joining the company in 2006, he investigated dipole and spin coherences in semiconductor nanostructures as a doctoral/postdoctoral researcher at the Universities of Oregon and California (Berkeley). He holds a degree in physics from the University of Karlsruhe.



Dr. Holger Neuhaus received his degree in physics and his Ph.D. from the Universities of Hanover and New South Wales in 1998 and 2002 respectively. He then worked at Pacific Solar as a characterization engineer. In 2003 he joined the SolarWorld Group, and since 2009 he has been the MD of its R&D organization.

Enquiries

Thorsten Dullweber
Institute for Solar Energy Research
Hamelin (ISFH)
Am Ohrberg 1
D-31860 Emmerthal
Germany

Tel: +49-5151-999-638
Email: t.dullweber@isfh.de
Website: www.isfh.de

Metallization: The technology with highest efficiency gain potential for c-Si cells

Radovan Kopecek, Lejo J. Koduvelikulathu, Enrique Cabrera, Dominik Rudolph & Thomas Buck, International Solar Energy Research Center (ISC) Konstanz, Germany

ABSTRACT

This paper summarizes the status and potential of screen-printing technology, and describes the results and thoughts of ISC Konstanz relating to the present and future of metallization technology. A microstructural investigation of contact formation and the possible electrical transport mechanism from the emitter into the metal finger is briefly discussed. In addition, the simulation results using Silvaco, which model the drop in V_{oc} due to so-called *metal-induced recombination*, are presented. Several options for reducing this recombination in order to improve solar cell efficiency are then proposed.

Introduction

In the last few years, efficiencies of 20% have been achieved with industrial-standard screen-printed passivated emitter and rear cell (PERC), passivated emitter and rear totally diffused (PERT) and interdigitated back contact (IBC) solar cells; even higher efficiencies have been demonstrated by some companies (e.g. TRINA, Solar World, LG electronics, Motech, ISC Konstanz with BiSoN and ZEBRA).

PERC p-type, and in particular PERT and IBC n-type, solar cells are almost perfect devices before undergoing screen-printing metallization. Implied open-circuit voltages (V_{oc}) of more than 700mV are achievable, before a screen-printing firing step is performed. During this step, recombination takes place underneath the metal fingers, causing one of the major losses in the finished device; in some cases, the resulting V_{oc} is reduced to a value of around 650mV, which is detrimental. If the V_{oc} could be kept at the same level as that before metallization, the efficiency could be increased by about 1.5% abs. This can be achieved by the use of (for example):

- Softer non-fire-through pastes, in combination with laser contact opening
- Evaporated contacts
- Plating (on the top as well)
- Passivated contacts

These and many other topics – for example replacing Ag by Cu, making plating more robust,

understanding the mechanism behind screen printing, and industrially interconnecting cells with conductive adhesives – have been discussed at metallization workshops organized in the last two years by ISC Konstanz [1]. ISC Konstanz's results and opinions regarding the present and future of metallization technology are presented in this paper.

Status of standard metallization

"Soccer is so popular, because it's a simple game." These words of wisdom could also loosely apply to the relationship of screen printing to solar cell metallization. Although there have been many efforts to replace screen printing in the past 10 years, this has never happened: the technique remains by far the predominant way

of establishing local metal contacts on crystalline solar cells.

"Amazing progress has been made in the field of paste development."

Apart from the convenience and the long-term experience in the PV industry of using screen printing, amazing progress has been made in the field of paste development. The workhorse and symbol for the technique's remarkable evolution are the silver pastes for front-side metallization. Excellent contact formation, for sheet resistances above $90\Omega/\text{sq.}$ and surface concentrations of $10^{20}/\text{cm}^3$, of phosphorus-doped emitters can be obtained with commercial fire-through silver pastes

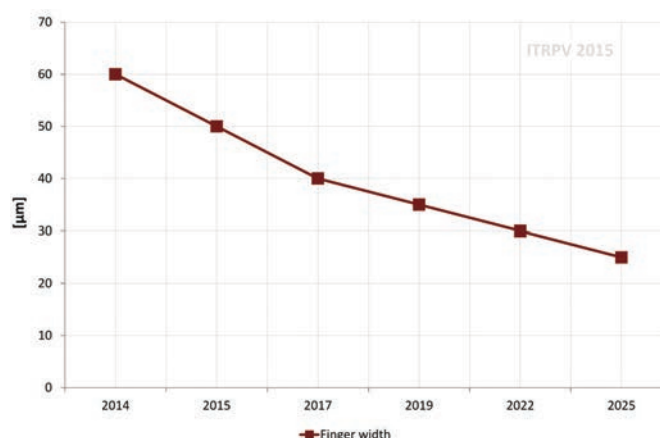


Figure 1. Predicted trend of finger width in screen printing, according to the ITRPV roadmap [2].

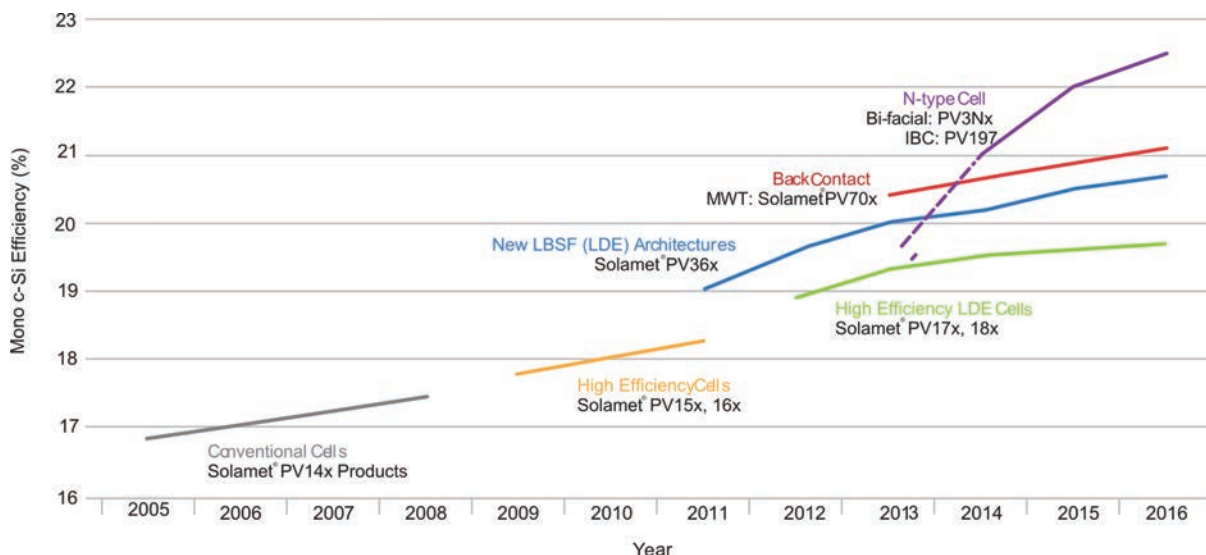


Figure 2. DuPont Solamet roadmap [3].

from various paste manufacturers.

At the same time, a reduced line resistance, mainly because of the high solid content of the metal paste, and an improved printability at a high aspect ratio, have opened the way for fine-line printing in the range of 30µm-wide apertures. In combination with the employment of finer mesh materials for the screens and innovative emulsion materials, a successful implementation was possible. As a consequence, the consumption of Ag paste was reduced, resulting in material costs savings of almost 70–100%. And this trend of narrower finger widths continues: as indicated in Fig. 1, according to the ITRPV roadmap [2], the finger width is expected to decrease further, to 25µm, in the next decade.

As an additional benefit of the thinner lines, the shadowing losses have also decreased. Increasing the number of busbars on the wafer to four or five and simultaneously minimizing their widths have also helped to reduce losses and to adapt to the improved power output of the devices. The enormous flexibility and demonstrated potential for cost reduction have so far curbed (at least for standard solar cells) any efforts to switch to another metallization approach. Fig. 2 illustrates – for example – how the paste supplier DuPont has customized its paste technology to different solar cell concepts over the last 10 years and contributed continuously

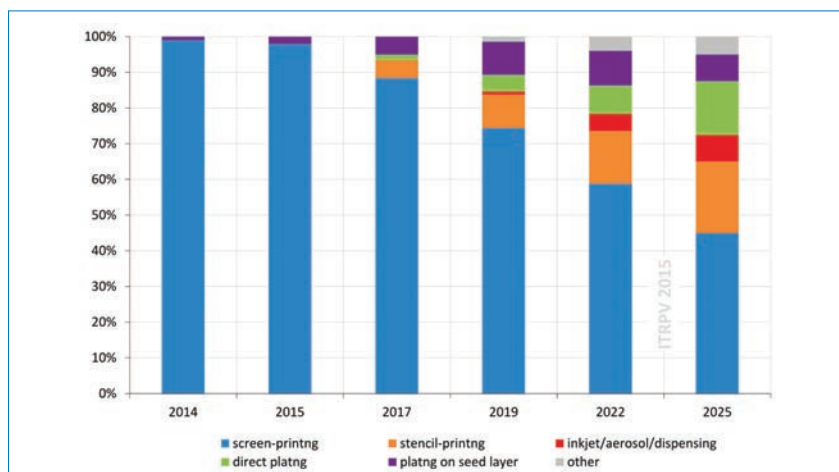


Figure 3. Trend of different metallization technologies, predicted by the ITRPV roadmap [2].

evolving products for improving device performance levels. This example is representative of the ongoing evolution of the entire solar cell industry in the last few years.

Potential of screen printing

Again, on a football theme, the German writer Ernst Probst once wrote: “The most important thing in football is the opponent. Nobody likes him but without him you cannot start.” This is also true for the free-market economy, and especially for the field of solar cell metallization; without the competition of other metallization schemes, screen printing would not

be where it is today. There are several other metallization techniques, such as seed and plate, inkjet printing, laser transfer printing, aerosol printing, flexographic printing and dispensing [4–8]. Most of these were developed by research institutes and never found their way into commercial production; some made it to production but failed, and others are still in development and might one day replace screen printing in solar cell metallization.

Because of its dominant status, screen printing is the benchmark process for the industrial application of metallization: the simple maintenance, low breakage rate (<0.15%) and inline throughput of 3,200 wafers/hour

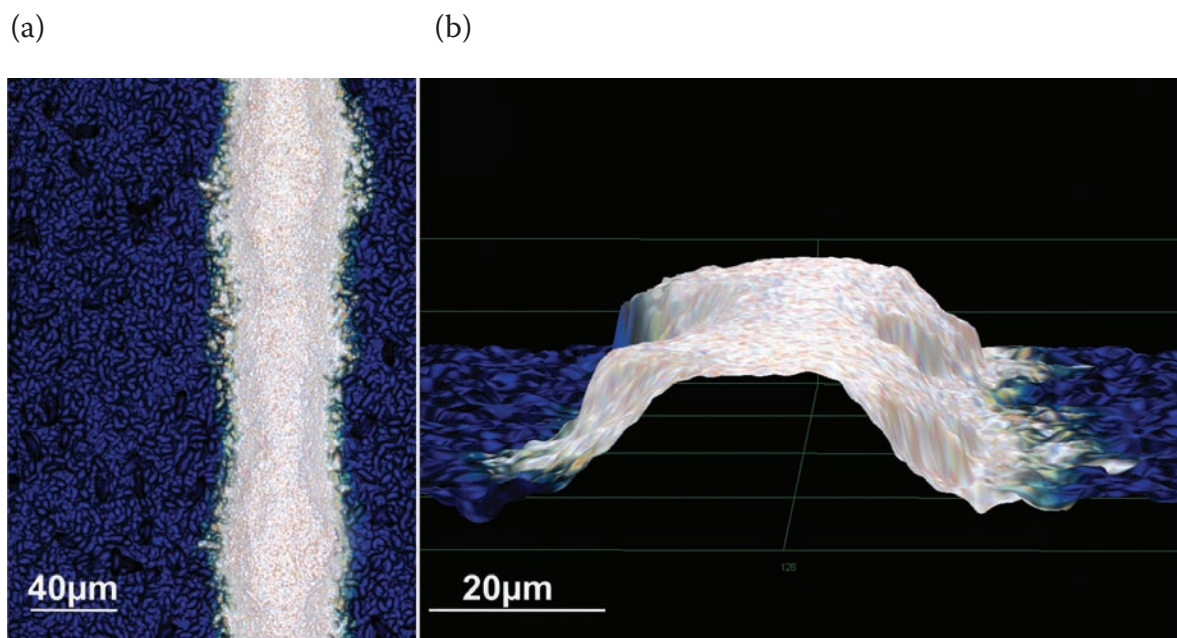


Figure 4. Ag finger, screen printed using the double-printing technique: (a) top view; (b) 3D image. (Images taken by laser scanning microscopy.)

collectively make up the standard to be beaten. To evaluate future potential, two questions are of significance: is the technology still compatible with cell concepts of the future, or even beneficial, and can it be implemented at competitive costs compared with alternative techniques? On the one hand, the convenience of a solution (such as the one represented by screen printing) that incorporates in one step the contact formation through a dielectric layer and good adhesion is attractive. On the other hand, the high-temperature steps required for sintering that are mainly used at present may cause problems and limitations for high-efficiency solar cells.

The improvements described above for silver fine-line pastes are a key benefit. Another is the enormous set of parameters that can be covered by this method with the use of various metal pastes. There have been many niche products in the past that were tailored to special requirements and trends, such as via pastes for metal wrap-through (MWT) applications or non-fire-through silver pastes that helped to avoid recombination losses. The simple combination of different materials, such as aluminium and silver, by spatially resolved patterns represents a platform for further adaptations. The competition of different paste suppliers guarantees further innovation in this field. A technique that could draw on these advantages, without the claim of a radical technological U-turn, is stencil printing; the roadmap shown in Fig. 3

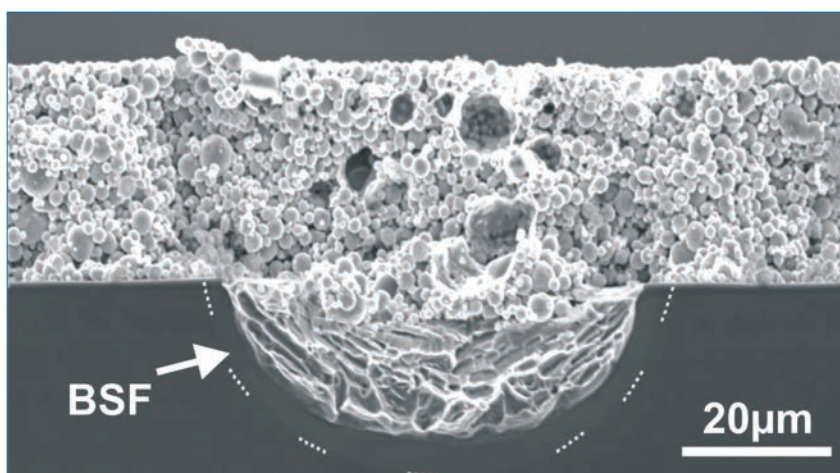


Figure 5. SEM cross-sectional view of the Al BSF of a locally opened passivated rear-side solar cell [12].

predicts that this metallization method represents the best opportunities for growth in the future. Thick-film paste technology, however, is still expected to dominate the market over the next 10 years.

Some representative thick-film pastes are discussed next, to illustrate the wide range that is available.

“Silver is currently the chief material used for fine-line fire-through metallization of passivated phosphorus emitters.”

Ag pastes

As already mentioned, silver is currently the chief material used for fine-line fire-through metallization of passivated phosphorus emitters and probably will remain so during the next few years. Improvements to glass additives have reduced the performance losses caused by the metallization. Research into the mechanisms for contact formation will make it possible to contact even more lightly doped emitters than those currently used in production, which is discussed in the next section. Fig. 4 shows a screen-printed Ag finger line manufactured by the double-printing technique.



SOLAR MEDIA

2016 INTERNATIONAL EVENTS

Business critical events for solar and clean energy industry professionals

SOLAR FINANCE & INVESTMENT SERIES

INCORPORATING: Solar Asset Management | 1 February 2016

MEET EUROPE'S BIGGEST ASSET OWNERS AND BUYERS

1-3 February 2016 | Grange City Hotel, London, UK
finance.solarenergyevents.com

Future Events in: India - June/July 2016
New York - October



DESIGNED TO CONNECT ENERGY USERS WITH INSTALLERS

March & April 2016 | Locations throughout the UK
ukroadshow.solarenergyevents.com



THE ONLY CTO SOLAR EVENT WHICH ADDRESSES THE
BALANCE BETWEEN COST AND EFFICIENCY

16 - 17 March 2016 | Kuala Lumpur, Malaysia
celltech.solarenergyevents.com

SOLAR & OFF-GRID RENEWABLES WEST AFRICA

ENERGY BUYERS AND THE SOLAR INDUSTRY WILL MEET
TO CLOSE THE POWER GAP

19 - 20 April 2016
westafrica.solarenergyevents.com



INCORPORATING: Solar O&M | Solar & Storage

26 - 28 April 2016 | Twickenham Stadium, UK
summit.solarenergyevents.com

DOING SOLAR BUSINESS IN A NEW MARKET

June 2016
solarenergyevents.com



CO-LOCATED WITH:



4 - 6 October 2016 | NEC, Birmingham, UK
FREE to attend - uk.solarenergyevents.com

INCORPORATING:



BOOK NOW AT www.solarenergyevents.com

Al pastes

Al pastes are a cheap and simple solution for rear-side metallization. Modifications have improved the V_{oc} of standard solar cells [9] in the past. A focus of the development is the tuning of the pastes to the new requirements of a passivated rear side with local contacts [10]. Good adhesion on the dielectric layer and the formation of a passivating back-surface field (BSF) at the contact areas are features of these pastes.

The scanning electron microscope (SEM) cross section in Fig. 5 gives an impression of the dimensions of such a local contact established during the sintering of the Al paste matrix. The interaction of the paste and the silicon is restricted to the area where Al was in direct contact with the silicon. Al paste, however, cannot be easily interconnected with solder contact strings. Applications proposing a treatment with, for example, an adhesion layer could be one solution for economizing expensive silver paste that is still being used for the solder pads [11].

AgAl pastes

Rear-side pad pastes, formerly a mixture of Ag and Al, have been improved in the past by gradually reducing the Ag content in order to cut the costs, while meeting the challenge of avoiding a negative effect on conductivity and solderability. Silver paste with a very small content of Al is still the main candidate for screen-printed contacts on p^+ emitters with low contact resistivity but high recombination because of Al spiking [13].

Cu pastes

A shortage of silver in the future, and the consequential increase in the price, could motivate the use of alternative materials for solar cell metallization. The potential for cost reduction was witnessed in the replacement of silver as the sintered metal. Copper pastes are already the focus of research efforts and could be a substitute for silver, at least for printing non-contacting bus bars [14,15].

The main problems of copper are its high diffusivity into silicon, with a detrimental effect on the minority-carrier lifetime, and its strong

oxidation in ambient air/oxygen, leading to soldering problems. Unless these issues are addressed or avoided, copper pastes will not be a viable candidate for replacing silver pastes.

Microstructure of screen-printed contacts

The contacts on the n-type emitters of industrial crystalline silicon solar cells are mainly formed by firing silver-based, screen-printable, thick-film pastes through passivating silicon nitride anti-reflection coatings, to contact the textured Si surface. The resulting contact resistivities, however, are orders of magnitude higher than the theoretically expected n-type Si emitter/Ag contact resistivities. The contact resistivity is directly related to the solar cell efficiency through the series resistance and thus the fill factor. Emitters with phosphorus surface concentrations well above the P solubility limit in Si are currently necessary in order to achieve acceptable contact quality.

Contrariwise, for achieving the highest solar cell performance,

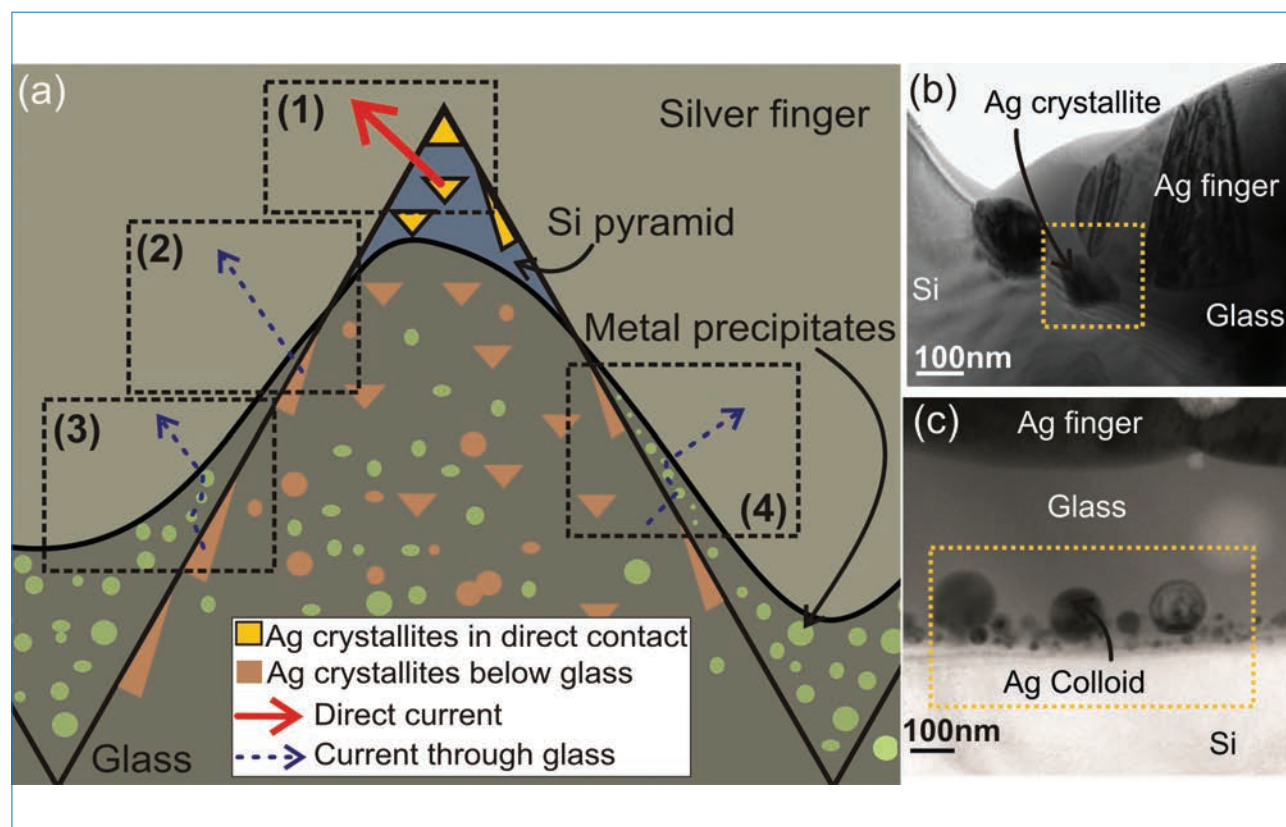


Figure 6. (a) Possible current transport mechanisms in textured Si solar cells [25]: (1) the current flows directly through Ag crystallites into the silver finger [16]; (2) the current flows through the Ag crystallites separated by a thin glass layer from the silver finger bulk [16–20]; (3) the current flows through the Ag crystallites separated from the silver finger by a glass layer, by means of the tunnelling effect due to metal precipitates in the glass [17,18] (the number of these metal precipitates can thereby enhance the conductivity of the glass); (4) the current is transported by means of multistep tunnelling from the n^+ emitter into the silver finger across nano-Ag colloids in the glass layer [21]. (b) TEM cross-sectional view of a Ag crystallite in direct contact with the silver finger. (c) TEM cross-sectional view of nano-Ag colloids in the glass layer close to the Si emitter.

emitters with low surface doping are desirable, and flat surfaces need to be contacted in the case of advanced concepts, such as the IBC solar cell; both of these requirements have the goal of minimizing recombination losses. For the fabrication of those highly efficient solar cells by the most cost-effective metallization technique available, namely screen-printing, it is therefore essential to understand, and thus accordingly improve the performance of, thick-film metallization.

Even though the continual progress in Ag paste manufacturing allows the contacting of higher-resistivity emitters without the need for a selective emitter or subsequent plating, there are still open questions: for example, how are the new pastes able to achieve better contact, and what is the dominant conduction mechanism of screen-printed Ag contacts on n^+ Si emitters? Fig. 6 illustrates the two current-transport models that are predominant in the literature [16–24], namely:

1. The current flows through the Ag crystallites grown into the Si emitter; these are separated by a thin glass layer or possibly in direct contact with the silver finger. See Fig. 6(a):(1),(2),(3), and Fig. 6(b).
2. The current is transported by means of multistep tunnelling into the silver finger across nano-Ag colloids in the glass layer; these are formed under optimal firing conditions and in locations where the formation of Ag crystallites into the Si surface is synonymous with over-firing. See Fig. 6(a):(4), and Fig. 6(c).

The most widely accepted model for explaining contact formation is that described in Schubert [17]: Ag crystallites grown into the Si are formed as a result of the redox reaction between silicon and metal oxides contained within the glass. Additional studies indicate that Ag crystallites result from the reaction between the dissolved Ag^+ and O_2 ions in the molten glass and the Si wafer, without the aid of liquid Pb formation [22] or Bi formation [23]. This reaction is strongly dependent on the ambient oxygen content during the firing process [23,24].

Microscopic investigations suggest that the largest influence on the topography-dependent contact resistance comes from the surface-sharpness-dependent glass coverage governing the number of Ag crystallites in direct contact with the

silver finger bulk [26]. Experimental evidence indicates that the major current flow into the silver finger is through Ag crystallites that are directly touching the silver finger [27]. The presence of glass-free regions, necessary for the direct connection of the Ag crystallites with the silver finger in order to achieve good-quality contact, depends on the paste composition and on the surface texture, and does not vary with the Si emitter properties [25]. Nevertheless, whether or not the Ag crystallites are in direct contact with the silver finger or in quasi-direct contact (separated from it by a very thin glass layer of less than 1nm) will continue to be up for discussion. The presence of Ag crystallites, however, is required for the transmission of the current. If it were possible to avoid the Ag crystallite formation while retaining a low specific contact resistance, an ideal

contact could be achieved, because there would be no metal penetration into the emitter, and therefore no contact-induced recombination losses; these losses are the main efficiency-limiting factor at present, as discussed in the next section.

“Contact-induced recombination losses are the main efficiency-limiting factor at present.”

Modelling of metal-induced recombination

From experimental observations of internal quantum efficiency (IQE) measurements, for samples with various metallization fractions, one could deduce the cause of the V_{oc}

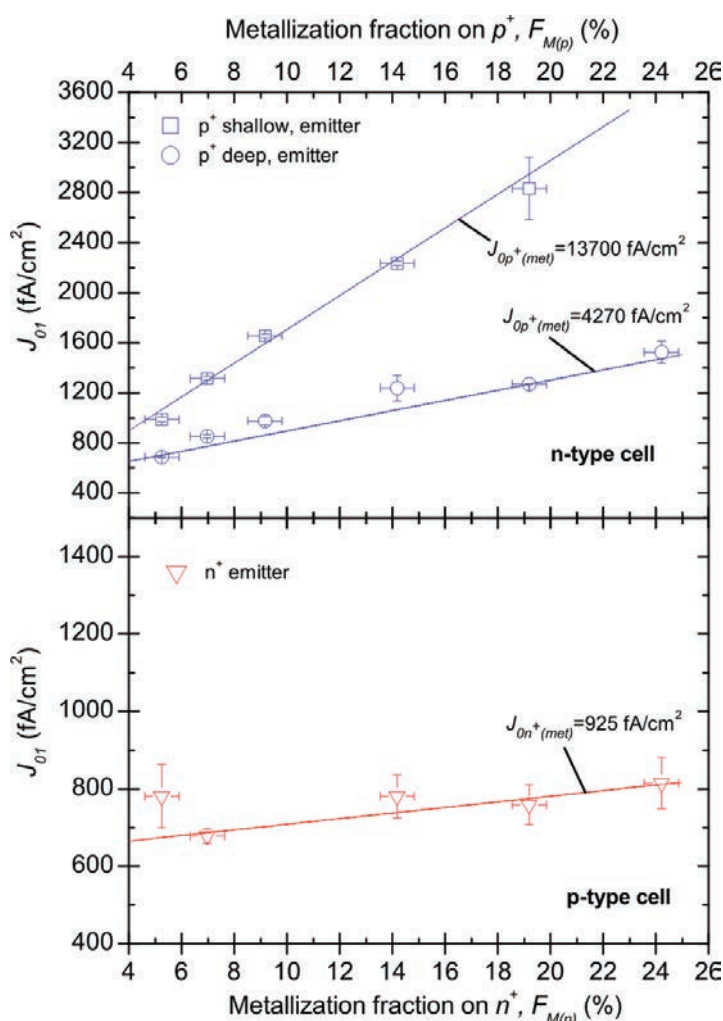


Figure 7. Modelling metallization-induced recombination losses. Experimental J_{01} for different metallization fractions on n-type and p-type cells. (Source: Edler et al. [30].)

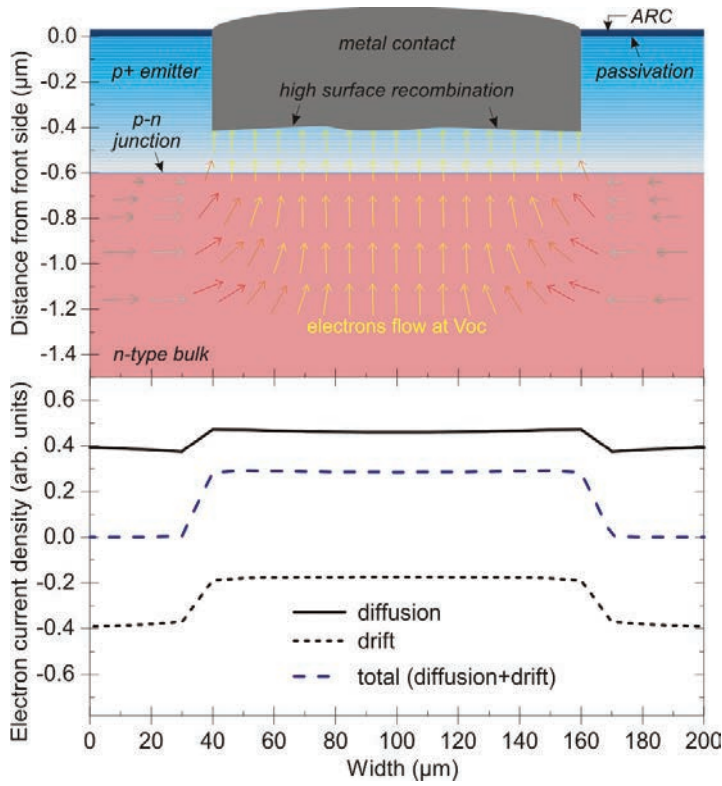


Figure 8. Electron current density map of the region under the p⁺ metal contact. Recombination currents are dominated by the diffusion currents (extracted from the ATLAS device simulation). (Source: Edler et al. [30].)

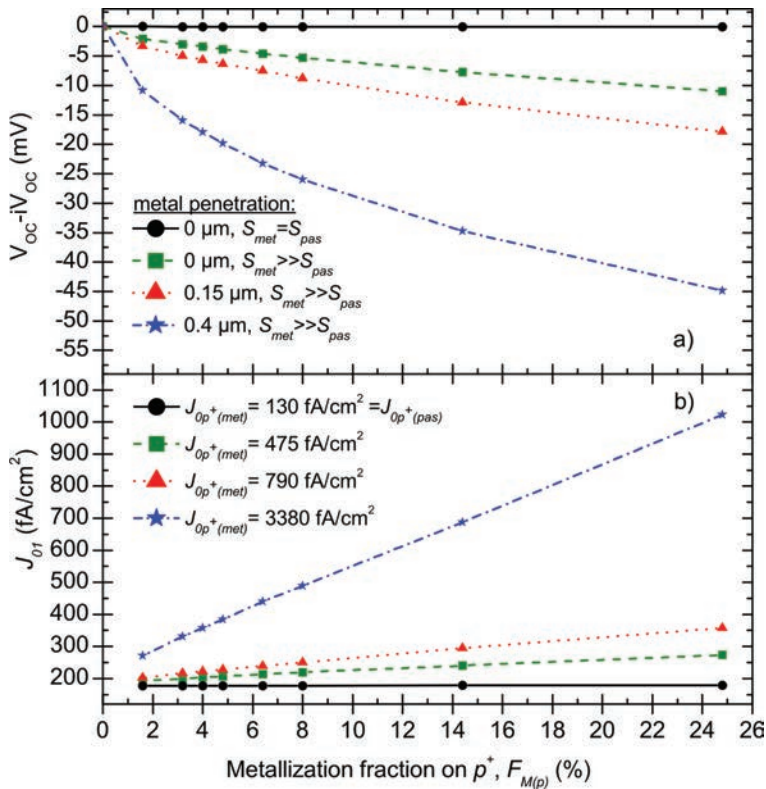


Figure 9. Simulation of the decrease in V_{oc} due to the increased J_{01} under the metal-p⁺ emitter interface, as a function of the fraction of front-side metallization and of the structural details of the p⁺ metal interface. (Source: Edler et al. [30].)

degradation as being a local effect directly beneath the metal contacts, causing an increase in recombination. Fig. 7 shows experimental dark saturation current density under the metal contacts (J_{01}) of a series of samples with different fractions of front-side metallization; the higher the J_{01} , the greater the V_{oc} losses, which reduces cell efficiency. Since J_{01} is much larger for p⁺ emitters than for n⁺ emitters, the recombination underneath the metalized regions of n-type cells limits the efficiencies more severely than it does for p-type cells.

With the use of 2D simulations, an attempt was made to capture and provide insight into the possible local effect causing V_{oc} losses after the metallization step. The ATLAS 2D device simulator tool [28] computes cell performance under V_{oc} conditions. The incorporation of microstructural details of a metal-n⁺ Si interface (p-type cell) into the simulation model classifies the role of each interface component with respect to the overall recombination under the metal contacts, and establishes a structural property correlation [29].

In order to reproduce the experimental V_{oc} , a series of simulations were performed with the assumption that the metal contact penetrates into the p⁺ emitter at various depths. The simulation model assigns a surface recombination velocity $S_{met} = 1 \times 10^7$ cm/s to an unpassivated ohmic contact between the metal and Si interface. The surface recombination velocity of the passivated area between the metal contacts, S_{pas} , is determined by means of a numerical fit to the experimental IQE measurements.

A highly recombinative (unpassivated) interface reduces the shielding of the diffused emitter layer and attracts minority-charge carriers (electrons) in the emitter; this phenomenon is captured in Fig. 8, which shows an ATLAS snapshot of drift and diffusion currents beneath the metal contact at V_{oc} conditions. The volume beneath the metal contact becomes depleted of electrons because of the highly recombinative interface, resulting in a leakage current across the junction due to diffusion. With increasing metal penetration, the leakage current also increases, and thus the overall dark saturation current density (J_{01}) of the cell increases.

Fig. 9 shows an estimate of the V_{oc} loss as a function of metallization fraction for different metal penetrations and interface conditions. The (metal contact) etching of the diffused emitter region during the

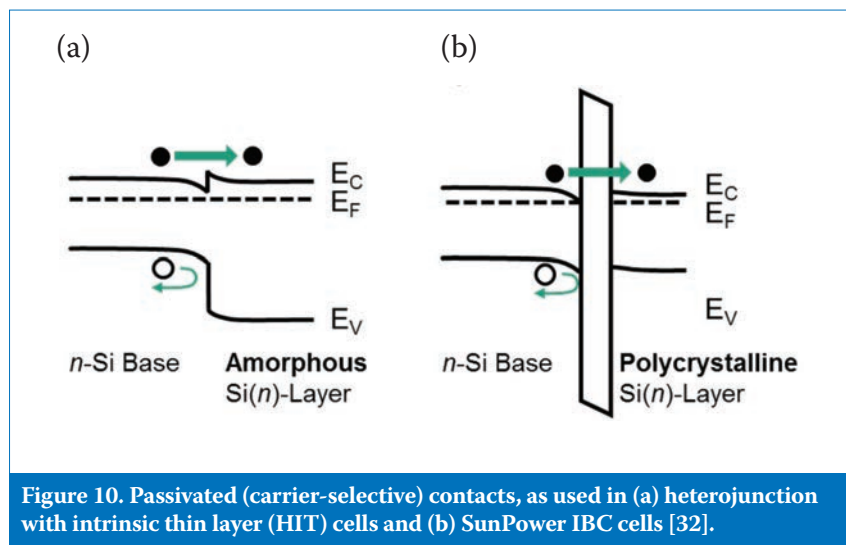


Figure 10. Passivated (carrier-selective) contacts, as used in (a) heterojunction with intrinsic thin layer (HIT) cells and (b) SunPower IBC cells [32].

firing process degrades the metal–Si interface. With increased damage to the diffused emitter, the leakage current increases and thus J_{01} increases.

Although the simulation model is a simplified representation of the actual process taking place, it does capture two important features: 1) the strong local increase in recombination, resulting in a leakage current across the junction; and 2) the reduction in the shielding effect of the diffused emitters as the metal penetrates into the Si, or the Si is etched by the glass frit. Using screen printing, a simple method to minimize the metal-induced recombination loss and the metal coverage on the emitter surface is to print floating busbars and thinner fingers; softer non-firing fingers in combination with laser ablation also demonstrate potential improvement of the cell V_{oc} [31], in addition to a reduced usage of expensive Ag. Evaporated and plated contacts also reduce the degradation of the metal–Si interface, thus offering the potential of overall lower cell J_{01} , which results in higher efficiencies.

“With further development of the metallization process, there is still significant potential for device efficiencies to reach the theoretical limit for c-Si.”

Summary and outlook

In recent years, it has mostly been screen-printing technology and the development of screen-printable metal pastes that has been responsible for the efficiency increases in the case of c-Si

solar cells. And this does not appear to be the end of it, since with further development of the metallization process, there is still significant potential for device efficiencies to reach the theoretical limit for c-Si. Similarly to c-Si being the dominant technology in the PV sector, screen-printing metallization will remain the dominant metallization technology for the next few years. Although alternative technologies, such as plating, remain of interest, they still need to prove their competitiveness in terms of robustness and cost.

What will surely also be implemented in low-cost devices in the future are passivated (or carrier-selective) contacts, similar to what Panasonic or SunPower are using to achieve the highest V_{oc} s. The Panasonic contacts, shown in Fig. 10(a), are based on amorphous Si as a passivation layer, whereas the SunPower version, shown in Fig. 10(b), uses a 1–1.5nm thin oxide and highly doped polycrystalline Si layer on top. FhG ISE also recently presented their TOPCon 4cm² solar cell, which boasts an efficiency of 25.13% and a V_{oc} of 718mV [32]. In order to be cost-effective, however, even this technology could (and may have to) be combined with low-temperature firing screen-printing pastes.

The future of metallization for c-Si solar cells is discussed in depth, and new findings presented by international scientists and industry, at the almost yearly metallization workshops organized by ISC Konstanz, other metallization specialists and various companies/organizations [1].

References

- [1] 6th Workshop on Metallization & Interconnection for Crystalline Silicon Solar Cells, May 2–3, 2016, Konstanz, Germany [http://www.

metallizationworkshop.info].

- [2] SEMI PV Group Europe 2015, “International technology roadmap for photovoltaic (ITRPV): 2014 results”, 6th edn (Apr.), Revision 1 (Jul.) [http://www.itrpv.net/Reports/Downloads/].
- [3] DuPont 2014, “DuPont™ Solamet® photovoltaic metallizations” [http://www.dupont.com/content/dam/assets/products-and-services/solar-photovoltaic-materials/assets/DEC-Solamet-Brochure.pdf]
- [4] Bartsch, J.M. 2009, “Advanced front side metallization for crystalline silicon solar cells with electrochemical techniques”, Ph.D. dissertation, Albert Ludwig University of Freiburg, Germany.
- [5] Tous, L. et al. 2015, “Evaluation of advanced p-PERL and n-PERT large area silicon solar cells with 20.5% energy conversion”, *Prog. Photovoltaics Res. Appl.*, Vol. 5, No. 2, pp. 660–670.
- [6] Mette, A. et al. 2007, “Metal aerosol jet printing for solar cell metallization”, *Prog. Photovoltaics Res. Appl.*, Vol. 15, No. 7, pp. 621–627.
- [7] Lorenz, A. et al. 2015, “Comprehensive comparison of different fine line printing technologies addressing the seed and plate approach with Ni-Cu-plating”, *Proc. 31st EU PVSEC*, Hamburg, Germany, pp. 732–736.
- [8] Pospischil, M. et al. 2015, “Dispensing technology on the route to an industrial metallization process”, *Energy Procedia*, Vol. 67, pp. 138–146.
- [9] Rauer, M. et al. 2010, “Effectively surface-passivated aluminum-doped p⁺ emitters for n-type silicon solar cells”, *physica status solidi (a)*, Vol. 207, No. 5, pp. 1249–1251.
- [10] Uruena De Castro, A. et al. 2009, “Local Al-alloyed contacts for next generation Si solar cells”, *Proc. 24th EU PVSEC*, Hamburg, Germany, pp. 1483–1487.
- [11] Woehl, R. et al. 2015, “All-screen-printed back-contact back-junction silicon solar cells with aluminum-alloyed emitter and demonstration of interconnection of point-shaped metalized contacts”, *Prog. Photovoltaics Res. Appl.*, Vol. 23, No. 2, pp. 226–237.
- [12] Urrejola, E. 2012, “Aluminum-silicon contact formation through narrow dielectric openings: Application to industrial high efficiency rear passivated solar cells”, Ph.D. dissertation,

- University of Konstanz, Germany.
- [13] Riegel, S. et al. 2012, "Review on screen printed metallization on p-type silicon", *Energy Procedia*, Vol. 21, pp. 14–23.
 - [14] Nakamura, K., Takahashi, T. & Ohshita, Y. 2015, "Novel silver and copper pastes for n-type bi-facial pert cell", *Proc. 31st EU PVSEC*, Hamburg, Germany, pp. 536–539.
 - [15] Wood, D. et al. 2015, "Non-contacting busbars for advanced cell structures using low temperature copper paste", *Energy Procedia*, Vol. 67, pp. 101–107
 - [16] Ballif, C. et al. 2003, "Silver thick-film contacts on highly doped n-type silicon emitters: Structural and electronic properties of the interface", *Appl. Phys. Lett.*, Vol. 82, No. 12, pp. 1878–1880.
 - [17] Schubert, G. 2006, "Thick film metallisation of crystalline silicon solar cells", Ph.D. dissertation, University of Konstanz, Germany.
 - [18] Kontermann, S. 2009, "Characterization and modeling of contacting crystalline silicon solar cells", Ph.D. dissertation, University of Konstanz, Germany.
 - [19] Hilali, M.M. et al. 2005, "Understanding and development of manufacturable screen-printed contacts on high sheet-resistance emitters for low-cost silicon solar cells", *J. Electrochem. Soc.*, Vol. 152, No. 10, pp. G742–G749.
 - [20] Hörteis, M. 2009, "Fine-line printed contacts on crystalline silicon solar cells", Ph.D. dissertation, University of Konstanz, Germany.
 - [21] Li, Z., Liang, L. & Cheng, L. 2009, "Electron microscopy study of front-side Ag contact in crystalline Si solar cells", *J. Appl. Phys.*, Vol. 105, No. 6, pp. 066102–066102-3.
 - [22] Hong, K.K. et al. 2009, "Mechanism for the formation of Ag crystallites in the Ag thick-film contacts of crystalline Si solar cells", *Sol. Energy Mater. Sol. Cells*, Vol. 93, No. 6–7, pp. 898–904.
 - [23] Huh, J.Y. et al. 2011, "Effect of oxygen partial pressure on Ag crystallite formation at screen-printed Pb-free Ag contacts of Si solar cells", *Mater. Chem. Phys.*, Vol. 131, No. 1–2, pp. 113–119.
 - [24] Cho, S.B. et al. 2008, "Role of the ambient oxygen on the silver thick-film contact formation for crystalline silicon solar cells", *Curr. Appl. Phys.*, Vol. 10, No. 2, pp. S222–S225.
 - [25] Cabrera, E. et al. 2013, "Impact of excess phosphorus doping and Si crystalline defects on Ag crystallite nucleation and growth in silver screen-printed Si solar cells", *Prog. Photovoltaics Res. Appl.*, Vol. 23, No. 3, pp. 367–375.
 - [26] Cabrera, E. et al. 2012, "Influence of surface topography on the glass coverage in the contact formation of silver screen-printed Si solar cells", *IEEE J. Photovolt.*, Vol. 3, No. 1, pp. 1–6.
 - [27] Cabrera, E. et al. 2011, "Experimental evidence of direct contact formation for the current transport in silver thick film metalized silicon emitters", *J. Appl. Phys.*, Vol. 110, No. 11, pp. 114511–114511-5.
 - [28] SILVACO 2015, ATLAS Device Simulation Framework and TCAD Suite [http://www.silvaco.com].
 - [29] Koduvelikulathu, L. et al. 2015, "Two-dimensional modeling of the metallization induced recombination losses of screen printed solar cells", *IEEE J. Photovolt.*, Vol. 5, No. 1, pp. 159–165.
 - [30] Edler, A. et al. 2015, "Metallization - induced recombination losses of bifacial silicon solar cells", *Prog. Photovoltaics Res. Appl.*, Vol. 23, No. 5, pp. 620–627.
 - [31] Dominik, R. et al. 2014, "Laser ablation of passivation stacks to enable metallization with non-fire-through pastes", *Proc. 29th EU PVSEC*, Amsterdam, The Netherlands, pp. 928–932.
 - [32] Glunz, S.W. et al. 2015, "The irresistible charm of a simple current flow pattern – 25% with a solar cell featuring a full-area back contact", *Proc. 31st EU PVSEC*, Hamburg, Germany, pp. 732–736.

About the Authors



Dr. Radovan Kopecek is one of the founders of ISC Konstanz. He has been working at the institute as a full-time manager and researcher since January 2007 and is currently the leader of the advanced solar cells department. He received his M.S. from Portland State University, USA, in 1995, followed by his diploma in physics from the University of Stuttgart in 1998. The dissertation topic for his Ph.D., which he completed in 2002 in Konstanz, was thin-film silicon solar cells.



Lejo J. Koduvelikulathu has been with ISC Konstanz since 2010, where he works in the field of PV, conducting simulations of solar cell

devices. He received his B.Tech. in electronics and telecommunication engineering from Dr. Babasaheb Ambedkar Technological University, Raigad, India, in 2005, followed by his master's in telecommunication engineering and professional master's in nano-micro systems, both from the University of Trento, Italy, in 2009 and 2010 respectively.



Dr. Enrique Cabrera received his Dipl.-Ing. (honours) in electrical engineering and electrical power systems from the Universidad de Santiago de Chile in 2008. In 2013 he received his Ph.D. in physics in the field of metallization of silicon solar cells at ISC Konstanz in cooperation with the University of Konstanz. He currently heads the BMBF SolarChilD Project and supports R&D cooperative projects in Chile.



Dominik Rudolph studied microsystems engineering in Freiburg and received his diploma in April 2008 with a thesis topic of laser-induced metallization of silicon solar cells from an aqueous electrolyte, the research for which was carried out at Fraunhofer ISE. He joined ISC Konstanz as a scientist in 2009, where he is responsible for the metallization processes and leads the ZIM Alf project, as well as working on the EU Hercules project.



Thomas Buck studied physics at the University of Konstanz, with research for his thesis on the characterization of PEM fuel cells carried out at the Daimler Chrysler Corporation. From 2003 he worked in the field of industrial n-type solar cells at the University of Konstanz, before joining ISC Konstanz in 2008. He is engaged in metallization topics and bifacial solar cells, and is the head of the BMWi IdeAl project. R&D organization.

Enquiries

Enrique Cabrera
International Solar Energy Research Center (ISC) Konstanz

Rudolf-Diesel-Str. 15
78467 Konstanz, Germany

Tel: +49 7531 3618356

Email:

enrique.cabrera@isc-konstanz.de

Website: www.isc-konstanz.de

Metallization and interconnection for silicon heterojunction solar cells and modules

Matthieu Despeisse, Christophe Ballif, Antonin Faes & Agata Lachowicz, CSEM, Neuchâtel, Switzerland

ABSTRACT

Silicon heterojunction (SHJ) solar cells demonstrate key advantages of high conversion efficiency, maximum field performance and simplicity of processing. The dedicated materials, processes and technologies used for the metallization and interconnection of this type of cell are reviewed in this paper. It is shown that fine-line printing, combined with multiple-wire interconnection, allows the cost of cell metallization to be drastically reduced, with as little as 30mg of Ag being used per cell side, which is compatible with high-performance and reliable modules. Copper-plating technology is demonstrated to be applicable to silicon heterojunction solar cells, allowing highly conductive fine fingers as well as high performance. While this process eliminates Ag usage, dedicated low-cost patterning technologies are nevertheless required.

Introduction

Silicon heterojunction (SHJ) technology is triggering a lot of interest in the PV community, owing to the high conversion efficiency achieved at an industrial production level with a limited number of production steps (a prerequisite for keeping costs low). The SHJ cell structure is an excellent demonstration of so-called 'passivating contacts'. Hydrogenated amorphous silicon (a-Si:H) layers and transparent conductive oxide (TCO) layers are deposited on both sides of a textured and cleaned n-type silicon wafer, over the entire surface, forming carrier-selective hetero-contacts with high-passivation properties [1,2].

The intrinsic a-Si:H layers deposited directly on the wafer surfaces provide excellent chemical passivation properties, yielding a minority-carrier lifetime that is potentially on a par with theoretical limits [3]. The doped a-Si:H layers then allow the selective collection of one type of carrier while blocking the other: the p-type doped layer acts as a hole-selective contact, and the n-type doped layer as an electron-selective contact. Finally, the TCO layers enable an efficient contact to be made between the a-Si:H doped layers and the cell metallization, and moreover provide lateral conduction and an anti-reflection effect. The typical structure of an SHJ cell is illustrated in Fig. 1.

“One of the key advantages of the passivated contacts of SHJ solar cells is that increased operating voltages are attainable.”

One of the key advantages of the passivated contacts of SHJ solar cells is that increased operating voltages are attainable; for instance, with this technology open-circuit voltages above 740mV can be achieved on commercial 180µm-thick (nominal thickness) Cz silicon wafers [3–7]. The main performance limitation is then linked to the fact that the full-area hetero-contacts exhibit parasitic light absorption in the thin TCO and a-Si:H layers. Advanced engineering of these layers is therefore required in order to maintain the high operating voltage while maximizing light

transmission. An optimum trade-off can be realized, and an efficiency above 22.5% at the production level can be achieved [6,8]. The hetero-structure can be further optimized, and a record conversion efficiency was recently demonstrated by the company Kaneka in Japan [7] at the R&D level using this SHJ cell structure, with up to 25.1% cell efficiency being achieved on 151.9cm². This is the highest efficiency ever achieved on such an area for a double-side-contacted silicon solar cell, and demonstrates the potential for high performance of the simple SHJ cell architecture.

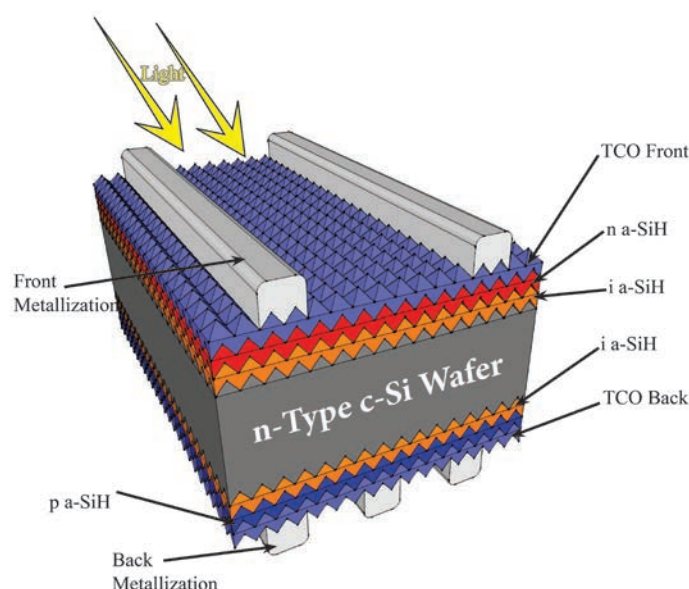


Figure 1. Schematic representation of the symmetrical structure of a bifacial silicon heterojunction solar cell with a rear-emitter configuration.

In addition, SHJ solar cells exhibit a key advantage of maximum field performance, or in other words improved kWh/kWp. These cells have a low temperature coefficient of -0.2 to $-0.3\%/^{\circ}\text{C}$, in contrast to around $-0.4\%/^{\circ}\text{C}$ for standard diffused-junction technologies. Moreover, they are bifacial 'by nature' and can be used and optimized either with the p layer on the sunny side (referred to as a *front-emitter structure*), or with the n layer on the sunny side (referred to as a *rear-emitter structure*). The symmetrical SHJ architecture therefore allows high bifaciality above 90%, and potentially up to 100%. The passivated contacts and symmetrical structure of cells of this type also make them perfectly suited to an efficient use of thin silicon wafers. The excellent surface passivation allows high performance to be maintained, even for thin wafers less than $100\mu\text{m}$ [4], while the symmetrical layer structure on both sides of the wafer equilibrates mechanical stress, reducing the risk of wafer bending and breakage. These factors make SHJ solar cells the technology of choice for pushing forward the industrial implementation of thinner wafers.

The SHJ process sequence is kept simple, with just a few well-established production steps consisting of full-wafer deposition by plasma-enhanced vapour deposition (a-Si:H based layers) and mostly sputtering (TCO), all occurring at a low temperature ($\sim 200^{\circ}\text{C}$). This simple process sequence enables the best efficiency to be achieved.

An intrinsic process limitation of SHJ solar cells, compared with diffused silicon technologies, is the requirement of a low-temperature processing step following the a-Si:H layer depositions, in order to avoid degradation of the passivation properties. At the metallization level this constraint imposes the use of low-temperature-cured Ag pastes, with curing temperatures typically below 250°C . The printing of state-of-the-art low-temperature-cured Ag pastes yields Ag lines demonstrating typical bulk resistivity higher than 6 to $10 \times 10^{-6}\Omega\text{-cm}$, or approximately a factor of two to three times higher than that for state-of-the-art metallization based on the firing-through of high-temperature Ag pastes. The higher Ag line bulk resistance for SHJ solar cells, compared with homojunction solar cells, therefore imposes economical and performance limitations for standard H-pattern metallization with two busbars (2BB) to five busbars

(5BB): not only is more Ag required to achieve similar line resistance, but also lines with higher resistivities or larger dimensions have to be employed. With the use of state-of-the-art low-temperature-cured Ag pastes for H-pattern cells with 3BB to 5BB, improved performance can be achieved by, for instance, multiple printing. A typical laydown mass of 180mg of Ag per side represents a metallization cost of 8\$cts/cell (assuming a Ag price of \$460/kg); for a cell efficiency above 22.5%, the costs are typically ~ 1.5 \$cts/Wp per side, or 3\$cts/Wp for a bifacial cell. (For simplicity, it is assumed that the Ag paste cost is the same as the Ag cost.) To overcome this cost and performance limitation because of the metallization, three approaches are taken: 1) a continuous enhancement of the electrical characteristics of low-temperature cured Ag lines; 2) a switch to multiple-wire interconnection; and/or 3) a switch to copper lines by employing electroplating processes.

Advanced metallization and interconnection for silicon heterojunction solar cells

Screen printing and busbar/ribbon interconnection

In the first approach, as SHJ cell technology continues to attract increasing industrial interest, certain

paste and ink manufacturers continue to improve their low-temperature-cured products, allowing the bulk resistivity of the printed Ag lines to be decreased. A reduction to less than $5 \times 10^{-6}\Omega\text{-cm}$, for instance, will allow the amount of Ag to be typically decreased to around 130mg, which reduces the cost to ~ 5.7 \$cts/cell.

For the interconnection of SHJ cells with busbars, standard ribbon soldering can be applied on optimized pastes for that purpose, as proposed in early 2013, for example, for a 5BB interconnection of SHJ cells [9]. To limit the temperature during ribbon contacting, alternative technologies have since been proposed, such as the printing or the dispensing application of electrically conductive adhesives for ribbon attachment (e.g. the method proposed by teamtechnik [10]). The latter approach further facilitates the introduction of light-capturing ribbons, which can increase the module power output by about 1 to 2% [11].

Fine-line printing and multi-wire interconnection

In the second approach, alternative advanced interconnection technologies using multiple wires can be employed to significantly relax the constraints on the SHJ solar cell metallization conductivity. SmartWire Contacting Technology (SWCT) makes use of copper wires supported by a polymer foil (see Fig. 2) [12–14]. The wires are

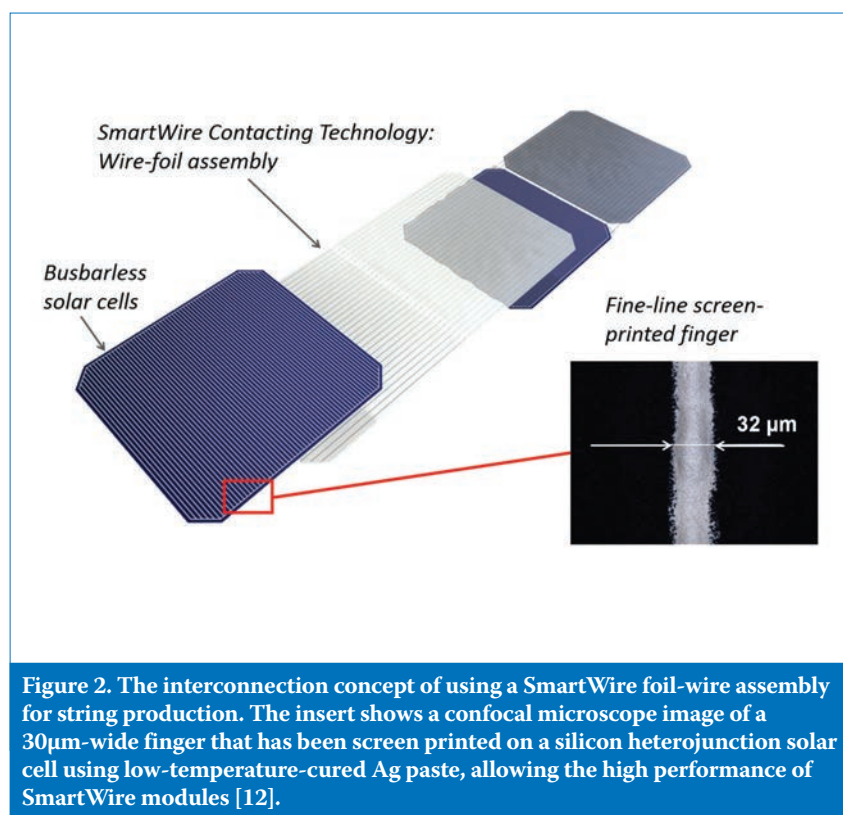


Figure 2. The interconnection concept of using a SmartWire foil-wire assembly for string production. The insert shows a confocal microscope image of a 30μm-wide finger that has been screen printed on a silicon heterojunction solar cell using low-temperature-cured Ag paste, allowing the high performance of SmartWire modules [12].

coated with a thin alloy layer that has a low melting point; this melts during the module lamination process and builds up a solder contact with the cell metallization fingers, thereby keeping the temperature budget low, which is perfectly suited to SHJ cells and to thin-wafer cell-module integration. This approach replaces state-of-the-art busbar and ribbon technology, and is applicable to cells having front metallization without busbars and solely fingers (see Fig. 2), referred to as *busbar-less cells*. First introduced by Day4 Energy [14], the technology is today mass produced by the Meyer Burger group with automated production equipment [12,13].

Because of a low wire optical dimension and the direct interconnection to the neighbouring cell, SWCT allows the use of more distributed current extraction paths perpendicular to the cell metallic fingers than with standard busbar technology. Wires with a diameter of 200µm are typically employed, exhibiting an optical dimension of about 140µm as a result of the re-collection of part of the light reflected onto the circular wire surface [12–15]. This allows the passage from standard interconnection schemes using three or five busbars/

ribbons to interconnections with more than 18 wires, without increasing the shadowing losses of the interconnections.

“The use of multiple-wire connections means that the ohmic losses in the cell metallization fingers are significantly decreased.”

The use of multiple-wire connections means that the ohmic losses in the cell metallization fingers are significantly decreased. By using 18 wires (the standard arrangement for SWCT), the power loss (P_f) in the cell metallic fingers can be divided by 13, compared with a 5BB design, provided the other parameters are kept constant (Equation 1). This because the power dissipation losses in the fingers, P_f , is inversely proportional to the square of the number of busbars:

$$P_f \propto \frac{J^2 L}{12 n_f} \frac{R_f}{n_{BB}^2} \propto C \frac{R_f}{n_{BB}^2} \quad (1)$$

where J is the current density, L is the width of the cell, n_f is the number of

fingers, R_f is the finger line resistance, n_{BB} is the number of busbars and C is a constant [12,16].

The increase in the number of interconnection wires (busbars) therefore enables the implementation of more resistive fingers than in the case of state-of-the-art busbar cells. Similar power losses can be achieved with a 5BB design and an 18-wire design having a finger line resistance 13 times higher than that of the 5BB case. Consequently, while fingers with a line resistance of less than 1Ω/cm should be implemented in 5BB cells to achieve optimum performance, the SWCT method with 18 wires allows the integration of fingers with a line resistance of up to 10Ω/cm, to realize similar electrical losses in the fingers.

The use of SWCT therefore significantly relaxes the constraints on the conductance of the printed fingers; this, in turn, completely changes the way of thinking when optimizing the metallization of the fingers. The challenge in the printing technology thus shifts from making the high aspect ratio fingers required for sufficient conductance and minimum shadowing (for instance achieved by multiple printing), to printing continuous fingers that are as fine as possible in order to reduce the silver

Cell Processing



SWISS MADE ■■■
INDEOTEC
PLASMA PROCESS EQUIPMENT

proudly unveils

Octopus

with

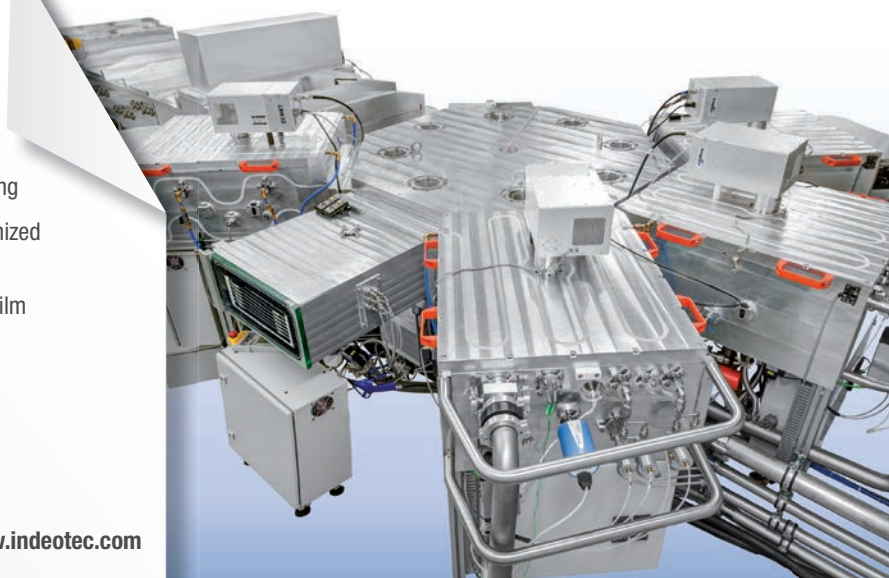
Mirror Reactor

A real innovation in PECVD
RF- and VHF-deposition technology

- Top & bottom thin film deposition in successive reactors without vacuum breakage or substrate flipping
- Special bifacial carrier plate hole design for minimized substrate edge bearing
- Secondary compensation electrode for excellent film thickness uniformity and passivation quality levels

▶ PV cell coatings
▶ Opto-electronic layers
▶ MEMS/semicon devices

www.indeotec.com



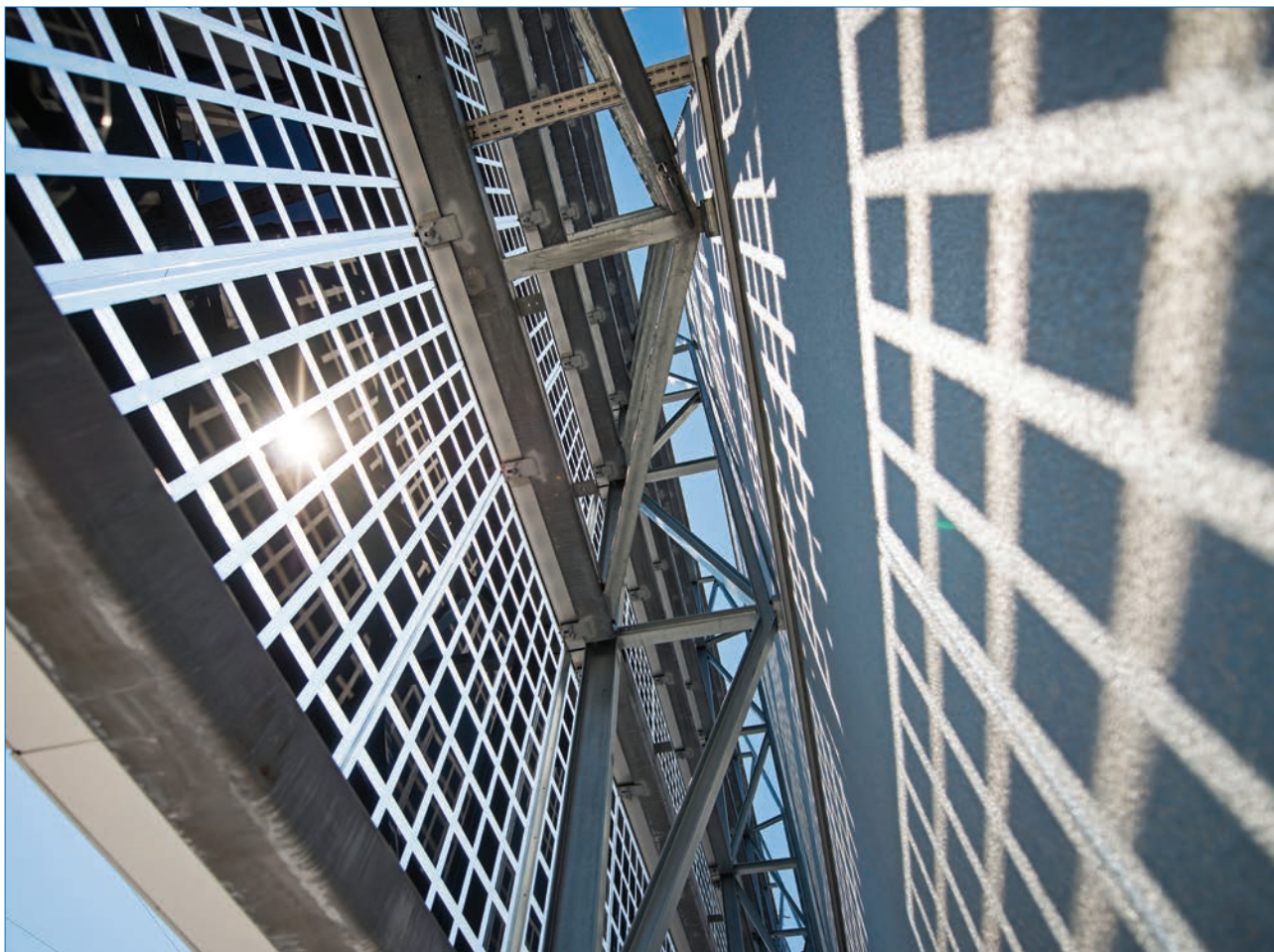


Figure 3. Semi-transparent facade of the renovated CSEM building in Neuchâtel, Switzerland, which comprises bifacial silicon heterojunction solar cells that are interconnected using SmartWire Contacting Technology [17].

lay-down (cost reduction) and to increase the current density (efficiency enhancement).

Recent developments in the fine-line printing of low-temperature cured Ag pastes have demonstrated the possibility of printing low-temperature cured Ag lines with sufficient conductivity using minimum screen openings down to 20µm; this has resulted in approximately 30µm-wide fingers with a line resistance of 5Ω/cm, which is sufficient for module integration using SWCT without adding electrical losses from the fingers [12,16]. This represents a double benefit: first, since only 30mg of Ag is necessary per side, considerable savings in metallization costs are realized; second, thanks to the reduced shadowing of the finer printed fingers, an increase in performance is achieved, with a relative gain of about 1% possible [12,16].

When SWCT is used, the consideration of a typical lay-down mass of Ag of 30mg per side represents a metallization cost of 1.33\$cts/cell (for an assumed Ag price of \$460/kg). Compared with a 22.5%

cell efficiency obtained using standard printing, an efficiency of 22.7% can be achieved using fine-line printing, yielding finger metallization costs of ~0.23\$cts/Wp, which is around one-sixth the cost of the standard case. SWCT technology therefore demonstrates how an initial weakness of SHJ technology can be turned into a strength, as record low usage of Ag is made possible, resulting in an ultra-low cost of the printed Ag and an increased cell performance.

In 2014 the high-performance potential was demonstrated with a 327Wp module which integrated 60 silicon heterojunction solar cells, corresponding to a total-area module efficiency of 20% [15]. In addition, high reliability with this technology can be demonstrated: a degradation of less than 5% after undergoing more than three times the IEC standard test criteria for accelerated degradation has been reported [8].

At the R&D level, there have been further developments in order to profit from the relaxed constraints provided by SWCT. For instance, the printing of copper lines was demonstrated to yield sufficient line conduction for use in

combination with SWCT, and reliable modules were also demonstrated [16]; moreover, the cost-reduction potential of SWCT has been shown by implementing an alternative coating material for the wires [16]. Yet further advancements have been demonstrated in the form of the first bifacial single-cell modules with an efficiency of 19.9% without any cell metallization on the front side or the back [16]. Direct contacting is realized between the wires and the conductive front surface of SHJ solar cells; this, however, necessitates the implementation of a large number of wires.

“By switching to copper-electroplating processing for the formation of the electrical grid, the use of silver can be suppressed and the metallization process maintained at room temperature.”

Meco Plating Equipment

Copper metalization for high efficiency solar cells

- HIT, IBC, bifacial
- PERC plating:
 - > 20.5% on p-type
 - > 22.5% on n-type
- > 65% reduction of metalization costs
- Inline process up to 30 - 100 MW tool capacity
- IEC61215 certified
- Eco-friendly processes with maximum material recycling
- Over 35 years of plating experience
- More than 800 plating tools installed
- Installed base at leading PV manufacturers

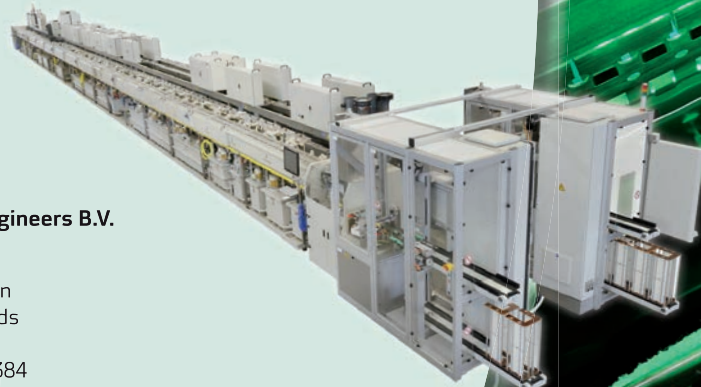


Besì

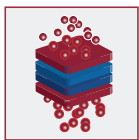
Meco Equipment Engineers B.V.

Marconilaan 2
5151 DR Drunen
The Netherlands

T: +31 416 384 384
meco.sales@besi.com



www.besi.com



2-sided deposition
is simple now

- RF deposition at top & bottom side in one system
- Excellent results for a-Si:H layers (intrinsic, doped), SiOx, SiNx
- NO substrate flipping
- NO vacuum breakage



Cut operation costs
Cut footprint

- Drastically reduced handling steps reduce risk of breakage
- Elimination of intermediate vacuum breakage cuts costs
- Substantial footprint savings by smart platform design

Octopus
with
Mirror Reactor



Regulate your
layer profile

- Customization of film thickness profile possible
- Adaption of film profile to slightly bended substrates
- NO change of plasma or stoichiometry



Send email request via QR code

sales@indeotec.com • Rue du Puits-Godet 12A, 2000 Neuchâtel (Switzerland)
+41-32-545 30 24
www.indeotec.com

INDEOtec

Finally, the aesthetics of SWCT modules are today highlighted by the CSEM PV facade, which comprises spaced bifacial SHJ solar cells that are interconnected using SWCT, as shown in Fig. 3 [17].

Copper electroplating

In the third approach, certain technologies that enable the application of silver-free metal stacks with improved line conductance can be implemented. By switching to copper-electroplating processing for the formation of the electrical grid, the use of silver can be suppressed and the metallization process maintained at room temperature. The plated copper lines typically demonstrate a low resistivity of down to $2 \times 10^{-6} \Omega \cdot \text{cm}$, which is only slightly higher than the resistivity of pure bulk copper ($1.7 \times 10^{-6} \Omega \cdot \text{cm}$).

Copper electroplating is a possible alternative to the screen printing of silver paste that is currently used for diffused-junction silicon solar cells. In this case, the dielectric anti-reflection layer can be used as a plating mask by opening it by, for instance, laser ablation. The standard process then consists of the growth of a nickel–copper stack by plating. The nickel layer will form a nickel silicide barrier to copper diffusion after annealing, while the copper acts as the conductive layer. Such metallization technology was recently demonstrated on commercial equipment to enable low resistivity contacts on lightly doped emitters as well [18].

For the application of copper electroplating to silicon heterojunction solar cells, the situation is different: the plating is performed on the conductive front TCO layer of the SHJ solar cell [19–20]. This TCO layer will already act as an efficient barrier to copper migration towards the silicon, and therefore limit potential degradation. Since the layer is conductive, however, it requires the application of additional protective layers and processes in order to achieve the definition of a patterning mask to permit the selective plating. The development of the application of copper electroplating to SHJ solar cells therefore focuses on achieving low contact resistance and high adhesion of plated materials onto TCO layers, as well as on cost-effective patterning technologies.

Electroplated copper front-contact metallization has been

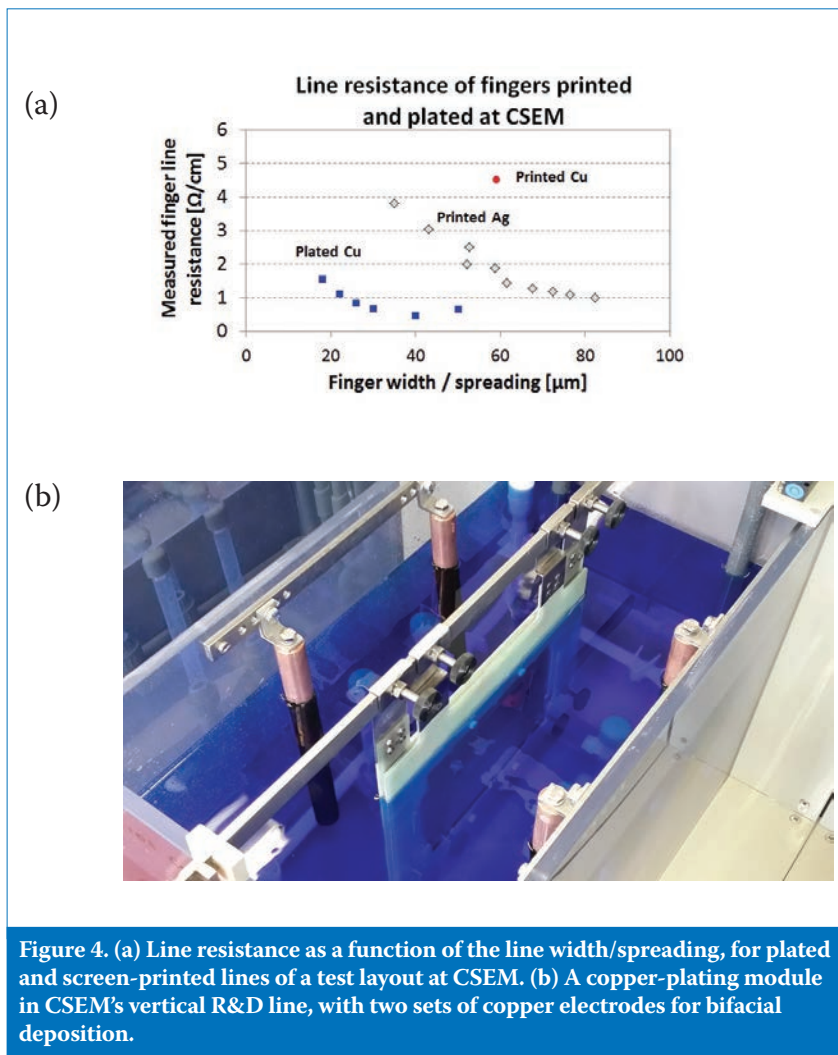


Figure 4. (a) Line resistance as a function of the line width/spreading, for plated and screen-printed lines of a test layout at CSEM. (b) A copper-plating module in CSEM's vertical R&D line, with two sets of copper electrodes for bifacial deposition.

successfully demonstrated for silicon heterojunction (SHJ) solar cells [19–20]. One patterning technique that potentially offers cost competitiveness with screen-printed metallization is the inkjet printing of a hot melt ink using a sophisticated process with significantly reduced ink consumption, as presented by Hermans et al. [21].

The possibilities of achieving fine-plated lines with low line resistance are illustrated in Fig. 4, in comparison to the use of low-temperature cured Ag paste; 20 μm -wide copper-plated fingers can be produced with a line resistance of about 1 Ω/cm . This therefore allows the achievement of high performance to be considered with silicon heterojunction solar cells that also use a three- to five-busbar H-pattern design, the fine, conductive plated fingers yielding low electrical and optical losses. Furthermore, the high finger conductivity may offer additional advantages for low-concentration solar devices, as well as in new interconnection technologies, such as shingling, also referred to as *dense cell interconnection* [22].

“20 μm -wide copper-plated fingers can be produced with a line resistance of about 1 Ω/cm .”

Conclusions

Various technological approaches have been purposefully developed during the last few years to completely overcome the initial limitation in performance and cost originating from the requirement of a low-temperature-cured silver paste for silicon heterojunction solar cells. A switch to copper-plating processes permits fine, highly conductive fingers to be realized, with today's established processes guaranteeing high adhesion and performance.

Further work is under way by the different industry players to determine their own cost-effective patterning technology. With some of the commercially available solutions, plating already offers the prospect of improved cost compared with screen printing in the case of busbar and

ribbon interconnection; moreover, plating facilitates alternative module technologies.

Importantly, multiple-wire interconnection was shown to be a paradigm shift in technology; the method relaxes the constraints of the metallization finger conductivity to the same level achieved by today's low-temperature-cured silver paste. Ultra-low Ag consumption has been demonstrated (down to 30mg per cell side), yielding a significant reduction in metallization costs, which is even more pronounced in the case of bifacial modules.

In conclusion, the different alternative metallization and interconnection technologies developed in recent years are now further advancing silicon heterojunction solar cell technology as a cost-competitive high-performance technology.

References

- [1] Tanaka, M. et al. 1992, "Development of new a-Si/c-Si heterojunction solar cells: ACJ-HIT (artificially constructed junction-heterojunction with intrinsic thin-layer)", *Jap. J. Appl. Phys.*, Vol. 31, pp. 3518–3522.
- [2] De Wolf, S. et al. 2012, "High-efficiency silicon heterojunction solar cells: a review", *Green*, Vol. 2, pp 7–24.
- [3] Descoeudres, A., Allebé, C. & Badel, N. 2015, "Silicon heterojunction solar cells: Towards low-cost high-efficiency industrial devices and application to low-concentration PV", *Energy Procedia*, Vol. 77, pp. 508–514.
- [4] Taguchi, M. et al. 2014, "24.7% record efficiency HIT solar cell on thin silicon wafer", *IEEE J. Photovolt.*, Vol. 4, pp. 96–99.
- [5] Masuko, K. et al. 2014, "Achievement of more than 25% conversion efficiency with crystalline silicon heterojunction solar cell", *IEEE J. Photovolt.*, Vol. 4, pp. 1433–1435.
- [6] Strahm, B. et al. 2015, "The Swiss Inno-HJT project: Fully integrated R&D to boost Si-HJT module performance", *Proc. 31st EU PVSEC*, Hamburg, Germany.
- [7] Yamamoto, K. et al. 2015, "Progress and challenges in thin-film silicon photovoltaics: Heterojunctions and multijunctions", *Proc. 31st EU PVSEC*, Hamburg, Germany.
- [8] Soderstrom, T., Yao, Y. & Grischke, R. 2015, "Low cost high energy yield solar module lines and its applications", *Proc. 42nd IEEE PVSC*, New Orleans, Louisiana, USA.
- [9] SOMONT [http://www.somont.com/en/].
- [10] teamtechnik [http://www.teamtechnik.com/en/solar/stringer-tt/stringer-tt1400-eca/].
- [11] Ebner, R. et al. 2013, "Increased power output of crystalline silicon PV modules by alternative interconnection applications", *Proc. 28th EU PVSEC*, Paris, France.
- [12] Faes A., Despeisse M., Levrat J. et al. 2014, "SmartWire Solar Cell Interconnection Technology", *Proc. 29th EU PVSEC*, Amsterdam, The Netherlands.
- [13] Papet, P. et al. 2014, "Metallization schemes dedicated to SmartWire Connection Technology for heterojunction solar cells", *Proc. 29th EU PVSEC*, Amsterdam, The Netherlands.
- [14] Schneider, A., Rubin, L. & Rubin, G. 2006, "Solar cell improvement by new metallization techniques – The DAY4™ electrode concept", *Proc. 4th WCPEC*, Waikoloa, Hawaii, USA, p. 1095.
- [15] Braun, S., Micard, G. & Hahn, G. 2013, "Solar cell improvement by using a multi busbar design as front electrode", *Energy Procedia*, Vol. 21, pp. 227–233.
- [16] Yao, Y. et al. 2015, "Module integration of solar cells with diverse metallization schemes enabled by SmartWire Connection Technology", *Proc. 30th EU PVSEC*, Hamburg, Germany.
- [17] CSEM [http://www.csem.ch/site/card.asp?pid=33107].
- [18] Horzel, J.T. et al. 2015, "Industrial solar cells with Cu-based plated contacts", *IEEE J. Photovolt.*, Vol. 5, No. 6.
- [19] Hernández, J.L. et al. 2012, "High efficiency copper electroplated heterojunction solar cells", *Proc. 27th EU PVSEC*, Frankfurt, Germany.
- [20] Geissbuhler, J. et al. 2014, "Silicon heterojunction solar cells with copper-plated grid electrodes: Status and comparison with silver thick-film techniques", *IEEE J. Photovolt.*, Vol. 4, No. 4, pp. 1055–1062.
- [21] Hermans, J. et al. 2014, "Advanced metallization concepts by inkjet printing", *Proc. 29th EU PVSEC*, Amsterdam, The Netherlands.
- [22] Cogenra [www.cogenra.com/dci-technology/].

About the Authors



Matthieu Despeisse received his Ph.D. in 2006 for his work on advanced detectors at CERN in Geneva, Switzerland. He then joined EPFL in 2009 as head of the thin-film silicon photovoltaics research team. Since 2013 he has led research activities at CSEM concerning crystalline silicon photovoltaics and metallization, with a special focus on silicon heterojunction technology, passivating contacts, metallization and interconnection.



Christophe Ballif received his Ph.D. from EPFL, Switzerland, in 1998. In 2004 he became a full professor with the Institute of Microengineering at the University of Neuchâtel, where he directs the Photovoltaics and Thin-Film Electronics Laboratory, which is now part of EPFL. Since 2013 he has also been the director of the CSEM PV-center. His research interests include materials for PV, high-efficiency c-Si solar cells, module technology, BIPV and energy systems.



Antonin Faes received his Ph.D. in 2006 for his work on solid oxide fuel cells at the Interdisciplinary Center for Electron Microscopy (CIME) and the Industrial Energy System Laboratory (LENI) at EPFL. In 2012 he joined the CSEM PV-center in Neuchâtel, where he is responsible for c-Si solar cell metallization and interconnection activities, with a particular focus on silicon heterojunction solar cells.



Agata Lachowicz studied chemistry at Heinrich Heine University Düsseldorf, and worked initially on the development of processes for manufacturing printed-circuit boards, such as final finishes, copper plating and conductive polymers. She worked at Schott Solar and Meyer Burger Germany, focusing on PERC processes, before joining CSEM PV-center to work on the development of plating for silicon heterojunction solar cells.

Enquiries

Matthieu Despeisse
Jaquet Droz 1
CH-2002 Neuchâtel
Switzerland

Email: mde@csem.ch

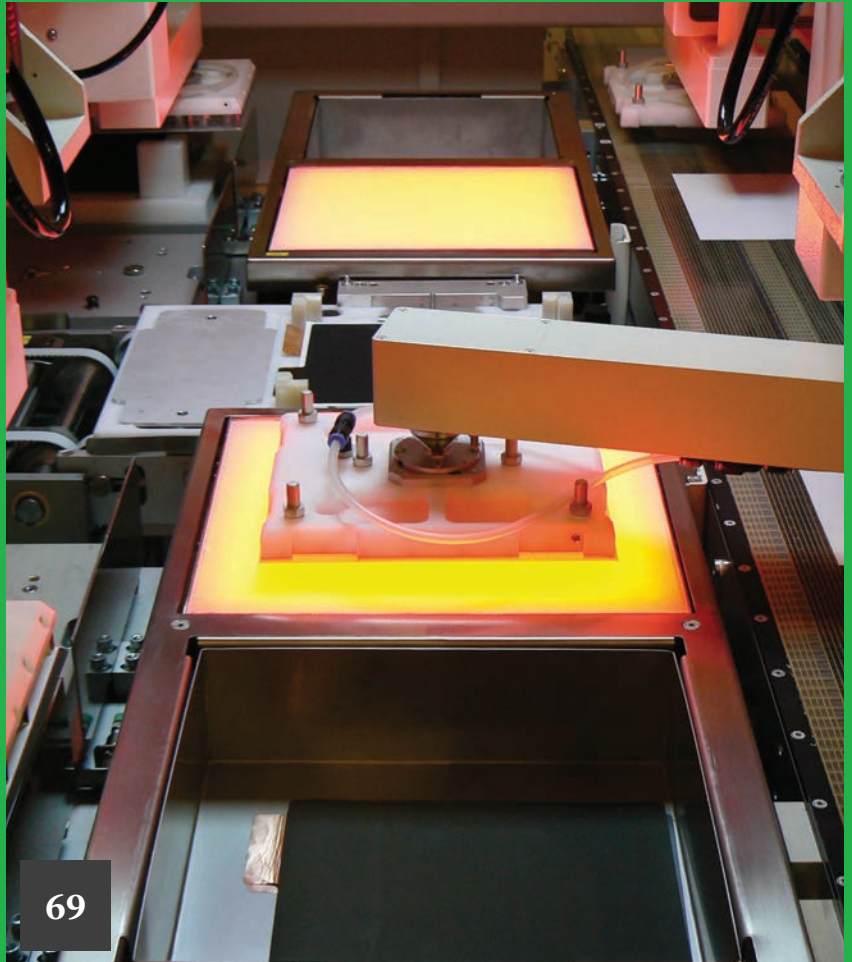
Thin Film

Page 69
News

Page 72
Predicting moisture-induced
degradation of flexible PV
modules in the field

Kedar Hardikar, Todd Krajewski &
Kris Toivola, MiaSolé, Santa Clara,
California, USA

.....



69

First Solar sets 2016 shipment guidance at 2.9-3.0GW

In early December, First Solar announced shipment guidance for 2016 of 2.9-3.0GW for 2016 and confirmed that it has no immediate plans to expand production capacity.

The shipment target translates to US\$3.9-4.1 billion of sales with earnings per share of US\$4.00-4.50.

First Solar said it would benefit from an additional 500MW of output as a result of the two additional production lines that went into service this year and improved conversion efficiency. The company said it expected its fleet to average around 16.2% efficiency next year. Further improvements to efficiency will be delayed till at least the second half of 2016 in order to maximise production.

First Solar said in November that it expects to be operating all of its production lines at full capacity next year.

The company said it will wait until it has visibility on 2017 and 2018 demand before making any major investment decisions.



Credit: First Solar

First Solar is guiding shipments of 2.9-3GW in 2016.

R&D

Solar Frontier's record CIS cell hits 22.3% efficiency

Solar Frontier achieved a conversion efficiency record for CIS thin-film solar cells, hitting 22.3% efficiency on a 0.5cm² PV cell.

The Japanese manufacturer developed the cell through a collaborative partnership with Japan's New Energy and Industrial Technology Development Organisation (NEDO).

Public research institution NEDO



Credit: Solar Frontier

Solar Frontier has hit a 22.3% efficiency record with a CIS cell.

and its CIS research consortium targets improvements in the mass production of CIS PV. The cell breaks the Stuttgart Centre for Solar Energy and Hydrogen Research (ZSW) record, which achieved 21.7% conversion efficiency on a similarly-sized PV cell in 2014. Solar Frontier's own previous best was 20.9% conversion efficiency.

Technology used in that previous best efficiency cells is already assimilated into manufacturing processes at Solar Frontier's newest 150MW production plant in Tohoku, Japan. Modules from that plant will have efficiencies of around 14.7% when commercial production begins.

Teams combine perovskite and silicon cells to reach record 18% efficiency

Teams from solar cell research institute Helmholtz-Zentrum Berlin (HZB) and the university École Polytechnique Fédérale de Lausanne (EPFL) in Switzerland have combined a silicon heterojunction solar cell with a perovskite solar cell monolithically into a tandem device and reached a record efficiency of 18%, claiming it has the potential to hit 30% after further modifications.

Perovskite layers absorb light in the blue region of the spectrum, which means they are useful to combine with silicon layers that mostly convert long-wavelength red and near-infrared light.

However, constructing these two types of cell in tandem is difficult, because high efficiency perovskite cells tend to require coating onto titanium dioxide layers,

which must first be sintered at around 500°C. The amorphous silicon layers that cover the crystalline silicon wafer in silicon heterojunction degrade at this temperature.

Kaneka continues solar cell R&D collaboration with imec

Nanoelectronics research centre imec and Japanese solar cell manufacturer Kaneka are expanding their collaboration on solar cell technology to incorporate life science and thin-film electronics.

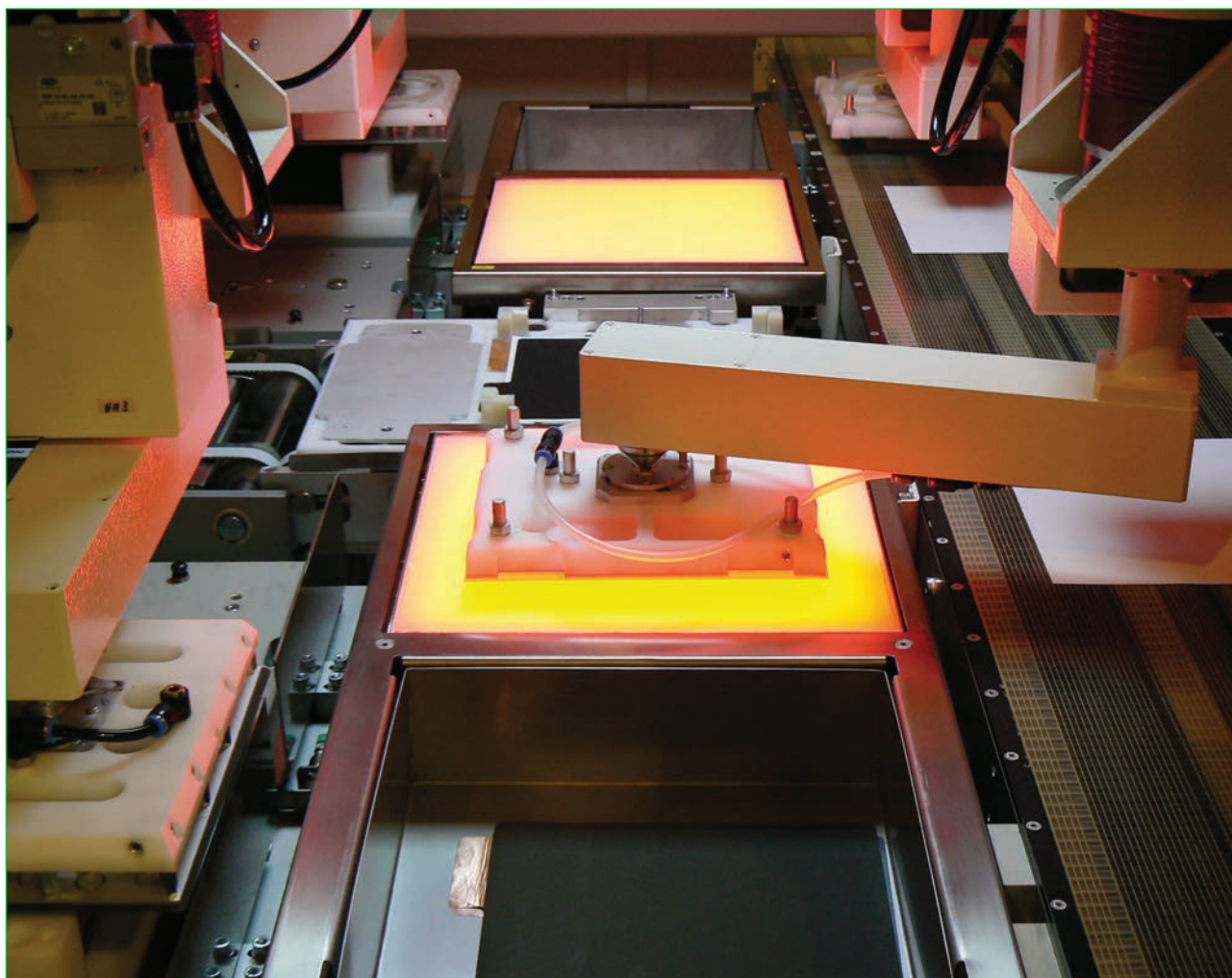
Recently, Kaneka announced a record of 25.1% efficiency for both-side-contacted crystalline silicon solar cell with copper contact metallisation and plans to establish a pilot production line using the technology.

Imec said that the extended work with Kaneka included using its thin-film electronics technology developed in cooperation with the Holst Centre, set up by imec and TNO in the Netherlands, to optimise applications in flexible, stretchable and low-cost electronic solutions.

Solar Frontier modules in Kuwaiti benchmarking project

A benchmarking project with c-Si technology for the Kuwait Institute for Scientific Research (KISR) will see Solar Frontier build a 5MW power plant in the Middle Eastern country.

Solar Frontier started shipping its CIS modules for the project at the beginning of December and expected the plant to be operational from June 2016 onwards.



Credit: Manz

Manz has been forced to lay off 174 staff as part of ongoing restructuring.

Partner TSK would be responsible for the construction and operation of the site for the next six years.

The project is part of the Shagaya Renewable Energy Project and run as part of the Innovative Renewable Energy Research program at KISR, which is testing the performance of multiple renewable technologies, including PV, concentrated solar power (CSP) and wind.

Company news

First Solar among investors in energy storage company Younicos

First Solar is among the investors in a US\$50 million funding round for grid-scale storage specialist Younicos, with the money raised set to fuel the latter's expansion.

Thus far, the only public expression of interest in the growing energy storage space by the Arizona-headquartered company has been a collaboration with heavy duty engineering and machinery

provider Caterpillar on micro grids that combine a variety of power and energy sources such as diesel gensets, batteries and solar.

Younicos develops energy storage projects as well as offering a consultancy business, and has offices in Germany and the US.

Manz lays off 174 employees following order delays

Manufacturing equipment supplier Manz laid off 174 staff at the beginning of December.

Part of an ongoing restructuring plan, Manz said it needed to implement cost-cutting measures. Other measures will be taken throughout the coming fiscal year.

This will lead to 101 employees internationally including some in Taiwan and China losing jobs, as well as 73 workers in Germany. Workforce cuts and other strategies including outsourcing more tasks to lower cost China, could save around €7 million (US\$7.6 million).

Manz' managing board is also mulling savings "in the lower two-digit million range" and is evaluating the future of its solar business. Manz reported revenue

in the first nine months of 2015 of €169 million, with several energy storage segment delays attributed to the Chinese stock market downturn.

IKEA terminates distribution partnership with Hanergy

IKEA cancelled its UK solar PV supply deal with beleaguered Chinese thin-film module manufacturer Hanergy at the beginning of November.

The Swedish furniture company and Hanergy originally partnered in September 2012 in a deal in the UK via an installer subsidiary but later expanded its sales of solar equipment into additional markets in 2014.

"...we have successfully rolled out a residential solar offer to stores in three markets; the Netherlands, Switzerland and the United Kingdom," an IKEA statement said.

A new business model has been decided upon, which includes the decision not to renew the contract with Hanergy Solar UK when their current contract ends on 1 November 2015.

IKEA is expected to roll out a "broader" solar offering in UK in the near future.



Hanergy Thin Film Power has been forced to cancel contracts worth US\$2 billion.

US\$2 billion of Hanergy contracts cancelled

Two contracts worth almost US\$2 billion have been cancelled by Hanergy Thin Film Power Group.

The deals, for BIPV manufacturing

equipment, were signed in March 2015 with a condition that 80% of the value be paid by the end of November. With the deadline passed, Hanergy cancelled the agreements with neither party held responsible.

Mongolia Manshi Investment Group had agreed to buy 600MW of equipment of US\$198 million with Hanergy providing "technical services" for a fee of US\$462 million.

Baota Petrochemical Group was to purchase production line equipment totalling 1200MW for US\$396 million with a service contract of US\$924 million.

Both companies were to receive hefty share allotments as part of the agreements.

Ascent Solar's raises cash to keep going, sales hit by cash constraints

Flexible CIGS thin-film consumer product producer Ascent Solar Technologies reported lower than expected third quarter sales while reducing full-year revenue guidance on liquidity constraints in the quarter.

Ascent Solar reported third quarter revenue of US\$1.3 million, compared to US\$2.2 million in the previous quarter. Net loss for the quarter was US\$6.1 million, compared to US\$11.3 million in the prior quarter.

As a result of the financial constraints said by management to have eased, Ascent Solar noted it expected to end the year's fourth quarter with approximately US\$3.1 million revenue and full year revenues of approximately US\$7.2 million.

The company announced a cash injection to help it along, securing US\$2.8 million in funding from the issue of three purchase agreements of its 'E' series stock in November.

Work underway on 1.5GW Avancis CIGS thin-film fab in China

Chinese-owned German CIGS thin-film module manufacturer has broken ground on a new factory in Bengbu, Anhui province, China.

The 300MW initial phase of the new fab is expected to begin production in early 2017 and heralds what is expected to become a much larger operation of some 1.5GW.

CTIEC, the engineering and project development branch of CNBM, the building materials group that bought Avancis last year, the Bengbu Investment Group and the Bengbu Gaoxin Investment Group jointly plan to invest €1.43 billion (US\$1.62 billion) in the facility.

Avancis' existing production line in Germany will also be expanded to serve the European market, the company said, without giving further details.

Predicting moisture-induced degradation of flexible PV modules in the field

Kedar Hardikar, Todd Krajewski & Kris Toivola, MiaSolé, Santa Clara, California, USA

ABSTRACT

Establishing the reliability of PV modules for a typical warranty period of ~25 years is challenging because of several failure mechanisms that can be triggered during outdoor exposure. A critical failure mechanism for PV modules is the degradation in performance as a result of exposure to temperature and humidity. In the case of flexible PV modules, moisture-induced damage becomes a greater concern, since the moisture resistance of barriers and polymer packaging is expected to be lower than that for conventional glass–glass PV products; hence developing a means to assess the field performance of flexible PV modules is essential. The time to failure of a PV module attributable to moisture-induced damage under given field conditions involves multiple factors, including the moisture resistance of the front/back sheets, the encapsulant and edge seal, and the degradation rate of particular solar cells when exposed to moisture. The work presented here is aimed at establishing, through the use of accelerated testing, the field lifetime of flexible PV modules with regard to moisture-induced degradation. A semi-empirical framework for such an assessment is developed using a combination of empirical and analytical models. Testing at different temperature and humidity conditions is carried out for representative flexible copper indium gallium selenide (CIGS) module configurations. The test results highlight the limitations of accelerated testing methodology for high-moisture-barrier systems. In particular, it is shown that for the high-moisture-barrier systems tested, the test times can become prohibitive for establishing humidity dependence through accelerated testing. Through the use of an analytical model, a method is proposed to translate test results to field performance using typical meteorological year (TMY) data.

Introduction

The degradation in performance of PV modules as a result of moisture ingress is a concern that has been raised for c-Si modules as well as for other PV technologies [1]. With the increasing interest in building-integrated photovoltaic (BIPV) products that demand light weight and flexibility, the use of non-glass barriers for PV products is inevitable. Moisture ingress concerns are even more critical in this case than for conventional glass–glass products, since the moisture barrier performance of polymer-based packages is expected to be lower than that of glass products. Some solar cell technologies, in particular copper indium gallium selenide (CIGS), are considered more prone to moisture-induced damage than c-Si, although c-Si modules are not completely free of these concerns.

“The moisture barrier performance of polymer-based packages is expected to be lower than that of glass products.”

The degradation of polymer-encapsulated electronic components is also a concern in the consumer electronics industry, where critical

components such as electronic displays and IC metallization may be at risk of performance degradation and failure because of moisture ingress and corrosion [2–3]. One factor that distinguishes degradation concerns and the assessment of field performance for PV modules, as compared with consumer electronics products, is the vast difference in expected product lifetime. While the typical timescale for assessing the performance of consumer electronics products is ~3–5 years, PV modules need to have a field performance assessment covering a typical warranty period of ~25 years. This makes the development of a means of assessing the long-term reliability of flexible PV modules quite critical.

There have been several attempts in the past to develop techniques and models to predict the life of PV modules with moisture ingress as a proposed mechanism leading to failures or degradation in performance [4–8]. For consumer electronics products, a typical approach to characterizing the field performance of encapsulated electronic components, based on accelerated testing with exposure to temperature and humidity, is an empirical approach commonly referred to as the *Hallberg-Peck model* [9–11]. While it may seem conceivable that a similar approach can be taken to assess the field performance of flexible PV modules, this approach is not well established or validated for PV

products. The Hallberg-Peck model is an empirical corrosion model, and its successful application to PV products can depend on whether or not the degradation in PV packages can be considered similar to corrosion mechanisms in encapsulated electronic components and metallization. Although there may be similarities which would suggest that such an approach is possible, the details of failure can differ between the two types of system. In particular, the barrier level of the packaging system for a PV module, and the manner in which a particular type of solar cell degrades when exposed to temperature and humidity, may be dramatically different from those of typically packaged electronic components.

In all of these scenarios, predicting the time to failure of the product on the basis of a threshold degradation level due to moisture ingress hinges upon the combination of two factors: the moisture barrier performance and degradation of the encapsulated components when exposed to moisture. A third factor involved in these predictions is the development of schemes to model fluctuations of ambient conditions to which the product is subjected during its lifetime, and relating these variations to the test conditions [5]. The charter of this paper is to explore a methodology based on relationships such as the Hallberg-Peck model for the assessment of the field performance of flexible

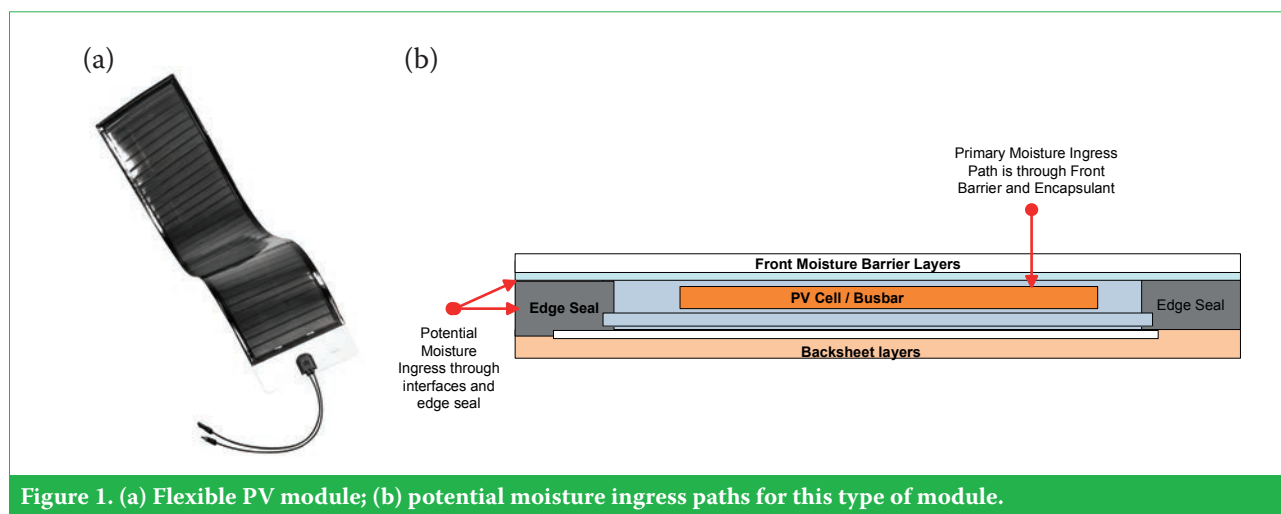


Figure 1. (a) Flexible PV module; (b) potential moisture ingress paths for this type of module.

PV modules with regard to moisture-induced degradation, using the results from accelerated testing. Candidate module configurations chosen for testing are CIGS thin-film flexible modules with different moisture barrier performance levels.

Fig. 1 shows a representative flexible PV module, and illustrates several potential moisture ingress paths that can be present in the system. In order to assess the moisture resistance of the product, it is important to understand the following:

1. The resistance of the edge seal alone to moisture ingress.
2. The resistance of the moisture barrier to moisture ingress.
3. The moisture ingress near the edges of the module, where the ingress through the edge seal may be modulated by the presence of interfaces susceptible to moisture penetration.

For the regions of the module near the edges, points (1) and (3) above are critical, whereas in the case of a sufficiently large module, the moisture ingress near the centre of the module is governed by (2).

A methodology for assessing the moisture resistance of the edge seal was developed for a glass-glass module by Hardikar et al. [12]. That method was based on an analytical model that was developed using the solution to a 1D diffusion equation; the model was validated by appropriate test results, and provided a method for assessing the field performance of the edge seal on the basis of the results of accelerated testing.

In the present work, the experience gained from the results in Hardikar et al. [12] is used in conjunction with additional testing to decide upon the preferred dimension of the edge

seal. The objective of these initial tests is to ensure that, for the chosen configurations, the dimension of the edge seal is such that the moisture ingress at the edges is sufficiently delayed and that the primary moisture path of concern is through the front barrier. Once this is ensured, further work can be carried out using appropriate edge seal configurations to characterize the performance degradation of a PV device when exposed to controlled temperature and humidity conditions. The results of this testing are then analysed to assess the field performance.

The rest of the paper is organized as follows. First, a candidate empirical model (Hallberg-Peck) and an analytical model are described, which form the basis of the experimental plan. This is followed by a description of the experiments performed, of which there are two sets: 1) measurements of barrier diffusivity, and 2) accelerated testing of flexible module samples, with performance monitoring. Finally, a method is presented for assessing the field performance of the product (on the basis of moisture-induced damage only) using the results of accelerated testing in a manner consistent with the model developed. The limitations of such testing and prediction are discussed, along with recommendations for further work.

Modelling moisture-induced degradation

As stated earlier, the degradation in performance of a PV module attributable to moisture-induced damage depends on several factors. The key factors affecting this degradation are: 1) the moisture resistance of the packaging, and 2) the degradation of a particular solar cell when exposed to temperature and humidity.

The degradation of a particular cell

when exposed to moisture will depend on the cell architecture and how moisture reacts with the components of the cell. A separate cell-level study, comprising either a characterization of the materials involved or appropriate modelling of reactions, is required in order to assess this degradation. However, as far as the characterization of product performance is concerned, one may take an empirical approach in which the degradation is measured and empirically modelled, without recourse to a detailed analysis of the mechanisms leading to this degradation. The approach taken in this study is based on a semi-empirical model in which the details of the mechanisms causing cell degradation are not modelled but are instead accounted for through assumptions which need to be verified later. The success of this approach depends on whether or not the implications of these assumptions and subsequent analyses can predict trends that are consistent with experimental results.

Empirical model for time to failure (Hallberg-Peck Model)

In the analysis of failure due to moisture for plastic- or epoxy-packaged electronic devices, it is customary to use an empirical approach for assessing field performance on the basis of the results of accelerated testing. The failures of interest are driven by moisture diffusing through epoxy-type packaging and ultimately driving component failures by corrosion. Typical timescales for which these predictions are desired correspond to the expected warranty period of approximately three years for these products. The approach is based on relationships proposed in the literature [9–11]; the empirical relationship used has the form:

$$TTF = A(RH)^n \exp\left(\frac{\varepsilon_a}{kT}\right) \quad (1)$$

where

TTF = time to failure when exposed to temperature T (K) and relative humidity RH

A = constant, to be obtained empirically

n = humidity exponent, to be obtained empirically (expected to be negative)

ε_a = effective activation energy (eV), to be obtained empirically

k = Boltzmann constant = $8.617 \times 10^{-5} \text{ eV/K}$

It should be noted that Equation 1 can be written in the form of an acceleration factor AF for translating test results to field conditions:

$$AF = \left(\frac{RH_{\text{field}}}{RH_{\text{test}}} \right)^n \exp \left[\frac{\varepsilon_a}{k} \left(\frac{1}{T_{\text{field}}} - \frac{1}{T_{\text{test}}} \right) \right] \quad (2)$$

Note that in order to exploit Equation 2, the field conditions used need to correspond to equivalent constant temperature and relative humidity conditions. For most indoor applications of consumer products this is not too difficult. It should be noted that this model is based on corrosion failures of encapsulated metallization. The empirical relationship has been demonstrated to correlate to a wide range of data relating to epoxy-based encapsulated metallization [9–11].

It is also worth noting that in Peck [11] this empirical model has been applied to applications involving semiconductor products in a military environment with a timescale of ~10 years. Peck [11] also provides recommended values for the range of effective activation energy and humidity exponents that can be used in such applications; in particular, the relative humidity exponent is expected to be negative, implying that as the relative humidity decreases the time to failure from moisture-induced damage increases.

While the use of this approach is well established for consumer electronics products, this is not the case for PV applications. It is the authors' belief, however, that such an approach may also be reasonable for the assessment of the long-term field performance of PV modules with regard to moisture-induced damage. In order to establish the validity and obtain the model parameters, namely the effective activation energy and humidity exponent, modules of identical construction need to be tested in controlled temperature and humidity conditions (i.e. for different temperatures at a constant relative humidity, and for different relative humidity values at a constant temperature).

Before such a test plan is discussed, a few points are worth noting. First, the degradation of PV cells in the presence of moisture can be thought of as somewhat similar to corrosion failures of encapsulated metallization, since the degradation is expected to be dependent on the reaction between moisture and the materials that constitute the PV cell. In addition, moisture-induced degradation of a PV module involves the diffusion of moisture through packaging materials, as well as the subsequent reaction with the cell in a manner similar to the way in which consumer electronics products might experience moisture-induced failures. It is acknowledged that the details of the reactions and failure mechanisms can differ between applications. Moreover, independently of moisture, for PV cells there can be other failure mechanisms based on temperature alone that can be different in nature from the degradation of electronic components exposed to temperature.

For flexible CIGS PV applications, the moisture barrier used needs to have a low water vapour transmission rate (WVTR) of less than $10^{-4} \text{ g/m}^2/\text{day}$. In particular, the moisture resistance of a flexible PV front sheet needs to be very high compared with that of epoxy packaging in semiconductor products, so that the front sheet can withstand the aggressive outdoor environmental exposure over long timescales. The expectation for a PV package is that the amount of moisture reaching the PV cell with such exposure will be very small in order to guarantee a lifetime of ~25 years. As a result, the humidity exponent and effective activation energy values that are recommended in Peck [11] may not work very well for PV packages. Thus, although the similarity in the two applications is compelling enough to consider this approach for a long-term reliability assessment, adequate testing and validation is warranted. In lieu of a full justification for the use of the Hallberg-Peck model in PV applications, an analytical model was first developed to explore the plausibility of an expression such as

Equation 2 holding good for flexible PV module degradation attributable to moisture.

Analytical model and functional form for the acceleration factor

The diffusion of moisture through a barrier material is a process which involves the adsorption of moisture on the exposed surface, followed by the diffusion of moisture through the barrier. The primary driving force for any diffusion process is the concentration gradient of the diffusing species (Fick's Law). Typically, the maximum concentration of moisture at the exposed surface is a function of the solubility of the material. The propagation of moisture through the barrier is a function of the diffusivity of the material.

As discussed earlier, once the configuration of the edge seal has been judiciously chosen, the primary moisture ingress path for a PV module is through the front barrier. This moisture ingress can be modelled using a 1D diffusion equation. For the high-barrier system used in PV modules, the moisture emerging near the solar cell after passing through the barrier and encapsulant is assumed to be consumed through a reaction with the materials constituting the PV cell, such as transparent conductive oxide (TCO) or CIGS material. This leads to a candidate model described by the following initial boundary value problem (see Fig. 2):

$$\frac{\partial C}{\partial t} = D \frac{\partial^2 C}{\partial x^2} \quad (3)$$

$$C(x, 0) = 0; C(x = 0, t) = C_1; C(x = l, t) = 0 \quad (4)$$

where

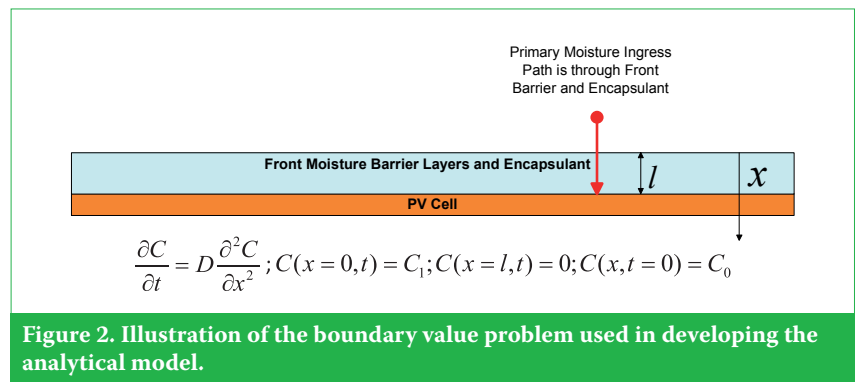
x = distance from the exposed surface

t = time

$C(x, t)$ = moisture concentration at position x at time t

D = diffusivity of the material between the exposed surface and the PV cell

l = effective thickness of the medium through which moisture diffuses between the exposed surface and the PV cell



A NEW PLAYING FIELD



Clean Energy

SUMMIT



HUAWEI

Headline Sponsor



Corporate Energy
FORUM



Solar
SUMMIT



Distributed Generation
FORUM

TWICKENHAM STADIUM | 26 - 28 April 2016

Incorporating the industry's leading spring event, Clean Energy Summit 2016 will bring together **major stakeholders in the growing clean technology space**. The event will allow the established UK solar industry to **explore opportunities in a post-subsidy world, engaging with energy consumers** and project developers to realise the vision for clean energy in the UK.

**SUPER
EARLYBIRD!**
BOOK NOW
for best
rates

summit.solarenergyevents.com

LEAD THE CONVERSATION

Contact us today to drive the clean energy movement and demonstrate the vital role solar has to play. Influence our programme and work with the team you can rely on for a good show at Twickenham!

For more information contact Dominic Barklem | dbarklem@solarmedia.co.uk | +44 (0) 207 871 0122

It should be noted that the boundary condition at $x = l$ is based on the assumption that the moisture arriving at this location is consumed through the reaction with PV cell, whereas the boundary condition at $x = 0$ is governed by ambient conditions. It can be shown [13] that this initial boundary value problem can be solved analytically, and the solution is given by:

$$C(x,t) = C_1 \left(1 - \frac{x}{l} \right) - \frac{2}{\pi} \sum_{n=1}^{\infty} C_1 \frac{\sin\left(\frac{n\pi x}{l}\right)}{n} \exp\left(-\frac{Dn^2\pi^2 t}{l^2}\right) \quad (5)$$

From this solution, the flux of the moisture reaching the PV cell can be evaluated analytically using $\frac{\partial C}{\partial x}\bigg|_{x=0}$. The expression for the amount of moisture Q_t reaching the cell in time t can be obtained by integrating the flux up to time t . The resulting expression is available in Crank [13] and is given by:

$$\frac{Q}{C_1 l} = \frac{Dt}{l^2} - \frac{1}{6} - \frac{2}{\pi^2} \sum_{n=1}^{\infty} \frac{(-1)^n}{n^2} \exp\left(-\frac{Dn^2\pi^2 t}{l^2}\right) \quad (6)$$

Fig. 3 shows the variation of the quantity of moisture Q_t reaching the PV cell over time t (non-dimensional quantities are used on the two axes). Now, it may be assumed that the degradation in performance of the PV cell up to time t due to reaction with moisture is proportional to the quantity of moisture that has reached the cell through the diffusion process. This assumption, however, needs to be validated by some means. One possible way is to provide a mechanistic understanding of the reaction between moisture and the PV cell, and the subsequent relationship of this reaction to the performance degradation. Another approach is to examine the implication of this assumption, namely study the trends it implies and then validate those trends by means of experimental data. In the study reported here, the latter approach is preferred, since the primary purpose is to provide a model for the assessment of product performance.

On the basis of the assumption that the degradation in performance of a PV module up to time t due to moisture ingress is proportional to the amount of moisture reaching the PV cell up to time t , and using the result in Equation 6, the following dependencies can be inferred:

1. The series in the solution given by Equation 6 converges rapidly. In fact, one can see that even a one-term approximation of the infinite series can be satisfactory for practical considerations with

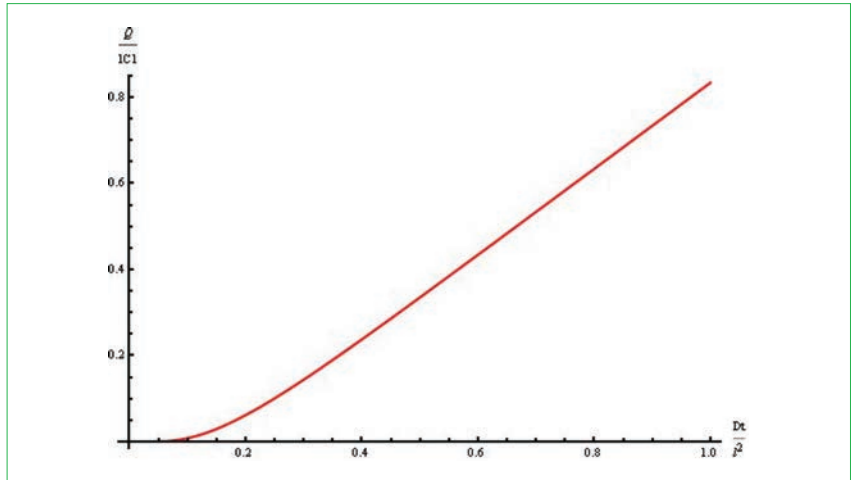


Figure 3. Quantity of moisture reaching the PV cell as a function of time.

$t \sim l^2/D$. For the representative values $l \sim 1\text{mm} = 0.1\text{cm}$ and $D \sim 10^{-9}\text{cm}^2/\text{s}$, the characteristic time is 2780 hours. From Equation 6 and the plot in Fig. 3, the performance degradation of the PV module, as characterized by the percentage change in power (equivalently, the amount of moisture consumed at the cell surface), can be expected to be linear in time, i.e. $\Delta P/P \propto t$.

2. The approximation for the expression in Equation 6 and the observed approximate linear behaviour in Fig. 3 imply that the degradation in performance may be expected to be approximately linear in diffusivity D . It is known that the diffusivity varies with temperature following an Arrhenius relationship:

$$D = D_0 \exp\left(-\frac{\varepsilon_a}{kT}\right) \quad (7)$$

This implies that the degradation in performance can be expected to have an Arrhenius dependence on temperature (using an effective activation energy ε_a , which in principle can differ from the activation energy ε_a' for the diffusion coefficient):

$$\frac{\Delta P}{P} \propto \exp\left(-\frac{\varepsilon_a}{kT}\right) \Rightarrow TTF \propto \exp\left(\frac{\varepsilon_a}{kT}\right) \quad (8)$$

3. From Fig. 3, one can infer that the quantity of moisture Q_t reaching the PV cell is linear in external concentration C_1 . If the reaction between moisture and PV cell material is assumed to be first order, and the degradation in performance of the PV cell is assumed to be proportional to the extent of the reaction, it would be concluded that the degradation in performance of the PV cell due to moisture is proportional to the

external concentration. On the basis of the discussion in Klinger [14], if the concentration of moisture on the surface is expressed in terms of a single variable independent of temperature, then there is reason to believe that the variable chosen should be relative humidity. If the temperature dependence is accounted for through an Arrhenius relationship, such as in Equation 8, the concentration dependence must be accounted for through relative humidity. Hence it may be conjectured that:

$$\frac{\Delta P}{P} \propto (RH) \Rightarrow TTF \propto (RH)^{-1} \quad (9)$$

Note that the exponent '-1' can change depending upon the assumption regarding the order of the reaction of moisture with the cell material.

4. When the above dependencies are combined, the functional form obtained for the time to failure of a flexible PV module based on this semi-analytical model is:

$$TTF = A(RH)^{-1} \exp\left(\frac{\varepsilon_a}{kT}\right) \quad (10)$$

The corresponding form for the acceleration factor is:

$$AF = \left(\frac{RH_{\text{field}}}{RH_{\text{test}}}\right)^{-1} \exp\left[\frac{\varepsilon_a}{k} \left(\frac{1}{T_{\text{field}}} - \frac{1}{T_{\text{test}}}\right)\right] \quad (11)$$

In summary, the semi-analytical model presented here provides a plausible approach to establishing a Hallberg-Peck type of relationship for the acceleration factor in analysing moisture-induced damage in flexible PV modules. The key point of the above discussion is that the test plan for analysing moisture-induced failures in flexible PV modules should be geared towards examining temperature and humidity dependence, by testing identical module constructions in different temperatures at the same

relative humidity, and for different humidity values at the same temperature in order to obtain the effective activation energy and RH exponent.

“The analytical model provides a means of assessing the expected values of activation energy and humidity exponent.”

While one must resort to extracting effective activation energy values and humidity exponent from experimental data, the analytical model provides a means of assessing the expected values of activation energy and humidity exponent; in other words, the activation energy is expected to be similar to the activation energy for the diffusion coefficient of the barrier material, whereas the relative humidity exponent is expected to be -1 on the basis of an assumed first-order reaction between moisture and the PV material. The relative humidity exponent could be different from -1 , but will be a negative value, depending on the details of the reaction. The activation energy will be dominated by the barrier diffusion if that is the rate-limiting step in the degradation process. In theory, the activation energy associated with degradation can be different from that for the barrier diffusion and needs to be verified by appropriate experimental data.

Experimental set-up, results and analysis

Two sets of experiments were performed in this study. First, the barrier material permittivity, diffusivity and solubility were measured at different temperatures through tests carried out at MOCON. The second set of experiments involved testing sample PV modules of identical construction at different temperature and humidity conditions. As stated earlier, a set of experiments was initially undertaken to establish the width of edge seal required to ensure that the primary path of moisture ingress for the samples (and for the corresponding product) was through the front barrier and not through the edges. The work in Hardikar et al. [12] indicates that (for their desiccated butyl edge seal, which is identical to that used in this study) the edge seal width of $\sim 10\text{mm}$ or greater is sufficient to delay moisture ingress beyond a typical warranty period of 25 years for a glass–glass product, even in aggressive field conditions such as in Bangkok. Extending that work further determined that an edge seal

width greater than 14mm ensures that the moisture breakthrough from the edge does not influence the test for a flexible product, since in that particular assembly the primary moisture ingress path is through the front barrier.

Measurement of barrier properties

In order to characterize the moisture resistance of barrier materials, it is customary to measure their WVTR; typically, this characterization begins with measurements of permittivity (P), diffusivity (D) and solubility (S). For this study, A4-sized sheet samples of a barrier were sent to the MOCON testing service [15]; the barrier, referred to as *barrier-1*, was a 0.0254cm -thick weatherable superstrate barrier system, with a nominal WVTR of $0.002\text{g}/\text{m}^2/\text{d}$ at $40^\circ\text{C}/90\%$ RH. The barrier-1 sample was tested on a MOCON AQUATRAN Model 2, using a remote cell to determine P, D and S. These tests were carried out at 37°C , 65°C and 85°C , with 100% RH; nitrogen was used as the carrier gas.

The goal of measuring diffusivity at different temperatures was to estimate the activation energy for the barrier diffusion from an expected Arrhenius relationship. Fig. 4 shows an Arrhenius fit for measured diffusivity values for barrier-1; in this case the activation energy is estimated to be 0.58eV . In principle, the estimation of lifetime can proceed using this estimated activation energy along with the acceleration factor derived from the analytical model in Equation 11. Before undertaking such a calculation, it is necessary to examine how this compares with the actual flexible module performance when exposed to different temperature and humidity conditions in a controlled manner. In this study it was also intended to examine the performance of another barrier, with a $\text{WVTR} < 5.0\text{e-}4\text{g}/\text{m}^2/\text{d}$ at $50^\circ\text{C}/100\%$ RH. However, this barrier, referred to as *barrier-2*, was

not amenable to MOCON testing, since the associated WVTR was below the detection level for the MOCON apparatus.

Accelerated testing of flexible module samples for field performance assessment

Accelerated testing was carried out on two representative module constructions: one configuration used barrier-1 (WVTR of $0.002\text{g}/\text{m}^2/\text{d}$ at $40^\circ\text{C}/90\%$ RH), whereas the second set of modules were constructed using barrier-2 ($\text{WVTR} < 5.0\text{e-}4\text{g}/\text{m}^2/\text{d}$ at $50^\circ\text{C}/100\%$ RH). The test modules consisting of eight cells in series were constructed for current–voltage–luminance (IVL) measurements using the same techniques as for the production process. Fig. 5 shows a schematic of module construction used in this study.

All cells were power matched (within 0.5% abs.) before the construction of the modules. A gap was included between the last cell of the string and the edge seal to allow the inclusion of CoCl_2 paper as an independent indicator of moisture penetration. One piece of indicator paper was centred in a segment of edge seal to serve as a reference. Five samples were made for each test condition for each barrier being evaluated; two glass–glass control samples were also constructed for each test condition. Samples were removed from the test chamber at one-week intervals and allowed to cool to ambient conditions before taking IVL measurements using a SPIRE flash tester at $1000\text{W}/\text{m}^2$. The drop in P_{max} was used to determine the degradation in performance. Fig. 6 shows the test conditions chosen for testing. (At the time of writing of this paper, data from barrier-1 were available for further analysis, whereas the testing of barrier-2 samples was still in progress.)

For the limited data available from

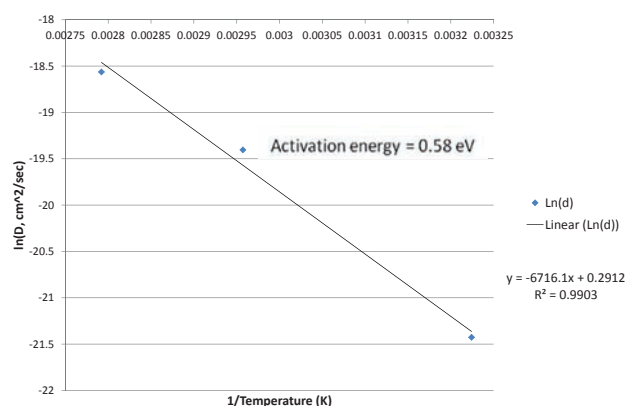


Figure 4. Arrhenius fit for the measured diffusivity values for barrier-1.

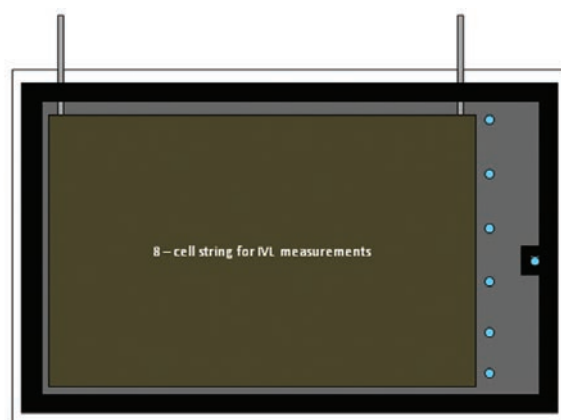


Figure 5. Module configuration for accelerated testing.

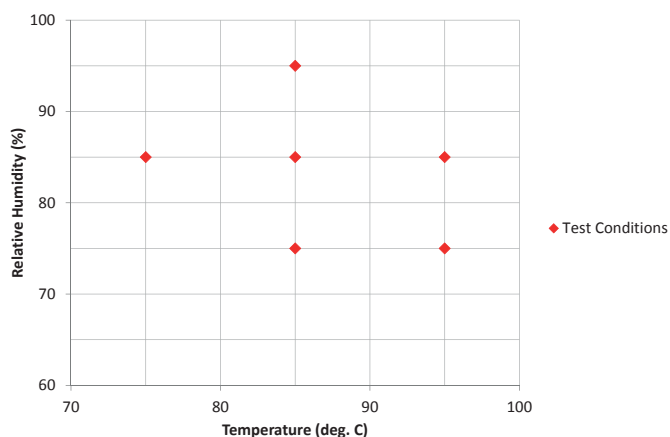


Figure 6. Test conditions chosen for accelerated testing. Five samples per barrier were used for each test condition.

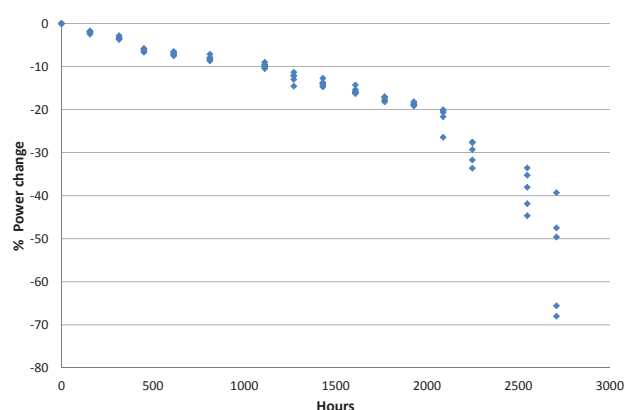


Figure 7. Degradation in P_{\max} for modules with barrier-1, tested at 85°C/85% RH.

barrier-1 samples there are two aspects of measured degradation that merit discussion here. On the basis of the analytical model discussed earlier, it is of interest to see if observed degradation is indeed linear in time; it is also of interest to obtain the effective activation energy and relative humidity exponent from these measurements. Both of these aspects are discussed next and apply to

barrier-1 samples only. Follow-up work is planned as and when data for barrier-2 samples become available.

Linear degradation and criterion for time to failure

Fig. 7 shows a representative degradation curve for modules tested at 85°C/85% RH: it is seen that the degradation appears to be close to linear up to a

~20% loss of P_{\max} , beyond which a 'crash behaviour' is seen. The scatter in the data also increases in the 'crash' region. At the outset it is not clear that the degradation can be considered consistent with a 'linear behaviour' predicted by the analytical model.

“Degradation appears to be close to linear up to a ~20% loss of P_{\max} , beyond which a 'crash behaviour' is seen.”

The data can be analysed on a log-log scale to identify if the crash behaviour is significantly different from the initial degradation, or if the entire degradation is indeed a power-law type of degradation. On the log-log scale two different regimes were seen: the 'pre-crash' behaviour was different from the 'post-crash' behaviour. On the basis of the examination of the data, it was determined that the linear degradation model was appropriate and acceptable for a degradation of up to 20%.

It is also possible that measurement errors can lead to deviations from linearity. The sample size can be improved and the measurement techniques refined in order to address possible sources of error and allow an improved statistical representation of the configurations tested. In one case, sample measurements were seen to deviate from others in the same group because of corrosion of the electrical contacts as a result of exposure to high-temperature and high-RH conditions. These deviations had to be addressed by repeating the measurements with another set of newly constructed samples. It was noted that for highly accelerated conditions using 95°C, the deviations and scatter were the most significant; this included an initiation of the crash behaviour before 20% degradation.

The onset of the crash behaviour was not quantified in this study because of the small sample size and the scatter in the data. A larger sample size and conducting tests under additional conditions would be required in order to fully understand this behaviour. It should be noted that these tests are resource intensive as a result of the test times involved for high-barrier systems. Additionally, increasing the sample sizes can be challenging because of chamber occupancy and associated costs.

In the authors' opinion, the assumption of linear degradation is acceptable for moderate field conditions where the temperatures do not reach these extremes (~95°C)

Under the patronage of
H. H. Sheikh Maktoum bin Mohammed bin Rashid Al Maktoum, Dubai Deputy Ruler



MIDDLE EAST
ELECTRICITY

1-3 March 2016

Dubai World Trade Centre, UAE

1,600 exhibiting companies
25 international pavilions
40 technical seminars
2 conferences



Find out more and register your attendance on www.middleeastelectricity.com
Email: info@middleeastelectricity , Phone: +971 4 336 5161

Co-located with:

THE REGION'S LARGEST SOLAR TRADE EVENT



1 – 3 MARCH 2016

DUBAI WORLD TRADE CENTRE, UAE

- **120+** exhibiting companies • **25** countries represented • **4,000** senior level decision makers
- **4,500** sqm of the latest solar technologies

REGISTER NOW FOR FREE FAST-TRACK ACCESS

E: info@solarmiddleeast.ae

T: +971 (0) 4 336 5161

W: www.solarmiddleeast.ae

Organised by

informa
exhibitions

Partner Events



Saudi Power



Saudi Aircon



POWER
NIGERIA

ELECTRICX

SOLAR-TEC

over extended periods of time. It seems possible that some temperatures used in highly accelerated test conditions (such as 95°C) over extended test times trigger other failure mechanisms that may not be representative of field failures attributable to moisture ingress; this requires further investigation. Nevertheless, for an initial assessment as undertaken in this study, the rest of the analysis is carried out directly using the results for time to failure as defined by a 20% degradation in power and using the models described earlier.

Analysis of time to failure using a 20% power loss as a criterion for obtaining model parameters

It is desirable to validate the model developed earlier using the data from accelerated testing; in particular, the objective is to obtain the activation energy and relative humidity exponent from the experimental data. Fig. 8 shows an Arrhenius plot for the time to failure as defined by a 20% power degradation for different temperature conditions at 85% RH. The activation energy derived from these results is $\epsilon_a = 0.63\text{eV}$.

It is interesting to note that the quality of regression is not as good as that for the diffusivity measurements, but the value of the activation energy calculated from module-level tests is consistent with the activation energy measured for barrier-1 using MOCON testing. It is also interesting to note that the activation energy estimated using just the mean time to failure at each condition is somewhat lower in value, namely $\epsilon_a = 0.6\text{eV}$, and the quality of regression is better.

It should be pointed out that the module-level tests, in principle, account for other degradation processes associated with the module construction when exposed to temperature and humidity, whereas the MOCON testing includes only the barrier material; hence, in theory, the two values can differ. For further analysis, the accepted value for the activation energy is 0.63eV .

Fig. 9 shows the log-log plot that is intended for the extraction of the humidity exponent; on the basis of this data, the relative humidity exponent is calculated to be $n = -3.41$. It is interesting to compare the values of activation energy and relative humidity exponents obtained in this study with those reported in Peck [11]: representative values given in Peck are $\epsilon_a = 0.79\text{eV}$ and $n = -2.66$ for encapsulated electronic components, whereas the current data set suggests $\epsilon_a = 0.63\text{eV}$ and $n = -3.41$ for the tested PV modules. While the consistency

between the two sets of values is promising, further considerations are necessary in order to assess the field life on the basis of the parameter values obtained from accelerated testing.

Prediction of field performance

Predicting field performance for flexible modules with regard to moisture ingress using the results of accelerated testing requires reconciliation with available meteorological data. The module performance is expected to be location dependent because of variations in local temperature and relative humidity. With that in mind, two aspects need to be examined:

1. A model based on given typical meteorological year (TMY) data for predicting cell and module temperatures.
2. An analysis framework for translating the results of accelerated testing and acceleration factor relationship, such

as Equation 11, to field conditions. It is desired that the analysis of TMY data be consistent with the framework used for Equations 2 or 11.

Modelling cell temperature using meteorological data

A well-known empirical model for cell temperature based on typical meteorological data is the Sandia model [16]. The expression for cell temperature is given by:

$$T_c = T_{\text{amb}} + I \exp(a + bv_{\text{wind}}) + \frac{1000}{I} T_{\text{offset}} \quad (12)$$

where

T_c = cell temperature at 1000W/m^2 irradiance

T_{amb} = ambient temperature

I = irradiance (W/m^2)

a = irradiance coefficient

b = wind speed coefficient

v_{wind} = wind speed

T_{offset} = offset ΔT between the back-side and cell temperatures

The coefficients for a variety of module constructions and mounting

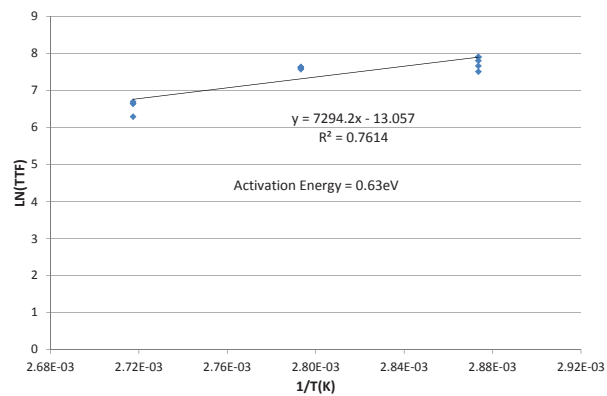


Figure 8. Arrhenius plot for time to failure (as defined by a 20% degradation in power) for samples subjected to different temperatures at 85% RH (activation energy = 0.63eV).

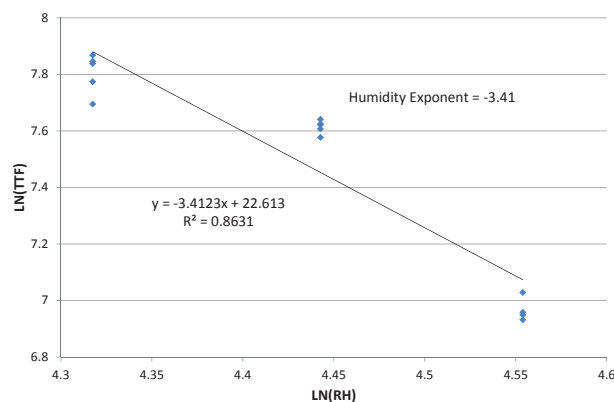


Figure 9. Log-log plot for the relative humidity exponent ($n = -3.41$).

configurations can be found in King, Boyson and Kratochvil [17].

For the flexible module construction used in this study, the coefficients were expected to be similar to an insulated back glass/cell/polymer sheet configuration ($a = -2.81$, $b = -0.0455$, $T_{\text{offset}} = 0$), as a polymer/cell/polymer sheet configuration with an insulated back was being tested. To obtain these coefficients by regression, module temperatures were measured with cell-level embedded thermocouples in outdoor testing for a year under variable atmospheric conditions at a location in Santa Clara, California, USA. The parameters derived using available data to date are $a = -2.96$, $b = -0.0178$, $T_{\text{offset}} = 0$. It should be noted that since the temperature offset for the flexible module is $T_{\text{offset}} = 0$, Equation 12 can be used to predict 'module temperature'. These values have been obtained using data at the California site, with further testing in progress at other sites. The data collected to date have shown strong consistency with these model parameters, but the parameter refinement will continue as more data become available.

A comparison of the model fit and measured temperatures at Santa Clara is shown in Fig. 10. The period chosen for the comparison corresponds to the week in which some of the highest average error values between the model prediction and measured data occurred. It is noted that this period also corresponds to the time when some of the highest module temperatures were reached. It is seen that there is good agreement between measured and predicted temperatures at midday, while the agreement is not so good during the evening and night time. The module temperatures at night time tend to be overestimated by the model, compared with the actual measured night-time temperatures (at the time when RH is expected to be high). This is a limitation of the model and is attributed to radiation losses that are not accounted for in Equation 12.

For the calculation of moisture-induced degradation, the Arrhenius variation with temperature would imply that matching the module temperatures at the high-temperature end is more important, and hence this fit is accepted. With this model, the module temperature can be predicted at different locations using available TMY data. Such a prediction using parameters obtained from data in California is used in this work for the field performance assessment of the barrier under consideration. The methodology for performance prediction is discussed in detail next.

Prediction of field performance with regard to moisture-induced damage

The prediction of field performance needs to be based on the acceleration factor relationship from Equation 2 or Equation 10; however, the variations in field temperature and humidity conditions need to be accounted for in this relationship. To this end, the assumption is made that the variations in field conditions (T , RH) are sufficiently slow that the ambient conditions may be assumed to be constant for the analysis of TMY *hourly* data (i.e. the conditions are approximately constant over each hourly interval). It should be noted that the temperature and humidity conditions for the module can change within an hour as a result of sudden changes in ambient conditions (e.g. rain); however, it is assumed that appropriate averaging will account for such deviations. On the basis of this consideration, a proposed averaged acceleration factor relationship is:

$$\langle AF \rangle = \frac{1}{t_{\text{yr TMY}}} \int \left(\frac{RH_{\text{field}}(t)}{RH_{\text{test}}} \right)^n \exp \left[\frac{\varepsilon_a}{k} \left(\frac{1}{T_{\text{field}}(t)} - \frac{1}{T_{\text{test}}} \right) \right] dt \quad (13)$$

where $\langle AF \rangle$ represents expected yearly averaged value of the acceleration factor.

Once the acceleration factor has been computed for a given location, reference test results can be scaled to field conditions using:

$$TTF(\text{field}) = \langle AF \rangle \times TTF(\text{test}) \quad (14)$$

The reference condition used in this calculation is the well-accepted high-acceleration condition of 85°C/85% RH.

Three features of the acceleration factor relationship to be used in Equations 13 and 14 merit attention:

1. For typical applications in the consumer electronics industry, the use of average temperature and average RH conditions in the operating environments may suffice for a prediction over shorter product lifetimes, since the conditions typically do not vary significantly in such usage environments. However, using *yearly* average values of temperature and RH for PV applications would be inappropriate, since such averages do not correctly reflect the conditions that correspond to maximum damage. Outdoor fluctuations of temperature and RH values need to be accounted for in PV applications in a consistent manner: hence the consideration of the integral representation of the acceleration factor relationship proposed in Equations 13 and 14. In addition, this relationship is typically evaluated using hourly TMY data, implying that the conditions are assumed to be constant over an hour in these calculations.

2. The prediction of the field life using this relationship is based on scaling a result obtained under a particular test condition. The prediction can in principle vary, depending on the test condition chosen as the reference. If the fit to experimental data is good for all conditions, this should not be a concern; however, the quality of fit under different conditions will alter the quality of prediction. To obtain a good predictive model, it is essential that the model parameters be derived from tests that are performed under many different conditions and that use statistically significant sample sizes. For this study, the limitation imposed by the available test resources was accepted, and the condition chosen as a reference was 85°C/85% RH.

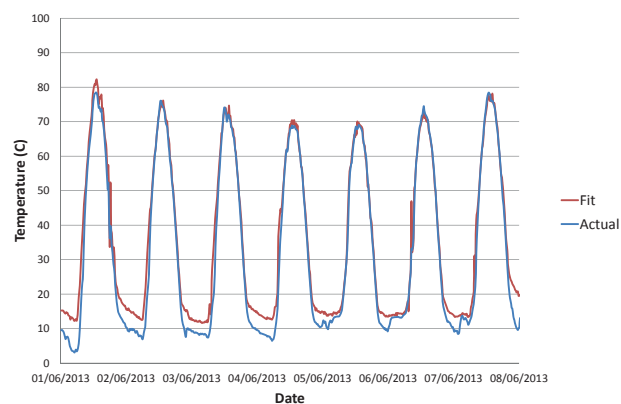


Figure 10. Comparison of predicted and measured module temperatures at Santa Clara.

3. A critical aspect of the relationship expressed in Equation 13 is that the implied time to failure for low-humidity conditions (low RH) is high. For smaller values of relative humidity exponent n , the singular behaviour at lower RH values will dominate the prediction. For instance, see Fig. 11 for the Hallberg-Peck acceleration factor for a constant field temperature of 50°C with the test conditions of 85°C for different RH values; in this case, below around 40% RH the acceleration factor starts to exceed 100. For reference, an acceleration factor of 100 would imply that 3000 hours at 85°C/85% RH is equivalent to ~34 years at 50°C/40% RH. The basis for this large time to failure prediction is that according to this model, the failure induced by moisture is significantly delayed, since the availability of moisture to drive the damaging reactions is affected. This does not, however, imply that the actual failure time of the module in the field is large. Fig. 11 illustrates that in hot and dry environments, Equations 13 and 14 will predict very large times to failure, while in reality other mechanisms, such as thermal degradation, can dominate module failure. The prediction from Equations 13 and 14 would be appropriate only with regard to *moisture-induced damage*.

With the above considerations, the mean times to failure calculated using TMY data for Bangkok and San Jose are given in Table 1. It should be noted that these predictions are intended to be the best assessment of the field performance of barrier-1 *for moisture-induced degradation only*; other potential modes of degradation, such as UV-induced degradation or delamination within the barrier layers, are not taken into account. It is noted that the results imply that the barrier-1 product may not meet typical warranty requirements for aggressive environments, such as those in Bangkok, while it may marginally survive in other locations.

In comparison, from the available data gathered to date (tests are ongoing), the barrier-2 product was seen to dramatically outperform the barrier-1 product with regard to moisture-induced degradation, showing a power degradation of less than 20%, even after ~7000h exposure to 85°C and 85% RH. Similar differences were also seen under other test conditions, indicating that barrier-2 performance is superior to barrier-1 performance.

On the basis of these results, the

barrier-1 product may not meet typical warranty requirements in aggressive environments, such as in Bangkok, and is seen to only marginally meet the requirements in environments such as San Jose, California. On the other hand, barrier-2 is expected to be adequate in resisting moisture ingress over a typical PV module lifetime of 25 years. To enhance this method for predicting field performance in different locations, including those which have low RH values, it is essential to carry out tests under low RH conditions. It seems possible that the singular behaviour at low relative humidity, as dictated by Hallberg-Peck-type relationships, may not hold because of failure modes driven by thermal effects alone. This merits further work and is currently under investigation.

There is another aspect of these results that is not obvious from the data presented so far. As mentioned earlier, the prediction methods based on Equations 13 and 14 will over-predict the time to failure of the module with regard to moisture ingress because of the singular behaviour implied by the negative RH exponent. It is also noted that in order to capture appropriate behaviour at low RH values, test data at low RH values is crucial. In principle, to obtain a power-law exponent from the log-log plot, data over a wide range of RH values would be desirable.

The singular behaviour in a relationship such as Equation 2 implies that it may be overly challenging to capture the behaviour at low RH

values using accelerated testing. There is practical difficulty in testing at low RH values, because the associated test times will be large. This concern is exacerbated for systems such as the module construction using very high barrier systems (e.g. barrier-2). As the barrier level increases, the fluctuations in external moisture content (ambient RH conditions) are even less detectable through its effect on cell performance. In the limiting case where the barrier level tends to be infinitely high, the primary degradation mode will switch to the one purely activated by thermally induced mechanisms or by the moisture ingress from the edge seal. The model based on a relationship such as Equation 2 will fail to capture such transitions. Furthermore, extensive testing will be necessary in order to identify threshold barrier levels (i.e. critical values of WVTR) below which the effects of ambient RH fluctuations are not detected in cell performance. Such a threshold level, of course, depends on the particular cell structure and composition as well as on the barrier WVTR.

On the basis of these considerations, the plan for future work is to explore similar tests at lower RH values in order to obtain a better estimate of RH dependence; in addition, lower barriers as well as very high barrier systems, such as a module construction using barrier-2, will be investigated further. At the time of writing this paper, testing is in progress for barrier-2 systems.

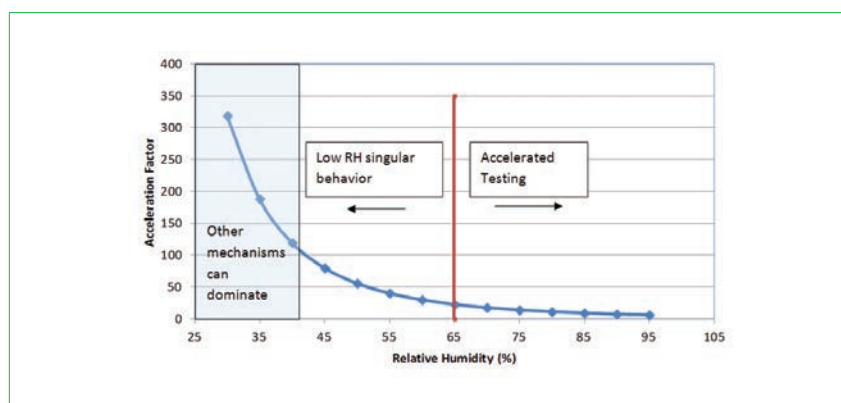


Figure 11. Hallberg-Peck acceleration factor for a constant field temperature of 50°C, with the test conditions of 85°C for different RH values. This highlights the limitations of accelerated testing with regard to conditions of low relative humidity (RH exponent $n = -3.41$).

Location	Power change at failure	Years to failure (RH exponent = -3.41)	Years to failure (RH exponent = -1)
Bangkok	20%	13.1	10.1
San Jose	20%	71.5	33.1

Table 1. Predicted field performance for barrier-1, considering moisture-induced degradation only.

Conclusion

A methodology based on accelerated testing has been presented for the assessment of the field performance of flexible PV modules with regard to moisture-induced damage. A framework based on an empirical relationship (the Hallberg-Peck model) used in consumer electronics industry has been proposed as a candidate for relating performance in accelerated testing to degradation in the field. An analytical model has been developed to justify the use of a Hallberg-Peck-type relationship in the testing and analysis of the performance of a PV module when exposed to temperature and humidity.

“In order to correctly capture relative humidity dependence, testing needs to be carried out under conditions that cover a wide range of relative humidity values.”

It was shown that, while Arrhenius temperature dependence can be demonstrated in the testing of the barrier alone, as well as through module-level tests, obtaining relative humidity dependence is challenging. In particular, it has been learnt that in order to correctly capture relative humidity dependence, testing needs to be carried out under conditions that cover a wide range of relative humidity values.

For high-barrier configurations used in PV modules, the associated test times can be prohibitive because of resource constraints. A framework, which uses a combination of test results and an analytical model, has been provided for predicting field performance from accelerated testing. For the configurations tested, and the limited data available, it has been shown that the barrier-1 product ($WVTR = 0.002\text{g/m}^2/\text{d}$ at $40^\circ\text{C}/90\%\text{ RH}$) considered in the study may not meet the typical warranty requirement of 25 years for PV modules in aggressive environments, such as in Bangkok; the barrier-2 product ($WVTR < 1.0\text{e-}5\text{g/m}^2/\text{d}$ at $40^\circ\text{C}/90\%\text{ RH}$), on the other hand, is likely to be adequate for resisting moisture ingress over the intended service life of the PV module. Further experimental work is necessary in order to establish a threshold value of WVTR for ensuring a product life of ~25 years for flexible PV modules.

Acknowledgement

The work presented in this article is the result of a team effort. The authors would like to thank Dr. Greg Kimball, Dr. Ting Cao, J. Poris and Underwriter Laboratory testing services for useful contributions to this work.

References

- [1] Pern, J. 2008, “Module encapsulation materials, processing and testing”, APP Internat. PV Rel. Worksh., Shanghai, China.
- [2] Livingston, H. 2002, “SSB-1: Guidelines for using plastic encapsulated microcircuits and semiconductors in military, aerospace and other rugged applications”, Report, Solid State Device Committee of the GEIA.
- [3] Shirley, C.G. 1994, “THB reliability models and life prediction for intermittently-powered non-hermetic components”, *Proc. 32nd Ann. Int. Rel. Phys. Symp.*, San Jose, California, USA, pp. 72–77.
- [4] Kempe, M.D. 2006, “Modeling of rates of moisture ingress into photovoltaic modules”, *Sol. Energy Mater. Sol. Cells*, Vol. 90, pp. 2720–2738.
- [5] Coyle, D.J. 2013, “Life prediction for CIGS solar modules. Part 1: Modeling moisture ingress and degradation”, *Prog. Photovoltaics Res. Appl.*, Vol. 21, pp. 156–172.
- [6] Kempe, M.D. et al. 2010, “Evaluation and modeling of edge-seal materials for photovoltaic applications”, *Proc. 35th IEEE PVSC*, Honolulu, Hawaii, USA.
- [7] Otth, D.H. & Ross, R.G. 1983, “Assessing photovoltaic module degradation and lifetime from long term environmental tests”, *Proc. 29th Inst. Env. Sci. Ann. Meet.*, Los Angeles, California, USA, pp. 121–126.
- [8] Osterwald, C.R. & McMahon, T.J. 2008, “History of accelerated and qualification testing of terrestrial photovoltaic modules: A literature review”, *Prog. Photovoltaics Res. Appl.*, Vol. 17, No. 1, pp. 11–33.
- [9] Hallberg, O. & Peck, D.S. 1991, “Recent humidity accelerations – a base for testing conditions”, *Qual. Reliab. Eng. Int.*, Vol. 7, pp. 169–180.
- [10] Peck, S.D. 1986, “Comprehensive model for humidity testing correlation”, *Proc. IRPS*, Anaheim, California, USA, pp. 44–50.
- [11] Peck, S.D. 1970, “The design and evaluation of reliable plastic encapsulated semiconductor devices”, *Proc. IRPS*, Anaheim, California, USA, pp. 81–93.
- [12] Hardikar, K. et al. 2013, “A methodology for testing, characterization and prediction of

edge seal performance in PV modules”, *Photovoltaics International*, 22nd edn.

- [13] Crank, J. 1975, *The Mathematics of Diffusion*, 2nd Edition. Oxford, UK: Oxford University Press.
- [14] Klinger, D.J. 1991, “Humidity acceleration factor for plastic packaged electronic devices”, *Qual. Reliab. Eng. Int.*, Vol. 7, pp. 365–370.
- [15] MOCON Testing Services, 7500 Midelsohm Ave., N. Minneapolis, MN 55428, USA.
- [16] Fuentes, M.K. 1985, “A simplified thermal model of photovoltaic modules”, Report No. SAND85-0330, Sandia National Laboratories, Albuquerque, New Mexico, USA.
- [17] King, D.L., Boyson, W.E. & Kratochvil, J.A. 2004, “Photovoltaic array performance model”, Report No. SAND2004-3535, Sandia National Laboratories, Albuquerque, New Mexico.

About the Authors

Dr. Kedar Hardikar is the director of reliability integration and modelling at MiaSolé and an adjunct faculty member at San Jose State University and Santa Clara University. He holds a Ph.D. from the Division of Engineering, Brown University. His role at MiaSolé includes leading and supporting product development activities, product reliability and computational modelling.

Todd Krajewski is the process development manager for flexible modules at MiaSolé. He has a bachelor's in chemistry and is the inventor/co-inventor of 15 issued patents and numerous patent applications. His work has focused on polymer synthesis, process scale-up, ultra barrier films and material integration in the semiconductor, OLED and solar fields.

Kris Toivola is a reliability engineer at MiaSolé, with responsibilities including accelerated testing, outdoor data collection and data analysis. He graduated from Stanford University with a B.S. in materials science and engineering in 2010 and an M.S. in materials science and engineering in 2011.

Enquiries

Kedar Hardikar
MiaSolé
2590 Walsh Ave
Santa Clara, CA 95051
USA

Email: khardikar@miasole.com
Tel: +1 408 919 5702

PV Modules

Page 85
News

Page 88
**Cost/kWh thinking and
bifaciality: Two allies for low-
cost PV of the future**

Radovan Kopecek, Ismail Shoukry &
Joris Libal, ISC Konstanz, Germany

Page 98
**Reliability and durability
comparison of PV module
backsheets**

Haidan Gong & Guofeng Wang, Wuxi
Suntech Power Co., Ltd., Wuxi, China



Quality of modules and project execution 'disregarded' in many Indian projects

Many solar projects built in India have compromised on the quality of execution and the modules used, according to an executive panel at Intersolar India in November. The executives also expressed concern that the extremely low bids quoted in the state solar auctions over the last six months may exacerbate this issue with efficiencies having to be prioritised over quality.

Gyanesh Chaudhary managing director and chief executive of India-based module manufacturer Vikram Solar, said: "There is a total disregard for quality of execution and sustainability of these large projects, which are eventually going onto the grid and possibly making the grid unstable. These are very significant issues which nobody is willing to talk about."

Vineet Mittal, vice chairman of Welspun Renewables, added: "People have compromised in evaluating the modules supplier."



Source: Solar Promotion gmbh

Welspun and Vikram Solar hit out at the poor quality and due diligence of some projects in the country.

News

Module ramp plans

JinkoSolar targeting 5.3GW of module capacity by mid-2016

JinkoSolar has said its ingot/wafer, solar cell and module production capacity would be expanded further in 2016 to meet growing demand. Reporting third quarter results in an earnings call, JinkoSolar's management updated preliminary plans to increase capacity. Its current ingot/wafer capacity of 3GW would be expanded by 300MW to 3.3GW by the first quarter of 2016, primarily by upgrading existing in-house equipment, the company said. Solar cell capacity would also be increased by a further 500MW from existing capacity of 2.5GW to total 3GW by mid-2016.

Management noted that a decision on how much of the additional capacity could be added in China and or overseas had not yet been made. The company also noted that module capacity would be increased by another 1GW to reach 5.3GW by mid-2016.

Sunpower announces plans to ramp 2GW of Cogenra module technology

Major PV energy provider SunPower is to ramp Cogenra Solar's module technology to 2GW by 2020 and only a further 800MW of its 'Maxeon' solar cell technology at its new facility, Fab 5, that it expects to ramp in early 2019.

SunPower said that it would be offering a new 'Performance' (P) Series module developed by US-based Cogenra Solar, which it said it acquired earlier in 2015. Cogenra Solar developed its Dense Cell Interconnect (DCI) technology, originally designed for low-cost CPV technology but further developed the technology for connecting conventional cell/modules, which is claimed to eliminate electrical losses from cell to cell.

compared to 10% of total revenue (US\$91.5 million) in the previous quarter. However, overall revenue was down 4.3% quarter-on-quarter due to shipments falling to 184.5MW, down 3.8% from 191.9MW in the first fiscal quarter of 2015. Self-branded module ASPs in the quarter were US\$0.58/W, unchanged from the previous quarter. ASPs for self-branded cells during the quarter were US\$0.26/W, compared to US\$0.27/W in the previous quarter.

Trina Solar hits record quarterly shipments of 1.7GW

Leading 'Silicon Module Super League' (SMSL) member Trina Solar reported record module shipments in the third quarter of 2015, surpassing previous guidance and setting a new quarterly shipment record in the PV industry.

Trina reported shipments of 1,703.2MW, consisting of 1,353.2MW of external shipments and 350MW of shipments to its own downstream PV power projects. Total module shipments increased 38.3% sequentially and 60.1% year-over-year. The company also significantly raised full year shipment guidance from a previously upward revision of between 4.9GW to 5.1GW to 5.5GW to 5.6GW, solidifying its position as the leading PV module manufacturer in the world in 2015. Jifan Gao, chairman and CEO of Trina Solar, commented: "We had a solid quarter of operations that came in ahead of our expectations, despite the one-off negative impact from the settlement of the Solyndra lawsuit and currency fluctuations that we experienced. We shipped a record 1.7GW of modules, which enables us to achieve a significant milestone of over 15GW of module shipments cumulatively since our inception."

Sales and shipments

China Sunergy's module sales jump in US

Struggling PV manufacturer China Sunergy (CSUN) experienced a significant increase in shipments and revenue from the US in its fiscal second quarter financial results. CSUN reported revenue from the US accounted for 34.4% of total revenue (US\$87.5 million) in its fiscal second quarter 2015 results,



Credit: Trina Solar



ReneSola downstream shift to hit 2015 shipments

PV module manufacturer and PV project developer ReneSola reported a rebound in shipments and sales in the third quarter of 2015, but shipment levels are unlikely to match nameplate capacity levels. ReneSola reported third quarter PV module shipments of 405.5MW, up 25.9% from the previous quarter, while solar wafer shipments also increased 21.3% to 341.6MW, said to be due to taking advantage of wafer market conditions of rising ASPs and tight supply.

It should be noted that the company had not provided PV module shipment guidance throughout 2015. However, based on ReneSola's nameplate capacity, PV module shipments in 2015 would

have been in the range of 2GW to 2.2GW if the company operated at full capacity. ReneSola has shipped 1,223.9MW of PV module shipments in the first nine months of 2015 and when taking quarterly run rates and inventory levels into consideration the company could potentially ship in a range of 1.7GW to 1.85GW for the full year.

Going, going...

Isofoton's 200MW of module equipment auctioned

Spanish industrial auctioneer Escrapalia, a subsidiary of Surus Inversa, has held

an online auction of module assembly equipment and a complete automated assembly line from defunct PV manufacturer Isofotón.

According to the auctioneer, the Isofotón facility in Malaga, Spain was the largest in the country before the company went into bankruptcy in late 2013. Individual lots from the 200MW module production facility were on offer as well as the entire 120MW complete automated turnkey line supplied by Reis and a second 100MW semi-automated line. Other equipment in the auction included a Maier laminator, a Komax 2800i string tester as well as a full suite of assembly tools.

Inside out

Fraunhofer installs MWT cells on its laboratory façade

Germany's Fraunhofer ISE has made a modest, 70-panel installation of new crystalline PV cell and module technologies produced by the institute on the outside of one of its laboratories. The institute, which researches solar energy and related clean energy technologies, including battery-based energy storage and hydrogen fuel cell vehicles, completed the test project, which started back in 2013 when the lab was inaugurated.

The institute claims the new cells and modules are lower cost than comparable technology, and said the installation



Fraunhofer has taken its MWT modules from the inside the lab to the outside of the lab.

shows that by the addition of the thermoplastic material TPS, they can be adapted for building façades. Fraunhofer has dubbed the new module 'TPedge'.

It integrates back-contacted cells made with the institute's patented 'High Performance Metal Wrap-through' concept. Group head of MWT solar cells and printing technology Dr Florian Clement said the use of automated production processes meant his team was able to produce the devices in cycle times similar to industrial fabrication.

Supply deals

Sunrun secures three new module supply deals for 2016

US residential installer signed three new module supply agreements for 2016.

The company increased its agreement with REC increasing it to a minimum of 120MW and up to 150MW. That's an increase on its 2015 contract for 50-100MW. Canadian Solar secured a 112MW deal and Hanwha Q CELLS will supply the NASDAQ-listed installer with up to 135MW of modules supplied from its Malaysian and South Korean manufacturing sites.

GCL signs off on 100MW module supply deal with CNI Energy

Nanjing GCL New Energy – a subsidiary of GNE – has signed off on a 100MW module supply agreement with CNI

Energy for RMB398 million (US\$61 million). The modules will be provided for Nanjing's GCL New Energy's 100MW PV project in Funan County, Anhui Province.

This is the fifth time that GNE has agreed to module supply deal with CNI Energy this year – all of which provided materials for projects in China.

Trina Solar to provide 96.2MW of PV modules for project in Japan

Trina Solar has signed off on a supply deal with Toyo Engineering to provide 96.2MW of solar modules to the Hosoe Mega Solar Project, which is currently being developed by Energy K.K. and is expected to be the largest solar plant in Kyushu, Japan.

The modules will be shipped starting in the fourth quarter of 2016 and will end by January 2018. The installation will be developed on 140 hectares of land where a golf course was originally planned. The project is expected to be operational by the spring of 2018 and will produce clean energy for up to 30,000 homes.

JA Solar to provide 100MW of modules for Zimbabwe project

Solar power products manufacturer JA Solar has won a contract to provide 100MW of PV modules to one of the first three large-scale ground-mounted solar power projects in Zimbabwe.

The projects will boast an installed capacity of 300MW, while the three contractors for the projects will be ZTE, China MCC17 Group and Intratek Zimbabwe. JA Solar will supply its PV modules to China MCC17 Group for the project it is developing. According to information offered by the State Procurement Board of Zimbabwe, the projects will be developed in Munyati, Insukamini, and Gwanda, the capital of Matabeleland.

The three projects hold a total PV module contract value of US\$544 million, US\$179 million of which was won by JA Solar. The projects are scheduled to begin construction in the closing months of 2016 and are expected to be completed by the end of 2017.

Testing and certification

WINAICO solar module passes tougher reliability testing at ITRI

Taiwan-based PV module manufacturer has received the Taiwan Excellent PV award by the Bureau of Energy, Ministry

of Economic Affairs, Taiwan after its 300W PERC 60-cell module passed advanced reliability tests conducted at Taiwan's research institute, ITRI.

New tougher reliability testing, designed to provide more improved real-world lab testing characteristics have been championed by NREL and make-up a proposed 'Qualification Plus' test that is expected to result in acceptance of new IEC 62804 and IEC 62892 testing standards, which is in draft development. According to WINAICO, ITRI tested its module for PID, UV, mechanical load, thermal cycling and humidity testing as part of more common tests on modules. The PID test period defined by ITRI was said to have been lengthened to 288 hours, three times the industry standard of 96 hours.

Seraphim receives 'A' rating certification for selling modules in Brazil

PV module manufacturer Seraphim Solar said it had been granted an 'A' rating certification for its modules with Brazil's National Institute of Metrology, Quality and Technology (Inmetro). The certification carries a scale of A through E for module quality, technical competence, and energy efficiency.

All of the tested Seraphim modules appearing on the list received an A rating, according to Seraphim. Justin Xi, global executive general manager of Seraphim Solar said: "Brazil will be a key PV market with local government the commitment, and their complete support and strong pursuance for renewable energies and solar. We anticipate rapid growth in Brazil."

HT-SAAE module exceeds 300W

The mass production output power for HT-SAAE's N-type PERT high-efficiency mono-crystalline silicon solar module has surpassed 300W, certification body TUV Rheinland confirmed after testing.

When compared with other mono-crystalline PV modules, the mass production output power for n-type PERT mono-crystalline modules is around 10 to 15W higher than the average industrial level.

The total output power of these modules have increased from February 2015, when they measured out at 285W. N-type PERT mono-crystalline silicon solar modules have also passed the full mechanical load test of 10800Pa, achieving the highest load level of the market, which is tested and certified by CSA – an international third party authoritative institution.



Credit: JA Solar

JA Solar will provide modules for one of three 100MW projects in Zimbabwe.

Cost/kWh thinking and bifaciality: Two allies for low-cost PV of the future

Radovan Kopecek, Ismail Shoukry & Joris Libal, ISC Konstanz, Germany

ABSTRACT

To bi(facial) or not to bi(facial) – that is the question, and has been for many years in the PV business. In early 2000 a renaissance of cost-effective bifacial PV started, and now more and more companies are beginning to believe in it. This paper summarizes the status of bifaciality and is a continuation of a previous article in *Photovoltaics International* on bifaciality and kWh cost reduction. The present paper concentrates more on the system side: bifacial gain data for large systems and for simulations of systems reveal that a bifacial gain of 30% on average can be obtained in an optimal situation. It is demonstrated in this paper that the future of the lowest-cost electricity generation from PV is not all about increasing cell and module efficiencies and minimizing cost/Wp, but rather squeezing the best out of a system using a few simple tricks, such as bifaciality, tracking and ground reflection improvements, to achieve the lowest cost/kWh.

Introduction

Bifaciality is becoming sexier every PV year. The EU PVSEC 2015 was announced to be a PERC conference, but in reality it was also a bifacial one. The reason for this is that the PV community has begun to realize that not only is direct sunlight responsible for high yield in a system, but also diffuse irradiance can increase system performance by up to 40% (Fig. 1). And this is true not only for free-standing modules but also for actual systems when properly installed.

“Not only is direct sunlight responsible for high yield in a system, but also diffuse irradiance can increase system performance by up to 40%.”

Even Solar World has now announced the development of a bifacial module, which will enter production in Q4 2015 [2]. In order to progress bifaciality into mass production, however, the three most important issues to be addressed are:

1. **Bankability:** proof of the bifacial gains for PV systems larger than 1MWp.
2. **Standardization:** creation of standards for bifacial measurements and lifetime testing conditions.
3. **Simulations:** improvement of bifacial simulations and their implementation in commercially available system-yield calculators, such as PVsyst.

This paper will address these three important points and report on their status (it is an update of an earlier bifaciality paper by Kopecek et al. [3], published in this journal).

The need for standards to sell the bifacial advantage: away from Wp mentality to kWh thinking

In PV R&D, as well as in the industry, module efficiency records (and sometimes power records) are quite often reported to show off the developers' muscles and to demotivate their competitors. However, the fact that these efficiencies were often achieved on a postage-stamp scale and complex and expensive processes were involved is not usually disclosed. If the cost of ownership (COO) were reported as well, then these records would be seen in another light. Basically, there should therefore be four categories for expressing cell and module records when the modules are implemented in a system:

1. Cell and module efficiency
2. Module power
3. Cost/Wp
4. Cost/kWh

The winners in each of these four categories are to be found within different technologies. Whereas categories (1) and (2) are led by SunPower (IBC cell efficiency: 25%), Sharp (heterojunction IBC: 25.1%) and Panasonic (heterojunction IBC: 25.6%) [4–6], category (3) is dominated by standard mc-Si module technologies at costs of around 50US\$/Wp (see Fig. 3).

In the author's opinion the most important category – the lowest levelized cost of electricity (LCOE), where the most powerful modules per area (occupied by the PV system) are necessary – is (and will be) dominated by bifacial technology when around 20% bifacial gain is achieved in large systems. This fact is explained in terms of numbers in Fig. 2.

The lowest-cost Cz-Si module per Wp is still a p-type Cz-Si module with

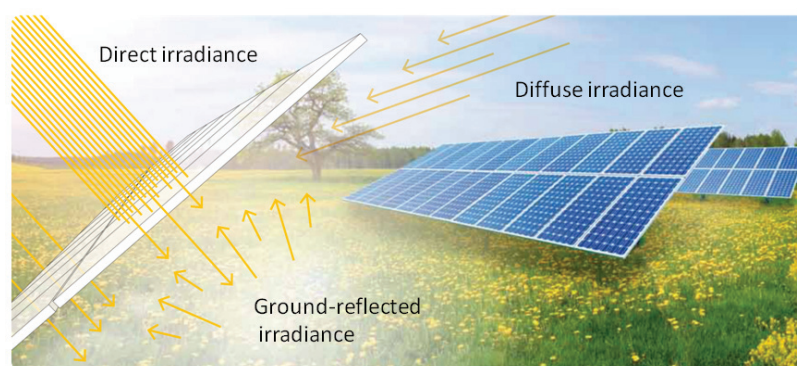


Figure 1. Visualization of indirect light striking the back side of a module, responsible for bifacial gains of up to 40% in a system [1].

Al-BSF or PERC technology. Monofacial modules with bifacial nPERT cells are 2–4US¢/Wp more expensive; even nPERT glass–glass modules are 1US¢/Wp more expensive, since more-

efficient cells are required in order to achieve the 280Wp front-side power, because of the transparent rear side of the module. However, if the advantage of the effective peak power (which is what

you actually have in a system compared with a monofacial module) were to be considered, then today's monofacial nPERT modules would already be comparable in cost (US\$/Wp) to monofacial p-type PERC modules, while a bifacial nPERT module would be even more cost-effective. If the LCOE is calculated for southern Europe with these modules, assuming a yearly global horizontal irradiation of 2,200kWh/m², the bifacial module with a bifacial gain of 20% already yields by far the lowest cost for electricity production. It will be seen later that even higher bifacial gains than that are also attainable in large systems.

The challenges of bifaciality lie in demonstrating its advantages in large systems and in setting standards in order to be able to promote this additional power generated by the rear side. Several meetings of a bifacial consortium led by Pasan, h.a.l.m. and others have already taken place, with the goal of setting standards for bifacial measurements, the most recent one being held at the EU PVSEC in Hamburg in September 2015. More and more companies are expressing their interest in participating in order to push this important topic.

Status of bifacial c-Si solar cells, module productions and PV systems

As already mentioned, the number of solar cell producers that build their business plans on bifaciality is steadily increasing, but mostly outside of China. The Asian Super League of the six largest solar cell producers (Yingli, TRINA, JA Solar, Jinko, Q-CELLS/Hanwha, Canadian Solar) produce about 90% of standard mc-Si BSF solar cells [7], mainly because of the lowest cost per Wp for this type of module. This, however, is extremely dependent on wafer costs, which in the last six months have changed in favour of Cz-Si technologies, as reported by PVinsights [8]: high-performance mc-Si wafers slightly increased in price, whereas mono Cz p-type and n-type dropped to US\$1/piece and US\$1.1/piece respectively. As shown in Fig. 3, even at the COO level, the costs for Cz-Si module technologies are getting closer to those for mc-Si modules.

The n-type solar cell and module producers

In 2015 n-type c-Si solar cell technology had a market share of around 6–7% [9]; Bloomberg has estimated that by 2025 it will have grown to 40% [10]. The dominating technology will be the PERT

PV
Modules

Market
Watch



Figure 2. COO and LCOE for different Cz-Si module technologies. (For the bifacial module, a bifacial gain of 20% was assumed.)

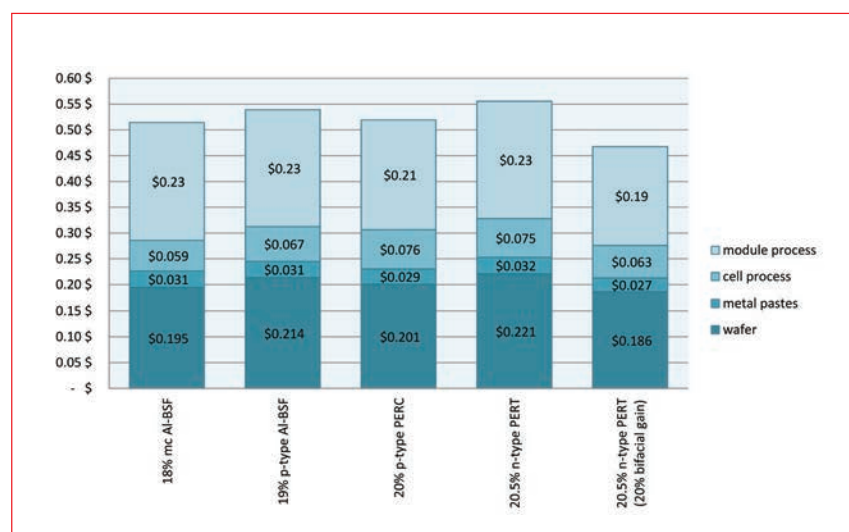


Figure 3. COOs for different technologies.

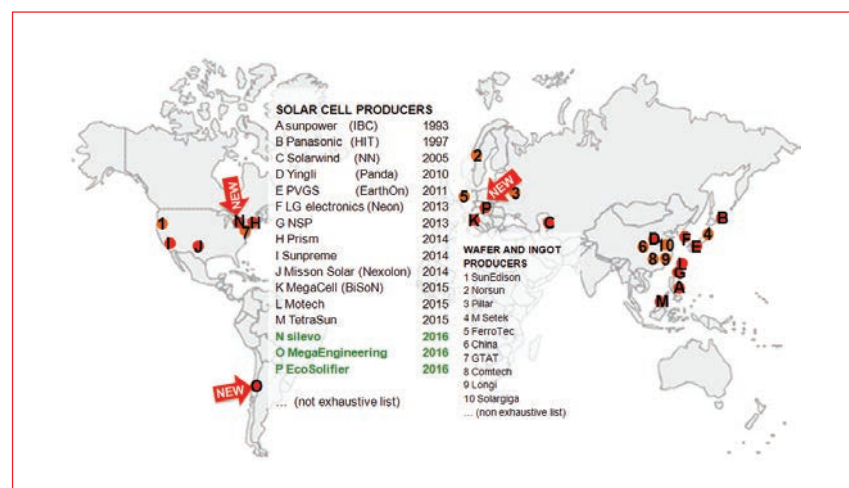


Figure 4. Producers of n-type solar cells and wafers since 1993, and new companies entering the market in 2016.

cell, with a 25% market share, which is bifacial in any case. Fig. 4 shows the list of n-type wafer and solar cell producers, beginning with existing n-type cell manufacturers which have been in the market the longest – SunPower and Panasonic (former Sanyo). PERT technologies, which are explicitly optimized for bifaciality, are produced by PVGS, NSP, Prism, Sunpreme, MegaCell, Motech, Inventech and Tetrasun.

In 2016 there will be new companies of note entering the n-type market, which are also outside of China: silevo in the USA [11], MegaEngineering in Chile and EcoSolifier in Hungary [12]. MegaCell also has plans to extend its cell and module production to Egypt.

Other companies – such as Panasonic, Yingli, LG electronics and Mission Solar – are instead producing monofacial modules with their bifacial solar cells. However, there is strong interest at the moment from companies like Panasonic and LG in also entering the bifacial market. In addition, many glass-glass module producers are buying cells from PVGS, NSP and MegaCell; they are doing so not just to optimize the LCOE but also on aesthetic grounds for the building integration sector.

If the COO of modules on the market in 2015 is examined (see Fig. 3), it can easily be seen that the mc-Si standard module is slowly losing its edge. The cost for the p-type PERC module is already extremely close to the lowest of the mc-Si costs. Monofacial PERT modules are slightly more expensive, but if the effective power (the additional contribution from rear-side irradiance) of bifacial

PERT modules is taken into account, this module technology would at this stage already be the cheapest. This is exactly what machine builders have realized in the last two years: Centrotherm is putting BiSoN from ISC Konstanz on the market, Tempres is making available nPASHA from ECN, and Meyer Burger is offering its own HIT technology.

Bifacial c-Si PV systems

On the system side, many things can also be done to increase the bifacial gain. The modules can be mounted at a greater height off the ground, and the ground itself can be conditioned for increasing the reflection. When the installation is done perfectly, up to 40% can be gained as compared with a monofacial module: 30% of that comes from the bifacial performance gain and

the other 10% from the reflection to the front side, even if this side is facing the sky. Even if a rather moderate gain of 20% is assumed, the LCOE for a bifacial system is lower than that of any of the monofacial technologies on the market, as illustrated in Fig. 5.

“The LCOE for a bifacial system is lower than that of any of the monofacial technologies on the market.”

If a single-axis tracking system were applied to a bifacial PV system, depending on the tracking costs, an LCOE of 4US¢/kWh calculated for a large ground-mounted system with a yearly global horizontal irradiance of

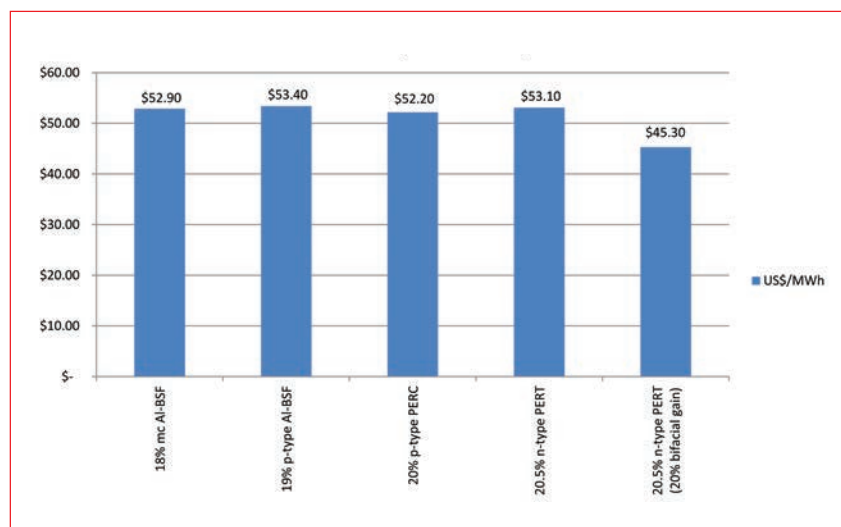


Figure 5. LCOEs for different technologies.



Figure 6. Commercial open-field installation in Saxony, Germany: 8 months with a 20% (0.2) reflectance ground albedo and 12 months with a 50% (0.5) reflectance ground albedo. Results: 17% bifaciality gain over the best module in the field and more than 60% gain in snowy conditions. (The bifacial system kept collecting solar energy through the back side even when the front side was covered with snow, in contrast to all the other systems, which stopped yielding power in these conditions.) The respective cell equivalent efficiency values are 21.7% and 29.6% [13].

GEMINUS – Bifacial Cell Technology

The new face of photovoltaics



Expect Solutions. **GEMINUS.**

The SCHMID's GEMINUS bifacial cell technology enables low manufacturing costs of multi and mono bifacial cells featuring over **30% more energy yield** (kWh/kWp)*. It combines outstanding manufacturing simplicity based on standard tools with highest efficiencies on all common p-type based material. The resulting multi crystalline based bifacial module operates at efficiency equivalents of over 18% and hence has a 7-10 USc / Wp BOS advantage as in comparison to current monofacial multi modules.

* Gain in energy depending on rear side illumination and module mounting.

Visit us at booth 7134 in the German Pavilion, hall 7 at
Abu Dhabi | National Exhibition Centre | January 18th to 21th, 2016

WORLD FUTURE
ENERGY SUMMIT
Abu Dhabi, 16-19 January 2012

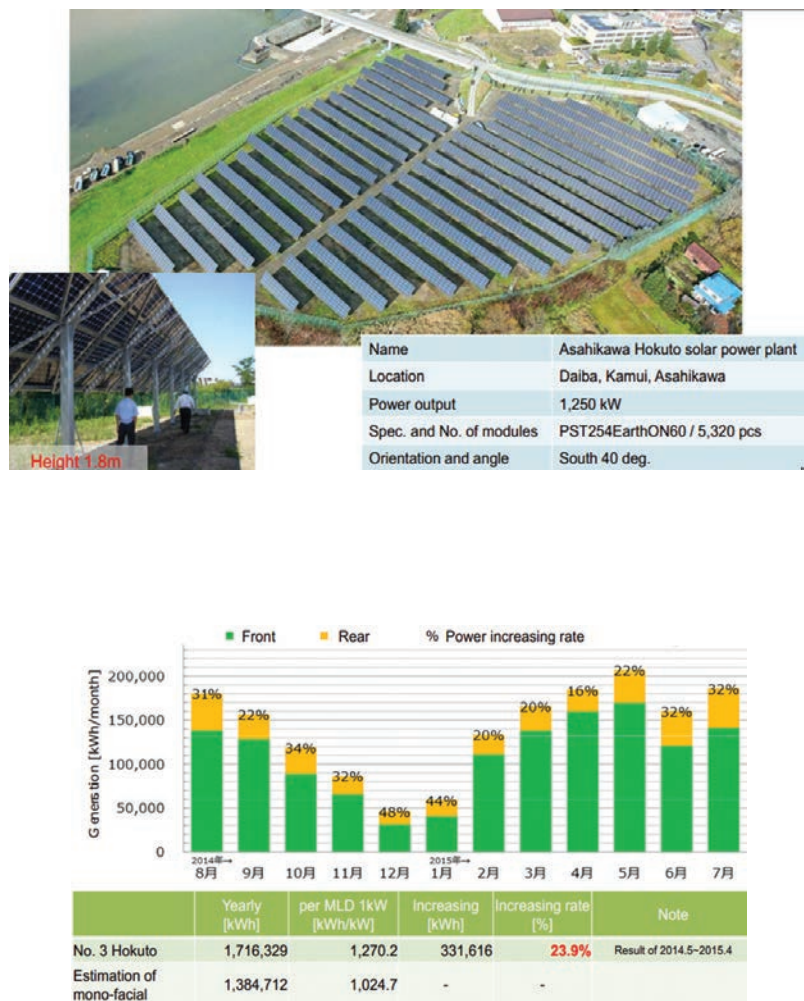


Figure 7. World's largest bifacial PV system so far, located in Japan [14].



Figure 8. The bifacial PV system currently being set up by MegaEngineering and Imelsa. With a total power of 2.5MWp and 3.25MWpe [15], the 'BiSoN farm' will become the world's largest bifacial PV system.

2,200kWh/m² (e.g. for southern Europe, North Africa and India) would already be possible today.

The images in Fig. 6 show an old installation of bSolar, where bifacial gains of 17–30% were observed during the year. Similar observations have been well documented at the world's largest bifacial PV system, located in Japan, with a power of 1.25MWp (Fig. 7). Even though the bifacial installation is not ideal (notice the rear-side shadowing from the metal installation), monthly bifacial gains of 20–48% are indicated, with an average of 24%. During the winter months, when the system is covered by snow, the rear side still produces electricity, giving rise to faster melting of the snow off the front.

What will become the world's largest bifacial system is currently being built in San Felipe in Chile (Fig. 8), close to Santiago de Chile. A joint venture of MegaEngineering and Imelsa, it will comprise a fixed-tilt PV field with BiSoN bifacial modules from MegaCell, with a total power of 2.5MWp – hence double the size of the current largest installation. MegaCell wants to demonstrate the high potential of bifaciality with this bifacial field, aiming for average bifacial gains of more than 30%.

The next section summarizes the bifacial gains of existing bifacial PV systems.

Summary of bifacial gains in large PV systems: bankability

An important contribution to making bifacial PV bankable is the collection of real-world energy-yield data; this means the monitoring of the energy production of large bifacial PV systems in different geographical locations and with various installation configurations. Ideally, part of the plant includes standard monofacial modules, allowing accurate calculations of the bifacial gain to be made.

Regarding the geographical location, apart from the total irradiance, the diffuse irradiance fraction plays an important role in the bifacial gain that can be obtained: the more diffuse light there is, the higher the irradiance of the rear side of the bifacial modules will be. On the other hand, various installation configurations enable the advantages of bifacial modules to be gained in different ways: for example, MW-size ground-mounted systems that have fixed-tilt or one-axis tracking, with natural ground or artificially enhanced albedo (white sand, reflective plates or sheets, etc.), and kW-size to MW-size PV systems on flat rooftops. Bifacial PV

systems vertically mounted in an east–west orientation reap particular benefits in snow-rich regions (no sticking of snow) or desert locations (no soiling), and also contribute to a more consistent energy production throughout the day ('peak-shaving'), thus improving the alignment between electricity production and demand.

In the past 10 years, some data regarding the energy yield of several bifacial PV systems have been published, for demonstration purposes, by various manufacturers of bifacial PV cells and modules, such as PVGS, bSolar and Sanyo/Panasonic. A summary of such data found in the literature is given in Fig 9. This data shows, on the one hand, that even under conditions that are not ideal (ground albedo less than 20%, which corresponds to, for example, grassland), the bifacial gain of a system is always higher than 10%; on the other hand, if measures are taken to increase the ground albedo to more than 60%, bifacial gains of 20% to 30% are possible (see, for example, the PV system by bSolar in Fig. 10).

If the values of the albedos for various ground types in Table 1 are examined, it becomes clear that an albedo between 20% (grassland) and 40% (dune sand) is possible without taking into account measures to artificially enhance the ground reflectivity. Accordingly, for many potential installation sites, sufficiently high bifacial gains can be achieved without additional investment for modification of the ground surface properties.

As mentioned in the previous section, a more recent installation is the 1.25MWp plant set up by PVGS in Japan, in operation since December 2013 and demonstrating a bifacial gain

of 24.9% over a 12-month monitoring period [14]. That will be overtaken by the 2.5MWp plant in Chile which is currently being constructed by MegaEngineering and Imelsa; the system is planned to be connected to the grid by December 2015, and at that point it will be the largest bifacial PV system in the world.

Status of simulations

Another prerequisite of making bifacial PV technology bankable is the capability to predict the energy yield of bifacial PV systems with the same accuracy as that which is already possible today for monofacial systems using commercially

available software tools. An accurate prediction of the total energy yield of a bifacial PV system during its entire lifetime is essential for making realistic calculations of the return on investment (ROI) and the LCOE of the system. In addition, the use of such simulation tools for determining the optimum installation configuration for a given location and a specific site contributes to minimizing the LCOE for the specific bifacial PV system. The simulation results for several studies have been published in the past; they demonstrate how various installation parameters impact the bifacial gain (for example, see Fig. 11).

ISC Konstanz (Shoukry [18]) as

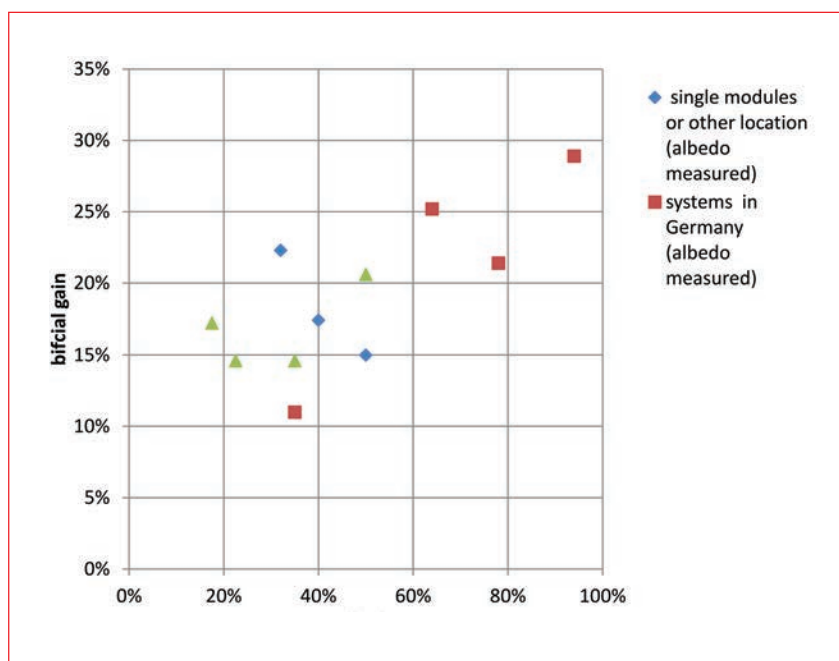


Figure 9. Bifacial gain as a function of the albedo of the surrounding ground at the installation site (data taken from the literature: bSolar, Sanyo/Panasonic, ISC Konstanz, PVGS).



Figure 10. A commercial installation in Geilenkirchen, Germany, monitored by Fraunhofer/ISE (20cm height above the rooftop, 78% reflectance white roof membrane, nine-month period). Results: bifaciality gain = 21.4%; effective cell efficiency = 22.5% [13].v

well as other researchers – such as Chiodetti [17] – have recently carried out extensive work on the modelling of bifacial PV systems. At ISC Konstanz an optical and electrical model has been developed and implemented as a software tool that allows the bifacial gain to be calculated for any

geographical location (with available meteorological data) and for a variety of configurations. Some of the most interesting results will be presented next.

One of the questions that have been studied is how big the difference in bifacial gain is between a stand-alone

bifacial module (which is a typical example that is often simulated and measured, but not very relevant for real-world applications) and a bifacial module located in the middle of a large ground-mounted solar farm. Consider the following scenario:

- Installation site: El Gouna (Egypt)
- Ground albedo: 50%
- Fixed module tilt: 25°
- Module height above the ground: 1.5m
- Row-to-row distance between modules: 2.5m
- Weather data for the year 2005, retrieved from the SoDa database [19]

In this case the bifacial gain over an entire year for a stand-alone bifacial module has been calculated to be 34% [18]. Values of the bifacial gains for modules located within a complete PV system are shown in Fig 12. In a large MW-size system the modules that are not located close to the edge (i.e. the red ones in Fig. 12) of the system, which feature a bifacial gain of 27.72%, represent a major part of the PV system; accordingly, the complete system will yield a bifacial gain of around 28%.

One possibility to further enhance the energy yield of a bifacial PV system is to use a tracking system; in the case of a cost-effective one-axis tracking system, this option will lead to a further reduction of the LCOE. A particularly cost-effective solution is the so-called sunbelt tracking system, whereby a module is rotated around a horizontally fixed north-south-running axis and tilted towards the east in the morning, upwards at noon, and towards the west in the evening. This is shown schematically in Fig. 13 and is ideal for installations in the equatorial regions.

Surface	Albedo
Dry dark soil	0.13
Grass	0.17 to 0.28 (avg. 22.5)
Dry sand	0.35
Dune sand	0.37
Old snow	0.4 to 0.7
Fresh snow	0.75 to 0.95

Table 1. Albedos for different ground types.

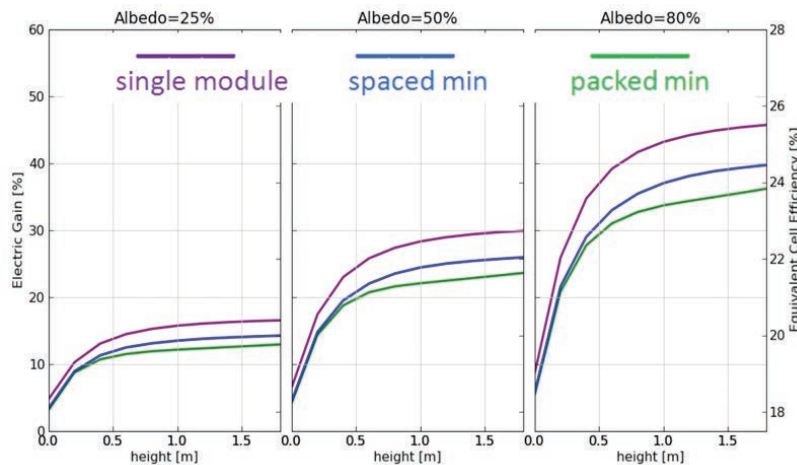


Figure 11. Simulations of the dependency of bifacial gain on both system configuration and ground albedo [16] ('packed min' = standard spacing between module rows; 'spaced min' = 150% of standard spacing).

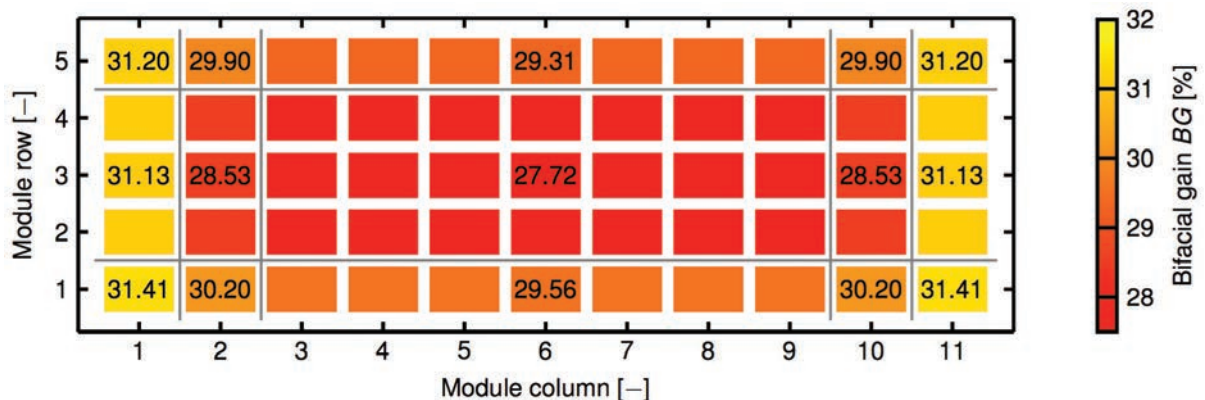


Figure 12. Results of the simulation of the bifacial gain of modules in various positions within a bifacial PV system. The location of the system (meteorological data and geographical latitude) is El Gouna (Egypt), and the modules (with a fixed tilt of 25°) are assumed to be installed at a height of 1.5m, with a row-to-row distance of 2.5m; the ground albedo is 50%.

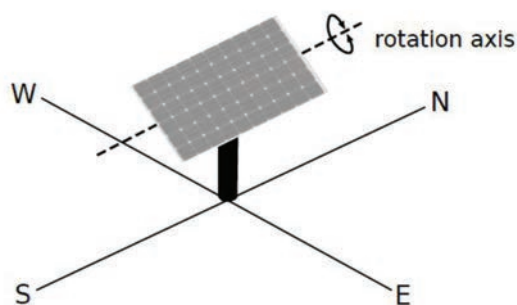


Figure 13. Sunbelt tracking system.

Kasese, Uganda					
No.	A	→	B	$\alpha = 0.2$	$\alpha = 0.5$
1	Monofacial fixed	→	Monofacial tracked	14.71%	17.93%
2	Bifacial fixed	→	Bifacial tracked	12.82%	20.30%
3	Monofacial fixed	→	Bifacial fixed	16.47%	43.77%
4	Monofacial tracked	→	Bifacial tracked	22.12%	37.53%
5	Monofacial tracked	→	Bifacial fixed	1.53%	21.91%
6	Monofacial fixed	→	Bifacial tracked	40.10%	62.20%

Table 2. Results of simulations of the bifacial gain for various monofacial and bifacial PV system configurations [18].

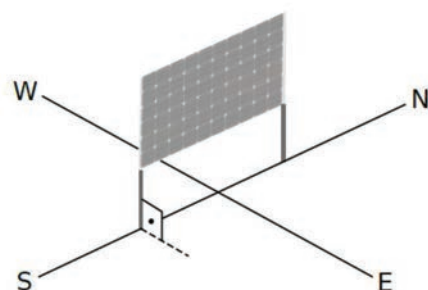


Figure 14. Vertical installation in an east-west orientation.

		El Gouna		Konstanz	
		$\alpha = 0.2$	$\alpha = 0.5$	$\alpha = 0.2$	$\alpha = 0.5$
BG	Monofacial optimum → Bifacial vertical	-14.88%	-5.99%	-4.52%	+15.77%

Table 3. Results of simulations of the yearly bifacial gain for a vertically mounted (east-west) bifacial PV module installed at El Gouna (Egypt) and at Konstanz (Germany) [18].

“One possibility to further enhance the energy yield of a bifacial PV system is to use a tracking system.”

The prediction of the energy yield of a bifacial PV system with one-axis tracking (sunbelt tracker) was therefore part of the study. The results were compared with monofacial tracked- and fixed-tilt installations as well as with bifacial fixed-tilt installations of PV systems in Kasese (Uganda), near the equator.

Table 2 shows the simulation results,

which demonstrate in particular that adding tracking support to a bifacial system enables bifacial gains of 40% for an albedo of 0.2, and 60% for an albedo of 0.5 (compared with standard monofacial fixed-tilt systems). A comparison of the tracked bifacial system with a tracked monofacial system reveals a bifacial gain ranging from 22% (albedo 0.2) to 37% (albedo 0.5). These results show the huge potential for reducing the LCOE by combining bifacial PV with robust, cost-effective tracking technologies. Another important element in this context is the development of albedo-enhancing techniques that are environmentally friendly and cost-effective and feature a long-term stable high reflectivity.

As mentioned earlier, a vertical installation in an east-west orientation is a very interesting option for bifacial modules (Fig. 14). While the advantages of such systems from an application point of view (e.g. along highways as a noise barrier, or in desert regions to avoid soiling) have not been questioned, the quantitative benefits in terms of energy production are dependent on the installation site and configuration.

The bifacial gain was simulated for two different geographical locations and for two different albedos. The results of these simulations (Table 3) show that for a high energy yield, vertically (east-west) installed bifacial modules require – apart from a high albedo – a higher geographical latitude as well as a higher diffuse irradiance fraction (both apply to Konstanz when comparing with El Gouna).

Last, but not least, the accuracy of the predictions obtained by the simulation tool has been validated by comparing simulation results with actual data from outdoor monitoring of a bifacial module installed in El Gouna. The following data served as input parameters for the simulation:

- Actual installation configuration: tilt, height, neighbouring module (Fig. 15).
- Experimentally determined albedo of the ground: 30%.
- Weather data acquired at the installation site during the time period when the actual energy yield of the bifacial module (and the monofacial reference) was monitored.

On the basis of these data, the bifacial gain was predicted by the simulation tool and was compared

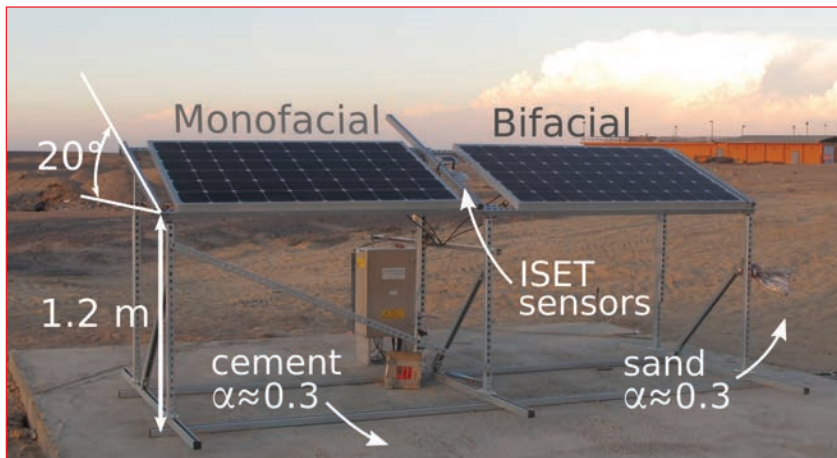


Figure 15. Relevant configuration parameters of the bifacial test installation in El Gouna, Egypt [18].

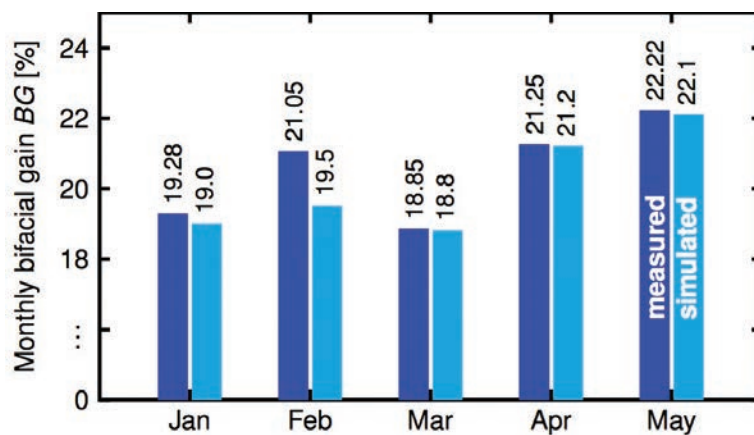


Figure 16. Comparison of simulated and measured bifacial gains, using data obtained from the ISC module test site in El Gouna, Egypt [18].

with the actual measurement data. The good correlation of the monthly values shown in Fig. 16 indicates that the simulation model is delivering realistic data, and therefore represents a very good starting point for the development of a tool that can be integrated into commercial software tools. Further development work will focus on faster computation times, a wider application range (e.g. to include various types of tracking) and further improvement of accuracy.

New companies entering the market

As already mentioned, new companies – such as silevo, MegaCell and EcoSolifier among others – are entering the n-type bifacial market. Furthermore, the p-type market is now working on bifacial solutions with PERT, PERCT and PERC structures. Even mc-Si is entering the bifacial equation: Schmid has developed a bifacial mc-Si cell architecture,

and RCT has already transferred its mcPERCT technology to Lu'an, a large Chinese cell and module manufacturer.

bSolar founders are coming back to the market under the company name SolAround, with new ideas and cell concepts. Yet another company – Solar World – has announced a bifacial PERC solar cell, namely PERC+, and expects to enter the bifacial market in Q4 2015. EDF has also shown strong interest in bifacial technology, as the company plans to install large PV plants in the future.

“How fast bifaciality penetrates the PV market will depend on how fast standards are developed and how fast the big investors are convinced about this technology.”

Prediction of bifacial future

The future of bifaciality looks extremely bright. No one can stop this technology, as c-Si PV is naturally developing in this direction. Solar cells are becoming bifacial and cost-effective, and are finding their way into the region of the cheapest standard mc-Si technology.

How fast bifaciality penetrates the PV market will depend on how fast standards are developed and how fast the big investors are convinced about this technology. For these reasons, to speed up the market take-up, ISC Konstanz organizes bifacial workshops [20], two of which have already taken place – in Konstanz (2012) and in Chambery (2014). The 2016 bifiPV workshop will be held in September in Miyazaki, Japan, while the 2017 meeting is planned to take place in the USA.

References

- [1] Solarfabrik, "Premium dual power module datasheet", http://www.solar-fabrik.de/fileadmin/user_upload/Premium_L_dual_power/Premium_L_dual_power.DT_1206.pdf
- [2] A. Colthorpe, "SolarWorld launches 72-cell bifacial PV module", pvtech.org, 09/2015, http://www.pv-tech.org/news/solarworld_launches_72_cell_bifacial_pv_module
- [3] R.Kopecek et al., "Bifaciality: One small step for technology, one giant leap for kWh cost reduction", Photovoltaics international issue 26 (2014)
- [4] D. D. Smith et al., "Towards the practical limits of silicon solar cells", IEEE Journal of Photovoltaics 4(6):1465-1469 (2014)
- [5] J. Nakamura et al., "Development of Hetero-Junction Back Contact Si Solar Cells", Proc. of 40th IEEE PVSC, Denver, USA (2014)
- [6] K. Masuko et al., "Achievement of More Than 25% Conversion Efficiency With Crystalline Silicon Heterojunction Solar Cell", IEEE Journal of Photovoltaics 4 (6): 1433-1435 (2014)
- [7] F. Colville, "PV technology roadmap stuck in roadblock as Super League stays with p-type multi", pvtech.org, 09/2015, http://www.pv-tech.org/editors_blog/pv_technology_roadmap_stuck_in_roadblock_as_super_league_stays_with_p_type
- [8] pvinsights, "Solar PV Wafer Weekly Spot Price", www.pvinsights.com
- [9] K. Pickerel, "Trending in solar generation: Advanced modules

- gaining ground", Solarpower world 05/2015, <http://www.solarpowerworldonline.com/2015/05/trending-in-solar-generation-advanced-modules-gaining-ground/>
- [10] Bloomberg New Energy Finance 2015, <http://about.bnef.com/>
- [11] J. Pernell, "SolarCity's Silevo gigafactory takes shape", pvtech.org, 08/2015, http://www.pv-tech.org/news/solarcitys_silevo_gigafactory_takes_shape
- [12] M. Osborne, "Tool Order: Meyer Burger wins heterojunction cell business from EcoSolifer", pvtech.org, 08/2015, http://www.pv-tech.org/news/tool_order_meyer_burger_wins_heterojunction_cell_business_from_ecosolifer
- [13] <http://www.b-solar.com/Technology.aspx?Sel=Field%20Results>
- [14] <http://www.nishiyama-s-denki.co.jp/>
- [15] image source: MegaEngineering
- [16] N. Eisenberg et al., "Outdoor bifacial module characterization: energy generation and gain", 1st bifi PV workshop, Konstanz, 2012
- [17] M. Chiodetti, "Bifacial PV plants: performance model development and optimization of their configuration", master

thesis at KTH Royal Institute of Technology, 2015

- [18] I. Shoukry, "Bifacial Modules - Simulation and Experiment", master thesis at IPV Stuttgart, 2015
- [19] <http://www.soda-is.com/eng/index.html>
- [20] <http://bifipv-workshop.com/>

About the Authors



Dr. Radovan Kopecek is one of the founders of ISC Konstanz. He has been working at the institute as a full-time manager and researcher since January 2007 and is currently the leader of the advanced solar cells department. Dr. Kopecek received his M.S. from Portland State University, USA, in 1995, followed by his diploma in physics from the University of Stuttgart in 1998. The dissertation topic for his Ph.D., which he completed in 2002 in Konstanz, was thin-film silicon solar cells.



Ismail Shoukry has a B.Sc. in renewable energies and an M.Sc. in sustainable energy production, both from the University of

Stuttgart. The work for his master's thesis was carried out at ISC Konstanz in 2015, and involved the development of a software tool to simulate the energy yield of bifacial PV systems, with a validation of the results using short-term and long-term measurements.



Dr. Joris Libal works at ISC Konstanz as a project manager, focusing on business development and technology transfer in the areas of high-efficiency n-type solar cells and innovative module technology. He received a diploma in physics from the University of Tübingen and a Ph.D. in the field of n-type crystalline silicon solar cells from the University of Konstanz. Dr. Libal has been involved in R&D along the entire value chain of crystalline silicon PV for more than 10 years.

Enquiries

ISC Konstanz
Rudolf-Diesel-Straße 15
78467 Konstanz
Germany

Tel: +49 7531-36 18 3-22
Email:
radovan.kopecek@isc-konstanz.de

PV
Modules



Technology and business solutions for commercial and utility-scale PV power plants – from the publisher of Photovoltaics International and www.pv-tech.org

SUBSCRIBE AT: www.pv-tech.org/power



Highlights from the latest issue:

MARKET WATCH

The price-busting Dubai project leading the way for Middle East solar

FINANCE

Global opportunities for solar securitisation

STORAGE & GRIDS

The vital role of Big Data in distributed energy management

Reliability and durability comparison of PV module backsheets

Haidan Gong & Guofeng Wang, Wuxi Suntech Power Co., Ltd., Wuxi, China

ABSTRACT

The backsheet is the first barrier for ensuring the reliability and durability of PV modules for 25+ years. To reduce cost, backsheets with a variety of compositions and constructions have been developed and introduced in PV modules. For PV module manufacturers, a major challenge is choosing a low-cost backsheet that can maintain the current levels of high reliability and durability performance. In the work reported in this paper, the properties of several backsheets of various compositions and constructions were compared. To distinguish the different backsheet properties, intensive and long-term weathering tests were performed. The results showed that the backsheet properties had a significant influence on the durability of the material. The ability of a backsheet to withstand extended high-humidity exposure is mainly affected by the hydrolysis performance of the core layer PET material, and is not affected by the outer layer material. Some backsheets – such as PVDF/PET/PVDF and PVF/PET/PE, which use a modified PE as the inner layer – also demonstrated a high ability to withstand extended UV exposure; PET-based backsheets, on the other hand, exhibited poor tolerance to UV exposure. In terms of weatherability, PA-based backsheets performed the worst.

Introduction

PV modules have a designed service life of at least 25 years, throughout which they will suffer a variety of environmental effects, such as high temperatures, high humidities and UV exposure. The module encapsulant material is expected to take up the challenge of ensuring long-term reliability and durability during the designed service life. The backsheet, as the outer layer of a PV module, is especially important for providing protection to the module in order for it to survive during its expected service life.

“Extensive testing is required in order to determine if the new types of backsheet can provide the same protection as the well-established PVF/PET/PVF backsheet.”

In the past, the multilayer structure comprising polyvinyl fluoride / polyester ethylene Tedlar / polyvinyl fluoride (PVF/PET/PVF) has been used for backsheets of PV modules because of its proven

long-term outdoor performance [1]. Since 2005, in an effort to reduce cost, backsheets with different compositions and constructions (other fluoropolymer films, non-fluoropolymer films, coatings, etc.) have been developed and introduced in PV modules; however, a long-term experience of the service life of some of the newer backsheets when used in PV modules is lacking. Extensive testing is therefore required in order to determine if the new types of backsheet can provide the same protection as the well-established PVF/PET/PVF backsheet.

This paper presents an evaluation of the durability of these new backsheets,

Sample	Layer composition and construction	Layer thickness [μm]
1	PVF / PET (PCT<36h) / PVF	38 / 250 / 38
2	PVDF / PET (PCT 48h) / PVDF	30 / 250 / 30
3	PVF / PET (PCT 60h) / PE (from PE supplier A)	25 / 250 / 60
4	PVF / PET (PCT 48h) / PE (from PE supplier A)	25 / 250 / 60
5	PVDF / PET (PCT 48h) / PE (from PE supplier D)	20 / 250 / 60
6	PVDF / PET (PCT 36h) / PE (from PE supplier E)	20 / 250 / 60
7	ETFE / PET (PCT<36h) / PE	25 / 188 / 110
8	PVDF / PET (PCT 48h) / fluorine coating	25 / 255 / 4
9	Fluorine coating / PET (PCT 60h) / fluorine coating	25 / 250 / 15
10	Non-fluorine coating / PET (PCT 48h) / PP	2 / 125 / 150
11	PET / PET(PCT 60h) / PE (from PE supplier F)	50 / 125 / 100
12	PA / PA / PA	350 (total)

PA = polyamide; PE = polyethylene; PET = polyethylene terephthalate; PVDF = polyvinylidene fluoride; PVF = polyvinyl fluoride; ETFE = ethylene tetrafluoroethylene; PP = polypropylene.

Table 1. Composition and construction of the various backsheets tested.

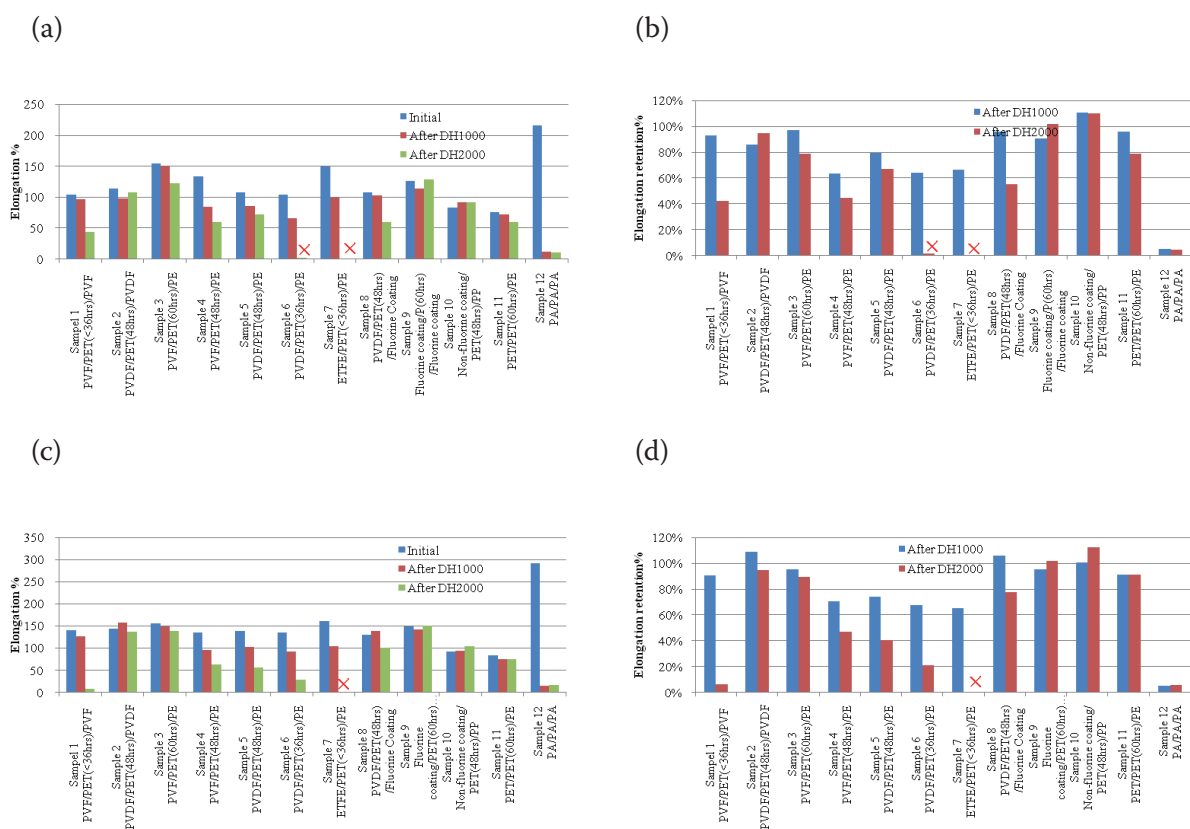


Figure 1. Comparison of elongation and elongation retention before and after the damp-heat tests: (a) TD elongation; (b) TD elongation retention; (c) MD elongation; (d) MD elongation retention.

with PVF/PET/PVF as a baseline. To distinguish the different backsheets properties, intensive and long-term weathering tests were performed: 2000h of damp heat, 400 cycles of thermal cycling, 40 cycles of humidity-freeze and more than 120kWh/m² of UV exposure.

Experimental set-up

Selection and classification of backsheets

Table 1 shows the different compositions and constructions of the tested backsheets that have been commercialized in the PV industry. All the backsheets, with the exception of PA/PA/PA, use modified PET as the core layer, which provides a barrier to moisture. PET is sensitive to moisture and prone to hydrolysis; hence modified PET can improve the hydrolysis resistance performance. Usually, PET suppliers use a pressure cooker test (PCT), consisting of 120°C and 100% relative humidity (RH) at 2 atm, to assess the hydrolysis resistance of PET. The elongation of PET is measured before and after the PCT test, until the elongation retention is below 40%; the test period then represents the hydrolysis resistance level of the PET.

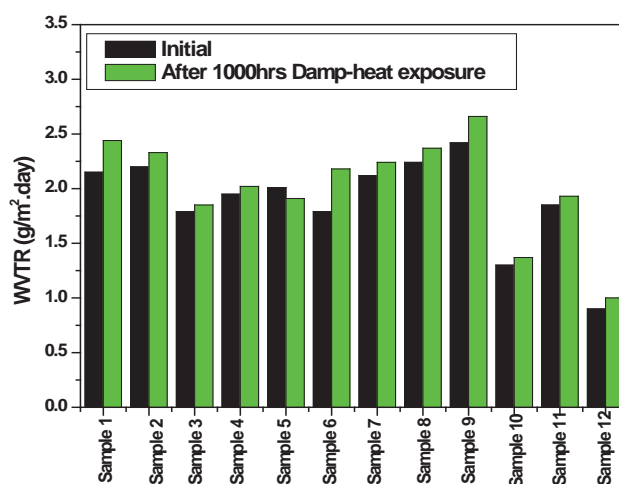


Figure 2. WVTR before and after 2000h damp-heat testing.

Experimental methods

Mechanical properties

The elongation of the backsheets was measured using an INSTRON 3365: the elongation in the transverse direction (TD) and machine direction (MD) of free-standing films was measured in accordance with ASTM D882. If the elongation retention of a backsheet is below 40%, the backsheet is usually considered to have failed the test.

Elongation was measured before and after damp-heat, thermal-cycling

and humidity-freeze tests, which were conducted in accordance with IEC 61215 [2]:

- Damp heat: 85°C and 85% RH
- Thermal cycling: -40°C to 85°C
- Humidity-freeze: -40°C to 85°C and 85% RH

Optical properties

The colour coordinate b^* and the metallographs were measured before and after UV exposure. The inner layer

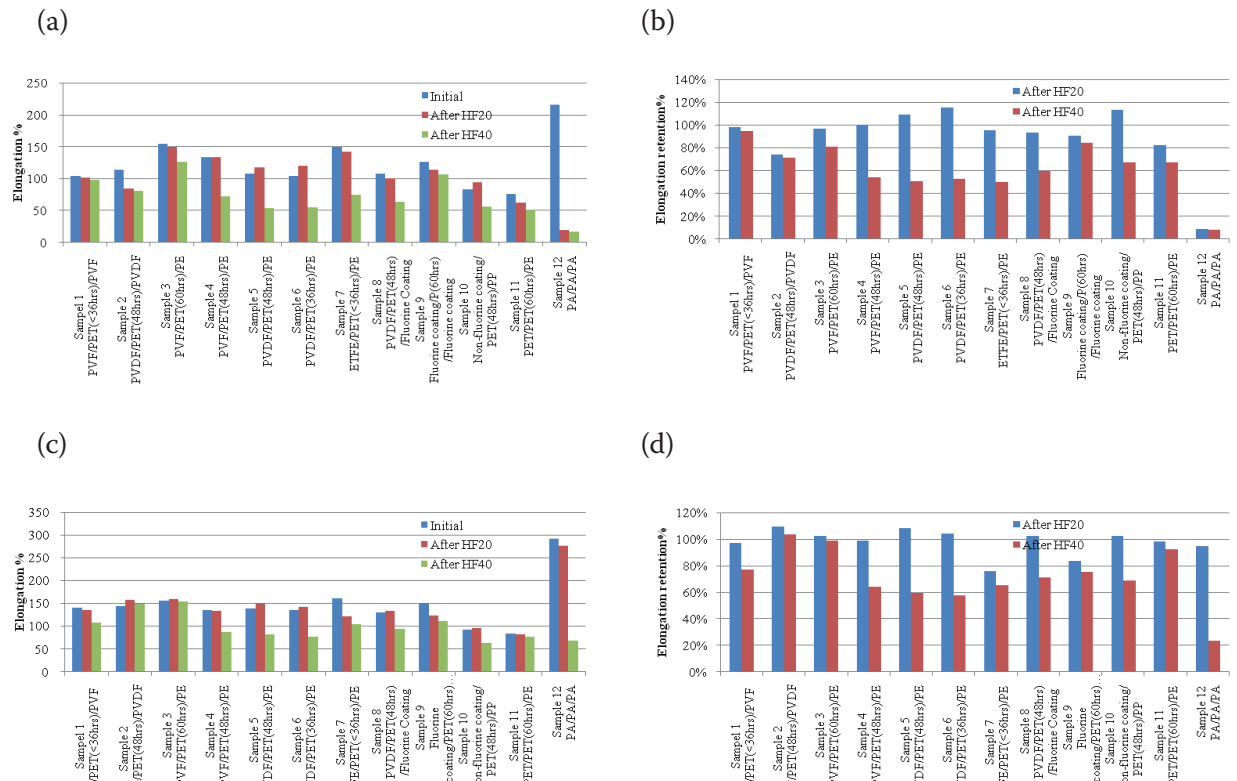


Figure 3. Comparison of elongation and elongation retention before and after the humidity-freeze tests: (a) TD elongation; (b) TD elongation retention; (c) MD elongation; (d) MD elongation retention.

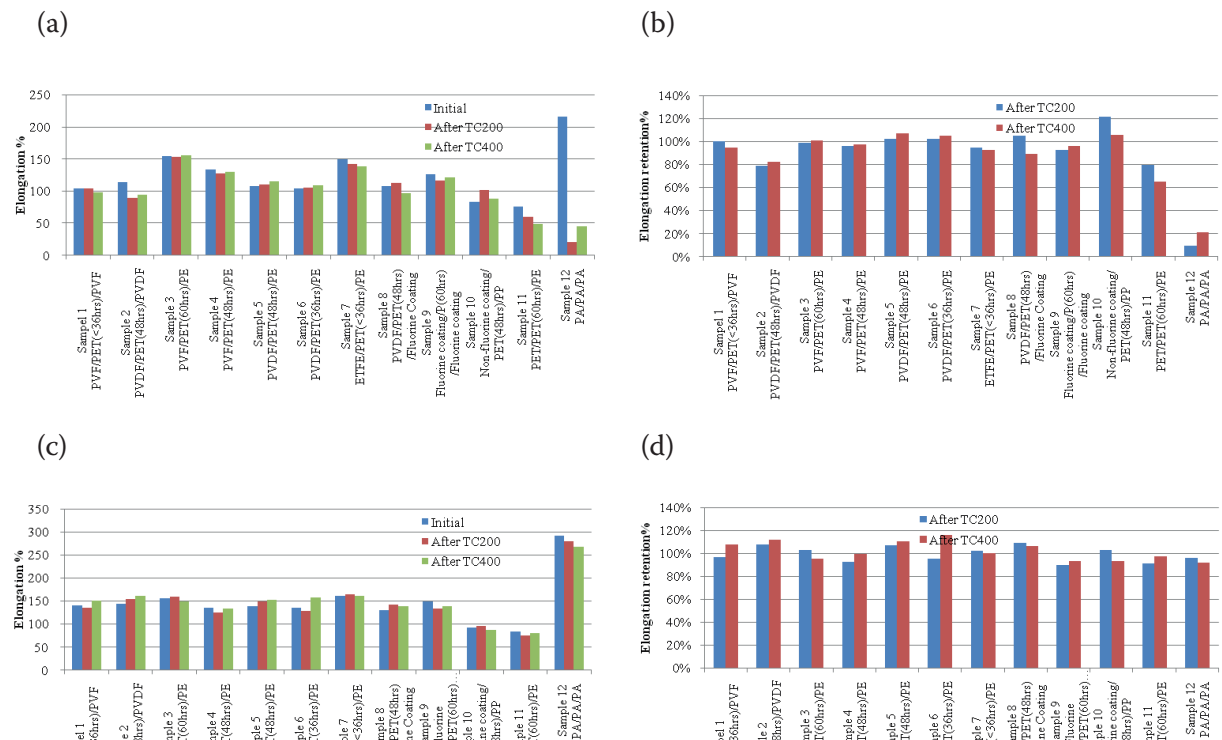


Figure 4. Comparison of elongation and elongation retention before and after the thermal-cycling tests: (a) TD elongation; (b) TD elongation retention; (c) MD elongation; (d) MD elongation retention.

📍 London, UK

📅 1-3 February 2016

Use Discount Code
'PVI15' for a
15% discount*

SOLAR FINANCE & INVESTMENT

🐦 #SFIUK

Over 40 speakers confirmed including:



Nick Boyle
CEO, Lightsource
Renewable Energy



Sir David King
UK Foreign Secretary's
Special Representative for
Climate Change



Armin Sandhoevel
CIO Infrastructure Equity
Allianz Global Investors GmbH



Thierry Lepercq
President
Solairedirect



Michael Bonte-Friedheim
CEO
NextEnergy Capital



David Kemp
Director Project &
Infrastructure Finance
M&G Investments



Christopher Mansfield
Head of Renewable Energy
DIF Infrastructure Fund



Angus MacDonald
CEO
British Solar Renewables



Tobias Reichmuth
CEO
SUSI Capital Partners AG



Giovanni Terranova
Founding Partner
Bluefield

Solar Media's 6th Solar Finance & Investment Europe Forum returns to London on 1-3 February 2016

FEB 1: Asset Management day

FEB 2 - 3: European Secondary Markets & Making Solar Work Post-Subsidy

WE ARE BRINGING TOGETHER:

- **Major European asset holders** looking to enlarge their portfolios
- **Banks** ready to refinance projects
- **Developers** with projects to sell
- **Institutional investors** looking how to balance their liabilities and assets with long-term investments

TO HELP YOU NAVIGATE HOW TO TAKE ADVANTAGE OF THE OPPORTUNITIES WITHIN:

- **European Secondary markets:** YieldCos and listed funds, project supply, M&A
- **Refinancing:** how to do it best
- **Asset management** and best practice O&M
- **Post-subsidy market**
- **Tendering** and development in Europe

**ASSET
MANAGEMENT
FOCUS DAY**
1st Feb, Separately
Bookable

*Exclusive to Photovoltaics International readers – offer end 31/12/2015.

finance.solarenergyevents.com



of the backsheet can be affected by the amount of UV light exposure, which will cause an aesthetic defect in the module and can lead to embrittlement and reduced dielectric strength.

The UV test (wavelength 280–400nm, with 3–10% UV irradiance in the wavelength range 280–320nm) was also conducted in accordance with IEC 61215 [2].

Water vapour transmission rate (WVTR)

The WVTR was measured using MOCON, with test conditions of 38°C and 100% RH. The barrier moisture property of the backsheet is important, since EVA encapsulants can produce acetic acid under moisture exposure; this can accelerate corrosion of the electrical components of the PV module and cause power degradation.

Results

Damp-heat impact on backsheets

The results of a comparison of TD and MD elongation of free-standing backsheet films before and after damp-heat testing are shown in Fig. 1. Sample 1 (PVF/PET/PVF backsheet) is used as the baseline. Apart from Sample 12 (PA/PA/PA), all the backsheets after 1000h damp-heat testing demonstrated a good elongation and elongation retention, similar to Sample 1.

“The common component of the failed backsheets is the use of PET with a lower hydrolysis resistance performance (PCT 36h or <36h) as the core layer.”

After 2000h of damp-heat testing, however, the elongation and elongation retention of Sample 1 began to decrease: in the MD in particular, the elongation retention was only 6%. Sample 6 (PVF/PET/PE) and Sample 7 (ETFE/PET/PE) also showed less than 40% of elongation retention in both the TD and the MD. The common component of the failed backsheets is the use of PET with a lower hydrolysis resistance performance (PCT 36h or <36h) as the core layer.

Other backsheets using PET with a high hydrolysis resistance (PCT 48h and PCT 60h) as the core layer showed higher elongation retention after 2000h damp-heat testing. Note that Samples 3 and 4 are from the same backsheet supplier and have the same composition, construction

and processing technique, the only difference being the hydrolysis resistance of the core layer PET. Sample 3 uses a higher hydrolysis resistance PET (PCT 60h) than Sample 4 (PCT 48h), resulting in significantly better mechanical properties.

The results indicate that the performance of backsheets using PET as the core layer in withstanding humidity is mainly affected by the hydrolysis resistance performance of PET. The PA/PA/PA backsheet performs very poorly in resisting humidity.

The backsheets also underwent WVTR testing before and after the 2000h damp-heat tests; the results are shown in Fig. 2. In all cases there was only a slight increase in the value of WVTR after exposure to 2000h damp heat, although some backsheets demonstrated low elongation and elongation retention. The barrier moisture property does not therefore correlate with obvious degradation.

Humidity–freeze impact on backsheets

The elongation properties in the TD and MD of free-standing backsheet films after humidity–freeze tests were measured; the results are shown in Fig. 3. Sample 12 (PA/PA/PA) showed poor weatherability performance once again; other backsheets were able to maintain a good elongation and elongation retention, even when the humidity–freeze test was prolonged to 40 cycles.

Thermal-cycling impact on backsheets

The results of 400 cycles of thermal-cycling are shown in Fig. 4: it can be observed that the ability to withstand thermal-cycling is mainly influenced by the composition of the backsheet material. Only the backsheet using PA material showed poor durability in the TD to the temperature stress; other backsheets, using PET as the core layer, demonstrated excellent temperature stress performance, similar to that of the baseline PVF/PET/PVF.

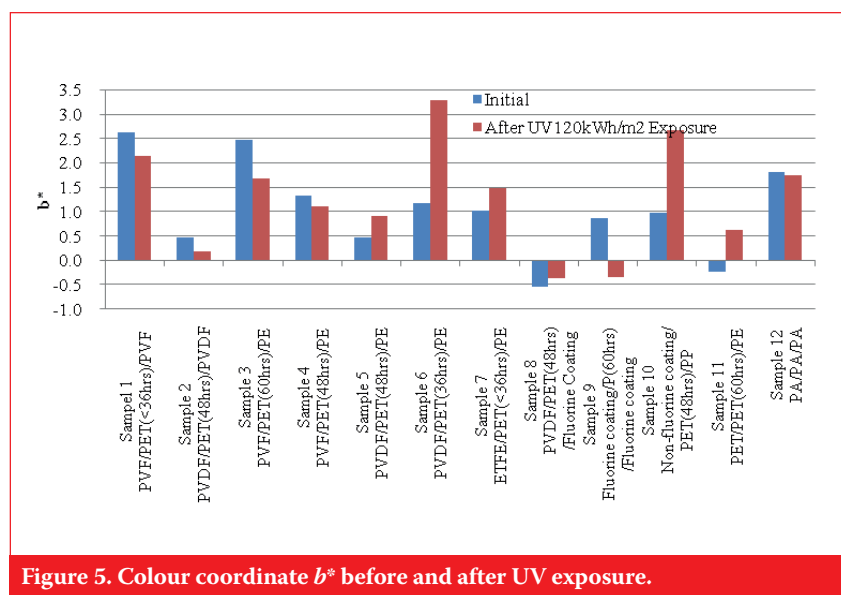


Figure 5. Colour coordinate b^* before and after UV exposure.



Figure 6. White powder from the Tedlar surface, observed after 330kWh/m² of UV exposure.

UV irradiance impact on backsheet

To simulate UV exposure from the front side, the EVA sides of free-standing backsheets were exposed to prolonged UV exposure of more than 120kWh/m²; the colour changes are shown in Fig. 5. Only Samples 6 and 10 demonstrated a significant change in colour after 120kWh/m² UV exposure, with all other backsheets showing low levels of colour change. Backsheets using PE or a fluorine coating on PA as an inner layer exhibited a lower level of colour change than TPT backsheets.

“Backsheets using PE or a fluorine coating on PA as an inner layer exhibited a lower level of colour change than TPT backsheets.”

The authors believe that the measured level of colour change will not accurately reflect the actual ageing of backsheet material in the field. It was noted that although some backsheets showed a low level of colour change, cracking was still observed (see the metallographs in Tables 2 and 3). For example, the level of colour change of Sample 11 (PET/PET/PE) is low, but obvious cracking was observed after 45kWh/m² of UV exposure. Cracking was also observed in both Sample 5 (PVDF/PET/PE) and Sample 6 (PVDF/PET/PE) after 120kWh/m² of UV exposure, but the level of colour change of Sample 5 was lower than that of Sample 6. There is no correlation between the colour change and the extent of the cracking. It is therefore speculated that some additives in backsheets can reduce the visible colour change, even if the materials have degraded.

Metallographic analysis

Metallographs were used to determine the degradation of the backsheet material. In Table 2, dark spots can be seen on Sample 1 (PVF/PET/PVF) after prolonged UV exposure to 330kWh/m². In addition, some white powder was observed on the PVF surface after 330kWh/m² of UV exposure, as shown in Fig. 6, which indicates that the material had begun to degrade.

A Fourier transform infrared (FTIR) measurement was also performed; the spectrogram is shown in Fig. 7. As speculated, it is observed that the FTIR spectrum of PVF changed after 330kWh/m² of UV exposure.

Sample 2 (PVDF/PET/PVDF) did not show any obvious change on the

metallographs or in the FTIR spectrum (Fig. 8); when used as the inner layer, PVDF is therefore expected to provide more stable UV resistance than PVF.

Surprisingly, Samples 3 and 4 demonstrated high UV resistance

because of the high UV resistance PE used by the supplier as the inner layer; however, these backsheets began to show evidence of slight cracking after 330kWh/m² UV exposure (Table 2).

The PET-based backsheet Samples 10







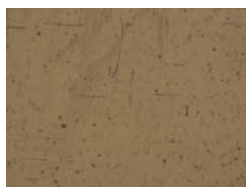



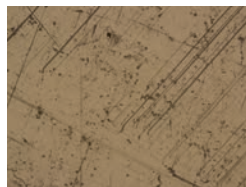
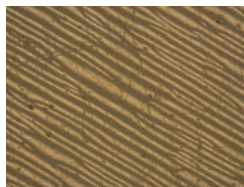
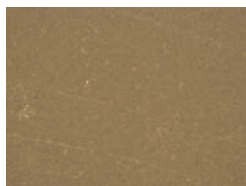
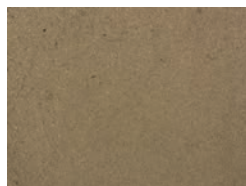

Sample 1 PVF/PET(<36h)/PVF			
Initial	120kWh/m ² UV exposure		330kWh/m ² UV exposure
			
Sample 2 PVDF/PET(48h)/PVDF			
Initial	120kWh/m ² UV exposure		330kWh/m ² UV exposure
			
Sample 3 PVF/PET(60h)/PE and Sample 4 PVF/PET(48h)/PE*			
Initial	120kWh/m ² UV exposure		330kWh/m ² UV exposure
			
Sample 5 PVDF/PET(48h)/PE			
Initial	60kWh/m ² UV exposure		120kWh/m ² UV exposure
			
Sample 6 PVDF/PET(36h)/PE			
Initial	60kWh/m ² UV exposure		120kWh/m ² UV exposure
			
* Since Samples 3 and 4 are from the same supplier and use the same PE for the inner layer, only the metallographs for Sample 3 are shown.			

Table 2. Metallographs of the backsheets after prolonged UV exposure (Samples 1–6).

Table 2. Metallographs of the backsheets after prolonged UV exposure (Samples 1–6).

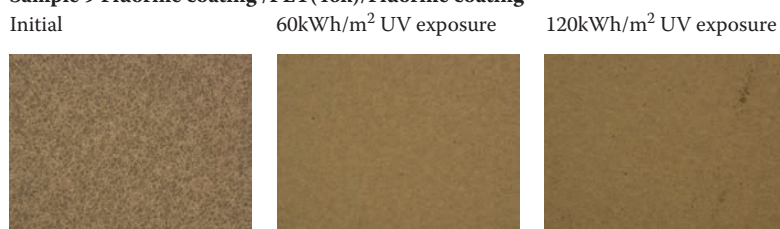
Sample 7 ETFE/PET(<36h)/PE**Sample 8 PVDF/PET(48h)/Fluorine coating****Sample 9 Fluorine coating /PET(46h)/Fluorine coating****Sample 10 Non-fluorine coating /PET(48h)/PP****Sample 11 PET/PET(60h)/PE****Sample 12 PA/PA/PA**

Table 3. Metallographs of the backsheets after prolonged UV exposure (Samples 7–12).

and 11 showed the worst UV resistance performance: they were only able to withstand 45kWh/m² of UV exposure, with obvious cracking observed.

Cracking was also evident with Sample 12 (PA/PA/PA) after 180kWh/m² of UV exposure. However, from the metallographs it was observed that the surface appearance of the inner layer of this backsheet began to change after 120kWh/m² UV exposure, which indicates that the material had already started to degrade.

The results of WVTR measurements for the backsheets before and after 120kWh/m² of UV exposure are shown in Fig. 9. It can be seen that the WVTR values for the backsheets that suffered cracking (Samples 5, 6 and 11) after 120kWh/m² of UV exposure are higher than their initial values. (Note that the measurement of WVTR for Sample 10 could not be performed, because of severe cracking of the backsheet.)

“The PVDF film was found to have outstanding UV resistance performance, and even better than PVF film.”

From the results presented above, it is clear that the UV resistance performance of backsheets is mainly determined by the composition of the materials used. With material containing fluorine as the inner layer, excellent UV resistance is demonstrated; likewise, the use of a modified PE material as the inner layer can also provide a high UV resistance. The PET-based backsheets showed poor UV resistance, whereas the PA/PA/PA backsheet demonstrated a medium level of UV resistance.

Conclusions

Several backsheets of various compositions and constructions have been put through extended accelerated ageing tests. The critical performance parameters – such as elongation, colour, surface appearance and WVTR – were evaluated and compared with a baseline PVF/PET/PVF backsheet, which has proven long-term reliability in the field.

The results show that the humidity performance of a backsheet is mainly affected by the hydrolysis resistance performance of the core layer PET material, and is not affected by the outer layer material. In damp-heat testing, the baseline PVF/PET/PVF does not yield satisfactory results owing to the low hydrolysis resistance PET. Apart from the PA/PA/PA backsheet, all the backsheets using PET with a high

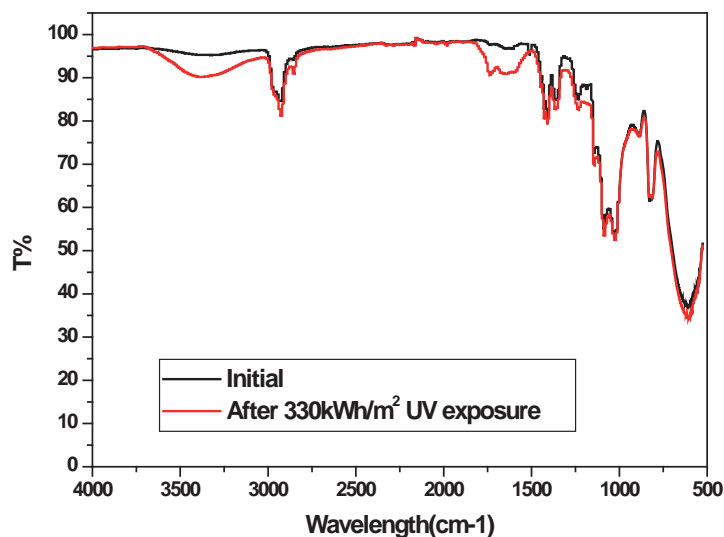


Figure 7. FTIR spectrum of PVF film used as the inner backsheet layer.

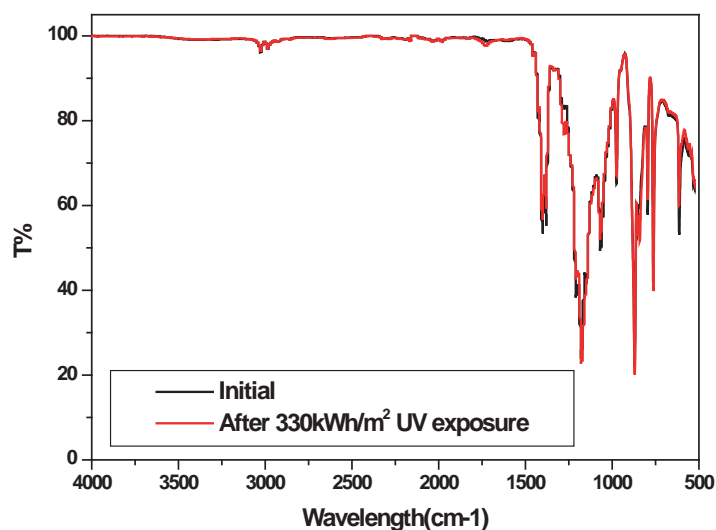


Figure 8. FTIR spectrum of PVDF film used as the inner backsheet layer.

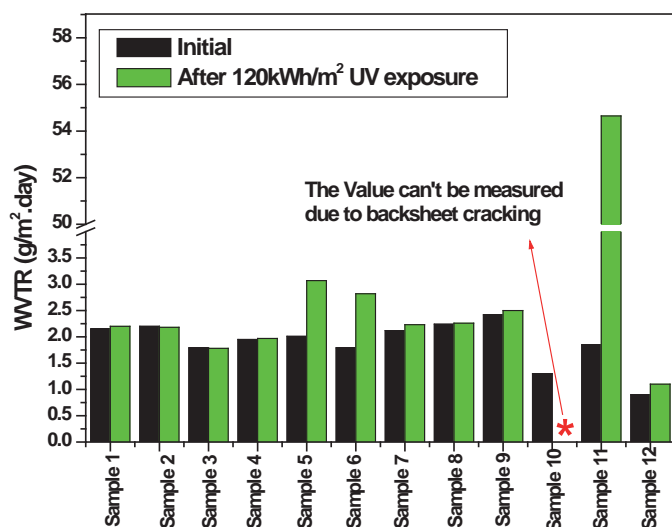


Figure 9. WVTR measurements for the backsheets after 120kWh/m² of UV exposure.

hydrolysis resistance (PCT 48h and PCT 60h) as the core layer demonstrate that they are better able to withstand exposure to humidity.

Humidity-freeze and thermal-cycling test results indicate that the weatherability performance is mainly influenced by the composition of the backsheet material; only the PA/PA/PA backsheet demonstrated poor weatherability performance.

The UV resistance performance of a backsheet is mainly determined by its composition and construction. The use of fluorine-containing materials offers excellent UV resistance performance. The PVDF film was found to have outstanding UV resistance performance, and even better than PVF film. When a modified PE is used as the inner layer of PVF-based and PVDF-based backsheets, the performance is also excellent in terms of UV resistance. In contrast, the UV resistance performance of the PET-based backsheet is poor, whereas that of the PA/PA/PA backsheet is only medium.

References

- [1] Skoczek, A., Sample, T. & Dunlop, E. 2009, "The results of performance measurements of field-aged crystalline silicon photovoltaic modules", *Prog. Photovoltaics Res. Appl.*, Vol. 17, p. 227.
- [2] IEC 61215:2005, "Crystalline silicon terrestrial photovoltaic (PV) modules – Design qualification and type approval".

About the Authors



Haidan Gong has a master's in polymer material science and is a staff engineer at Wuxi Suntech's PV Test Center.



Guofeng Wang has over 20 years' experience in semiconductor and PV technology. He is the director of Wuxi Suntech's PV Module Technology, PV Test Center and Product Management departments.

Enquiries

Haidan Gong
Wuxi Suntech Power Co., Ltd.
16 Xinhua Road
New District, Wuxi
Jiangsu Province
214028 China

Tel: +86 (510) 8531 8888-5751
Email: haidan.gong@suntech-power.com

Market Watch

Page 107
News

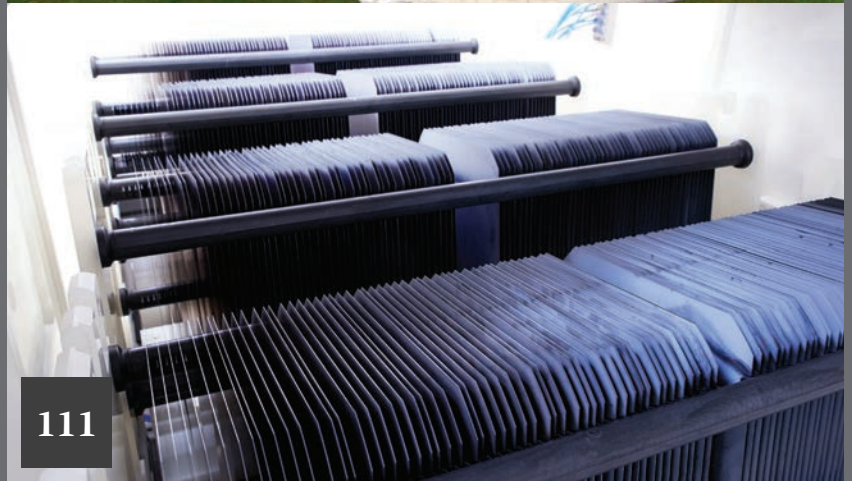
Page 111
Competing PV cell
technologies set to co-exist
out to 2020

Finlay Colville, Head of Market
Intelligence, Solar Media Ltd.

.....



107



111

PV capacity set for 64.7GW growth in 2016, says Mercom

Global PV capacity is expected to increase by 13% next year, the slowest rate of growth since 2012, according to Mercom Capital's latest market forecast.

The Texas-based analyst firm has predicted 64.7GW of new installations in 2016, up from the 57.8GW it expects to be built in 2015. That 13% increase equals the 13% year-on-year growth recorded in 2012, the slowest since before 2007.

China, the US and Japan look set to reinforce their global dominance next year, accounting for almost two-thirds of total new installations, Mercom said. The US will overtake Japan as the second largest market after China.

"The largest markets in 2016 will again be China, the United States and Japan; the United States is set to overtake Japan as the second largest solar market behind China. These three countries will account for about 65% of installations next year," said Raj Prabhu, CEO of Mercom Capital.

Mercom expects China to install 19.5GW in 2016. In the first three quarters of the year China completed almost 10GW 9GW of new capacity, a sizeable chunk of the 17.8GW target set for 2015. The US meanwhile is expected to notch up its best year so far for solar installations, with 13GW anticipated as companies rush to complete projects ahead of the expected step-down to the investment tax credit at the end of 2016. Japan will complete 9GW, according to Mercom, despite two feed-in tariff cuts in 2015. Further strong demand is expected due to the country's pending energy reforms.



Credit: SunPower

The US is expected to overtake Japan as the world's second largest PV market in 2016.

News

Asia

India approves 27 solar parks at combined 18.5GW capacity

India's government has now approved 27 solar parks, bringing the aggregate capacity to 18,418MW across 21 states and union territories at a total cost of INR40.5 billion (US\$606 million).

Until now the government's 'Development of Solar Parks and Ultra Mega Solar Power Projects' initiative only earmarked 25 solar parks for development and the government had also said these 25 parks would add up to 20GW capacity.

Each of the 'ultra mega' solar parks will have a minimum capacity of 500MW.

MNRE joint secretary Tarun Kapoor recently announced that India would also be introducing 'Solar Zones,' which will be even larger than the mega solar parks.

Green funding pours into Indian projects

The Asian Development Bank (ADB) is to lend US\$1 billion to Power Grid Corporation of India (Powergrid) to help India progress its Green Energy Corridors scheme.

The Green Energy Corridors scheme was brought in to transport power from states that are rich in renewable resources such as Rajasthan to centres of high power consumption such as Delhi and Maharashtra.

The ADB funds will be used to upgrade

high voltage transmission lines and substations in Rajasthan and Punjab to increase energy delivery from the west to southern regions. Investment will also be used for new high-voltage direct current terminals in the states of Chhattisgarh, Tamil Nadu, and Kerala to boost interconnectivity between the regions from around 10GW to 16GW.

In related funding news, Indian state-owned bank IDBI raised US\$350 million through the issue of green bonds, which also received orders of around US\$1 billion. The bonds are reported to be built around a mixed pool of assets including solar and wind energy, and other renewables initiatives.

The bank has taken up Prime Minister Narendra Modi's programme to grow clean energy and green infrastructure in India. The country is planning to reach 175GW of installed renewable energy by 2022.

Softbank and Mitsui activate 111MW Japan PV array

SB Energy, the offshoot of telecoms group Softbank, and conglomerate Mitsui have flipped the switch on a 111MW PV array in northern Japan.

The companies said in a statement the plant on Hokkaido island was set to be activated on 1 December after initially being scheduled for launch earlier this year.

Built on 166ha of land near the town of Abira, the project is expected to provide power to around 30,000 households.

Mitsui and SB Energy are

collaborating on a number of other utility PV projects in Japan.

Huawei wins order for 200MW greenhouse install

Huawei's Smart PV solution has been selected for a 200MW install at an industrial-scale greenhouse in Mongolia.

The company will work with Xiangdao Agriculture on the project. The rooftop panels will also reduce soil moisture loss and cut the acreage that would otherwise be needed for a separate ground-mounted solar facility and greenhouse.

PV monitoring networks are extended to incorporate data on the environmental conditions in the greenhouse from sensors monitoring temperature, soil moisture levels and more.

Americas

Scatec Solar switches on Utah's first utility PV plant

Norway-based IPP Scatec Solar has completed its first project in the US, a 104MW PV power plant in Utah.

The Red Hills Renewable Park is the state's first utility-scale solar plant and will more than double its current solar footprint, according to Scatec. It comprises some 340,000 modules mounted on single-axis trackers and is expected to generate up to 210 million kWh a year.



Solar has completed its first project in the US, which is also Utah's largest PV system to date.

News

"The commissioning of the Utah plant is a significant landmark for Scatec Solar. The fact that we were able to build this 104MW plant within 12 months is the proof of our company's capability to deploy solar power rapidly. The Utah plant also underlines the importance of delivering results and choosing partners whose core values match our own – in this case, Swinerton, Google and Prudential Capital Group," said Scatec Solar CEO, Raymond Carlsen.

SunPower seeks to raise US\$350 million to power corporate strategy

SunPower is seeking to raise US\$350 million in funding as it looks to power its corporate growth strategy.

The US solar developer has proposed to offer senior convertible debentures to mature in January 2023, with interest rate, offering price and various other terms to be agreed by both SunPower and initial purchasers.

The company says the net proceeds of the offering would be used for "general corporate purposes", and suggested that proceeds could be used to fund "potential acquisitions of complementary businesses".

Total Energies Nouvelles Activites USA, which owns a majority 57.5% stake in SunPower, has agreed to purchase US\$100 million of the total principal amount, which is subject to the company issuing at least US\$300 million of the amount.

Latin America installs 181MW PV in Q3, record 1.4GW forecast for Q4

The Latin America region saw 181MW of utility-scale solar PV projects come online in Q3 2015, down 50% from the historic 363MW of installations in Q2, but still helping the market's ability to move towards maturity in 2016, according

to GTM Research's 'Latin America Q3 Playbook'.

Furthermore GTM has forecast that Q4 will be the largest in the region's history with a surge of 1.4GW installed.

In Q3, 1.45GW of projects were announced bringing the total Latin America project pipeline to 38.5GW. A further 74MW of PV entered the construction phase in the same period.

Brazil's Development Bank raises US\$100 million for renewables investment

Brazil's Development Bank (BNDES) has raised US\$100 million from three Japanese banks in order to invest in clean energy projects.

The Japan Bank for International Cooperation (JBIC) was the main source of funding, supported by the Bank of Tokyo-Mitsubishi UFJ and Mizuho Bank.

The fundraising is part of BNDES's green line, which aims to support renewable energy projects, and is the fourth fundraising agreement signed

between the BNDES and JBIC as part of the green line since 2011.

A BNDES statement said: "Following this new loan agreement, the BNDES is now able to continue with its strategy of expanding its relationship with international financial institutions, thus increasing the Bank's scale of investments in partnership with multilateral institutions and governmental agencies."

Europe

PV tenders in Germany oversubscribed again

The third round of tenders in 2015 to build ground-mount PV power plants in Germany has been oversubscribed, with some 562MW of hopefuls entering the bidding for just 200MW of capacity.

German regulator Bundesnetzagentur (Federal Network Agency) said on 11 December that 43 out of 127 bids had been successful, representing 204MW of new capacity. Successful bidders would be informed by email, the agency said. The tenders had been opened up beyond project developers to allow cooperatives or individuals to take part with two cooperatives among the bidders awarded projects.

The second round in August was oversubscribed three times over, while the first round in April saw 700MW of bids for 150MW of available capacity.

France names winning solar projects

Over 200 projects are set to benefit from the feed-in tariff programme run by the French Ministry of Ecology, Sustainable



Germany's third PV tender in 2015 has been oversubscribed.

Under the Patronage of H.H. General Sheikh Mohammed bin Zayed Al Nahyan, Crown Prince of Abu Dhabi and Deputy Supreme Commander of the U.A.E. Armed Forces

WORLD FUTURE ENERGY SUMMIT

PART OF ABU DHABI SUSTAINABILITY WEEK 2016

18-21 JANUARY 2016
ABU DHABI NATIONAL EXHIBITION CENTRE

Hosted by

Masdar
A MUBADALA COMPANY



Principle
Sponsor



Associate Sponsor



Diamond Sponsor



Efficiency Sponsor

هيئة كهرباء ومياه دبي
Dubai Electricity & Water Authority



Strategic Sponsor



غرفة أبوظبي
ABU DHABI CHAMBER

POWERING THE FUTURE OF ENERGY

- Discover cutting-edge technologies from leading innovators at the **EXHIBITION**
- Explore the latest solar projects and investments at **WFES SOLAR EXPO**
- See innovations in motion at our dedicated **SUSTAINABLE TRANSPORT ZONE**
- Deepen your knowledge and insights at **WFES CONFERENCE**
- Maximise your visit and plan your meetings with **SUSTAINABILITY BUSINESS CONNECT**

REGISTER ONLINE NOW!

WIN A CONFERENCE DELEGATE PASS

By entering your promotion code upon registration, you stand a chance to win a complimentary delegate pass worth over AED 10,000 to the WFES World Class Conference.



www.worldfutureenergysummit.com

#WFES16

Platinum Sponsors



Gold Sponsor



Official Carbon Offset Partner



Official Hotel Partner



Co-located with



Organised by





The latest tender round in Dubai's flagship PV project has attracted significant interest.

Development and Energy (MEDDE).

The 212 winning projects from the 800MW solar energy auction range from 0.4MW to 12MW in capacity.

The average tariff for large rooftop solar installations was €129/MWh (US\$140), down 18% from €158/MWh in the previous auction held nearly two years ago. The average price for ground-mount facilities also fell, down 15% from €146 to €124.

In addition, the ministry announced that nearly €1 billion will be invested in solar parks - expected to produce 1.1TWh of electricity annually - to give impetus to solar in the French industrial sector.

New solar tenders will be launched in early 2016.

Middle East and Africa

Dubai's 800MW solar tender attracts international attention

Around 20 bidders have entered the frame for the latest 800MW phase of Dubai's flagship solar project, according to the Middle East Solar Industry Association.

The third tender in the Mohammed bin Rashid Al Maktoum Solar Park drew attention from a wide range of players, with

a number of international partnerships emerging throughout the bidding process.

Dubai recently extended the targeted size of the solar park from 3GW to 5GW by 2030. It was originally planned as a 1GW facility with CSP and PV technologies installed.

The next stage of the tender process will take place in early 2016.

The competition follows the launch of a new energy strategy for Dubai, which includes a provision to make rooftop solar mandatory from 2030.

Luxra lining up 300MW pipeline in Nigeria

The UK branch of Swiss PV manufacturer Luxra claims to have lined up a 300MW PV pipeline in Nigeria.

The company has signed a memorandum of understanding with the Delta State Government to develop 300MW of PV. Luxra is also looking at sites in the northern and central parts of the country that it estimates could open the door to a further 700MW.

Mike Judge, CEO of Luxra UK, told PV Tech that the national and state governments have indicated a commitment to solar. According to Judge, solar is viewed by Delta state officials as a means to tackling persistent power cuts.

EBRD allocates US\$500 million for Egypt's solar programme

The European Bank for Reconstruction and Development (EBRD) has allocated up to US\$500 million in support of Egypt's solar energy programme in 2016.

The programme is aiming for up to 2GW of utility-scale solar capacity delivered through 40 projects of 50MW each. This will be part of the country's target to source 20% of its electricity from renewables by 2020.

Many of these projects will be located on a planned 1.8GW site near Benban in north Egypt.

The EBRD expects to finance several such plants and mobilise up to US\$1.5 billion in debt and equity from other financiers for these ventures. The total cost of the projects is expected to be in the region of US\$4 billion.

The solar projects, to be constructed entirely by private firms, have been supported by recent reforms. The EBRD said it has worked closely with the Egyptian authorities to provide technical cooperation during the development of a legal and regulatory framework for renewable energy. This included contractual agreements, the solar grid code and environmental and social due diligence.

Competing PV cell technologies set to co-exist out to 2020

Finlay Colville, Head of Market Intelligence, Solar Media Ltd.

ABSTRACT

The solar industry is going through the final stages of correcting its supply–demand imbalance, with the decision-making on technology choice for the next generation of GW-scale factory expansions becoming a key strategic issue for leading manufacturers. In contrast to previous capacity expansion phases – where new entrants largely copied known process flows and technology types – the next round of technology additions is seeing a broader range of influences, indicative of a new type of technology roadmap unfolding for the industry as a whole.

Introduction

This paper provides a detailed overview of current crystalline silicon (c-Si) cell solar photovoltaic (PV) manufacturing technologies, and the factors that are influencing decision-making for new capital expenditure (capex) and capacity expansions.

A discussion is provided first that will help in understanding the current segmentation of c-Si cell technologies, across n-type and p-type substrates, and their different processing methods. Reference is also made here to the legacy solar PV cell roadmaps that have been promoted heavily by academic research institutes in the last five to ten years.

The results of new market research undertaken by PV-Tech are then presented, including conclusions from interviews undertaken with leading cell manufacturers and materials and equipment suppliers, backed up by data from a detailed analysis of the forecast top-20 cell producers by MW-volume in 2015.

The conclusions highlight a more complex blend of factors that are creating a broader mix of options for c-Si cell manufacturing going forward, and suggest that the industry's previous desire to choose a winning technology type (n-type or p-type, mono or multi, standard or advanced process flows) may be somewhat misleading, and that different technology options are likely to continue to co-exist in the short to mid term (three- to five-year time frame).

Understanding legacy PV cell technology roadmaps

During the early growth phase of the solar industry (from annual end-market demand levels of around 10GW to the 30–50GW level of 2012–2014), the industry went through two stages of technology roadmap consensus. The first, illustrated in Fig. 2(a), was based on an assumption that thin-film technologies (covering each of a-Si, CIGS and CdTe) would see gradual market-share gains, with many of the roadmaps projecting that thin-film modules would be



Figure 1. BiSon solar cell production: low-cost manufacture of high-efficiency n-type bifacial monocrystalline silicon solar cells.

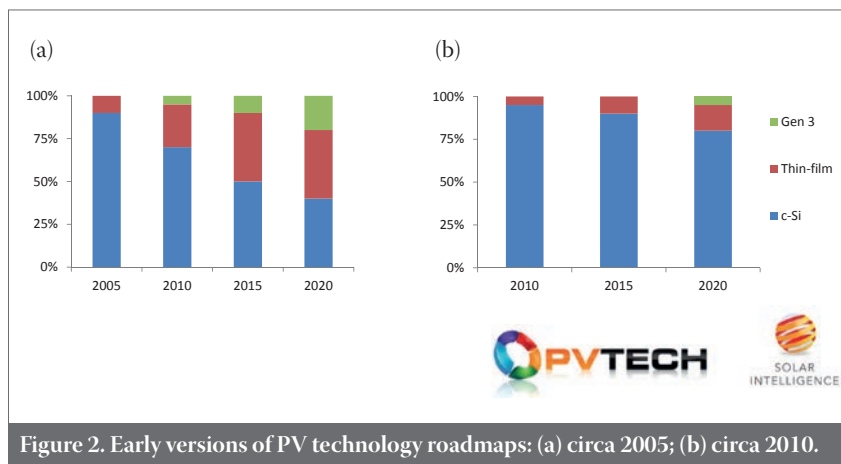


Figure 2. Early versions of PV technology roadmaps: (a) circa 2005; (b) circa 2010.

the dominant technology type by 2020. In fact, most of these roadmaps also factored in the adoption of so-called generation 3 (Gen 3) cell technologies based on dye-sensitized and organic-based technologies.

The failure of a-Si technologies to move beyond 10% efficiency levels – coupled with the challenges in transferring large-area deposition equipment originally conceived for flat-panel displays to solar PV – effectively eliminated a-Si from any credible technology roadmap from 2011 onwards.

“Solar technology roadmaps by 2010 sought to focus more on c-Si.”

Fast forward to 2015, and thin-film activity in the solar industry is all but confined to the strategies, and technology excellence, of two companies: First Solar for CdTe, and Solar Frontier for CIGS. Consequently, solar technology roadmaps by 2010 (see

Fab & Facilities

Materials

Cell Processing

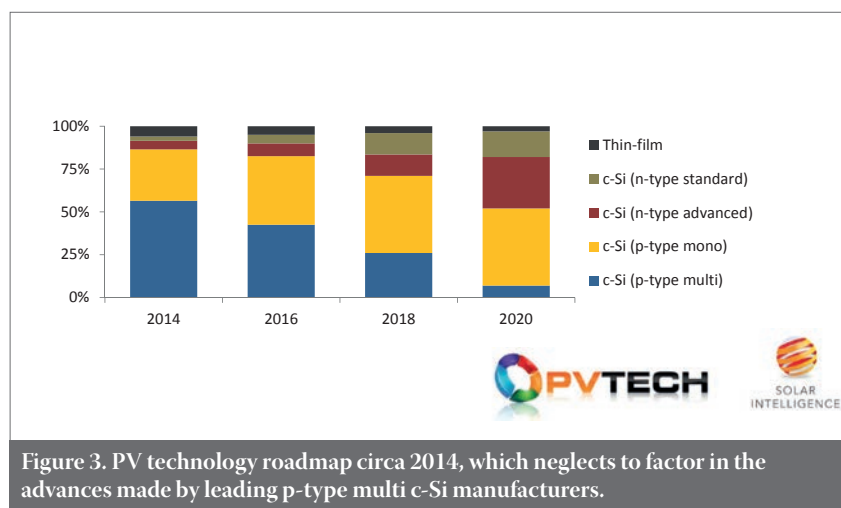
Thin Film

PV Modules

Market Watch

Credit: MegaCell

© Solar Media Ltd., PV-Tech, November 2015



Market Watch

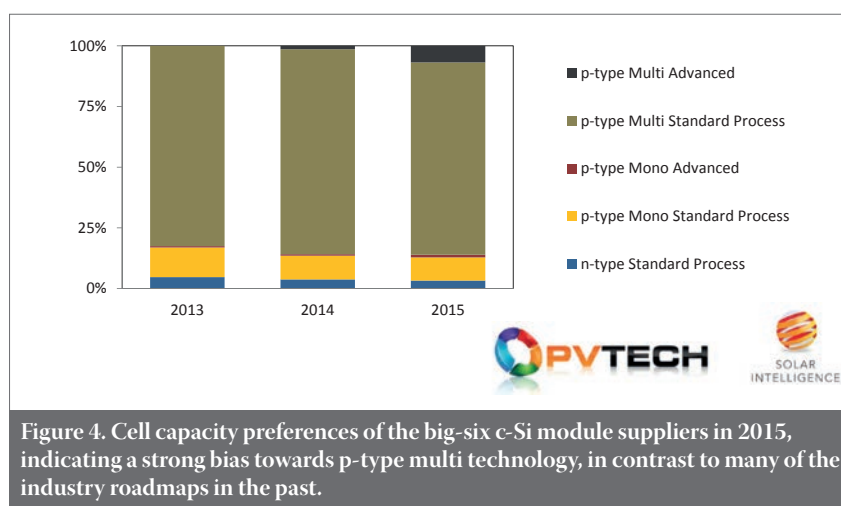


Fig. 2(b)) sought to focus more on c-Si, largely confining thin-film market shares to the production capacity and shipments driven by the two above-mentioned thin-film specialists, and assigning new entrants, such as Hanergy, to the thin-film sector. Gen 3 activity was by this time getting squeezed into a smaller wildcard contribution by 2020.

The c-Si roadmap consensus at the start of 2015

Concentrating on c-Si cell manufacturing as the leading indicator for module shipment trends, PV roadmaps from 2012 became heavily influenced by dedicated research laboratories again, and not directly by the leading c-Si cell producers, many of whom by then had accumulated manufacturing capacities at the GW level.

The fundamental assumption for most of these roadmaps was that p-type substrates, and corresponding cell processing using this wafer type, would ultimately be superseded by the higher efficiencies that were inherent in using better-quality n-type silicon material. Furthermore, p-type multi c-Si manufacturing was largely regarded as something of a passing phase in the industry, and in use across much of Asia simply because of its lower barriers-to-

entry for manufacturing.

As a result, c-Si roadmaps until recently were strongly biased towards market-share gains for p-type mono over p-type multi, and ultimately moving to an industry using n-type cells that would largely comprise thin silicon wafers and either back-junction or heterojunction cell types (see Fig. 3). Intrinsic to these assumptions was a perceived limit to p-type multi c-Si efficiency pegged below the 20% level.

While forecasting efficiency and cost at the multi-GW level over a three- to five-year period is fraught with challenges and always difficult, a major drawback of these roadmaps was the assumption that technologies had to compete directly with one another, ultimately leading to a single technology type (or small subset) that would reign supreme in the solar industry.

The reality of c-Si cell manufacturing going into the 60GW-plus end-market landscape of 2016 indicates that this concept of head-to-head competition is largely misplaced, as will be explained in more detail in the next section.

Technology production reality in 2015

Putting aside previous forecasts and legacy roadmaps for the solar industry,

the starting point for technology over the next three to five years should be what is actually happening in manufacturing today. While there is no immediate need to over-complicate the rationale for the breakdown of n-type and p-type, and mono and multi, a quick overview now will help to set the stage for the later discussion on roadmaps.

During 2015 it is likely that approximately 60GW of solar cells will be manufactured (note that here, for accurate methodology, thin-film manufacturing is classed as both cell and module production). This 60GW will probably end up including about 5% from thin-film manufacturing (dominated by CdTe from First Solar) and about 5% from n-type c-Si variants; therefore 90% is most likely to come from p-type solar cell production, of which about 80% comes from p-type multi. The final split could then end up being approximately 70% p-type multi, 20% p-type mono, 5% thin-film and 5% n-type. This is similar to the split seen during 2014, but with p-type multi seeing increased use at the expense of p-type mono.

At this point, it is useful to look at the cell manufacturing capacities of the leading c-Si module suppliers of 2015: this group includes Canadian Solar, Hanwha Q CELLS, JA Solar, JinkoSolar, Trina Solar and Yingli Green. Collectively, these six leading module suppliers – grouped by PV-Tech under the banner of Silicon Module Super League – are expected to ship approximately 24GW of modules during 2015, or about 40% of the entire industry requirements for 2015.

“The strong preference for p-type multi is at the heart of why the industry urgently needs a rethink on technology forecasts going into 2016.”

Fig. 4 shows the cell capacity breakdown for the Silicon Module Super League between 2013 and 2015; this helps to explain the differences between the legacy PV technology roadmaps and what is happening in the industry at the end of 2015. The strong preference of this leading module-supplier grouping for p-type multi is clear to see, and is at the heart of why the industry urgently needs a rethink on technology forecasts going into 2016.

Within the p-type options, the main difference in the past 12 months has been the increase in the use of passivated layers on the rear surfaces, with a move away from the industry-standard full aluminium back-surface field (Al-BSF) architectures employed in the past. More commonly referred to by the acronym PERC (passivated emitter and rear contact cell), coined by the University of New South

SOLAR & OFF-GRID RENEWABLES WEST AFRICA

Accra, Ghana

19 - 20 April 2016

Use Discount Code
'PVI15' for a
15% discount*


Secure clean & reliable energy for West African consumers and businesses
Hear from projects in:

 **Senegal:** Tenergie and Greenwish Partners will present their 50MW and 20MW respective projects

 **Nigeria:** Gigawatt Global and NSCP will elaborate on their 125MW project and the barriers to reaching financial closure

 **Burkina Faso:** Windiga will explain the realities of developing a 20MW project amidst political uncertainty

 **Ghana:** First Solar and Windiga will talk us through their Ghana project and issues relating to grid connection and land acquisition

 **Equatorial Guinea:** See Maeci talk about their development and construction of a 5MW island mini grid

Over 50 speakers confirmed including:



Wisdom Ahiataku-Togobo, Director of Renewable Energy Ministry of Energy Ghana



Dr. Ifeabunike Joseph Dioha Ag., Director, Renewable Energy, Nigerian Energy Commission



Joel Abrams, Managing Director, Nigeria Solar Capital Partners



Oliver Andrews, CIO AFC



Christopher J. Massaro, Senior Vice President, MAECI

Benefits of attending:

- Discover strategic business opportunities in the region
- Network with international and local key industry players including financiers, project developers, government, end users and manufacturers
- Hear policy and regulation updates from government officials
- Attend interactive sessions and learn from innovative case studies
- Learn about energy user's concerns at our bespoke end users' sessions

westafrica.solarenergyevents.com

For all enquiries contact marketing@solarenergyevents.com

 **#sorwa16**

Gold sponsors:



Silver sponsor:



Supporting sponsors:



Exclusive to PVI readers. Offer ends 31/12/2015

Wales, the technology has seen upgraded line activity for both p-type mono- and multi-based production.

The default way of forecasting the market-share trends of the different cell technologies (p-type, n-type, mono, multi) is simply to estimate which will win market share against the others, and to continue to do a side-by-side comparison. This also leads to conclusions about technologies 'winning' against the others, and as a consequence, it is all too easy to piece this together and call it the roadmap of the industry.

This somewhat naïve process has not, however, worked in the past, and there is also no evidence at all that it will work – or indeed provide any great help to manufacturers – going forward. Instead, we are now seeing that a different type of research methodology is needed, which will next be explained in more detail.

Shifting from technology competition to co-existing competitive alternatives

As background research undertaken by PV-Tech ahead of its inaugural solar cell manufacturing conference in Malaysia in March 2016 (PV CellTech [1]), an exhaustive series of interviews has just been completed with the leading cell manufacturers, as well as with the main materials and equipment suppliers to the industry. The study was initially geared towards scoping out the optimum session topics and issues for presentation and discussion at the conference; the findings, however, uncovered more than was originally targeted, in particular key inputs relating to the solar cell

roadmap of 2016 and beyond.

At the p-type and n-type levels, there was broad consensus not to pitch these as competitive cell manufacturing approaches, but to separate out n-type activity more as an overall business approach by the companies with know-how and intellectual property regarding manufacturing.

In fact, despite many leading p-type manufacturers having had n-type on corporate technology roadmaps on show to the outside world, there now appears to be a more pragmatic assessment of in-house skill sets. Basically, most p-type producers – even those at the multi-GW level – seem to be coming to the conclusion that the transition from p-type to n-type is not only an extremely difficult proposition, but also not necessary in order to have a market-competitive offering as a business. While to many this may seem rather obvious, plenty of cell manufacturers had got bought into the assumption that p-type was just a passing phase and that within five years, n-type would be essential; therefore, for the outside world, they were almost forced to include this in technology roadmaps when talking about in-house R&D activities.

“The transition from p-type to n-type is not only an extremely difficult proposition, but also not necessary in order to have a market-competitive offering as a business.”

Looking at n-type against p-type is not entirely dissimilar to comparing c-Si and thin-film technologies. Thin-film works for the two leading manufacturers because they have manufacturing excellence coupled with a downstream business model that is adaptive and works, and each company has the ability to supply a quality brand offering, either in-house or via third parties.

Furthermore, even when purely p-type was looked at in isolation, there were similar conclusions emerging from just comparing p-type mono and multi options. While flipping cell and module lines between mono and multi is an easy transition, the strategies of p-type cell makers still seem to be firmly dedicated to one of the two substrate types on offer; there are actually very few cell makers with balanced mono and multi cell production levels today. If any member of the Silicon Module Super League needs to increase short-term mono module supply, the easiest route is to simply increase the mono portion of outsourced cells.

With this in mind, some of the key c-Si manufacturers at the start of 2016 will be looked at in the next section, which will be a useful way of illustrating the concept of co-existence over competition for cell manufacturing going forward three to five years.

Grouping the leading players by strategy

To provide some colour to the above summary, the top-20 (approximately) cell producers in the industry will be examined, along with some of the new

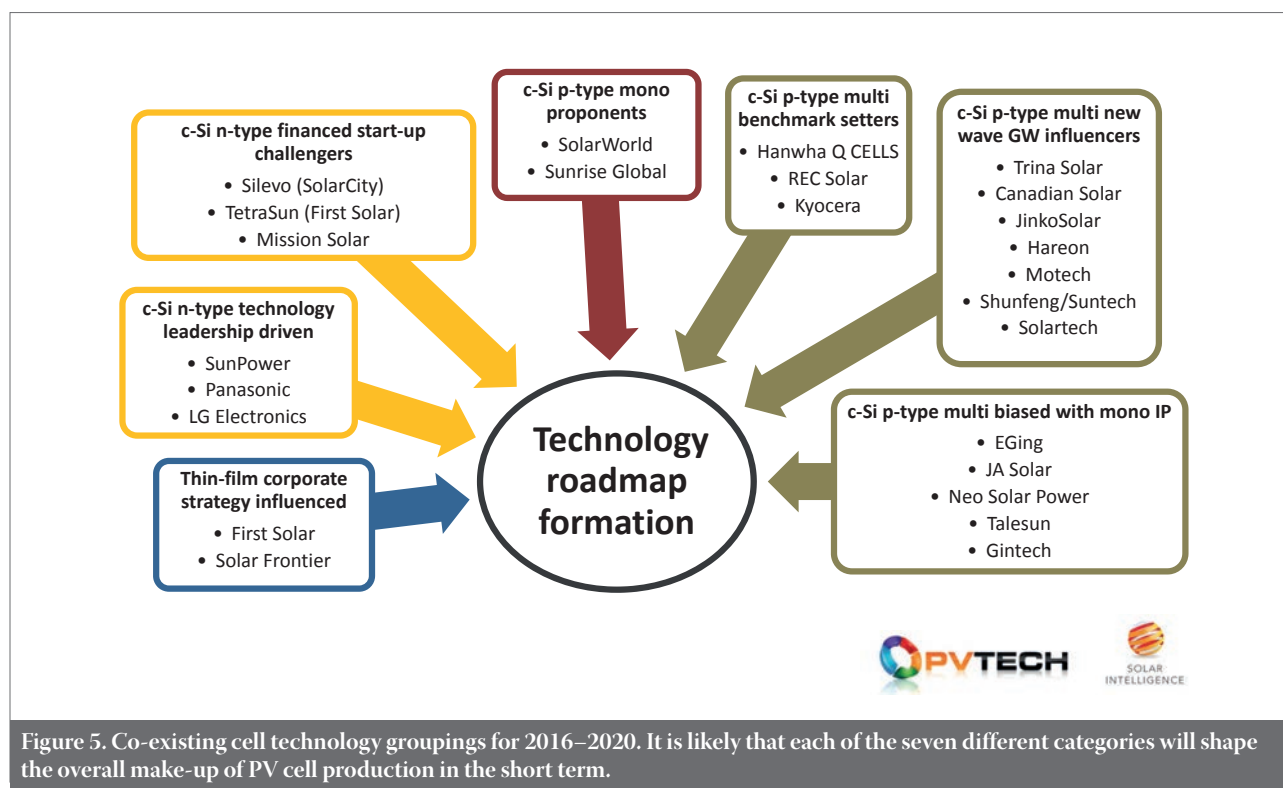


Figure 5. Co-existing cell technology groupings for 2016–2020. It is likely that each of the seven different categories will shape the overall make-up of PV cell production in the short term.

start-ups looking to disrupt the current technology mix. Ultimately, the top-20 cell producers shape the current segmentation of solar cell manufacturing; they do not follow a predestined path set out by any external think-tank seeking to offer guidance on how they should change their technologies to remain competitive.

Additionally, the disruptive approaches (most notably being championed by SolarCity through its Silevo operations, and First Solar with TetraSun) are not seeking to gain market share against p-type suppliers per se, but instead to open up new opportunities as part of company-specific downstream deployment growth. In this context, it has to be remembered that strong year-on-year growth of the solar industry is forecast to continue in the next three to five years, effectively creating the space for various technologies to expand and co-exist, rather than competing within a finite and static end-market space.

First, the thin-film activities are filtered out, leaving only c-Si technologies. Direct competition between First Solar or Solar Frontier and mainstream p-type c-Si producers is becoming less of an issue within the industry today, with the business deals being won and lost on the project side, within which the blend of module price, efficiency and levelized cost of energy (LCOE) is just one of a complex set of variables dictating the final choice.

Similarly, n-type activity can be largely segmented, especially in the case of SunPower. The other leading n-type producers (Panasonic and LG Electronics) are less influential in the downstream channels but still have a very different company approach to solar panel distribution when compared with today's mainstream p-type solar cell suppliers. It is entirely reasonable, therefore, to pull out SunPower and Panasonic as having a dedicated n-type strategy that operates largely decoupled from the issues affecting GW-scale p-type cell producers. Although LG Electronics are not yet fully aligned to an n-type strategy, it was decided to group the company within this category too, assuming that LG's solar business is based on differentiation from Chinese and Taiwanese manufacturing, and heavily driven by long-term R&D and technology development investments.

Sitting on the periphery of this n-type grouping are Silevo and TetraSun. While each has its own set of risks and challenges ahead before any volume production can be shown, it could be argued that if these two companies were running at the GW level today, the overall technology/end-market penetration strategy would look not entirely dissimilar to that of SunPower today.

The more interesting outcome of PV-Tech's new research relates to p-type

mono and multi approaches, and the clear preference from one company to another, each with an internal roadmap that has been carefully and strategically selected.

Given these findings, it could be strongly argued that the current dominance and share gains for p-type multi are largely coming from the sheer volume of capacity and number of companies in China that made technology decisions based on having the easiest market-entry route some years ago, coupled with the very tangible impact that GCL Poly has had on the solar industry through its polysilicon/wafer capacity and supply. Further impacting this equation is the fact that many of the Chinese p-type multi c-Si cell makers have been somewhat gifted a captive domestic end-market that has one of the lowest global price points and is easily receptive of p-type multi modules for ground-mount installations.

When the remaining (p-type) subset of cell makers that comprise the top-20 (approximately) producers this year is inspected, a clear divide can be seen between those shifting to mono-based approaches (SolarWorld, Sunrise Global), those historically attached to p-type multi (REC Solar, Hanwha Q CELLS), and those that entered the industry post-European manufacturing and are now dominated by p-type multi (Trina Solar, Canadian Solar, JinkoSolar, Yingli Green, Hareon, Motech, Shunfeng/Suntech and Solartech).

Currently sitting somewhat on its own is Kyocera, a company that has its own lineage, comparable to SunPower, Panasonic, REC Solar and Q CELLS, but is now the only Japanese c-Si cell maker of note with domestic production capacity, and is best grouped together with REC Solar and Hanwha Q CELLS.

Completing the technology categorization is a group of cell makers that are historically p-type multi producers but have significant mono activities (Gintech, JA Solar, Neo Solar Power, Talesun). Also included in this category is EGing, but coming from the opposite starting point (mono dominant to multi dominant). The overall grouping is shown in Fig. 5.

In terms of forecasting solar cell technology into 2016, it is useful to look at these groups and how their efforts to improve efficiency and yield, and reduce manufacturing costs, will unfold. In many cases, the approaches to maintaining competitive cell production will probably include a unique subset of variables, from wafer supply to processing tools and material supply. However, for most there is an overlap of issues (wafer quality, handling, PERC, inspection, metallization) that will ultimately help to drive the entire segment forward, and for most of the equipment and materials suppliers, these are potentially the most important issues to understand.

Setting the scene for 2016

Perhaps the main takeaway from the analysis outlined above is that it is simply not possible to decouple the upstream and downstream parts of the solar industry, which precludes any head-to-head comparison between chosen production approaches.

“It is simply not possible to decouple the upstream and downstream parts of the solar industry.”

Of course, each of the categories shown in Fig. 5 has to be market competitive in terms of cost and efficiency, but the boundaries here are certainly blurred and are clearly different for a downstream-focused, domestically entrenched, vertically integrated, US-centric thin-film producer and a China-based, state-favoured c-Si cell/module maker targeting domestic EPCs as part of its own government-driven end-market installation targets.

When the mix of technologies and approaches co-existing in the PV industry is examined, another conclusion is that all manufacturers have been forced to move efficiencies higher and costs lower, simply to justify sustaining a manufacturing presence. And in this respect, one is left to contemplate what could really be achieved by the solar industry if a common approach to implementing technology and reducing cost was followed, notwithstanding making the best use of locations that would ultimately favour the lowest-cost labour market at the time.

Reference

- [1] PV CellTech Conference, 16–17 March 2016, Kuala Lumpur, Malaysia [<http://celltech.solarenergyevents.com/>]

About the Author



Finlay Colville joined Solar Media as head of the new Solar Intelligence activities in June 2015, before which he was vice president and head of solar at NPD Solarbuzz until October 2014. Widely recognized as a leading authority on the solar PV industry, he has presented at almost every solar conference and event worldwide, and has authored hundreds of technical blogs and articles in the past few years. He holds a B.Sc. in physics and a Ph.D. in nonlinear photonics.

ADVERTISER	WEB ADDRESS	PAGE NO.
Centrotherm	www.centrotherm-pv.com	43
Clean Energy Summit	summit.solarenergyevents.com	75
Hellmann Worldwide Logistics	www.hellmann.net/secureSupplyChain	19
Heraeus Precious Metals	www.pvsilverpaste.com	Outside Back Cover
INDEOtec SA	www.indeotec.com	63/65
Intersolar	www.intersolarglobal.com	15
JA Solar Holdings Co., Ltd.	www.jasolar.com	Inside Front Cover
Meco Equipment Engineers B.V.	www.besi.com	65
PV CellTech Conference Malaysia	celltech.solarenergyevents.com	47
PV-Tech Power Technology Journal	www.pv-tech.org/power	97
Renolit Belgium NV	www.renolit.reflexolar.com	5
Schmid Group	www.schmid-group.com	91
SNEC 2016	www.snec.org.cn	Inside Back Cover
Solar & Off-grid Renewables West Africa	westafrica.solarenergyevents.com	113
Solar Finance & Investment Europe Forum	finance.solarenergyevents.com	101
Solar Media Events 2016	www.solarenergyevents.com	55
Solar Middle East	www.solarmiddleeast.ae	79
Von Ardenne GmbH	www.vonardenne.biz	11
World Future Energy Summit	worldfutureenergysummit.com	109
Wuxi Suntech Power Co., Ltd.	www.suntech-power.com	3

To advertise within Photovoltaics International, please contact the sales department: Tel +44 (0) 20 7871 0122

NEXT ISSUE:

- Polysilicon versus UMG: technology, quality and costs
- Cell-to-module loss analysis
- The present and future silver cost component in crystalline silicon PV module manufacturing

THE INDISPENSABLE GUIDE FOR MANUFACTURERS IN SOLAR

Photovoltaics International contains the latest cutting edge research and technical papers from the world's leading institutes and manufacturers.

Divided into six sections – Fab & Facilities, Materials, Cell Processing, Thin Film, PV Modules and Market Watch – it is an essential resource for engineers, senior management and investors to understand new processes, technologies and supply chain solutions to drive the industry forward.

An annual subscription to **Photovoltaics International**, which includes four editions, is available at a cost of just \$199 in print and \$159 for digital access.

Make sure you don't miss out on the ultimate source of PV knowledge which will help your business to grow!



SUBSCRIBE TODAY.

WWW.PHOTOVOLTAICSINTERNATIONAL.COM/SUBSCRIPTIONS



SNEC 10th (2016) International Photovoltaic Power Generation Conference & Exhibition

Gather worldwide PV industry leaders and enterprises.
Grasp the newest trends in PV technologies and the PV industry.
Build international co-operation and trade platforms for the PV industry.
Attract tens of thousands of powerful buyers.

www.snec.org.cn

Welcome to Shanghai

May 24-26 2016

 **SNEIA** Shanghai New Energy Industry Association

Shanghai New International Expo Center
(2345 Longyang Road, Pudong District, Shanghai, China)



180,000m²
Exhibition Space

1,800+
Exhibitors

5,000+
Professionals

150,000
Visits

Shanghai, China

Tel: +86-21-64276991
+86-21-33561099

For exhibition: info@snec.org.cn
For conference: office@snec.org.cn

California, USA

Tel: +1-510-219-6103

For exhibition: Petersnec@gmail.com

efficiency



Wisdom creates efficiency.



Our Research and Development team is constantly thinking about paste. We are committed to developing leading-edge solutions, which improve the power output and performance of solar cells at a lower cost per watt. We are always mindful of the current and future technology needs of our customers, and are driven to deliver results. So when you think of paste...think of Heraeus.

Leadership through R&D. Breakthroughs via innovation.
Achievement by tradition.

Visit us at:

PV EXPO 2016 | Tokyo Big Sight, Japan | March 2nd - 4th
SNEC 2016 | Shanghai, China | May 24th - 26th

Heraeus Photovoltaics Business Unit

www.pvsilverpaste.com

China | Singapore | Taiwan | Europe | America | Japan